Role of Protein Kinase D (PKD) in migration, invasion and cell adhesion of pancreas ductal adenocarcinoma cells

Von der Fakultät Geo- und Biowissenschaften
der Universität Stuttgart zur Erlangung der Würde
eines Doktors der Naturwissenschaften (Dr. rer. nat.)
genehmigte Abhandlung

Vorgelegt von

Tim Eiseler

aus Leutenbach

Hauptberichter: Prof. Dr. Klaus Pfizenmaier
Mitberichter: Prof. Dr. Peter Scheurich
Tag der mündlichen Prüfung: 10. April 2006

Institut für Zellbiologie und Immunologie
Universität Stuttgart
2006

Role of Protein Kinase D (PKD) in migration, invasion and cell adhesion of pancreas ductal adenocarcinoma cells

Tim Eiseler

Hiermit versichere ich, dass ich die Arbeit selbst und nur unter Verwendung der angegebenen Hilfsmittel verfasst habe.

Stuttgart, 13.03.06

Tim Eiseler

Index

1. Abbreviations

Ab	Antibody
ADP	Adenosine diphosphate
AP	Alkaline phosphatase
APS	Ammonium persulfate
ATP	Adenosine triphosphate
bp	Base pairs
BSA	Bovine serum albumin
Cdna	complementary-DNA
CO_2	Carbon dioxide
DAG	Diacylglycerol
ddH_2O	Double distilled H_2O
DMSO	Dimethylsulfoxide
DNA	Deoxyribonucleic acid
DTT	Dithiothreitol
ECL	Enhanced chemiluminescence
ECM	Extracellular matrix
EDTA	Ethylendiamintetraacetate
EGF	Epidermal growth factor
EGFP	Enhanced green fluorescent protein
EGTA	Ethylene glycolbis(aminoethylether)-tetra-acetic acid
$F(ab')_2$	Fragment of antigen binding 2
FAK	Focal adhesion kinase
Fc	Immunoglobulin fragment constant
FCS	Fetal calf serum
Fig	Figure
GFP	Green fluorescent protein
h	Hour
H_2O_2	Hydrogen peroxide
HRP	Horseradish peroxidase
IB	Immunoblot
IF	Immunofluorescence
Ig	Immunoglobulin
IHC	Immunohistochemistry
JNK	c-Jun N-terminal kinase
KD	Kinase-dead mutant
kDa	Kilo-Dalton
l	Litre
Lab	Laboratory
LSM	Laser scanning microscope
M	Molar [mol/l]
mAb	Monoclonal antibody
min	Minute
NFκB	Nuclear factor kappaB
NGS	Normal goat serum
ºC	Degree Celsius
PAGE	Polyacrylamide gel electrophoresis
PBS	Phosphate buffered saline
PDGF	Platelet derived growth factor
PFA	para-formaldehyde
PKD	Protein kinase D
PLC	Phospholipase C
PLL	Poly-L-lysine
POD	Peroxidase
RNA	Ribonucleic acid
RNAi	RNA interference
RNAse	Ribonuclease
rpm	Revolutions per minute

1 – Abbreviations

RT	Room temperature
SDS	Sodium dodecylsulfate
siRNA	Small interfering RNA
Sol	Solution
T	Timepoint
TGFβ	Transforming growth factor β
TGN	Trans Golgi network
TNF	Tumour necrosis factor
U	Enzyme unit
uPA	Urokinase-like Plasminogen-activator
WT	Wildtype

2. Summary

The pancreas ductal adenocarcinoma (PDAC) is one of the most common types of cancer, accounting for a large number of cancer related deaths. Due to its unfortunate characteristics, like resistance to chemo-, radio- and immunotherapy, the only way of treatment is surgical resection. Rapid tumour metastasis is a major problem in pancreatic cancer, and little is known on the molecular events governing this process, however, features like resistance to apoptotic stimuli, changes in cell shape, modulation of cell-to-cell adhesion, enhanced cell motility and matrix degrading potential seem to be important. In the literature the Protein kinase D (PKD) family of serine/threonine kinases, which consists of 3 structurally related isoforms, PKD1/PKCμ, PKD2 and PKD3/PKCν, has been implicated in the regulation of some of these processes, yet the molecular mechanisms involved largely remained unclear. That's why this study, using PDAC cell lines, focused on the functions of PKD in cell migration, the invasion of cancer cells, cell-substratum adhesion, cell-to-cell adhesion and the regulation of cancer related genes. In this work, PKD was found to be strongly expressed and also active in Panc89 cells, as indicated by trans-, and autophosphorylation of the kinase in total cell lysates. Focusing on this cell line, a potential link of PKD to the modulation and turnover of the Actin cytoskeleton was discovered. PKD was shown to colocalise with F-Actin and respective markers, indicating active Actin remodeling. For example, Arp3, a member of the Actin-related Arp2/3 protein complex, which is responsible for *de novo* Actin nucleation and dendritic branching of Actin filaments, colocalised with PKD. Further, PKD colocalised with a subcellular pool of Vinculin at the edge of membrane protrusions, again indicating active Actin turnover, possibly at nascent focal complexes, however PKD was not localised to Vinculin-positive mature focal adhesion to the substratum. In addition, PKD localised with Cortactin, which is enriched within lamellipodia and membrane ruffles. It is implicated in the stabilisation of F-Actin branch points and therefore exhibits important functions at the cortical F-Actin cytoskeleton, which are directly linked to cell migration. Surprisingly, PKD was also found to directly bind to F-Actin *in vitro*. The binding domain was mapped to 46 amino acids in the N-terminal region of PKD, close to the starting position at amino acid 98. An alignment of the respective PKD sequence indicated highly conserved motifs, both amongst PKD isoforms and also between *human*, *mouse*, and *Drosophila* species, pointing to a general feature of PKDs. Apart from the binding to F-Actin, PKD and Cortactin also interacted biochemically and PKD was shown to phosphorylate Cortactin *in vitro* at S298, as well as at additional unspecified sites. Unfortunately an *in vivo* phosphorylation of Cortactin could not be demonstrated up to now. Employing stable Panc89 cell lines, PKD1 impaired 3D cell migration, while for PKD1KD expressing cells, migration was enhanced. These effects can either be explained by a model implicating Cortactin phosphorylation by PKD in the regulation of F-Actin turnover and rigidity, or by the phosphorylation of yet unknown PKD substrates at the respective F-Actin-rich structures, negatively regulating cell migration. Since mutation of the potential Cortactin phosphorylation site Ser298 to an alanine residue also increased cell migration in stable Panc89 cells, Cortactin might be a potential target of PKD in the regulation of F-Actin dynamics.

PKD has also been implicated in the regulation of cell-to-cell adhesion, possibly by the phosphorylation of E-Cadherin itself. As shown in this work, PKD isoforms and kinase-dead mutants influenced Ca^{2+}-dependent cellular adhesion in Panc89 cells in a diverse fashion. PKD2KD and, to lesser extent, PKD1KD, strongly enhanced cell-to-cell adhesion of stable Panc89 cells, whereas E-Cadherin expression in the respective parental cell lines was reduced. At least in the case of PKD2KD cells, aggregation was only partially dependent on E-Cadherin, pointing to the expression of additional Cadherin isoforms. PKD1 also increased cell-to-cell adhesion, yet if this effect is mediated via a phosphorylation of E-Cadherin, remains to be analysed. In the PKD2 expressing cell line, aggregation was very weak, in some assays even resembling the vector control. This phenotype was correlated with processed E-Cadherin fragments in the supernatant of PKD2 expressing cells, which have been implicated in the literature in the inhibition of cell-to-cell adhesion of cancer cell lines, thereby also increasing their invasive potential. Initial results demonstrated that the E-Cadherin fragments from the supernatant of stable PKD2 expressing Panc89 cells were not processed by matrix metalloproteases, but rather by a serine-protease, possibly Plasmin or cationic Trypsin. How the PKD2 isoform is implicated in this process remains to be investigated further. Yet, these findings are in line with data obtained from expression profiling experiments with the respective stable Panc89 cells, indicating that the PLAUR gene (urokinase-like Plasminogen-activator-receptor) is strongly up-regulated in PKD2 expressing cells, triggering the activation of the uPA-Plasminogen-Plasmin-cascade, which has been demonstrated to be involved in the processing of E-Cadherin. The cluster analysis of the expression profiling experiments, using the stable Panc89 cell lines expressing wildtype and kinase-dead PKD1 and 2 variants, also revealed genes generally regulated via PKD kinase activity, independent of the isoform, as well as PKD1/PKD2-specific, differentially regulated genes. An initial cross-referencing with literature data showed interesting candidates, like PLAUR, or SPP1 (Secreted phosphoprotein 1), which is correlated with cancer progression and enhanced cell migration in breast cancer cell lines. These initial results have to be reproduced and verified through independent experimental approaches. Taken together, PKD isoforms seem to be involved in the regulation of cancer related genes, some of which might even be linked to the biological effects characterised during the analysis of PKD function in this work.

During the course of this work novel aspects concerning the role of PKD in cell migration and cellular adhesion of cancer cells were revealed. The localisation of PKD at the F-Actin cytoskeleton and its *in vitro* binding to F-Actin implicate possible functions for the PKD protein family in the regulation of F-Actin dynamics and remodelling processes, which might influence cell adhesion and motility.

3. Introduction

3.1 Activation and functions of PKD

3.1.1 Characterisation of Protein kinase D

The Protein kinase D (PKD) family of serine/threonine kinases consists of 3 structurally related isoforms: PKD1/PKCμ (Valverde et *al.*, 1994; Johannes et *al.*, 1994), PKD2 (Sturany et *al.*, 2001) and PKD3/PKCν (Hayashi et *al.*, 1999). They have been implicated in various cellular functions ranging from Golgi organisation and plasma membrane directed transport to immune response, proliferation, apoptosis, cytoskeletal reorganisation, and metastasis (Rykx et *al.* 2003; VanLint et *al.* 2002). PKD1/PKCμ was first described 1994 as an atypical member of the PKC family (Valverde et *al.*, 1994; Johannes et *al.*, 1994). Due to differences in the catalytic domain that displays very low homology to the conserved kinase domains of PKCs and sequence similarities between PKD and Calcium/Calmodulin-dependent (CAMK) kinase domains, PKDs were classified as a novel subgroup of CAMK (Manning et *al.*, 2002).

3.1.2 Structure, regulation and localisation of PKD

The three isoforms PKD1, 2 and 3 share similar modules. They consist of an N-terminal regulatory domain and a C-terminal kinase domain. While PKD1 and PKD2 posses an apolar alanine/proline-rich region at their N–terminus, in PKD3 this hydrophobic domain is absent. All isoforms contain two cysteine-rich Zn-fingers (CRD) separated by a long linker region. In PKD2 this linker region contains also a serine-rich stretch of amino acids. PKDs possess an acidic region consisting of negatively charged amino acids and a pleckstrin homology domain (PH). These characteristic motifs are also important for the regulation of enzyme activity and localisation within cells. The regulatory domain of PKD1 exerts an inhibitory effect on the kinase activity, since the deletion of this domain leads to its full activation (Vertommen et *al.*, 2000). Likewise, individual regions within this regulatory domain have an inhibitory effect on kinase activity. Mutation or deletion of the PH domain leads to full activation of PKD1 (Iglesias et *al.*, 1998a). PKD1 can also be fully activated when both Zn-fingers are deleted (Iglesias et *al.*, 1999), although the two Zn-fingers are functionally different. CRD1 is a minor phorbol dibutyrate (PDBu) binder but exerts an inhibitory effect on PKD activity. CRD2 binds PDBu with high affinity (Iglesias et *al.*, 1998b), yet it is not essential for the PDBu-induced activation of the kinase. CRD2 is necessary to mediate the PDBu-dependent translocation of PKD1 (Iglesias et *al.*, 1998b, 1999). In the case of PKD2 and PKD3 similar functions for the different sub-domains are predicted, but small variations in the respective sequences can also result in profound regulatory differences.

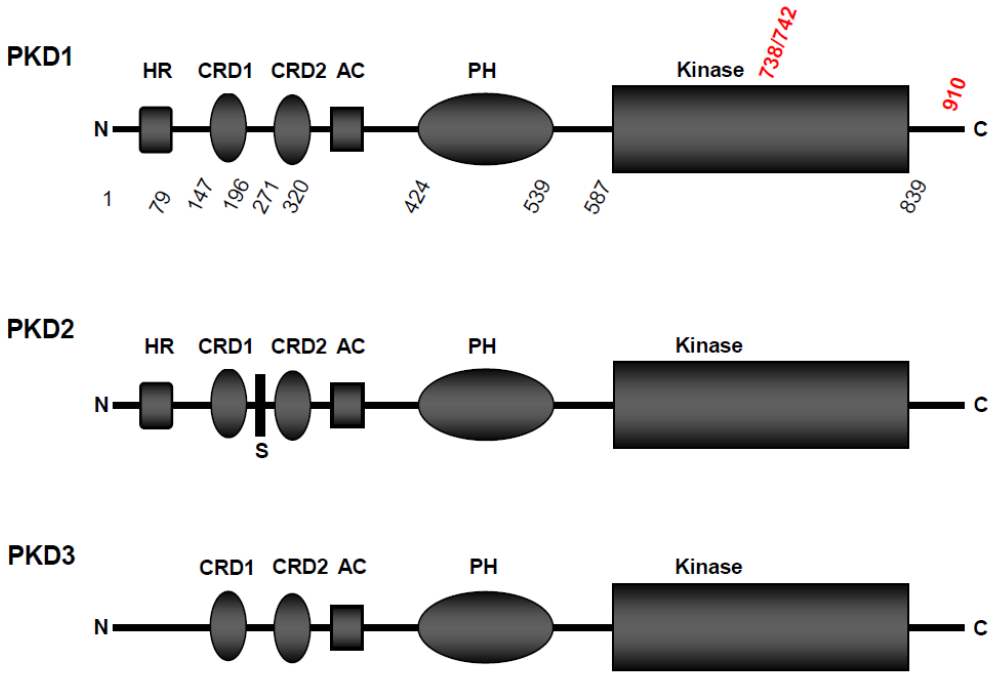

Fig. 1: Molecular architecture of Protein kinase D family members: PKD1, PKD2, PKD3. Abbreviations: HR, hydrophobic region; S, serine-rich domain; CRD1 and 2, cysteine-rich zinc-finger domain 1 and 2; AC, acidic domain; PH, pleckstrin-homology domain; Kinase: kinase catalytic domain. Black coloured numbers indicate amino acid positions in human PKD1, red coloured numbers indicate Ser738/742 activation loop and Ser 910 autophosphorylation sites (modified from Van Lint et *al*., 2002).

3.1.3 PKD activation and protein interaction

Activation of PKD is a complicated process depending on multiple phosphorylation events at different sites thereby regulating its diverse biological functions (Vertommen et *al*., 2000; Waldron et *al.*, 2001; Storz et *al.*, 2003). Up to now, six phosphorylation sites have been identified in PKD1: two sites in the regulatory domain (*mouse*: Ser203; Ser255; *human*: Ser205; Ser249), two in the catalytic domain, the so-called activation loop of the kinase *(mouse*: Ser744; Ser748; *human*: Ser738; Ser742), one at the C-terminus (*mouse*: Ser916; *human*: Ser910) (Rykx et *al.*, 2003; Iglesias et *al.*, 1998b) and a tyrosine phosphorylation site (*human*: Tyr463) in the PH domain of PKD, which is transphosphorylated by Abl in response to oxidative stress and mediates the release of the autoinhibitory PH domain leading to activation of PKD1 (Storz et *al.*, 2003). Ser203 (*human*: Ser205) is an autophosphorylation site located within a region that interacts with 14-3-3τ proteins (Hausser et *al.*, 1999). Ser255 (*human*: Ser249) is a transphosphorylation site targeted by PKC-dependent pathways. The two activation loop serines 744/748 play a crucial role in the activation of PKD1. Substitution of these amino acids with alanine completely inhibits activation of the kinase while substitution to glutamic acid, mimicking phosphorylation, results in a constitutive activation (Iglesias et *al.*, 1998b). Ser916 at the C-terminus is phosphorylated by PKD itself. It is not required for initial activation of the kinase but rather regulates conformation and duration of PKD activation (Matthews et *al.*, 1999b). The exact function and sequence of each phosphorylation event in the activation process of PKD1 remains still to be elucidated and

involvement of different PKC isoforms is very likely to be cell-type dependent. The activation loop serines 744/748 are thought to be phosphorylated by members of the novel PKC family PKCη, PKCε, PKCδ, PKCθ (Waldron and Rozengurt, 2003; Storz et *al.* 2004) although it has also been shown that Ser748 can slowly be autophosphorylated contributing to transphosphorylation of Ser744 by PKCε (Waldron and Rozengurt, 2003). In addition to phosphorylation, PKD can be activated via Caspase-3 mediated cleavage between the acidic domain and the PH domain releasing the catalytic domain of the kinase (Endo et *al.*, 2000). Moreover Gβγ subunits can activate PKD1 *in vitro*, presumably by direct interaction with the PH domain of PKD, since this effect can be abolished by adding free PKD PH domain (Jamora et *al.*, 1999). As for PKD1, PKD2 can also be activated downstream of G-protein coupled receptors (GPCRs), via the activation of PLCγ, which in turn activates PKCα, PKCε or PKCη. In the case of human PKD2 three phosphorylation sites have been identified so far: Ser876 corresponding to Ser910 in PKD1 and Ser706/Ser710 corresponding to the activation loop serines (Sturany et *al.*, 2001, 2002). In human B-cells, PKD3 transphosphorylation of activation loop Ser731/Ser735 was found to be mediated by a DAG-PLC-PKC-dependent pathway. Putative upstream kinases for PKD3 are PKCε, PKCη or PKCθ (Matthews et *al.*, 2003). However, in contrast to PKD1 and PKD2, PKD3 does not possess a C-terminal autophosphorylation site (Rykx et *al.*, 2003).

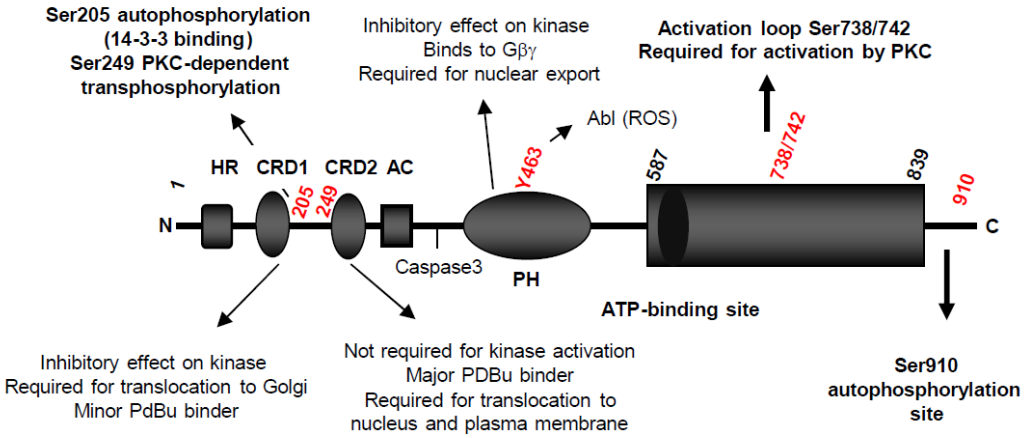

Fig. 2: Structure and its functional implications for human PKD1. The regulatory domain (amino acids 1–586) inhibits kinase activity. The cysteine-rich zinc-fingers CRD1 and CDR2 show different properties in terms of PDBu (phorbol 12, 13-dibutyrate) binding and importance for kinase translocation to the plasma membrane, the Golgi apparatus or the nucleus. The pleckstrin-homology (PH) domain inhibits kinase activity and this is relieved upon binding of Gβγ. The Caspase-3 cleavage site is located between the acidic domain (AC) and the PH domain. PKD1 is phosphorylated at multiple sites. Ser205 and Ser910 are autophosphorylation sites, which regulate 14-3-3 binding (Ser205), and conformation as well as signal duration (Ser910). Ser249 and activation loop Ser738/742 are transphosphorylation sites, which are phosphorylated by a PKC-dependent pathway (modified from Van Lint et *al.*, 2002). The novel phosphorylation of the tyrosine residue Tyr463 in the PH domain by Abl is implicated in the activation of PKD in response to oxidative stress signals (Storz et *al.*, 2003).

3.1.4 Protein interactions, substrates and subcellular localisation

3.1.4.1 Protein interactions

Interactions with other proteins are thought to play a vital role in activation of PKD and in directing it to different intracellular locations, where the kinase exerts its diverse biological functions.

14-3-3τ was suggested to be such a regulator in activation of PKD1. Binding of 14-3-3τ to a phosphoepitope in the regulatory region of PKD1 down-regulates kinase activity, thereby acting as a negative feedback regulator of PKD1 (Hausser et *al.*, 1999). Furthermore the chaperon p32 associates with PKD at mitochondrial membranes and probably inhibits its phosphorylation sterically by binding to the kinase domain of PKD1 (Storz et *al.*, 2000). PKD1 was also found to be associated with the B-cell receptor complex (BCR) and is activated upon cross-linking of the BCR and CD19 on B-cells (Sidorenko et *al.*, 1996). Johannes et *al.* also showed that endogenous PKD1 forms a complex with the tyrosine kinase Btk in SKW 6.4 B-cells via the regulatory CRD1 and the kinase domain (Johannes et *al.*, 1999). Direct interaction of Gβγ subunits with the PH domain activates PKD *in vivo* and inhibition of PKD activity via the addition of free PH domain prevented Gβγ-mediated Golgi breakdown (Jamora et *al.*, 1999). In addition PKD was also shown to form a complex with a Phosphatidylinositol 4-kinase and a Phosphatidylinositol 4-phosphate 5-kinase at the Golgi apparatus. The regulatory region of PKD may also act as a scaffold for enzymes involved in phosphoinositide synthesis at specific membrane locations (Nishikawa et *al.*, 1998).

A number of studies have shown interactions of PKD family members with PKC-subtypes. Storz et *al.* (2004) found PKCδ to be the main upstream kinase of PKD in response to oxidative stress signalling and Tan et *al.* (2003) demonstrated that Thrombin rapidly and transiently induces PKD activation via a PKCδ-dependent pathway in vascular smooth muscle cells. A recent report also demonstrated a complex of PKD and the A-kinase anchoring protein AKAP-Lbc, which has been proposed to be involved in the activation of PKD by recruiting the upstream kinase PKCη and also by coordinating phosphorylation events by protein kinase A (PKA) that release activated PKD of the complex (Carnegie et *al.*, 2004). Uhle et *al.* (2003) copurified PKD with the COP9 signalosome (CSN), a multiprotein complex that mediates phosphorylation of a number of proteins including c-Jun and p53. This phosphorylation was shown to induce the formation of ubiquitin conjugates of c-Jun and p53, resulting in their ubiquitin-dependent degradation and PKD was thought to be recruited to the CSN to regulate this process. Bowden et *al.* placed PKD into a ternary complex with Paxillin and Cortactin in invadopodia, Actin-rich membrane protrusions representing sites of extracellular matrix degradation in invasive cancer cells (Bowden et *al.*, 1999).

3.1.4.2 Substrates

For PKD only a few physiological substrates are known so far. One of the downstream targets of PKD is Kidins220 (Kinase D interacting substrate of 220 kDa), an integral membrane protein selectively expressed in the brain and neuroendocrine cells. Kidins220 was found to be phosphorylated by PKD1 at Ser919 (Iglesias et *al.*, 2000). Hurd et *al.* were

also able to show that c-Jun is a putative substrate of PKD1 and is phosphorylated on sites that are different from those phosphorylated by Jun N-terminal kinase (JNK) (Hurd et *al.*, 2002). The Ras effector Rin1 is phosphorylated by PKD1 at Ser351 causing its dissociation from Ras and subsequent sequestering by 14-3-3 proteins binding to the phosphorylated epitope. In turn, the release of Rin1 from Ras allows its interaction with Raf initiating downstream signalling events (Wang et *al.*, 2002). PKD has also been identified as a mediator of cardiac Troponin I (cTnI) phosphorylation regulating myofilament function. cTnI is phosphorylated on Ser22/23 *in vitro* by PKD reducing myofilament Ca^{2+}-sensitivity (Haworth et *al.*, 2004). During the last two years histone deacetylases (HDACs) were identified as PKD substrates, too. Vega et *al.* showed that PKC and PKD mediate agonist-dependent cardiac hypertrophy through nuclear export of Histone deacetylase 5. Class II histone deacetylases are phosphorylated in response to stress signals, triggering Crm-1 dependent nuclear export of HDACs, thereby suppressing cardiac hypertrophy. The authors demonstrated that PKD, a downstream effector of PKC, directly phosphorylates HDAC5 and stimulates its nuclear export (Vega et *al.*, 2004). Moreover Dequiedt et *al.* reported that phosphorylation of HDAC7 by PKD mediated T-cell receptor-induced Nur77 expression and apoptosis (Dequiedt et *al.*, 2005). Taken together, the phosphorylation of HDACs and regulation of their nuclear export reveals a novel mechanism of coupling extracellular signals via PKD to chromatin modifications and the regulation of gene expression. The transmembrane glycoprotein E-Cadherin, which plays a critical role in cell-to-cell adhesion, has also been proposed to be a substrate of PKD1. Phosphorylation of E-Cadherin is associated with altered cellular aggregation and motility of prostate cancer cells. Overexpression of PKD1 in C4-2 prostate cancer cells increased cellular aggregation and decreased cellular motility (Jaggi et *al.*, 2005). The Phosphatidylinositol 4-kinase IIIβ (PI4KIIIβ), a key player in the structure and function of the Golgi complex has also been identified as a novel physiological substrate of PKD. Phosphorylation of PI4KIIIβ at a highly conserved motif stimulates its lipid kinase activity resulting in enhanced vesicular stomatitis virus G-protein transport to the plasma membrane (Hausser et *al.*, 2005). Recently, advances in the generation of phosphorylation specific antibodies also led to the identification of the human heat shock protein Hsp27 as a *in vivo* substrate of PKD: Doppler et *al.* described the development and use of an antibody directed against the optimum phosphorylation consensus motif of PKD, involving a degenerated phosphopeptide library with fixed residues corresponding to the consensus LXR(Q/K/E/M)(M/L/K/E/Q/A)S*XXXX. Using this so-called pMOTIF-antibody the authors were able to identify Hsp27 as a novel *in vivo* substrate of PKD, phosphorylated at Ser82, as well as to verify Rin1 and HDAC5 as PKD *in vivo* substrates (Doppler et *al.* 2005). Taken together, the use of pMOTIF and other substrate specific antibodies should greatly enhance the ability to find additional physiological PKD substrates in the future.

3.1.4.3 Subcellular localisation of PKD

PKD can be recruited to multiple cellular compartments such as the plasma membrane, the Golgi apparatus or the nucleus via its different regulatory subdomains. In quiescent cells a large fraction of PKD resides in the cytosol, while a smaller fraction can be found at the Golgi (Prestle et *al.*, 1996). PKD is also localised at the mitochondria in some specialised cells (Storz et *al.*, 2000) and can be detected at secretory granules (Matthews et *al.*, 2000a). The two Zn-fingers of PKD1 have different lipid binding specificities (Iglesias et *al.*, 1998) resulting in a different subcellular localisation of PKD. Stimulation of cells with PDBu or mitogenic agonists results in a CRD2 domain mediated translocation of PKD from the cytosol to the plasma membrane, followed by a rapid redistribution to the cytosol, which requires phosphorylation of the PKD activation loop (Rey et *al.*, 2004; Rey et *al.*, 2001b). PKD1 can also shuttle between the nucleus and the cytosol. Accumulation in the nucleus is dependent on the CRD2 domain, while Crm-1 dependent nuclear export is mediated by the PH domain of PKD (Rey et *al.*, 2001a). Binding of PKD to TGN is mediated by the CRD1 domain and is dependent on local DAG production (Maeda et *al.*, 2001; Baron and Malhotra, 2002). Recruitment of PKD to the Golgi compartment was shown to be a two step process. First, PKD1 is constitutively recruited from the cytosol independent of activation loop phosphorylation, subsequently the activation loop of Golgi associated PKD is phosphorylated by a transacting kinase followed by auto-, and transphosphorylation of N-terminal sites in the regulatory domain of PKD, which are thought to provide phosphoepitopes for protein interactions (Hausser et *al.*, 2002). Unlike other PH domain-containing kinases such as PKB/Akt, PKD1 does not need its PH domain for membrane translocation (Matthews et *al.*, 2003; Rey et *al.*, 2001a) or Golgi recruitment (Maeda et *al.*, 2001), nor does it interact with phosphoinositol lipids. To elucidate the relationship between translocation, subcellular localisation and activation of PKD in mediating its different biological functions further detailed investigations are still needed.

3.1.5 Activation of PKD by different signalling pathways

PKD is activated in response to a variety of signals and pathways involving PKC-dependent transphosphorylation, signals transduced via the interaction with $G\beta\gamma$ subunits, as well as caspase-mediated cleavage. The PLC-DAG-PKC mediated activation loop phosphorylation of PKD plays a major role in activation mediated in response to several agents. Treatment of cells with tumour-promoting phorbol esters (Chiu and Rozengurt, 2001), Bryostatin (Matthews et *al.*,1997), neuropeptides e.g. Bombesin, Vasopressin, Bradykinin (Zugaza et *al.*, 1997), oxidative stress (Waldron et *al.*, 2004 Storz et *al.*, 2004), Thrombin (Tan et *al.*, 2003) as well as second messengers like diacylglycerol (DAG) all result in PKD activation. Phospholipase C catalyses the formation of cytosolic phosphatidyl inositol-1,-4,-5-trisphosphate (IP_3) and membrane bound DAG from phosphatidyl inositol-4,5-bisphosphate (PIP_2). IP_3 leads to the release of Ca^{2+} from intracellular storages thereby contributing to Ca^{2+}-mediated PKC activation, while binding of DAG directly activates PKC isozymes via the release of the inhibitory pseudosubstrate domain from the active site (Newton, 2002).

Moreover, PKD1 is also targeted to the plasma membrane by its CRD1 region in response to DAG production and is phosphorylated by membrane bound PKCs at the activation loop (Zugaza et *al.*, 1996, 1997; Waldron et *al.*, 2001). This phosphorylation event is thought to relieve the autoinhibition exerted by the PH domain and thereby lead to the activation of PKD (Waldron and Rozengurt, 2003). A number of signals are known to induce DAG production through receptor-mediated activation of PLCβ or γ, e.g. receptor tyrosine kinases such as PDGF (Van Lint et *al.*, 2002; Stafford et *al.*, 2003), ligation of T-and B-cell receptors (Sidorenko et *al.*, 1996; Matthews et *al.*, 2003), antigen triggering of the high affinity IgE receptor (FcεR1) on mast cells (Matthews et *al.*, 2000), and lysophosphatidic acid (LPA) (Paolucci et *al.*, 2000). Binding of Gastrin to its receptor triggers the heterotrimeric Gαq protein, which in turn activates PLC. DAG formation then leads to the activation of PKCs α, ε and η, in turn inducing the activation of PKD2 (Sturany et *al.*, 2002). Production of DAG at the plasma membrane in response to GPCR signals also results in a recruitment of PKD1 from the cytosol to the plasma membrane via the PKD CRD1 domain. PKD1 is then activated through phosphorylation at the activation loop by PKCs, but instead of rapid dissociation from the membrane, catalytically active PKD1 can bind to activated Gαq-subunits via its CRD2 domain and remain at the membrane for hours. This mechanism allows the translation of a transient DAG signal triggered by a short-term hormonal stimulus into a long-term cellular response (Oancea et *al.*, 2003). Furthermore, it has been described that in the course of apoptosis induction by TNFα or genotoxic agents the activation of Caspase-3 leads to cleavage of PKD, resulting in the release and activation of the catalytic domain (Johannes et *al.*, 1998; Endo et *al.*, 2000), yet the role of PKD in the apoptotic pathway still remains to be elucidated. G$\beta\gamma$ subunits of heterotrimeric G-proteins are able to activate PKD1 independently of PKC via the interaction with its PH domain. At the Golgi apparatus, this interaction is involved in the organisation of Golgi stacks and protein secretion (Jamora et *al.*, 1999). Furthermore the ATP-gated Ca-channel P2X7 (Bradford and Soltoff, 2002) mediates activation of PKD downstream of PKC. Recently, another PKC independent mechanism for PKD activation has been reported during osteoblast differentiation. Bone morphogenetic protein 2 (BMP-2) induces activation of mitogen-activated protein kinases JNK and p38 via a selective Ser916 phosphorylation and activation of PKD (Lemonnier et *al.*, 2004).

3.1.6 Biological functions of PKD

Van Lint et *al.* proposed a model for the regulation of different cellular functions by PKD1, whereby it is targeted to different intracellular destinations to recruit different proteins into multiprotein complexes. PKD1 targeted to the plasma membrane functions as a regulator of signals by immune receptors and growth factors and is likely to be involved in regulation of cell shape and tumour cell invasion. PKD targeted to the Golgi regulates vesicular traffic to the plasma membrane. PKD in the nucleus could perhaps contribute to its role in potentiating DNA synthesis and cell proliferation as well as PKD1-induced gene expression of anti-apoptotic genes (Van Lint et *al.*, 2002).

3.1.6.1 Golgi organisation and vesicular transport

An important function of PKD appears the regulation of Golgi organisation and protein transport en route to the plasma membrane. The Golgi apparatus is a key component of the secretory pathway involved in protein sorting. It consists of stacks of cisternae and is located in the perinuclear region of mammalian cells. PKD was found to bind to the trans-Golgi network (TGN) via DAG. The TGN represents the outermost cisternae of the Golgi stack from which vesicles are released by fission destined to the cell surface, lysosomes and the secretory pathway (Glick and Malhotra, 1998). The interaction of PKD with DAG at the TGN is mediated via its CRD1 domain (Prestle et *al.*, 1996; Maeda et *al.*, 2001; Baron and Malhotra, 2002). Activation of PKD at the TGN occurs through the interaction with Gβγ subunits of G-proteins (Jamora et *al.*, 1999). The function of PKD in the vesiculation process at the Golgi is not well understood. Ilimaquinone, a marine sponge metabolite can be used to hyperstimulate PKD resulting in an inappropriate elevation of Golgi-derived vesicle formation (Jamora et *al.*, 1997). Furthermore Iglesias et *al.* showed that a kinase-dead PKD1 acts dominant-negative (Iglesias et *al.*, 1998b) and that this mutant localises to the TGN causing an extensive Golgi-tubulation. These tubes are thought to contain proteins destined for the plasma membrane, yet they do not detach from the TGN (Lijedahl et *al.*, 2001). Corroborating, the results indicate that PKD1 somehow regulates the fission of vesicles from the TGN targeted to the plasma membrane. A very recent report of Diaz et *al.* (2005) identified G protein subunits beta1gamma2 and beta3gamma2 to be responsible for the activation of PKD via the Golgi apparatus-associated PKCη. They were able to show that compromising the kinase activity of PKCη also inhibited protein transport from the TGN to the cell surface and that constitutively active PKCη caused Golgi fragmentation, which was inhibited by a kinase-inactive form of PKD. According to a model presented by Bankaitas, recruitment of effector proteins to TGN-bound PKD (e.g. PI-4-P 5 kinase, PI-4 kinase, 14-3-3 proteins) leads to the formation of a vesicle budding machinery that deforms TGN membranes into short tubules. Moreover, this machine is thought to support the fission process by mediating the conversion of DAG into the lipid phosphatidic acid (Nishikawa et *al.*, 1998; Bankaitis, 2002). A novel interlink between PKD and lipid kinases has also been demonstrated by the *in vivo* phosphorylation of PI4KIIIβ through PKD1 and PKD2. This PKD-mediated phosphorylation stimulates PI4KIIIβ lipid kinase activity and enhanced vesicular stomatitis virus G-protein transport to the plasma membrane. The identification of PI4KIIIβ as one of the PKD substrates at the TGN should help to reveal the molecular events that enable transport-carrier formation (Hausser et *al.*, 2005). Recently, Yeaman and colleges reported also that the PKD isoforms possess different specificities in regulating protein trafficking from the TGN in polarised MDCK cells and non-polarised HeLa cells. They found that kinase-dead mutants of PKD1 and PKD2 lead to accumulation of cell surface destined cargo within TGN tubules in non-polarised HeLa cells and had no effect on other transport pathways. Investigating polar traffic in MDCK cells they were able to show that PKD1 and PKD2 are not required for apical transport, but overexpression of kinase-dead isoforms led to apical missorting of a basolateral destined exocytosis marker, possibly by the inhibition of a basolateral transport pathway. Yeaman et *al.* also elucidated different functions for PKD1

and PKD2 in polarised MDCK cells, since only expression of kinase-dead PKD1 led to an accumulation of the exocyst component Sec6 at the TGN. The exocyst is an octameric complex of proteins contributing to the final stages of vesicle delivery from the TGN to the basolateral membrane in polarised MDCK cells (Yeaman et *al.*, 2004b). Overexpression of kinase-dead PKD3 was not found to effect apical or basolateral transport. In conclusion the authors propose that apical transport is PKD-independent and that for basolateral transport PKD is required, yet each PKD isoform shows a distinct effect on cargo transport from the TGN (Yeaman et *al.*, 2004a).

3.1.6.2 Immune response

PKD1 activation after BCR cross-linking depends on Syk and PLCγ activity and is regulated by the Btk tyrosine kinase. Therefore PKD1 was proposed to function in a negative feedback loop on the BCR by reducing the ability of Syk to phosphorylate PLCγ. Data from Matthews et *al.* (2003) also indicated an abundant expression of PKD3 in B-cells and activation upon BCR engagement. PKD was also shown to be activated by Fcγ-receptor stimulation on neutrophils (Davidson-Monacada et *al.*, 2002). Results of Marklund et *al.* suggest a role for PKD in early T-cell development. They found that modification of intracellular localisation of PKD influences T-cell-receptor (TCR) rearrangement, T-cell maturation and selection in a cell context dependent manner (Marklund et *al.*, 2003)

3.1.6.3 Cell proliferation and differentiation

PKD1 is thought to have an important role in proliferation and differentiation. Several reports indicated a participation of PKD1 in the mitogen-activated Erk and JNK pathways (Hausser et *al.*, 2001; Brändlin et *al.*, 2002a/b). In this respect PKD was reported to phosphorylate Rin (Wang et *al.*, 2002). Following phosphorylation of Rin by PKD1, Rin is thought to interact with 14-3-3 via a phosphoepitope around the PKD phosphorylation site, thereby releasing its interaction with Ras, in turn allowing a more efficient Ras-Raf interaction and Erk activation. Studies have also indicated an inhibitory effect of PKD1 on the c-Jun-N-terminal kinase (JNK) signalling pathway. Overexpression of PKD1 prevents the epidermal growth factor (EGF) from signalling to JNK (Bagowski et *al.*, 1999). This inhibitory effect requires phosphorylation of the EGF receptor on two sites that are required for negative regulation of the EGF receptor by PDGF. It is not known whether these sites are phosphorylated directly by PKD1, but there seems to be an important link in the down-regulation of EGF by PDGF signalling. Furthermore PKD1 physically interacts with JNK inhibiting phosphorylation of c-Jun and it also phosphorylates c-Jun itself at sites different from those phosphorylated by JNK (Hurd and Rozengurt, 2001; Hurd et *al.*, 2002). Rennecke et *al.* showed a correlation between PKD1 expression and keratinocyte proliferation, since PKD1 is highly expressed in basal dividing cells, while differentiating cells exhibit a low expression level. Moreover, NIH3T3 fibroblasts overexpressing PKD1 show enhanced proliferation, corroborating increased PKD1 expression in mouse skin carcinomas (Rennecke et *al.*, 1999). An independent study confirmed that overexpression of PKD1 in NIH3T3 fibroblasts causes a potentiation of DNA synthesis and cell proliferation in response to G protein-coupled receptor

agonists Bombesin and Vasopressin as well as phorbol esters (Zhukova et *al.*, 2001). Recently, it has been reported that this effect is due to an increase in the duration of Erk signals through PKD1 (Sinnett-Smith et *al.*, 2004). Further, studying osteoblasts, Lemonier et *al.* found PKD to be involved in stimulation of JNK and p38 signalling in response to BMP2, which is required for optimal cell differentiation.

3.1.6.4 Regulation of apoptosis and cell survival

Overexpression of PKD1 in murine and human cell lines caused a reduced sensitivity to TNF-mediated apoptosis correlating with enhanced NFκB-dependent gene expression, e.g. cIAP2 (inhibitor of apoptosis protein) and TRAF1 (TNF-receptor-associated protein 1) (Johannes et *al.*, 1998). Treatment of lymphoma cells with TNF, chemotherapeutic agents or γ-radiation results in the caspase-mediated cleavage of PKD1 releasing the catalytic fragment of PKD. This sensitises cells to the apoptosis-inducing effect of the genotoxic agents (Haussermann et *al.*, 1999; Endo et *al.*, 2000). Trauzold et *al.* reported that PKD1 expression strongly correlated with resistance to CD95-(Fas) mediated apoptosis in pancreatic ductal adenocarcinoma cells. They were able to demonstrate an up-regulation of the anti-apoptotic proteins c-$FLIP_L$ and Survivin in PKD overexpressing Colo357 cells. Immunohistochemical analysis of pancreatic cancer tissue of 48 patients and 10 normal tissue controls also revealed a marked overexpression of PKD1 in tumours pointing to important function of PKD *in vivo*. In addition, PKD overexpression led to enhanced cellular growth and to a significant increase in telomerase activity. Therefore PKD is thought to play an important role in acquiring the malignant phenotype of pancreatic tumours (Trauzold et *al.*, 2003). Additional functions of PKD1 in cellular survival are induced in response to oxidative stress. Treatment of cells with reactive oxygen species (ROS) leads to the activation of PKD1 in a coordinated two step process. First, Abl phosphorylates Tyr463 in the PH domain of PKD1 promoting a second phosphorylation step whereby PKCδ phosphorylates the activation loop of PKD resulting in a synergistic PKD1 activation and subsequent NFκB induction. The activation of both kinases, Abl and PKCδ, in this process is mediated by Src. The PKD-mediated induction of NFκB then induces protective genes and leads to cell survival (Storz et *al.*, 2003, 2004).

3.1.6.5 Regulation of cell shape, adhesion, motility and invasion

There are several studies involving PKD1 in cell shape regulation, cell motility, and adhesion, as well as cancer cell invasion. Bowden et *al.* found PKD1 to form a complex with the Actin-binding protein Cortactin and the focal adhesion protein Paxillin in invadopodia of breast cancer cells. Invadopodia are Actin-rich membrane protrusions extending into the extracellular matrix. They are involved in proteolytic matrix degradation thus being correlated with enhanced invasive potential of cancer cells. Since Cortactin has a role in cell motility and cellular invasion, the authors suggested that this function might be modulated by Paxillin and PKD1 in the above mentioned complex. Interestingly this complex is absent in non-invasive cells (Bowden et *al.*, 1999). Kidins220, the first physiological substrate of PKD1, localises at neurite tips and growth cones of PC12 pheochromocytoma cells (Iglesias et *al.*,

2000) as well as in motile immature dendritic cells. There, Kidins220 is localised to a raft compartment on the poles or membrane protrusions at the leading edge. Immature dendritic cells migrate onto an extracellular matrix changing their shape cyclically from a highly polarised morphology to a symmetrical shape (Riol-Blanco et *al.*, 2004) supporting a role for PKD1 in cytoskeletal reorganisation and cell shape modulation. Locomoting cells exhibit a constant retrograde flow of membrane proteins from the leading edge of the lamellipodia backwards, which when coupled to substrate adhesion might drive forward movement of the cell. Prigozhina et *al.* reported that a kinase-dead, dominant-negative mutant of PKD1 specifically blocks budding of secretory vesicles from the TGN to the plasma membrane in NIH3T3 fibroblasts thereby inhibiting cell motility and retrograde flow of surface markers as wells as filamentous Actin. Inhibition of PKD elsewhere in the cell neither blocked anterograde membrane transport nor cell motile functions (Prigozhina et *al.*, 2004). Jaggi et *al.* reported that phosphorylation of the transmembrane glycoprotein E-Cadherin, which plays a critical role in cell-to-cell adhesion is associated with altered cellular aggregation and motility of prostate cancer cells. Jaggi and colleagues demonstrated a colocalisation of PKD and E-Cadherin at cell junctions in LNCaP prostate cancer cells as well as a coimmunoprecipitation of both proteins from lysates. PKD phosphorylated E-Cadherin *in vitro* and inhibition of PKD1 activity using the Gö6976 inhibitor in LNCaP cell resulted in decreased cellular aggregation, whereas overexpression of PKD1 in C4-2 prostate cancer cells increased cellular aggregation and decreased cellular motility (Jaggi et *al.*, 2005). Taken together PKD seems to play important roles in cell shape modulation and motility, nevertheless its exact function and interaction partners need to be investigated further. There were also differences in the effects of PKD1 on cell motility with Prigozhina et *al.* reporting PKD1KD having an inhibitory effect on cell migration in fibroblasts while Jaggi et *al.* show active PKD1 to inhibit cell motility in C4-2 prostate cancer cells. Whether these differences represent cell type-dependent effects, or are dependent on the assays used to quantify cell motility e.g. random 2D cell motility in the case of Prigozhina et *al.* versus cell migration through Transwell filters, i.e. in a 3D space, is an important question that needs to be answered.

3.2 Cell motility and dynamic regulation of the Actin cytoskeleton

The dynamic regulation of the Actin cytoskeleton plays a vital role in a variety of cellular events like adhesion, division, spreading and motility (Mitchison and Cramer, 1996). Cell migration is a highly regulated multistep process orchestrating morphogenesis, tissue regeneration and disease progression e.g. mental retardation, artherosclerosis, and tumour metastasis. Dynamic Actin is important in remodelling of the plasma membrane, e.g. lamellipodia. These are thin, sheet-like protrusive structures at the leading edge of migrating cells and consist of a lattice-like meshwork of Actin filaments. Membrane ruffles are closely related structures, which form on the dorsal surface of cells when nonadherent lamellipodia fold back over the dorsal surface. In contrast, filopodia are thin, cylindrical projections consisting of cross-linked, bundled Actin filaments. The formation of these structures at the leading edge of cells together with the coordinated retraction of the tail-end are fundamental to cell motility (Lauffenburger and Horwitz, 1996; Ridley, 2001; Daly, 2004). A migrating cell

is highly polarised with complex regulatory pathways that spatially and temporally integrate different processes (Ridley et *al.*, 2003). The major force driving cell motility is Actin polymerisation extending the leading edge of a migrating cell (Tilney et *al.*, 1981, 1983; Zigmond, 1993). Like migrating cells, Actin filaments are also polarised. They consist of a rapidly growing so-called barbed end and a slow growing pointed end. The designation barbed end is based on the arrowhead pattern generated when Myosin binds to the fast growing end of the Actin filaments. The movement of the leading edge depends on elongation of filaments at their fast-growing barbed ends, organisation of filaments into mechanically stable networks, and regulated depolymerisation of filaments (Cooper et *al.*, 1983; Tobacman and Korn, 1983; Frieden, 1983). The engagement of cell surface growth factors and adhesion receptors thereby influences the assembly and arrangement of F-Actin networks (Zigmond, 1996; Schoenwaelder and Burridge, 1999).

3.2.1 F-Actin and monomer binding proteins

Since the elongation of an Actin filament is a bimolecular reaction between monomers and filament ends, it can be regulated by controlling the ability of either monomers or filaments participating in the reaction. Applying physiological conditions, the massive pool of monomeric Actin bound to Mg^{2+}-ATP (Rosenblatt et *al.*, 1995) would instantly polymerise, considering a critical concentration for polymerisation (Kd) of 0.1 µM at the barbed end and 0.6 µM at pointed ends of Actin filaments. Therefore two groups of proteins evolved controlling the polymerisation reaction: capping proteins like CapZ (in muscle cells) or Gelsolin act in micromolar concentrations and with a high affinity (Kd = 0.1nM) to cap most of the free barbed ends (Schafer et *al.*, 1996) preventing the addition of monomers to the growing ends of Actin filaments. The second group, monomer-binding proteins, modify the properties of the monomeric G-Actin. The two main monomer-binding proteins in vertebrates are Profilin and Thymosin-β4 (Safer and Nachmias, 1994). The vertebrate Thymosin-β4 is a very effective sequestering protein which binds about 50 fold stronger to ATP-Actin than to ADP-Actin (Carlier et *al.*, 1993; Pantaloni et *al.*, 1993; Vinson et *al.*, 1998). Actin bound to Thymosin-β4 does not polymerise (Carlier et *al.*, 1993; Goldschmidt-Clermont et *al.*, 1992), thus Profilin is thought to compete for the binding to ATP-Actin, shuttling G-Actin away from Thymosin towards the fast growing barbed end of Actin filaments (Pantaloni et *al.*, 1993; Pollard et *al.*, 1984). In combination, both machineries guarantee a metastable state with a huge pool of unpolymerised Actin ready for rapid filament growth, when free barbed ends are produced (Pollard et *al.*, 2000).

Actin polymerisation can be initiated either by the uncapping of F-Actin, by severing of filaments to create new barbed ends or by *de novo* nucleation involving the Actin-related Arp2/3 complex (Pollard et *al.*, 2000). Uncapping involves the interaction of capping proteins, e.g. Gelsolin and CapZ, with polyphosphoinositides (PIP_2) (Janmey, 1994; Schafer et *al.*, 1996). The Actin depolymerising factors ADF/Cofilins are both involved in severing of filaments as well as Actin depolymerisation (Bamburg et *al.*, 1999; Carlier et *al.*, 1999). In mammals, there are three different isoforms: Cofilin-1, Cofilin-2, and ADF (Bamburg et *al.*, 1999).

3.2.2 Regulation of Actin polymerisation in cortical Actin networks

Transmission of extracellular signals to the Actin cytoskeleton is directed by small GTPases of the Rho family, as well as by a variety of Actin-binding proteins (Ayscough, 1998; Hall, 1998). The small GTPases Cdc42 and Rac govern vital steps in the formation and organisation of cortical Actin networks in mammalian cells (Weed et *al.*, 2000). Treatment of cells with agents that increase GTP-bound Cdc42 stimulate filopodia formation (Kozma et *al.*, 1995), whereas activation of Rac induces membrane ruffles and lamellipodia formation (Ridley et *al.*, 1992). Both, EGF stimulation (Chan et *al.*, 1998) or activated Rac (Machesky and Hall, 1997) induce the formation of cortical Actin networks and require *de novo* formation of Actin filaments, indicating that Cdc42 and Rac are important factors in the integration of signals resulting in Actin polymerisation. In addition, the activation of Rac is closely coupled to activation of Cdc42 (Nobes and Hall, 1995). This allows the coordinated formation of filopodia and lamellipodia, often noticed jointly at the leading edge of motile cells (Rinnerthaler et *al.*, 1988). Cortical Actin polymerisation initiated by Cdc42 and Rac requires the presence of members of the Wiskott-Aldrich syndrome protein (WASp) superfamily (Bi and Zigmond, 1999). Binding of activated Cdc42 to N-WASp induces filopodia (Miki et al., 1998a), whereas Rac-induced membrane ruffling utilises the structurally related Scar1/WAVE (Machesky and Insall, 1998; Miki et *al.*, 1998b).
Since formation of new Actin filaments from pure Actin monomers is unfavourable, cells need a molecular apparatus to drive *de novo* Actin nucleation. This function is provided by the Arp2/3 complex.

3.2.3 The Arp2/3 complex

The Arp2/3 complexes consist of seven subunits, the two Actin-related proteins Arp2, Arp3 and five other proteins designated p40-, p35-, p19-, p18-, and p14-Arc (ARPC1–5) (Machesky and Gould, 1999). It is abundant (Kelleher et *al.*, 1995), essential (Schwob et *al.*, 1992) and conserved (Welch et *al.*, 1997) across eukaryotic phyla. In isolation the Arp2/3 complex has very low Actin-nucleating activity, yet this can be enhanced by binding of specific nucleation promoting factors (NPFs). *In vitro* the Arp2/3 complex also attaches the slowly growing pointed end of pre-existing Actin filaments to the side of other filaments creating characteristically 70° branched Actin networks, a process termed “dendritic nucleation” model of cortical Actin assembly (Mullins et *al.*, 1998). This coupling between nucleation and branching defines the morphology of the leading edge in cells. As predicted by the model, the Arp2/3 complex locates to branch points of Actin networks in lamellipodia (Svitkina and Borisy, 1999), and is localised to sites of dynamic Actin assembly and motility in living cells (Schafer et *al.*, 1998).

3.2.4 Integration of signals to the Arp2/3 complex

External stimuli driving the assembly of cortical Actin networks act via extracellular receptors and multiple connected signalling pathways, several of which converge on WASp/Scar family proteins to the Arp2/3 complex, acting as NPFs. The WASp proteins integrate a number of

diverse signals, including those transmitted by the Rho family GTPases, Rac and Cdc42 (Machesky et *al.*, 1999). The Wiskott-Aldrich protein family in mammals is comprised of 5 members: WASp is the protein defective in the Wiskott-Aldrich syndrome, a human X-linked genetic disorder with deficiencies in the Actin cytoskeleton of platelets and leukocytes (Ochs, 1998). N-WASp (neural-WASp) exhibits a much broader expression pattern with expression in the brain and many other tissues and finally Scar/WAVE 1-3 (Suetsugu et *al.*, 1999). WASp/Scar proteins share similar molecular features like C-terminal WH2 (WASp homology domain 2, W) motifs, a central proline-rich region (C) followed by an acidic domain (A), but differ in the N-terminal third of the protein. The WH2 domain, originally discovered in Verprolin (Vaduva et *al.*, 1997), binds monomeric Actin and is found in many proteins that regulate Actin (Paunola et *al.*, 2002). The C and A sequences of WASp proteins bind to and activate the Arp2/3 complex. Both, the WH2- and the CA-terminal module are required for efficient activation of the Arp2/3 complex and together they are sufficient (Pollard et *al.*, 2000; Machesky et *al.*, 1998, 1999). This minimal C-terminal activation module is henceforth termed WCA-domain in this work. The N-termini of WASp-family proteins are more divergent among family members, but each possesses a proline-rich stretch (P) adjacent to the WCA domain that acts as a binding site for various SH3 domain containing proteins, like Nck and Grb2. Nck and Grb2 possess Src homology 2 (SH2) domains that associate directly with activated tyrosine kinase receptors by binding to specific phosphotyrosine containing motifs (Buday et *al.*,1999), thereby providing a link between ligand engagement of tyrosine kinase receptors and activation of Arp2/3-mediated Actin assembly. WASp and N-WASp, but not the Scars, possess a Cdc42 and Rac interactive binding domain (CRIB, GTPase binding domain, GB) (Higgs et *al.*, 2000, Rohatgi et *al.*, 2000). They also posses N-terminal WH1 domains, which are folded like PH domains and are involved in binding of proline-rich domains (Fedorov et *al.*, 1999; Prehoda et *al.*, 1999). Adjacent to the GB domain, WASp and N-WASp have a basic stretch of amino acids (B) which is bound by the phospholipid PIP_2 (Prehoda et *al.*, 2000), resulting in a potentiation of WASp activation. When not activated, N-WASp and WASp exist in an autoinhibited state, in which the C-domain interacts with the GB domain (Miki et *al.*, 1998a, Kim et *al.*, 2000). When in the autoinhibited conformation, WASp and N-WASp are unable to induce activation of the Arp2/3 complex, since the WCA domain cannot interact fully with the Arp2/3 complex (Panchal et *al.*, 2003). Binding of activator proteins to proline-rich sequences or of GTP-Cdc42 to the GB domain (Aspenstrom et *al.*, 1996) destabilises the autoinhibitory conformation, allowing full binding of the WCA domain to Arp2/3 (Kim et *al.*, 2000, Rohatgi et *al.*, 2001). The Scar proteins do not possess a GB domain and do not form an autoinhibited state (Machesky et *al.*, 1998).

3.2.5 The cortical Actin-binding protein Cortactin

Apart from the Arp2/3 complex, several other Actin-binding proteins are selectively recruited to cortical Actin structures upon activation of Cdc42 or Rac (Kobayashi et *al.*, 1998; Mishima and Nishida, 1999; Kessels et *al.*, 2000), such as the Src kinase substrate and PKD1 interaction partner Cortactin (Wu et *al.*, 1991; Bowden et *al.*, 1999), which is enriched within lamellipodia (Wu and Parsons, 1993). The localisation of Cortactin in membrane ruffles and lamellipodia is controlled by activation of Rac (Weed et *al.*, 1998). Cortactin possesses a multidomain structure consisting of an acidic domain at the amino-terminus (NTA), followed by 6½ 37–amino acid tandem repeats, a helical region (H), a proline-rich segment (P), and a SH3 domain located at the carboxyl-terminus (Wu et *al.*, 1991). Direct binding to F-Actin is mediated via sequences within the tandem repeat region (Wu and Parsons, 1993), with the fourth repeat being indispensable for binding (Weed et *al.*, 2000), while a DDW motif in the NTA region mediates binding to the Arp2/3 complex (Uruno et *al.*, 2001). The SH3 domain interacts with several postsynaptic density (PDZ) domain–containing proteins like ZO-1, a protein involved in the organisation of transmembrane protein complexes in tight junction (Katsube at *al.*, 1998), CortBP1 (Du et *al.*, 1998), SHANK3 (Naisbitt et *al.*, 1999) and an unrelated protein CBP-90 (Ohoka and Takai, 1998). Cortactin function and activity is regulated by protein interactions, as shown for the WASP-interacting protein WIP (Kinley et *al.*, 2003), which enhances the NPF activity, and by phosphorylation (Daly, 2004). Tyrosine phosphorylation of Cortactin is observed in response to multiple cellular events, including v-Src transformation (Wu et *al.*, 1991), growth factor treatment (Maa et *al.*, 1992; Zhan et *al.*, 1993), bacterial invasion (Dehio et *al.*, 1995; Fawaz et *al.*, 1997), osmotic stress (Kapus et *al.*, 1999), and Integrin or Syndecan-3 ligation with the extracellular matrix (Vuori and Ruoslahti, 1995; Kinnunen et *al.*, 1998). The ability of Cortactin to promote migration of human endothelial cells is dependent on Src-mediated tyrosine phosphorylation (Huang et *al.*, 1998). Cortactin was shown to reduce the time to reach a steady state of Actin polymerisation and also to enhance the rate of polymerisation itself, but only when instead of 10 nM of Arp2/3 complex, a 10 fold higher concentration (100 nM) was used in Actin polymerisation assays (Uruno et *al.*, 2001; Weaver et *al.*, 2001). Although these effects were relatively weak, when compared with the WCA fragment of N-WASp, Cortactin was able to further enhance WCA-stimulated Actin polymerisation. Weaver et *al.* (2001) also reported a synergistic effect on the formation of new Actin barbed ends. Unlike WASp/Scar proteins, the NPF activity of Cortactin is not inhibited by intra- or intermolecular interactions. In addition, Cortactin also increased Actin filament branching in the presence of Arp2/3 complex, and WCA and Cortactin enhanced this process in a synergistic manner. Stimulation of Actin polymerisation by Cortactin required both the NTA domain as well as the repeat regions required for binding the Arp2/3 complex and F-Actin, respectively (Daly, 2004). Chemical cross-linking studies also revealed that the NTA region of Cortactin interacts with Arp3, while N-WASp WCA associates with Arp3, Arp2 and ARPC1, and that a ternary complex consisting of Arp2/3-WCA-NTA could form (Weaver et *al.*, 2002). Another study led to a model in which Cortactin acquires a higher affinity for Arp2/3 by interacting with both Arp2/3 and F-Actin at a branching site, arguing for a sequential binding of N-WASp and Cortactin to

the Arp2/3 complex (Uruno et *al.*, 2003), since Cortactin was able to displace recombinant N-WASp WCA from the Arp2/3 complex, but only when the assay was performed in the presence of Actin polymerisation. Corroborating data from other reports, showing distinct localisations of N-WASp and Cortactin in the Actin comet tails induced by intracellular pathogens (Uruno et *al.*, 2003; Zettl et *al.*, 2001), favour the model of sequential interaction with the Arp2/3 complex. Cortactin and its associated proteins perform several functions at the cell cortex, relating to remodelling of the plasma membrane and the underlying Actin cytoskeleton. A role of Cortactin in lamellipodia and ruffles is presumably to enhance the formation of branched Actin networks via the Arp2/3 complex and/or to stabilise those formed by the activity of the Rac-stimulated NPF, Scar. However, Cortactin also recruits specific binding proteins to cortical regions of the cell via its SH3 domain (Daly, 2004). Among its diverse physiological roles, Cortactin has also functions in association with transmembrane complexes such as tight junctions (Wu and Montone, 1998) and cell-to-cell adherens junctions formed upon homophilic E-Cadherin interaction. In MDCK cell monolayers Cortactin was shown to localise to E-Cadherin based cell contacts, and Cortactin is also recruited to the extending outer margins of Cadherin-based lamellipodia (Helwani et *al.*, 2004). Moreover, inhibition of Cortactin function reduced Cadherin-based lamellipodia formation, altered cell morphology and prevented accumulation of E-Cadherin and β-Catenin at cell-cell contacts (Daly, 2004).

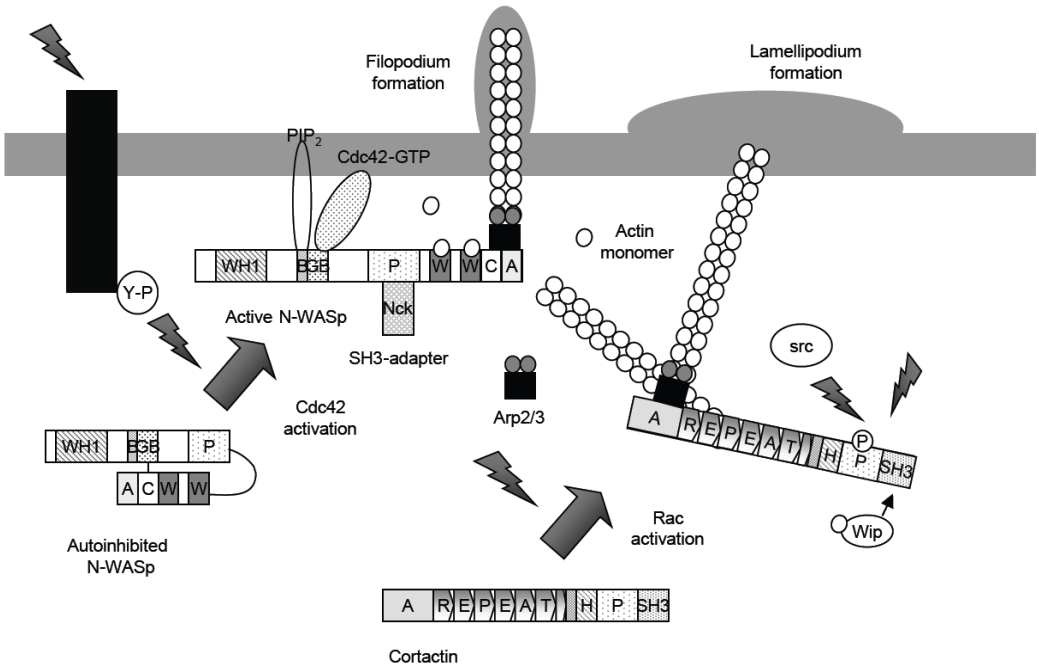

Fig. 3: Comparison of N-WASp and Cortactin regulation in response to growth factor receptor activation: Upon receptor activation, the auto-inhibited conformation of N-WASp is released by binding of Cdc42–GTP and PIP_2 to the GTPase binding (GB) and basic regions (B) respectively, resulting in Arp2/3 complex activation and Actin filament nucleation. Binding of specific SH3 domain-containing adaptor proteins (e.g. Grb2, Nck) can further stimulate NPF activity. In contrast, Cortactin is not auto-inhibited in the basal state. It is translocated to the cell periphery in a Rac-dependent manner upon growth factor stimulation, where it functions as coactivator of the Arp2/3 complex in concert with other NPFs, or to stabilise Actin branch points formed following *de novo* nucleation of filaments. The activity of Cortactin towards the Arp2/3 complex can be modulated by binding of SH3 adaptors. E.g. WIP can enhance NPF activity by inducing dimerisation of Cortactin, or by providing Actin monomers respectively. Phosphorylation of Cortactin on tyrosine and/or serine/threonine residues can induce conformational changes and regulate intermolecular interactions. In the case of the tyrosine phosphorylation, this may inhibit F-Actin binding or cross-linking, and hence the rigidity or turnover of Actin networks (adapted from Daly, 2004).

Considering the involvement of PKD and Cortactin in cell motility, cell adhesion and Actin cytoskeleton remodelling, as well as their mutual interactions, numerous questions emerge that need to be answered and which might help in elucidating the function of PKD in the regulation of cell migration and invasion of cancer cells, including pancreas ductal adenocarcinoma cells (PDAC), which will be used in this study.

3.3 Introduction in PDAC cell lines

The pancreas ductal adenocarcinoma (PDAC) is a common malignancy and probably the most aggressive form of cancer known to date, with the lowest overall 5-year survival rate (Grutzmann et *al.*, 2005; Jemal et *al.*, 2003). There is no effective therapy, apart from surgery and even resected patients mostly die within 1 year.
As it is the case for most studies on cell biology and genetics of other cancers cells, investigation of pancreatic ductal adenocarcinomas also relies on a number of commonly available cell lines, previously established from tumour samples of patients.

Cell line	Source of tumour cells	Histology and grade of primary tumour (WHO grading)	Histology and grade of transplanted tumour (in nude or SCID mice)	Principal investigator
Capan1	Liver metastasis	PDAC, G1	G1 Kyriazis et *al.*, 1998	J. Fogh (USA) Fogh et *al.*, 1977
Colo357	Lymphnode metastasis	PDAC, G1-G2	G2/G3 (focally G1 and adenosquamous components) Meitner et *al.*, 1983	R. Morgan (USA) Morgan et *al.*, 1980
Panc1	Primary tumour	PDAC, G3	G3 Lieber et *al.*, 1975	M. Lieber (USA) Lieber et *al.*, 1975
Panc89	Lymphnode metastasis	PDAC, G2	G2/G3 Okabe et *al.*, 1983	T. Okabe (Japan) Okabe et *al.*, 1983
PancTul	Primary tumour	PDAC, G2-G3	G3 unpublished data	M. von Bülow Moore et *al.*, 2001

Table 1: Characterisation of PDAC cell lines used in this study adapted from Sipos et *al.*, 2003

Sipos and colleagues performed a study to comprehensively characterise different PDAC cell lines, available as an *in vitro* research platform.

3.3.1 Features of monolayer and spheroid cultures

According to Sipos et *al.*, PDAC cell lines in general grew as adherent monolayers, yet Capan1, Colo357, and, to some extent, also Panc1 cells tended to form multiple layers in post confluent cultures. Capan1 cells, detached from the surface after cultures, became confluent and grew as floating aggregates. The different PDAC cell lines varied highly in size and shape. Capan1 cultures were rather monomorphic and consisted of polygonal, cuboid, or round-oval cells, while Panc89 cells were moderately polymorphic, polygonal, or oval. The other cultures exhibited a marked polymorphism, with cell shapes ranging from polygonal, oval-round to spindle-shaped fibroblastoid. Some cell lines, e.g. Colo357, also contained abnormal giant cells with atypical morphology. All PDAC cell lines tend to form spheroids within 24 h, when cultured without adhesive substrates. Capan1 cells were found to form cohesive spheroids, consisting of smaller cell aggregates with lumen formation, while Colo357, Panc89, and PancTuI cells developed circumscribed spheroids. In contrast, Panc1 spheroids had an irregular outer surface. These *in vitro* grown multicellular spheroids are thought to represent a model system that is intermediate in complexity when compared to monolayer cultures and solid *in vivo* grown tumours. Speroids facilitate direct cell-to-cell interactions, thereby allowing the study of cell-to-cell adhesion processes as well as the influence homo- and heterotypic cell interactions on proliferation, differentiation and metabolism of the involved cells. PDAC cells growing in spheroids were found to show cell polarisation and lumen formation. Based on these criteria, Capan1 cells were graded by the authors to be highly differentiated, since their spheroids even resemble hollow spheres (Sipos et *al.*, 2003). In addition to the degree of differentiation, the genetic background of the different cells lines needs to be considered for the evaluation of obtained results.

3.3.2 Genetic alterations of PDAC cell lines

When working with PDAC cell lines, genetic aberrations have to be taken in consideration. A study by Moore et *al.* (2001) analysed the genetic status of 22 cell lines derived from pancreas ductal carcinomas, including the cells that will be used in this study. Mutations in K-ras, p53, $p16^{Ink4}$, and DPC4/Smad4 were found to be the most common genetic alterations in *human* PDAC. K-ras, p53, and p16 genes were mutated in more then 90% of cell lines, followed by alterations in Smad4 in approximately 50% of cells (*table 2)*.

Cell line	Grade	K-ras	p53	P16	Smad4
Capan1	1	Mut (p.m.) Berrozpe et *al.*, 1994 Kalthoff et *al.*, 1993	Mut (p.m.) Berrozpe et *al.*, 1994	Mut (no gene product detected) Naumann et *al.*, 1996	Mut (p.m.) Schutte et *al.*, 1996
Colo357	2	Mut (p.m.) Kalthoff et *al.*, 1993	W.t. Kalthoff et *al.*, 1993 Barton et *al.*, 1991	W.t. Naumann et *al.*, 1996	Mut (h.d.)
Panc1	3	Mut (p.m.)	Mut (p.m.)	Mut (h.d.)	W.t.
Panc89	2	W.t. Kalthoff et *al.*, 1993/ Mut (p.m.) Hirai et *al.*, 1985	Mut (p.m.)	Mut (meth)	W.t.
PancTul	3	Mut (p.m.)	Mut (p.m.)	Mut (h.d.)	W.t.

Table 2: Genetic alterations of PDAC cell lines used in this study adapted from Sipos et *al.*, 2003. (p.m.) point mutation; (meth) hypermethylated; (h.d.), hyperdyploid; W.t., wildtype. (For detailed references see Sipos et *al.*, 2003)

Since immunohistochemical analyses of tumour biopsies from PDAC patients also indicated overexpression of PKD (Trauzold et *al.*, 2003), a potential function of PKD family members in processes implicated with cancer progression was elucidated further in this work.

3.4 Aim of this work

Based on this clinical observation, one aim of this study was to investigate the function of PKD in cell shape regulation, migration, and invasion of pancreatic adenocarcinoma cells. A particular focus of the work shall be the identification and analysis of the functional link of PKD interaction partners, like Cortactin, in the regulation of cell motility and Actin remodelling processes. Understanding the regulation of cell motility and invasion of pancreatic tumour cells might reveal novel molecular targets for anti-invasion and anti-metastasis therapies against these to date incurable cancer.

4. Materials & Methods

4.1 Materials

4.1.1 Chemicals & Biochemicals

Acrylamide, RotophoreseGel30	Roth, Karlsruhe
2-Mercaptoethanol (2-ME)	Roth, Karlsruhe
5-Bromo-4-chloro-3-indolylphosphate toluidinium salt (BCIP)	Roth, Karlsruhe
Agarose, low EEO	Applichem GmbH, Darmstadt
Ammoniumpersulfate (APS)	Roth, Karlsruhe
Aprotinin	Roth, Karlsruhe
ATP	Sigma-Aldrich, Deisenhofen
Bio-RAD protein assay solution, 5x	Bio-RAD Laboratories, München
Blocking reagent for ECL	Roche Diagnostics, Basel, CHE
BSA A-6003, fatty acid free	Sigma-Aldrich, Deisenhofen
BSA bovine serum albumin 10mg/ml	New England BioLabs, Frankfurt a.M.
Collagen, Type I, from rat tail	Sigma-Aldrich, Deisenhofen
Collagen, Type IV, from human placenta	Sigma-Aldrich, Deisenhofen
Complete protease inhibitor cocktail (EDTA-free)	Roche Diagnostics, Basel, Switzerland
Diethyl pyrocarbonate (DEPC)	Sigma-Aldrich, Deisenhofen
Dimethylformamide (DMF)	Roth, Karlsruhe
Dimethysulfoxide (DMSO)	Roth, Karlsruhe
dNTP Set (100mM)	Invitrogen, Karlsruhe
DRAQ5	5 mM, Biostatus Ltd., Shepshed, UK
Dry milk powder	Merck, Darmstadt
DTT	Sigma-Aldrich, Deisenhofen
EDTA	Roth, Karlsruhe
EGTA	Roth, Karlsruhe
Ethidium bromide	Roche Diagnostics, Basel, Switzerland
FCS (foetal calf serum)	Sigma, Taufkirchen
Fluoromount® G	Biozol, Eching
Glycerol	Roth, Karlsruhe
2-Glycerophosphate	Sigma-Aldrich, Deisenhofen
Glycine	Roth, Karlsruhe
hydrogen peroxide H_2O_2	Roth, Karlsruhe
Isopropanol	Roth, Karlsruhe
Leupeptin	Roth, Karlsruhe
Luminol for ECL substrate	Sigma-Aldrich, Deisenhofen
Maleic acid	Roth, Karlsruhe
Matrigel™ (Phenol-red-free)	BD Bioscience,Heidelberg
Methanol	Roth, Karlsruhe
Sodium fluoride (NaF)	Sigma-Aldrich, Deisenhofen
Sodium orthovanadate	Sigma-Aldrich, Deisenhofen
NGS normal goat serum	Invitrogen, Karlsruhe
Nitroblue tetrazollum salt (NBT)	Roth, Karlsruhe
OptiMEM®I	Invitrogen/Gibco, Karlsruhe
PageRuler™ prestained prot. ladder	MBI Fermentas, St. Leon-Rot
PDGF-BB human	R&D Systems, Wiesbaden-Nordenstadt
PFA, granular	Elektron Microscopy Science, Fort Washington, PA, USA

Phenylmethylsulfonylfluoride (PMSF)	Sigma-Aldrich, Deisenhofen
Poly L-lysine 0.1% (w/v) in H_20	Sigma Diagnostics (Cat P8920), St.Louis, MO, USA
Ponceau	Sigma-Aldrich, Deisenhofen
Protein marker SDS-7B, prestained standard mixture	Sigma-Aldrich, Deisenhofen
Rabbit muscle G-actin	AKL99, Cytoskeleton Inc., Denver, USA
Rhodamine-Phalloidin	Sigma-Aldrich, Deisenhofen
SDS	Roth, Karlsruhe
TEMED	Sigma-Aldrich, Deisenhofen
Triton X100	Roth, Karlsruhe
Tryp/EDTA, 10x	PAA Laboratories, Pasching, Austria
Trypan blue solution 0.2 % (w/v)	Sigma-Aldrich, Deisenhofen
Tween20	Roth, Karlsruhe

4.1.2 Enzymes

Restriction endonucleases were obtained from MBI Fermentas, (St. Leon-Rot), Roche Diagnostics, (Basel, Switzerland) or New England BioLabs (Frankfurt a.M.). Additional enzymes used are listed below:

T4-DNA Ligase	MBI Fermentas, St. Leon-Rot
DNAseI, RNase-free	Roche Diagnostics, Basel, Switzerland
Expand High Fidelity Kit	Roche Diagnostics, Basel, Switzerland
KOD-Polymerase	Novagen/EMD-Bioscience, Darmstadt
Pfu HF-Polymerase	Stratagene, Amsterdam, Netherlands
Pfu Turbo-Polymerase	Stratagene, Amsterdam, Netherlands
Taq DNA-Polymerase	Eppendorf, Hamburg
Titan One-Tube RT-System	Roche Diagnostics, Basel, Switzerland

4.1.3 Buffers and Solutions

Acrylamide running gel buffer	10%/12,5% (v/v) acrylamide, 375 mM Tris, 0.1% SDS, pH 8.8
Acrylamide stacking gel buffer	4% (v/v) acrylamide, 125 mM Tris, 0.1% SDS, pH 6.8
AP-detection buffer	100 mM Tris-HCl, 100 mM NaCl, 50 mM $MgCl_2$ pH 9.5
AP-blocking solution	Dry milk powder 3% (w/v), 0.05% (v/v) Tween 20 in PBS
Aprotinin stock solution	10 mg/ml ddH_2O
APS solution	10% (w/v) ammonium persulfate in H_2O
BCIP stock solution	50 mg/ml BCIP in DMF
Blocking solution 1% for ECL	Blocking solution 10x, diluted 1:10 in TBS/Tween
Blocking solution 10x for ECL	10% (w/v) blocking reagent in 100 mM maleic acid buffer, 150 mM NaCl, pH 7.5
Blocking solution for IHC	5% (v/v) NGS, 0.05% (v/v) Tween20 in PBS, sterile filtered
Blotting buffer	25 mM Tris, 192 mM glycine, 20% (v/v) methanol, pH 8.3
Collagen I, IV stem solution	1 mg/ml Collagen, 0.1 M Acetate in PBS
Crystal violet staining solution	0.5% (w/v) crystal violet, 20% (v/v) Methanol
DNA sample buffer (6x)	250 pg/ml xylene cyanol, 250 pg/ml bromophenol blue, 50 mM EDTA, 80% (v/v) glycerol
Leupeptin stock solution	10 mg/ml ddH_2O
Lysis buffer	20 mM Tris, 1% (v/v) TritionX100, 5 mM $MgCl_2$, 150 mM NaCl, pH 7.4
Methanol/acetone fixative	50% (v/v) Methanol, 50% (v/v) Acetone
NBT stock solution	50 mg/ml NBT in 70% (v/v) DMF/H_2O
PBS (phosphate buffered saline)	140 mM NaCl, 2.7 mM KCl, 8 mM Na_2HPO_4, 1.5 mM KH_2PO_4, pH 7.2
PBS/Tween	PBS + 0.05% (v/v) Tween20
PDGF stock solution	10 µg/ml PDGF, 4 mM HCl, 0.1% BSA
PFA fixing solution	4% PFA in PBS
PMSF solution	100 mM in isopropanol

POD substrate for ECL	Sol. A: 0.1 M Tris, 250 mg/ml Luminol, pH8.6, 4°C Sol. B: 1.1 mg/ml para-hydroxycoumarinacid in DMSO, RT
Ponceau staining solution	0.1 % (w/v) Ponceau, 1 % (v/v) glacial acetic acid
SDS sample buffer (5x)	312.5 mM Tris-HCl, 25% (v/v) β-mercaptoethanol, 25% (v/v) glycerol, 10% (w/v) SDS, 0.05% (w/v) bromophenol blue, pH 6.8
Sodium orthovanadate	1 M in ddH_2O
Stripping buffer	62.5 mM Tris, 2% (v/v) SDS, 0.7% (v/v) β-mercaptoethanol (added freshly), pH 6.8
TBE (10x)	900 mM Tris-borate, 20 mM EDTA (5.5% (w/v) boric acid)
TBS buffer	20mM Tris, 136 mM NaCl, pH 7.6
TBS/Tween	TBS buffer + 0.05% (v/v) Tween20
TGS buffer for SDS-PAGE	192 mM glycine, 25 mM Tris-HCl, 0.1 % (w/v) SDS, pH 7.4
Tryp/EDTA solution 1x	10% (v/v) Tryp EDTA (10x) in sterile PBS

Additional special buffers and solutions are described in the respective parts of the Methods section.

4.1.4 Antibodies

4.1.4.1 Primary antibodies

Antibody	Dilution	Manufacturer
mouse anti-HECD-1 (Human E-Cadherin)	IB: 1:1.000	Calbiochem, Bad Soden
mouse-anti-Actin (AC-40, monoclonal)	IB: 1:400	Sigma-Aldrich, Deisenhofen
mouse-anti-Arp3 (monoclonal)	IB: 1:100	250 µg/ml, Becton Dickinson San Jose, CA, USA
mouse-anti-E-Cadherin (monoclonal)	IB: 1:1.000 IHC: 1:400	250 µg/ml, Becton Dickinson San Jose, CA, USA
mouse-anti-FAK (monoclonal)	IB: 1:100	250 µg/ml. Becton Dickinson San Jose, CA, USA
mouse-anti-FLAG-M2 (monoclonal)	IB: 1:2.000	Sigma-Aldrich, Deisenhofen
mouse-anti-GAPDH	IB: 1:5.000	Abcam, Cambridge, UK
mouse-anti-GFP (monoclonal)	IB: 1:2.000	Roche Diagnostics, Basel, Switzerland
mouse-anti-GM 130 (monoclonal)	IHC: 1:400	250 µg/ml, Becton Dickinson San Jose, CA, USA
mouse-anti-Paxillin (monoclonal)	IB: 1:1.000 IHC: 1:200	250 µg/ml, Becton Dickinson San Jose, CA, USA
mouse-anti-PKD1 (JP2, polyclonal)	IHC: 1:200	1 mg/ml, Protein-A-purified, epitope: N-terminus of PKD1, Dr. H. Böttinger, Stuttgart; provided by Dr. A. Hausser, Stuttgart
mouse-anti-Tubulin (Ab-4, monoclonal)	IHC: 1:400	200 µg/ml, NeoMarkers, Fremont, CA, USA
mouse-anti-Vinculin (monoclonal)	IB: 1:200	Sigma-Aldrich, Deisenhofen
rabbit-anti-Cortactin (polyclonal, H-191)	IB: 1:1.000 IHC: 1:200	200 µg/ml, Santa Cruz Biotechnology Santa Cruz, CA, USA
rabbit-anti-PKD (polyclonal, C-20)	IB: 1:1.000	200 µg/ml, epitope: C-terminus of PKD1 Santa Cruz Biotechnology Santa Cruz, CA, USA
rabbit-anti-PKD (polyclonal, D-20)	IB: 1:1.000	200 µg/ml, epitope: N-terminus of PKD1 Santa Cruz Biotechnology Santa Cruz, CA, USA
rabbit-anti-PKD1/2 pSer9l0 (*P9*, polyclonal)	IB: 1:3.000 IHC: 1:200	3 mg/ml, Protein-A-purified, epitope: MKALGERVpSIL (Dr. J. Pineda Ab GmbH); provided by Dr. A. Hausser, Stuttgart
rabbit-anti-PKD1/2/3 pSer738/742 (*P10*, polyclonal)	IB: 1:100 IHC: 1:40	Affinity purified against peptide, epitope: activation loop IGEKpSFRRpSVV (Dr. J. Pineda Ab GmbH) Provided by Dr. A. Hausser, Stuttgart
rabbit-anti-PKD2 (polyclonal)	IB: 1:2.000	200 µg/ml, epitope: C-terminus of PKD2 Calbiochem, Bad Soden
rabbit-anti-PKD3 (polyclonal)	IB: 1:1.000	Epitope: KHFIMAPNPDDMEEDP (C-terminus of PKD3). Provided by V. Malhotra, UCSD, San Diego, USA
sheep-anti-TGN46 (polyclonal)	IHC: 1:400	Acris Antibodies, Hiddenhausen

4.1.4.2 Secondary antibodies

goat-anti-mouse F(ab')$_2$ of IgG - Alexa Fluor 546 conjugated	IHC: 1: 400	Molecular Probes, Göttingen
donkey-anti-sheep IgG- Alexa Fluor 546 conjugated	IHC: 1: 400	Molecular Probes, Göttingen
goat-anti-rabbit IgG- Cy5 conjugated	IHC: 1: 100	Jackson Immuno Research Lab, Soham, UK
goat-anti-rabbit (H+L) of IgG- AP conjugated	IB: 1: 5.000	Jackson Immuno Research Lab, Soham, UK
goat-anti-mouse (H+L) of IgG- AP conjugated	IB: 1: 5.000	Jackson Immuno Research Lab, Soham, UK
goat-anti-rabbit F(ab')$_2$ of IgG- HRP conjugated	IB: 1: 10.000	Jackson Immuno Research Lab, Soham, UK
goat-anti-mouse F(ab')$_2$ of IgG- HRP conjugated	IB: 1: 10.000	Jackson Immuno Research Lab, Soham, UK
goat-anti-mouse F(ab')$_2$ of IgG - Alexa Fluor 488 conjugated	IHC: 1: 400 For α-Arp3/JP2 IHC: 1: 200	Molecular Probes, Göttingen
goat-anti-rabbit F(ab')$_2$ of IgG - Alexa Fluor 488 conjugated	IHC: 1: 400	Molecular Probes, Göttingen
goat-anti-rabbit F(ab')$_2$ of IgG - Alexa Fluor 546 conjugated	IHC: 1: 400 For α-P9/P10 IHC: 1: 200	Molecular Probes, Göttingen

4.1.5 Media & components

4.1.5.1 Bacterial media components

Tryptone	Roth, Karlsruhe
Yeast extract	Roth, Karlsruhe
Agar-agar	Roth, Karlsruhe
Ampicillin	Roth, Karlsruhe, 100 mg/ml in ddH_2O
Kanamycin	Roth, Karlsruhe, 30 mg/ml in ddH_2O
Tetracyclin hydrochloride	Merck, Darmstadt, 12.5 mg/ml in 70% EtOH

4.1.5.2 Bacterial media

LB medium	10 g/l tryptone, 5 g/l yeast extract, 10 g/l NaCl, pH 7.0
LB_{Amp} medium	LB medium, 0.1% (v/v) Ampicillin stock solution
LB_{Kan} medium	LB medium, 0.1% (v/v) Kanamycin stock solution
LB agar plates	15 g/l agar agar in LB medium
LB_{Amp} agar plates	15 g/l agar agar in LB medium, 0.1% (v/v) Ampicillin stock solution
LB_{Kan} agar plates	15 g/l agar agar in LB medium, 0.1% (v/v) Kanamycin stock solution

4.1.5.3 Cell culture media and components

FCS (fetal calf serum)	PAA Laboratories, Linz, Austria
Freezing solution for PDAC cells	20% (v/v) FCS, 5% (v/v) DMSO, 1mM sodium pyruvate in RPMI
Geneticin (G418)	Chemicon/Merk, Darmstadt
Geneticin (G418) stock solution	50 mg/ml in ddH_20, sterile filtered
PDAC cell selection media	standard growth media, 1mg/ml G418
PDAC cell standard growth media	RPMI 1640 supplemented with 10% (v/v) FCS and 1mM sodium pyruvate
Penicillin/Streptomycin (PEN/STREP, 10 mg/ml)	Sigma-Aldrich, Deisenhofen
RPMI 1640	Invitrogen/Gibco, Karlsruhe
Sodium pyruvate	Invitrogen/Gibco, Karlsruhe

4.1.6 Consumables

Bio-Trace™ nitrocellulose membrane	PALL Gelman Laboratory, Dreieich
24 well Transwell filter inserts, 8µM pore diameter (Cat 4244)	Corning, New York, USA
Cover slips 15 x 15	Roth, Karlsruhe
Filter paper	Whatman International, Maidstone,UK
Microscopy object slides	Roth, Karlsruhe
Sterilin boxes (100 mm, 25 compartment dish)	Bibby Sterilin, Staffs, UK
Tissue culture flasks and dishes	Greiner, Frickenhausen
X-ray films	Fujifilm, Düsseldorf

4.1.7 Kits

Effectene Transfection kit	Qiagen, Hilden
NuceloSpin Extract Kit	Machery-Nagel, Düren
Nucleobond plasmid isolation kit	Machery-Nagel, Düren
RNeasy Mini kit	Qiagen, Hilden
peqGOLD RNAPure™	PeqLab, Erlangen
α-FLAG M2-Agarose (A2220)	Sigma-Aldrich, Deisenhofen
First-Strand cDNA systhesis kit	MBI Fermentas St. Leon-Rot
TOPO TA cloning ® kit	Invitrogen, Karlsruhe
TransIT® 293 Transfection kit	Mirus Corporation, Madison, WI, USA
Lipofectamin 2000 kit	Invitrogen, Karlsruhe

4.1.8 Plasmids

pEGFP N1-Vector	Clontech, Palo Alto, USA
pCDNA3-PKD2	Provided by Dr. A. Hausser, Stuttgart
pCDNA3-PKD1	Provided by Dr. A. Hausser, Stuttgart
pCDNA31-PKD1K612Wmyc	Provided by Dr. A. Hausser, Stuttgart
pCDNA3-PKD1Δ1-79	Provided by Dr. A. Hausser, Stuttgart
pCDNA3-PKD1Δ1-98	Provided by Dr. A. Hausser, Stuttgart
pCDNA3-Vector	Invitrogen
pCR3.V62-Met-Flag-Cortactin	T. Eiseler, Stuttgart
pCR3.V62-Met-Flag-CortactinS113/S298A	T. Eiseler, Stuttgart
pCR3.V62-Met-Flag-CortactinS113A	T. Eiseler, Stuttgart

pCR3.V62-Met-Flag-CortactinS298A	T. Eiseler, Stuttgart
pCR3.V62-Met-Flag-Vector	Provided by Dr. A. Hausser, Stuttgart
pECFP N1-Vector	Clontech, Palo Alto, USA
pEGFP N1-Cortactin	T. Eiseler, Stuttgart
pEGFP N1-CortactinS113A	T. Eiseler, Stuttgart
pEGFP N1-CortactinS298A	T. Eiseler, Stuttgart
pEGFP N1-PKD1	Provided by Dr. A. Hausser, Stuttgart (Hausser et *al*., 2002)
pEGFP N1-PKD1K612Wmyc (henceforth PKD1KD)	Provided by Dr. A. Hausser, Stuttgart (Hausser et *al*., 2002)
pEGFP N1-PKD1Δ340	Provided by Dr. A. Hausser, Stuttgart (Hausser et *al*., 2002)
pEGFP N1-PKD1ΔAD	Provided by Dr. A. Hausser, Stuttgart (Hausser et *al*., 2002)
pEGFP N1-PKD1ΔCRD	Provided by Dr. A. Hausser, Stuttgart (Hausser et *al*., 2002)
pEGFP N1-PKD1ΔPH	Provided by Dr. A. Hausser, Stuttgart (Hausser et *al*., 2002)
pEGFP N1-PKD2	Provided by Dr. A. Hausser, Stuttgart
pEGFP N1-PKD2K580W (henceforth PKD2KD)	Provided by Dr. A. Hausser, Stuttgart
pSuppressor-PKD1	Provided by Dr. A. Hausser, Stuttgart RNAi mediated against: base pairs 959-978 of PKD1

4.1.9 Bacterial strains

E. Coli XL1-blue	**relevant genotype:** recA1 endA1 gyrA96 thi-1 hsdR17 relA1 lac [F' proAB $lacI^qZ\Delta M15$ TN10 (Tet^r)], Stratagene, Amsterdam, Netherlands

4.1.10 Eukaryotic cell lines

HEK 293T cells	ATCC, Manassas,USA
Panc1 cells	Provided by Prof. Dr. H. Kalthoff, Christian-Albrechts-Universität, Kiel
Panc89 cells	Provided by Prof. Dr. H. Kalthoff, Christian-Albrechts-Universität, Kiel
Colo357 cells	Provided by Prof. Dr. H. Kalthoff, Christian-Albrechts-Universität, Kiel
Capan1 cells	Provided by Prof. Dr. H. Kalthoff, Christian-Albrechts-Universität, Kiel
PancTul cells	Provided by Prof. Dr. H. Kalthoff, Christian-Albrechts-Universität, Kiel
KIF-5 fibroblasts	Provided by Prof. Dr. H. Kalthoff, Christian-Albrechts-Universität, Kiel

4.1.11 Devices

Optima TCL ultracentrifuge	Beckman Coulter, Krefeld
Cell sorter FACStar PLUS	Becton Dickinson, Franklin Lakes, USA
Flow cytometer EPICS XL-MCL	Beckman Coulter, Krefeld
Leica DM-IRB fluorescence microscope	Leica Microsystems, Bensheim
Confocal Laserscanning Microscope Leica TCS SP2	Leica Microsystems, Bensheim
Confocal Laserscanning Microscope Leica TCS SL	Leica Microsystems, Bensheim
Film processor Kodak X-Omat1000	Kodak, Stuttgart
SpectraMax340^{PC}, microplate reader	Molecular Dynamics, Krefeld
Axiovert 35 inverted microscope	Zeiss, Jena
Storm Phosphoimager	Molecular Dynamics, Krefeld

4.1.12 Specialised software

Leica confocal software V2.61	Leica Microsystems, Mannheim
Leica confocal software lite V2.61	Leica Microsystems, Mannheim
Zeiss LSM Image browser V3.2	Zeiss, Aalen, Germany
ImageQuant 5.2	Amersham, Biosciences, Freiburg
WinMDI 2.8	Josef Trotter
pDRAW	AcaClone Software, Kjeld Olesen
GraphPad Prism 3.0	GraphPad Software Inc., San Diego, CA, USA
Gene Cluster	Eisen et *al*., 1998
TreeView	M. Eisen, Stanford University

All non listed materials have been purchased either from Sigma-Aldich (Deisenhofen), Roth (Karlsruhe) or Merck (Darmstadt).

4.2 Methods

4.2.1 General methods

General methods, like restriction endonuclease digestion, phenol-chloroform extraction, agarose gel electrophoresis, measurement of DNA concentration, ligation and transformation of chemically competent E. *coli* were performed as described in Sambrook et *al.*, 1998. Plasmid isolation and purification of DNA fragments was done using the Nucleobond plasmid isolation or the NuceloSpin Extract kit (Machery-Nagel, Düren). RNA was isolated by the RNeasy Mini Kit (Qiagen, Hilden) and the peqGOLD RNAPure^{TM} system (PeqLab, Erlangen) according to manufacturer's protocol. DNase I digestion of RNA for subsequent RT-PCR was performed using DNase I, RNase-free (Roche Diagnostics, Basel, Switzerland) as stated by the manufacturer. Reverse transcription was done using the First-strand cDNA systhesis Kit (MBI Fermentas St. Leon-Rot). 4 µg of total-RNA were used for first-strand cDNA synthesis as described in the manufacturer's protocol.

4.2.2 Qualitative and semi-quantitative RT-PCR reactions

For qualitative analysis of PKD isoform expression, PDAC cell lines were grown to approximately 80% confluence, total RNA was isolated using the respective kits, followed by DNase I digestion and phenol-chloroform extraction and first strand cDNA synthesis as described in *4.2.1*. 3 µl of template cDNA was used in PCR reactions. For qualitative RT-PCRs 30 amplification cycles were performed, while for semi-quantitative RT-PCR care was taken to be within the linear range of amplification. Starting from a basal 17 cycles, every third amplification cycle 5 µl of PCR reaction was removed and analysed on a 2% agarose gel to adapt the PCR reaction for a linear amplification range.

PCR reaction: 5 µl
5 x reaction buffer
5 µl 2mM dNTP-Mix
2.5 µl Primers for/rev 10pmol
3 µl template first-strand cDNA
0,2 µl Taq DNA-Polymerase (Eppendorf, Hamburg)
add H_2O to 50µl

Annealing: 55°C 30 sec
Extension: 72°C 1 min

Primers used for RT-PCR analysis of PKD isoform expression:

Primer	Sequence	Product size (bp)
PKD1 forward	5'-CAGATTTCTATGCACGCTCTCTTTGTTCATTCATAC-3'	500 bp
PKD1 reverse	5'-CTGGATCCAGGCAGTTGTTTGGTACTTTCGGTGC-3'	
PKD2 forward	5'-AGCTTCTCTGAGCATCTCTGT-3'	332 bp
PKD2 reverse	5-TAATACGACTCACTATAGGGCGCAGCTTCTCCATCACCACAA-3'	
PKD3 forward	5'-GGTGAAGCTGTGTGACTTTGG-3'	372 bp
PKD3 reverse	5'-TAATACGACTCACTATAGGGCAGCCAGGGATGACTAAGAGAT-3'	
GAPDH forward	5'-TGATGACATCAAGAAGGTGGTGAAG-3'	250 bp
GAPDH reverse	5'-TCCTTGGAGGCCATGTAGGCCAT-3'	

4.2.3 Qualitative RT-PCR of tumour sample total-RNA

For qualitative analysis of PKD isoform expression in PDAC tumour samples the Titan One-Tube RT-System (Roche Diagnostics, Basel, Switzerland) was used according to the manufacturer's protocol with 100 ng of total-RNA per reaction. For PCR-reaction amplifying PKD2, PKD3 and GAPDH annealing was done at 55 °C, annealing for PKD1 was performed at 57°C.

PCR-Program Titan One-Tube RT-System:

Step	Temperature	Time	Comment
1	50°C	30 min	RT-reaction
2	95°C	60 sec	
3	95°C	30 sec	35 cycles
4	55/57°C	30 sec	
5	68°C	60 sec	
6	68°C	10 min	

4.2.4 Cloning of Cortactin cDNA-constructs

Human Cortactin transcript variant 1 (NM_005231) was amplified from Panc89 cDNA using Expand High Fidelity Kit (Roche Diagnostics, Basel, Switzerland). Primers used were generated as following:

Cortactin EcoRI for 5'-CGGAATTCATGTGGAAAGCTTCAGCA-3'
Cortactin ApaI rev 5'-AAGGGCCCTCTGCCGCAGCTCCACATA-3'

After cloning into TOPO TA-(pCR2.1)-Vector (Invitrogen, Karlsruhe) according to the manufacturer's protocol, the respective pEGFP-N1-, pECFP-C1- and pCR3.V62-Met-Flag-Cortactin constructs were obtained by subcloning the Cortactin cDNA sequence in frame into EcoRI - ApaI sites within the polylinker of the respective Vectors.

4.2.5 Site-directed mutagenesis of pEGFP-N1- and pCR3.V62-Met-Flag-Cortactin

Site-directed mutations in pEGFP-N1- and pCR3.V62-Met-Flag-Cortactin resulting in single amino acid substitutions (S113A, S298A) were performed using QuickChange™ site-directed mutagenesis system (Stratagene, Heidelberg) according to the manufacturer's instructions. The integrity of the PCR-amplified Cortactin cDNA as well as the mutant constructs was verified by sequencing.

Mutagenesis Primer:

Primer	Sequence	Mutagenesis
CortactinS113A for	5'-CAGTCGAAACTTGCCAAGCACTGCTCG-3'	Template 100ng; Pfu-Turbo Program: 1) 95°C 1' 2) 95°C 30'' 3) 56°C 30'' 4) 72°C 7' 30'' 5) 2)- 4) 12 cycles 6) 72°C 10'
CortactinS113A rev	5'-CGAGCAGTGCTTGGCAAGTTTCGACTG-3'	
CortactinS298A for	5'-CTGGCCAAGCACGAGGCCCAGCAAGAC-3'	
CortactinS298A rev	5'-GTCTTGCTGGGCCTCGTGCTTGGCCAG-3'	

4.2.6 Cell culture of eukaryotic cells

4.2.6.1 Cell culture of PDAC and HEK 293T cells

Panc89, Panc1, Colo357, Capan1 and PancTuI pancreas ductal adenocarcinoma (PDAC) cell lines were obtained from Prof. Dr. H. Kalthoff (Christian-Albrechts-Universität, Kiel). PDAC cells were cultured in RPMI supplemented with 10% FCS, 1mM sodium pyruvate. KIF-5 fibroblasts for invasion assays were also obtained from H. Kalthoff and were cultured in RPMI supplemented with 10 % FCS. HEK 293T cells (ATCC) were cultured in RPMI + 5% FCS. All cell lines were held under standard growth conditions 37°C/ 5% CO_2/ 95 % humidity.

4.2.6.2 Transient transfection of HEK293T cells

293T cells were transfected using the TransIT293 reagent (MoBiTec GmbH, Goettingen; Mirus, Wisconsin, USA). For transfection of 500.000 cells/well 2µg DNA and 4µl TransIT293 according to the manufacturer's instructions were used. For total cell lysates of 293T cells transiently expressing cDNA constructs, the cells were harvested the next day, washed once in PBS and lysed according to *4.2.7.1*.

4.2.6.3 Transfection and creation of stable of Panc89 and Panc1 cells

Transfection of Panc89 and Panc1 cells was done using Effectene (Qiagen, Hilden) and Lipofectamin 2000 (Invitrogen, Karlsruhe) according to the manufacturer's protocol. Stable Panc89 cell lines expressing pEGFP-N1-Vector, PKD1-GFP, PKD1KD-GFP, PKD2-GFP, PKD2KD-GFP, Cortactin-GFP and CortactinS298A-GFP constructs were created by selection with G418 (Invitrogen, Karlsruhe) 1mg/ml (w/v) following several rounds of cell sorting (FACS star plus, Becton Dickinson, Franklin Lakes, USA) to enhance GFP-expressing cells. Panc1 and Panc89 PKD1-pSuppressor clones were created by transfection of the PKD1-pSuppressor construct in 300.000 cells/6well and subsequent selection using 1mg/ml (w/v) G418 until cells stopped dying. Then cells were subjected to a limited dilution in 96 well plates with an approximate density of one cell every fourth well. Individual surviving clones were harvested and expanded. Resulting PKD1-knockdown clones were subsequently evaluated using Western blotting and semi-quantitative RT-PCR analysis *(4.2.2)* as indicated in the respective figures.

4.2.6.4 Migration assays using Transwell filter inserts

Migration assay with Panc89 and Panc1 cells, as well as derived stable cell lines and PKD1-pSuppressor-knockdown clones were performed using 24 well Transwell filter inserts (Corning, New York, USA) with 8 µm pore diameter: Cells were removed from selection and grown for 3 days on standard growth media. For migration assays, Panc89 cells were seeded at a density of 60.000 cells/insert in media containing 1% FCS and 1mM sodium pyruvate. For Panc1 PKD1-pSuppressor clones, 20.000 cells/insert were used and cells were cultivated on selection media until the start of the assay to induce a maximum RNA interference effect. Migration was induced by an FCS gradient of 1% - 10% FCS (top of insert/well) for 40 hours. Cells on the filter were fixed using 4% para-formaldehyd and subsequently washed three times with PBS. The inside of the Transwell insert was wiped with a cotton swab to remove cells, which had not migrated and washed again two times with PBS. To quantify migration, cells on the filter were stained with DAPI 1µg/ml in PBS for 20 min at room temperature (RT). Filters were washed three times with PBS and then documented using a widefield fluorescence microscope (Leica, Bensheim) equipped with a CCD camera, and a monochromator light source controlled via OpenLab Software (Improvision, UK) with 10 x magnification. At least 6 visual fields (1024 x 1022) per filter were photographed. Results were calculated as median number of migrated cells/visual field with at least 6 images per filter.

4.2.6.5 Invasion assays using Transwell filters coated with Matrigel™

Migration assays with stable Panc89 cell lines were essentially done as described in *4.2.6.4*, except that both migration (uncoated filter control) and invasion through Matrigel™-coated filters was measured. Filters were coated by incubation with Matrigel™ (basement membrane matrix, Phenol-red-free, 11.9 mg/ml, BD Bioscience, Heidelberg) 1:5 in RPMI supplemented with 1% FCS and 1mM sodium pyruvate for 30 min at 37°C. Subsequently the stable Panc89 cell lines were seeded at a density of 60.000 cells/insert on control and Matrigel™-coated filter inserts in media containing 1% FCS and 1mM sodium pyruvate. Migration/invasion was induced for 40 h and filters were processed as described in *4.2.6.4*. Percent invasion was calculated as number of invading cells/number of migrating cells x 100.

4.2.6.6 Cell invasion assays in KIF-5 fibroblast layers

In this assay the invasive potential of cancer cells is determined using a modified trypan-blue dye-based model to show cell invasion into KIF-5 fibroblast layers. The assay was a modification of a protocol provided by Dr. A. Trauzold (Christian-Albrechts-Universität, Kiel). Briefly, KIF-5 fibroblasts were seeded at a density of 150.000 cells/well in a 24 well plate. At the 4th day, after KIF-5 cells had formed a confluent monolayer, the cells were rinsed twice with PBS, permeabilised with 500 µl of DMSO for 1h at room temperature and washed again twice with PBS. KIF-5 monolayers were overlayed with stable Panc89 cell lines grown for 3 days without selection on standard growth media at a density of 20.000 cells/well in RPMI supplemented with 10% FCS and 1mM sodium pyruvate. A strongly invasive positive control

(Colo357 cells) and an untouched KIF-fibroblast layer as negative control were also included in the assay. Tumour cells were left to grow for 60 h, daily exchanging the growth media then cells were rinsed with PBS and stained for 20 min using 0.2% trypan blue solution (Sigma-Aldrich, Deisenhofen). After 2x washing with PBS, tumour cell invasion was immediately documented using a widefield fluorescence microscope (Leica, Bensheim) equipped with a CCD camera, and a white light source controlled via OpenLab Software (Improvision, UK) with 10 x magnification using the translucent settings of the software. Trypan-blued stained only the dead cells of the permeabilised KIF-5 fibroblast layer while the living carcinoma cells remained unstained.

4.2.6.7 Cellular adhesion assay towards different substrates

For cell adhesion assays towards different adhesive substrates 96 well TC-plates were coated in triplicate for each cell line assayed for 1h at 37°C using 50µl/well:

Collagen IV :	22.5 µg/ml in PBS (Sigma-Aldrich, Deisenhofen)
Poly-L-Lysine:	0.1% (v/v) in H_20 (1:10 of stem solution, Sigma-Aldrich, Deisenhofen)
Matrigel™:	1:8 dilution of Matrigel™ in PBS (Phenol-red-free, BD Bioscience, Heidelberg)
BSA:	5% BSA in PBS (A-6003, fatty acid free, Sigma Diagnostics, St. Louis, USA)

Uncoated TC-plate surfaces as well as BSA-coated wells served as controls. Prior to the assay Panc89 cells were held without selection on standard growth media for 3 days. Following trypsination they were left to recover for 1h resuspended in standard growth media before seeding on coated plates. Following coating, plates were washed twice with media and stable Panc89 cell lines were seeded at a density of 30.000 cells/well in standard growth media. After 1h 30 min cells, which had not adhered were gently washed away by rinsing the wells 3 times with PBS. To quantify cell adhesion on different adhesive substrates, plates were subjected to crystal violet staining as described in *4.2.6.10*. Relative adhesion was shown by calculating OD 550 means of triplicate wells and respective standard deviations for each cell line and coating condition assayed.

4.2.6.8 Cell-to-cell aggregation assays

Cell-to-cell aggregation assays were adapted from Jaggi et *al.* (2005) and Redfield et *al.* (1997). Prior to the assay, Panc89 cell lines were held without selection on standard growth media for 3 days. For aggregation assays Panc89 cells were diluted to a density of 30.000 cells/100µl in standard growth media and 20 µl of the resuspended cell solution (~6.000 cells) were dropped on the inner surface of the lid of a 10 cm cell culture dish. The lid was inverted and the cell culture dish was filled with PBS to avoid evaporation of the droplets. For each cell line tested, triplicate droplets were analysed. After cultivation of the cells in "hanging drops" for 24 h, the lid was inverted and droplets were resuspended ten times using a 10 µl micropipette. Cell aggregates were documented by an Axiovert 35 inverted microscope equipped with a camera and controller unit (Zeiss, Jena) with 10x magnification.

When indicated in the different experimental settings, 2mM EGTA, inhibitors, α-HECD1-E-Cadherin antibody, as well as respective controls were included in the initial cell suspensions as described in the figure legends.

4.2.6.9 Proliferation assays

For proliferation assays serial dilutions of 10.000, 5.000 and 2.500 stable Panc89 cells/100µl were seeded in triplicate in three 96 well TC-plates in standard growth media. Before starting the assay, the stable Panc89 cells were held for 3 days without selection. After culturing the cells for 40 h with daily medium exchange, the first plate T0 h was subjected to crystal violet staining *(4.2.6.10)*. Plates 2 and 3 were cultured to T24 h and T48 h respectively followed by crystal violet staining. Cell density and hence proliferation was quantified by calculating OD 550 means of triplicate wells as well as respective standard deviations for each cell line and dilution assayed. To calculate doubling times, starting dilutions of 5.000 cells/100µl were used since they were in the linear range of proliferation. Linear equations of growth curves were calculated using EXCEL trend line function. Subsequently doubling times for the respective cell lines were calculated using the linear regression terms.

4.2.6.10 Crystal violet staining

Supernatant was removed from 96 well TC-plates and cells were stained by applying 100 µl of crystal violet solution (0.5% crystal violet in ddH_20, 20% (v/v) Methanol) to each well. After incubation for 20 min at room temperature, plates were washed extensively with H_20 to remove unbound crystal violet and air-dried over night. Cell-bound crystal violet then was dissolved in 100 µl methanol/well and quantified by measuring the absorbance at OD 550 nm using a Spectra-Max 340PC ELISA-reader (Molecular Dynamics, Krefeld). Data was processed by calculating OD 550 means of triplicate wells and respective standard deviations for each cell line and condition assayed. Further data processing was done as indicated in the different experimental settings.

4.2.6.11 Flow cytometry analysis of GFP-expressing stable Panc89 cells

To analyse the GFP-expression of stable Panc89 cell lines. Cells were held for 3 days without selection on standard growth media, harvested by trypsination, washed once with PBS and resuspended in PBA (PBS, 5% BSA, 0.05 % sodium azide). Cell solutions were then subjected to flow cytometry determining GFP-expression using an Epics XL-MCL cytometer (Beckman Coulter, Krefeld) by gating on the population of living cells in the FS/SS Log histogram. 10.000 cells were measured per analysis in the FL1- channel.

4.2.6.12 Analysis of E-Cadherin surface expression on Panc89 cells

Binding of E-Cadherin antibody α-HECD1, generated against the extracellular domain of E-Cadherin, was assessed by flow cytometry. Following trypsination, Panc89 cells were left to recover for 1h in standard growth media. In order to stain the cells for flow cytometry analysis, 1 x 10^6 cells were suspended in 1ml PBA (PBS, 5% BSA, 0.05% sodium azide) and incubated on ice for 20 min. 1µg/ml α-HECD1 antibody or the respective isotype control were added and incubated for 45 min at 4°C on a roller incubator. After washing the cells two times with PBA at 4°C, α-mouse-IgG conjugated with Rhodamine (Sigma-Aldrich, Deisenhofen) diluted 1:200 in PBA was added for 1h at 4°C. Cells were washed again two times with PBA at 4°C and then subjected to flow cytometry using an Epics XL-MCL cytometer, gating on the population of living cells in the FS/SS Log histogram. 10.000 cells were measured per analysis in the FL2-channel.

4.2.7 Protein analyses

4.2.7.1 Total cell lysates

Total cell lysates were prepared by resuspending pelleted and washed cells in the appropriate volume of lysis buffer (20 mM Tris pH 7.4, 150 mM NaCl, 1% Triton X-100, 5 mM $MgCl_2$) supplemented with protease and phosphatase inhibitors 0,5 mM PMSF, 10 µg/ml leupeptin, 10 µg/ml aprotinin, 1 mM sodium orthovanadate, 10 mM sodium fluoride, 20mM β-glycerophosphate. Cells were lysed by vortexing three times and incubation on ice for 30 min. Following centrifugation at 10.000 g for 20 min at 4°C to pellet the cell debris, cleared lysates were transferred to fresh reaction tubes and equal amounts of protein, as determined by Bradford assay according to manufacturer's description (Bio Rad, München) were used to prepare total cell lysate samples for Western blot analysis. 5x SDS sample buffer was added to a final 1x dilution in equal volumes of cell lysate normalised for total protein content and heated to 100°C for 5 min. In some assays instead of protease inhibitors also "Complete" inhibitor mix (EDTA-free, Roche, Basel, Switzerland) was used.

4.2.7.2 Deglycosilation of total cell lysate using PNGaseF

For deglycosilation of E-Cadherin in total cell lysates, 100 µg of protein was used and processed as described in the PNGaseF protocol (New England Biolabs, Ipswich, USA). Subsequently deglycosilated samples were fractionated by 12.5% SDS-PAGE and blotted against E-Cadherin using α-E-Cadherin antibody (Cat.-Nr. 610181, BD Bioscience, Heidelberg).

4.2.7.3 Immunoprecipitations

Panc89/Panc1 and derived stable cell lines, as well as transiently transfected HEK293T cells expressing the indicated constructs were lysed at 4 °C in 1 ml lysis buffer (20 mM Tris/HCl, pH 7.4, 1% Triton X-100, 150 mM NaCl, 5 mM $MgCl_2$, Complete (EDTA-free, Roche, Basel), 10 mM sodium fluoride, 20mM β-glycerophosphate. After 30 min the samples were centrifuged (10.000 g, 20 min, 4 °C), the supernatant was collected and equal amounts of total protein, as described in the individual figures, were subjected to immunoprecipitations with respective α-Cortactin H191 (5µl, 200µg/ml), α-PKD phosphoSer$_{910}$ (3µl, 1mg/ml), α-GFP (3µl, 200ng/ml) and α-FLAG M2 (3µl, 200ng/ml) antibodies. After incubation for 2h at 4°C on a roller incubator 30 µl of Protein G-Sepharose (Amersham Bioscience, Freiburg) was added and the mixture was incubated for an additional hour at 4°C. Subsequently the sepharose pellet was washed tree times in lysis buffer, then 2,5x SDS sample buffer was added and pellets were heated to 100°C for 5 min to release the precipitated proteins.
For immunoprecipitation after removal of the cellular F-Actin cytoskeleton, cells were lysed in binding-buffer supplemented with 1% Triton X-100 and protease inhibitors PMSF, aprotinin, leupeptin as well as β-glycerophosphate for 30 min on ice (3x vortexing). Then the lysates were centrifuged in an Optima TCL ultracentrifuge (Beckman Coulter, Krefeld) at 100.000 x g for 1h at 4°C. The supernatant was collected and equal amounts of protein were used for immunoprecipitations in 1ml lysis buffer including all inhibitors as mentioned above. Immunoprecipitations were then processed as described earlier.
Immunoprecipitations from Panc89 cell culture supernatant were done by conditioning 10 ml standard growth media. 3.5 x 10^6 GFP-Vector, PKD2-GFP, PKD2KD-GFP Panc89 cells were seeded in 10 cm TC-dishes. After adhesion over night, cells were washed three times with serum-free RPMI and then incubated for 16 h with serum-free RPMI supplemented with 25µM GM6001 or respective amounts of vehicle. Subsequently the conditioned cell culture supernatant was centrifuged at 4.000 x g for 10 min to pellet cells in suspension. 6ml supernatant were subjected to immunoprecipitation using 3µl of α-HECD1 antibody (1µg/µl) for 2 h at 4°C on a roller incubator. 30µl Protein G-Sepharose were added and incubated for 1h at 4°C. The precipitated immuncomplexes were washed three times with PBS, then 2,5x SDS sample buffer was added and pellets were heated to 100°C for 5 min to release the precipitated proteins.

4.2.7.4 *In vitro* kinase assays

HEK 293T cells transiently expressing the indicated constructs were lysed at 4 °C in lysis buffer *(see 4.2.7.1)*. After 30 min lysis, the samples were centrifuged (10.000 g, 20 min, 4 °C), the supernatant was collected and immunoprecipitation of GFP-, and FLAG-fusion proteins was performed using 400 ng of respective α-GFP and α-FLAG M2 antibodies. After incubation for 2h at 4 °C, 30 µl of Protein G-Sepharose was added and the mixture was incubated for 1h at 4°C. The sepharose pellet was then washed three times in lysis buffer and once in kinase buffer (50 mM Tris, pH 7.4, 10 mM $MgCl_2$, 2 mM DTT). PKD auto-, as well as Cortactin substrate phosphorylation was determined either by incubating

immuncomplexes or purified FLAG-Cortactin/FLAG-Cortactins298A with PKD1/PKD1KD proteins as indicated in the experimental settings, with 30 µl of kinase buffer containing 2 µCi [γ-32P]-ATP (Amersham Pharmacia, Braunschweig) at 37 °C for 15 min. Reactions were terminated by the addition of 15µl SDS-PAGE sample buffer and analysed by SDS-PAGE, Western blotting, and autoradiography. Autoradiographs were analysed by quantitative phosphoimage analysis (Storm, Molecular Dynamics, Krefeld).

4.2.7.5 Western blot analyses

Western blots were performed according to standard procedures. In brief, protein samples for Western blot analysis were fractionated by 10% or 12.5% SDS-PAGE and transferred to a nitrocellulose membrane. Membranes were blocked by 3% milk in PBST (0.05% Tween 20) for 1h, followed by incubation with respective primary antibodies in PBST as stated in *4.1.4.1*. After washing and incubation with alkaline phosphatase–conjugated anti–mouse IgG or anti–rabbit IgG secondary antibodies, immunoblots were developed according to standard procedures (Ausubel, 1994). For enhanced chemiluminescence detection (ECL), membranes were blocked with 1% Blocking in PBST (Roche, Basel, Switzerland) for 1h and primary as well as secondary antibodies were incubated in 0.5% blocking. After incubation with respective horseradish-conjugated secondary antibodies membranes were subjected to ECL as described in the protocol of Stefan Jean-Pierre Haas (Institute for anatomy, University of Rostock). For 1ml ECL-solution A, 0.3 µl 30% H_2O_2 and 100 µl solution B were added. Membranes were incubated for 2 min with ECL solution and then exposed on X-ray films (Fujifilm, Düsseldorf). X-ray films then were developed by an X-OMAT 1000 processor (Kodak, Stuttgart).

4.2.7.6 F-Actin cosedimentation assays

F-Actin binding assays were adapted from Weed et *al.* (2000). HEK 293T cells in 6 well plates (500.000/well) were transfected using TransIT 293 (Mirus) with 2µg of the indicated expression constructs and 4 µl TransIT293 according to manufacturer's protocol. The next day cells were pelleted, washed once with PBS and then lysed in 200 µl of binding buffer (10mM imidazole, pH 7.2, 75mM KCl, 5mM $MgCl_2$, 0.5 mM DTT and 1mM EGTA) supplemented with 1% Triton X-100 and protease inhibitors PMSF, aprotinin, leupeptin as well as β-glycerophosphate for 30 min on ice (3 times vortexing). Then the lysates were centrifuged in an Optima TCL ultracentrifuge at 100.000 g for 1h at 4°C. Rabbit muscle G-Actin (AKL99, Cytoskeleton Inc., Denver, USA) was diluted to 2.5 mg/ml in binding buffer (without Triton X-100, inhibitors) and then polymerised for 1h at room temperature. For long-term storage at 4°C, ampicillin at 100 µg/ml was added as an antibacterial agent. In binding assays 5 µM of F-Actin (~ 17 µl) were incubated with 50 µg of total protein lysate (~15-20 µl) following ultracentrifugation in a final volume of 200 µl binding buffer supplemented with inhibitors (without Triton X-100) for 30 min at room temperature. In the case of cosedimentation assays using purified proteins, 1 µg of purified PKD1 and PKD1KD were added to 5 µM F-Actin in 200 µl binding buffer, while for the assays with purified FLAG-Cortactin and FLAG-CortactinS298A, 0.5 µg of protein was incubated with 10 µg F-Actin in

the same volume of binding buffer. Samples then were centrifuged at 100.000 g for 1h at 20°C in an Optima TCL ultracentrifuge, the supernatant was removed and the pellet was incubated for 1h at 4°C in 200 µl of G-buffer (5mM Tris-HCl, pH 8.0, 0.5 mM DTT and 0.2 mM $CaCl_2$) supplemented with 0.2 mM fresh ATP to depolymerise the F-Actin (Wu and Parsons, 1993). Subsequently, the 200 µl supernatant and pellet fractions were solubilised with 50 µl of 5x SDS sample buffer and heated to 100°C for 5 min. Equal amounts of the fractions (150 µl) were then analysed by 12.5% SDS-PAGE and Western blotting with the respective antibodies.

4.2.7.7 Purification of FLAG-Cortactin and FLAG-CortactinS298A from 293T lysates via FLAG-M2 affinity purification

FLAG-Cortactin and FLAG-CortactinS298A each were transfected in three 10cm dishes of HEK 293T cells seeded at a density 4 x 10^6 cells/dish using TransIT 293 (14 µg DNA and 21 µl TransIT 293 in 700µl serum-free RPMI). The next day cells were harvested, washed once with PBS and then lysed in 4 ml of lysis buffer supplemented with Complete (EDTA-free), 1 mM sodium orthovanadate, 10 mM sodium fluoride, 20 mM β-glycerophosphate according to the standard protocol in *4.2.7.1*. Cleared lysates were incubated with 400 µl of activated α-FLAG M2-Agarose (A2220, Sigma-Aldrich, Deisenhofen) for 1h 30 min at 4°C on a roller incubator. Activation of α-FLAG M2-Agarose was done according to the manufacturer's descriptions. M2-Immunoprecipitates were subsequently loaded onto a column (Bio Rad, München) equilibrated with lysis buffer. The packed column was washed three times with ice-cold lysis buffer followed by three times PBS. Elusion of the bound FLAG-Cortactin was done by 3 times 200 µl 100mM glycine pH 2.3 in reaction tubes containing 60 µl 1,5M Tris pH 8.8 to buffer the eluate. Eluted proteins were stabilised by the addition of sterile glycerol to a final concentration of 10 % (v/v) and stored at -80°C. FLAG-Cortactin/FLAG-CortactinS298A concentrations as well as purity were subsequently assed by fractionation on SDS-PAGE and comparing coomassie- stained bands to a BSA standard dilution series.

4.2.8 Confocal immunofluorescence analyses

4.2.8.1 Coating of cover slips for immunohistochemistry using Collagen I and IV

Coating of cover slips was done by incubation with 1ml Collagen solution (22.5 µg/ml in PBS, type I or IV, Sigma-Aldrich, Deisenhofen) at room temperature for at least 1h in sterilin boxes (Bibby Sterilin, Staffs, UK). The Collagen solution was removed and the coated cover slips were washed once with standard growth media before seeding cells as indicated in the respective experiments.

4.2.8.2 Immunohistochemistry

Wildtype and stable Panc89 cells were grown for 24 hours on glass cover slips coated with Collagen I or IV as indicated in the figure legends, washed once in PBS and fixed in 4% para-formaldehyde (pH 7.4) for 20 min at 37 °C. For PDGF stimulation cells were serum starved over night and subsequently stimulated with PDGF-BB (R&D Systems, Oxon, UK) 30ng/ml in serum-free media at 37°C for the indicated time points, following fixation with 4% para-formaldehyde as described above. Serum starved cells were used as a control. Fixed cells were washed three times with PBS and then blocked, as well as permeabilised in blocking solution (PBS, 5% NGS and 0.05% Tween-20) for 30 min at room temperature. Cover slips were incubated with the respective primary antibodies in blocking solution for 2h at room temperature (concentrations as indicated in *4.1.4.1*). Samples were washed three times in PBS and incubated with respective α–rabbit/α–mouse IgG Alexa 546/488–labelled secondary antibodies (1:400) and in the case of α-Cortactin H191 also with a goat α-rabbit Cy5 antibody (1:100) in blocking for another 2h at room temperature. F-Actin was stained using Rhodamine-Phalloidine (Sigma-Aldriche, 1:200). Nuclei were stained using DRAQ5 (Biostatus Ltd., Shepshed, UK 1: 2.000 in PBS) for 10 min at room temperature after three times washing in PBS following incubation with secondary antibodies. Cover slips were mounted in Fluormount G (Dianova GmbH, Hamburg). Images were acquired using a confocal laser scanning microscope (TCS SP2; Leica Microsystems GmbH, Heidelberg) equipped with a 100/1.4 HCX PlanAPO oil immersion objective. GFP was excited with an argon laser (488-nm line), whereas Alexa 546 was excited with a helium-neon laser (543-nm line). DRAQ5 and Cy5 were excited with a helium-neon laser at (633-nm line).

5. Results

Despite intensive research to improve therapeutic options, most pancreas carcinomas are resistant to radiotherapy (Klinkenbijl et *al*., 1999, Permert et *al*., 2001, Wanebo et *al.*, 2000). Chemotherapy and immunotherapy also did not significantly improve the overall 5 year survival rate (Staib et *al.*, 1999, Yeo and Cameron, 1999, Keleg et *al*., 2003, Westphal and Kalthoff, 2003).
A second unfortunate hallmark of pancreatic cancer is its early systemic dissemination and the extraordinary rapid local tumour progression (DiMagno, 1999). Metastasis is a major problem in the therapy of pancreatic tumours. Even if resection of the primary tumour is possible, metastatic disease often makes a curative treatment impossible and contributes to high mortality rate amongst patients with pancreatic cancer. How metastatic progression develops is unknown, and little is known on how malignant cells detach from the primary tumour site and grow in distant organs (Kim et *al*., 1998).
Previous studies have suggested a potential role for PKD in processes mediating cell shape modulation, motility, cell adhesion as well as invasion of cancer cells. These are all key processes in the metastasis of cancer and therefore important cellular functions to focus on, when searching for potential new targets for treatment of pancreatic cancer cells, which are not responding to established therapeutic regimens.
The PDAC cell lines used in this study were obtained from Prof. Dr. H. Kalthoff (Christian-Albrechts Universität, Kiel).

5.1 Characterisation of PDAC cell lines used in this study

5.1.1 Expression of PKD isoforms using qualitative RT-PCR

Since at the time this study started, no reliable isoform specific antibodies against PKD1, 2, and 3 were available, the expression of the respective isoforms was investigated by performing a qualitative RT-PCR analysis *(4.2.2)* of the different PDAC cell lines grown to approximately 80 % confluence **(Fig. 4A)**. Although the amount of transcript detected cannot be necessarily translated into protein expression, this analysis gives a first insight, which PKD isoforms may be important in the respective cell lines, and also if correlations between isoform expression and different phenotypes are possible. The PKD isoform expression in **Fig. 4A** represents 30 cycles of amplification. Qualitative RT-PCR was done according to *4.2.2*. GAPDH was included as a loading control to show the integrity of the first-strand transcripts. As seen in **Fig. 4A**, GAPDH was equally strong expressed in all cell lines, indicating that RT-reactions from the isolated total RNA were successful. PKD1 was expressed in Panc1, Panc89, Capan1, and Colo357 cells, while in the PancTuI cell line a PKD1 specific band was not clearly visible, or to faint to be visualised. Colo357 cells ectopically expressing PKD1, a vector control, as well as PCR reactions with cDNA constructs for PKD1, 2, 3 served as positive controls for the respective isoforms, while PCR reactions without template were used as negative control. PKD2 was equally strong expressed in all PDAC cell lines, while PKD3 was strongly expressed in Panc1, Panc89,

Capan1, and Colo357 cells, whereas PancTul cells only showed a weak band appearing at the appropriate length. Additional, non specific, higher molecular weight amplificates were observed, too.

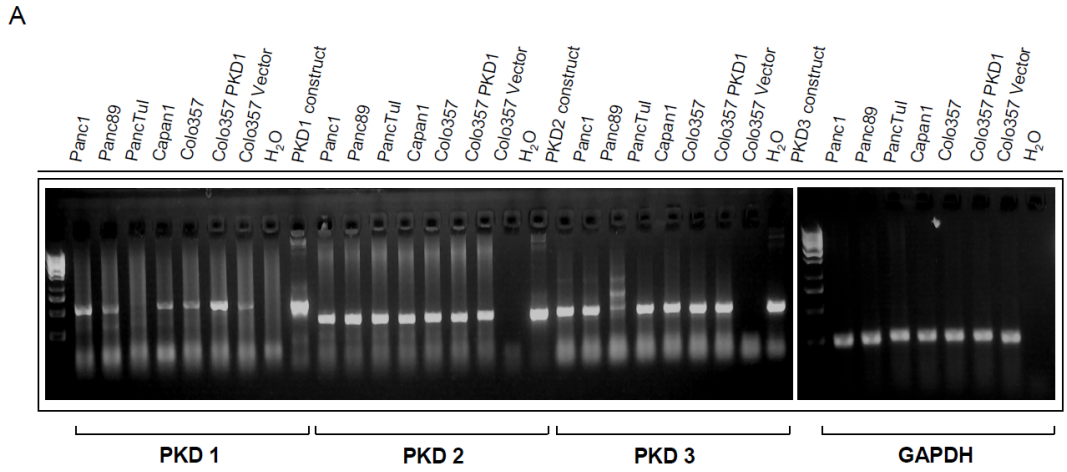

Fig. 4: Characterisation of PDAC cell lines: **(A)** Qualitative RT-PCR analysis of PKD1/2/3 isoform expression in pancreas ductal adenocarcinoma (PDAC) cell lines at 80% confluence after 30 amplification cycles. Equal amounts of total-RNA were used for reverse transcription. GAPDH was included as loading control. PCR from cDNA-constructs as well as stable Colo357 PKD1 and vector cell lines were included as positive controls, while H_20 served as a negative control. PCR amplificates were separated by 2% agarose gels. **(B)** Expression and activation state of PKD isoforms in different PDAC cell lines: 120µg total cell lysate per lane. α-Tubulin (*blot panel 4*) is included as a loading control. Pan-PKD expression is shown in *blot panel 1*; the asterisk (*) marks immunoreactive bands running not at the appropriate molecular weight to be PKD2. Active autophosphorylated PKD ($pPKD_{S910}$) is shown in *blot panel 2*, while the T-Loop phosphorylation state ($pPKD_{S738/742}$) can be seen in *blot panel 3*.

5.1.2 Expression and activation state of PKD in total cell lysates of PDAC cells

To investigate PKD protein expression and the activation status of the kinase in the different cell lines, Western blot analysis of total cell lysates from the respective PDAC cell lines was performed with the PKD selective reagents meanwhile available **(Fig. 4 B)**.

PKD expression in total cell lysates from PDAC cell lines at 80% confluence was detected using the α-PKD D20 antibody (Santa Cruz Biotechnology Inc., Santa Cruz, CA, USA) reactive against both PKD1 as well as PKD2, since there was no reliable isoform specific antibody available at that time **(*Fig. 4B*, *blot panel 1*)**. Although PKD1 (~115 kDa) and PKD2 (~105 kDa) can be separated by SDS-PAGE, is was impossible to decisively differentiate between the different isoforms in the PDAC cell lysates, taken also in consideration the different bands created by mobility shifts due to the different activations states (auto-, and transphosphorylation) of the kinases. The immunoreactive bands migrating at the appropriate

molecular weight to be either PKD1, or PKD2 were therefore labeled as PKD, a strong immunoreactive band also detected by the antibody, but not with the molecular weight required was marked by an asterisk (***Fig. 4B**, blot panel 1*). As demonstrated in the blot, Panc89 as well as PancTuI cells show a strong PKD expression followed by Capan1 and Colo357 cells with much weaker immunoreactive bands. Whether the band seen in PancTuI lysates represents PKD2, since RT-PCR analysis failed to detect visible PKD1 transcript levels, can not be decided conclusively, although it is likely to be so. Active, autophosphorylated PKD ($pPKD_{S910}$) is shown in *blot panel 2*. Compared to the other PDAC cell lines, PKD in Panc89 lysates is strongly autophosphorylated. Noticeably the $pPKD_{S910}$ band in PancTuI cells migrated at a reduced molecular weight, further emphasising the possibility that in this case PKD2 was detected. T-Loop phosphorylated, transactivated PKD ($pPKD_{S738/742}$) can be seen in *blot panel 3*. Panc89 cells also show a clearly visible transactivation of PKD in the total cell lysates, followed by Capan1, and PancTuI cells. Summarising the data from the Western blot experiments, Panc89 cells exhibit a strong PKD expression, in an active, autophosphorylated and transphosphorylated state, thereby indicating activation by upstream kinases.

In order to gain more insight in the expression of PKD isoforms in different pancreas ductal adenocarcinoma tumour samples, a qualitative RT-PCR analysis of total tumour RNA from biopsy material provided by Prof. Dr. H. Kalthoff (Christian-Albrechts Universität, Kiel) was done.

5.2 PKD isoform expression in tumour sample RNA

For each tumour sample 100 ng of total RNA were subjected to a qualitative RT-PCR *(see 4.2.2)*. The obtained tumour sample RNAs were characterised by histopathological examination as follows: Samples **15500/0** and **15909/03** were well differentiated carcinomas with normal tissue in block, while samples **19299/03**, **17323/03**, and **9511/03** were low differentiated carcinomas with strong desmoplasia and lacking apparent normal tissue in the preparation. As shown in **Fig. 5**, all samples tested, expressed detectable amounts of PKD1, 2 and 3 transcripts. GAPDH was included as a control to ensure the integrity of the used total-RNA. Yet, from the results obtained in this analysis no correlation between PKD isoform expression and differentiation as well as tumour progression state was possible. Lacking a normal pancreas control sample, further conclusions on a correlation of isoform expression with the state of tumour progression were impossible **(Fig. 5)**.

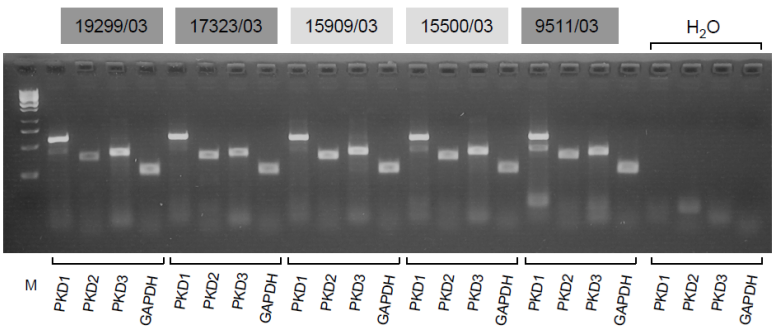

Fig. 5: Qualitative RT-PCR analysis of PKD1/2/3 isoform expression in pancreas ductal adenocarcinoma tumour samples. 100 ng of total-tumour-RNA were subjected to RT-PCR analysis using Titan-One-Tube RT-System (Roche Diagnostics). GAPDH was included as loading control while H_20 served as a negative control. PCR amplificates were separated by a 2% agarose gel. Samples **15500/0** and **15909/03**: well differentiated carcinomas with normal tissue in block; samples **19299/03**, **17323/03**, and **9511/03**: low differentiated carcinomas with strong desmoplasia, containing no normal tissue.

To investigate a potential link of PKD to cell shape modulation (van Lint et al., 2003; Riol-Blanco et *al.*, 2004), motility (Prigozhina et *al.*, 2004, Jaggi et *al.*, 2005), and invasion (Bowden et *al.*, 1999) in more detail, additional experiments were now focused on the Panc89 cells, because they exhibited a strong PKD expression in an active, autophosphorylated and transphosphorylated state **(Fig. 4B).**

Since all of the above mentioned processes are tightly linked to a rearrangement of the cellular Actin cytoskeleton (Pollard et *al.*, 2000), involving a coordinated depolymerisation of Actin filaments, *de novo* Actin nucleation and also filament branching, it was an important aim of this work, using Panc89 cells as a model, to investigate a putative function of PKD in the modulation of the Actin cytoskeleton and in the cellular behaviour/functions mentioned above. In order to obtain initial data on PKD-involvement in these processes, immunohistochemical stainings for PKD and different cytoskeletal markers were performed and subjected to confocal immunofluorescence analyses.

5.3 Immunohistochemical analysis of parental Panc89 cells

Parental Panc89 cells were costained for PKD or autophosphorylated, active $pPKD_{S910}$ and filamentous Actin (F-Actin), Arp3, Cortactin, as well as Vinculin, depending on the antibody combinations possible. F-Actin was stained using Phalloidine conjugated to Rhodamine. Phalloidine is a fungal toxin, which specifically interacts with F-Actin and thereby stabilises Actin filaments. As explained in *3.2.3* and *3.2.4*, Arp3 is a member of the Actin-related Arp2/3 protein complex, which is responsible for Actin nucleation and dendritic branching of Actin filaments. It has been shown to locate at sites of dynamic Actin assembly and motility in living cells. The marker Cortactin is enriched within lamellipodia and membrane ruffles *(see in 3.2.5)*. It was shown to bind directly to F-Actin as well as the Arp2/3 complex thereby exhibiting important functions in the organisation and remodulation of the cortical Actin cytoskeleton. Vinculin is an Actin-binding protein bound to Talin and α-Actinin (Jockusch and Isenberg, 1981; Johnson and Craig, 1995), which in turn are localised in complexes with Integrins, transmembrane proteins linking the cytoskeleton to the extracellular matrix (Nishizaka et *al.*, 2000; Kiosses et *al.*, 2001). DeMali et *al.* (2002) also showed a direct, but transient interaction of Vinculin and the Arp2/3 complex. Vinculin has been shown to be a prominent component of focal adhesions, yet the Arp2/3 complex has not been detected in these structures (Welch et *al.*, 1997; DeMali et *al.*, 2002), indicating that different cellular pools of Vinculin exist. Vinculin therefore is not only a marker for focal adhesions, it is also localised at sites of active Actin polymerisation in protrusive membrane structures, as indicated by its colocalisation and interaction with the Arp2/3 complex.

Taken all this facts in consideration, PKD was costained with the above mentioned markers and analysed by confocal microscopy.

5.3.1 Localisation of PKD with F-Actin, Cortactin and Arp3 in parental growing Panc89 cells

Panc89 cells were seeded on collagen coated cover slips and processed for immunohistochemical staining as indicated in the figure legends and *4.2.8.1/2*. In **Fig. 6A** confocal image sections of Panc89 cells were costained for PKD and F-Actin, Actin-related protein complex member Arp3, and Cortactin. Areas of colocalisation are indicated by yellow colour in overlays, respective structures were marked by white arrows. Panc89 cells stained for active $pPKD_{S910}$ and F-Actin showed a colocalisation of both proteins in membrane protrusions (*A-H*). Cortactin and PKD also colocalised in membrane protrusions and cortical Actin structures (*I-L*) and in addition active autophosphorylated $pPKD_{S910}$ localised with Arp3 at the edge of protrusive membrane structures (*M-P*), thereby indicating a possible function for the active PKD kinase at these sites.

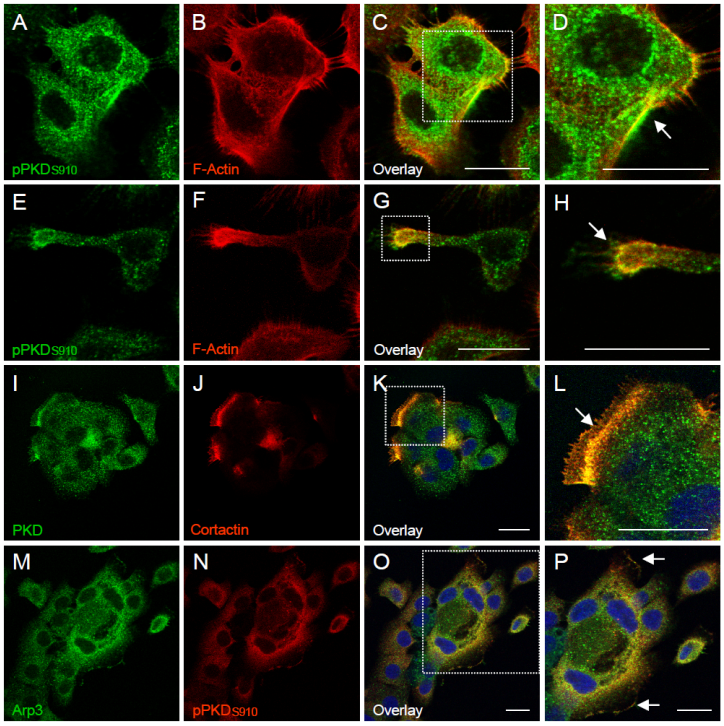

Fig. 6: **(A)** Confocal image sections of Panc89 cells stained for PKD, F-Actin, Arp3, and Cortactin. Cells were seeded at a density of 100.000 cells on Collagen IV coated cover slips in standard growth media. (A-H) Costaining of F-Actin (Phalloidine-Rhodamine) and active, autophosphorylated PKD (α-$pPKD_{S910}$). (I-L) Costaining of Cortactin and PKD. (M-P) Colocalisation of active, autophosphorylated PKD and Arp3. Images were taken by a Leica TCS SP2 confocal microscope at 100x magnification. Colocalisation in overlay images is indicated by yellow colour, respective structures are marked by a white arrow. Nuclei were stained using DRAQ5. The scale bar represents 20 µm.

Due to limitations of the antibodies used, the immunohistochemical stainings observed with Arp3 were very weak, and therefore the full extent of a colocalisation with the equally weak $pPKD_{S910}$ signal was difficult to assess. That's why in **Fig. 6B** the respective markers used in **Fig. 6A** were analysed to demonstrate both specificity and colocalisation. As expected, colocalisation of Arp3 and Cortactin in cortical structures and membrane protrusions was found **(Fig.6B**, *A-D***)**, while Arp3 and F-Actin colocalised at sites of active Actin polymerisation in lamellipodia and membrane ruffles **(Fig.6B**, *E-H***)**. Cortactin and Actin were also found to colocalise in cortical Actin-rich structures of membrane protrusions, indicating that the different markers used showed the localisation expected from published data.

Colocalisation of Arp3 in structures strongly stained for Cortactin **(Fig. 6B**, *A-D***)** suggested that sites exhibiting a colocalisation of PKD and Cortactin **(Fig. 6A**, *I-L***)** might also be Arp3 positive.

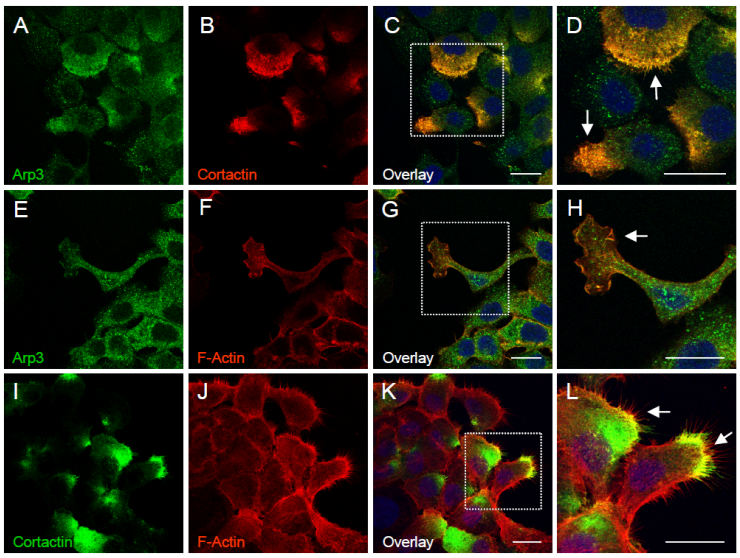

Fig. 6: **(B)** Mutual colocalisation of respective markers Arp3, Cortactin and F-Actin. Cells were seeded at a density of 100.000 cells on Collagen IV coated cover slips in standard growth media. (A-D) Colocalisation of Arp3 and Cortactin. (E-H) Costaining of Arp3 and F-Actin. (I-L) Colocalisation of Cortactin and F-Actin. Images were taken at 100x magnification. Colocalisation in overlay images is indicated by yellow colour, respective structures are marked by a white arrow. Nuclei were stained using DRAQ5. The scale bar represents 20 µm.

In order to see if the observed colocalisations could be further enhanced by an external stimulus, both activating PKD and triggering Actin cytoskeleton remodelling, in subsequent experiments PDGF-BB was used to stimulate the Panc89 cells before processing cells for immunohistochemical staining.

5.3.2 Stimulation of Panc89 cells using PDGF-BB

Engagement of PDGF-receptors has been shown to activate PKD via a DAG dependent signal pathway through receptor-mediated activation of PLCβ or γ (Van Lint et *al.*, 1998; Stafford et *al.*, 2003). In addition, PDGF is known to stimulate Src kinase signalling cascades, enhancing cell motility by reorganisation of the Actin cytoskeleton (Parsons and Parsons, 1997; Heldin *et al.*, 1998). It also induces the redistribution of cytoskeletal proteins, like Cortactin (Krueger et al., 2003). Therefore, it was postulated that PDGF treatment of Panc89 cells might give more insights into the dynamics of the PKD-Actin cytoskeleton interdependency.

For the analyses shown in **Fig. 7 A-E,** Panc89 cells were seeded on Collagen coated cover slips. After being serum-starved over night, Panc89 cells were stimulated using 30 ng/ml PDGF-BB for 10, and 30 minutes respectively, while serum-starved cells (-FCS) served as control. Following stimulation, cells were processed for immunohistochemical staining (*4.2.8.2*) with reagents specific for F-Actin, Cortactin, Arp3, and Vinculin, as well as PKD, or autophosphorylated $pPKD_{S910}$. As described previously, colocalisation in overlay images is indicated by yellow colour and respective structures were marked by arrows. The scale bar represents 20 µM. In **Fig. 7A** colocalisation of active $pPKD_{S910}$ with F-Actin was observed in serum-starved control cells (-FCS) in membrane protrusions and in membrane ruffles (*A-H*). After 10 minutes of PDGF stimulation, colocalisation was enhanced in membrane ruffles (*E-*

H), while after 30 minutes there was a strongly increased colocalisation of active PKD and F-Actin at filamentous and cortical structures in membrane protrusions as well as at the edge of protrusive membranes (*I-L*).

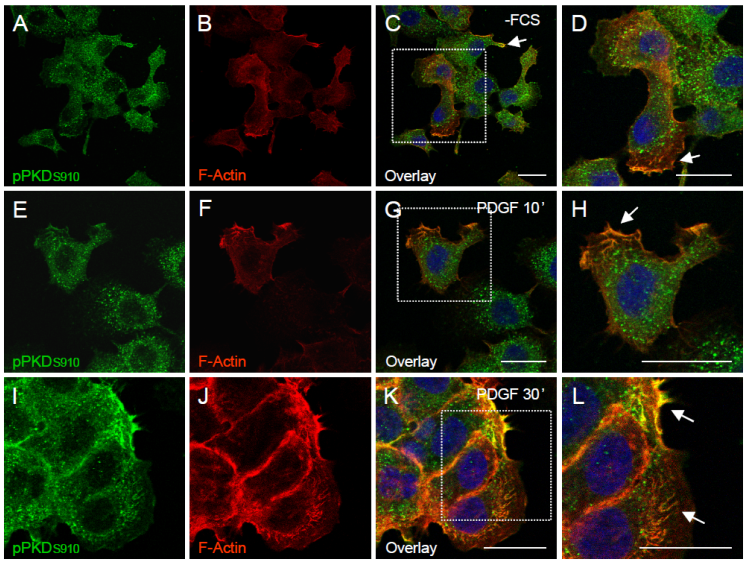

Fig. 7: **(A)** Confocal image sections of Panc89 cells costained for PKD and F-Actin (A-L). 70.000 cells were seeded on Collagen IV coated cover slips, serum starved over night and stimulated with PDGF-BB 30ng/ml for the indicated time points at 37°C. Serum starved cells (-FCS) served as a control. Cells were stained for autophosphorylated $pPKD_{S910}$ and F-Actin. (A-D) Serum starved Panc89 cells. (E-H) Panc89 cells stimulated with PDGF-BB 30ng/ml for 10 min. (I-L) Panc89 cells stimulated with PDGF-BB 30ng/ml for 30 min. Colocalisation in overlay images is indicated by yellow colour, respective structures are marked by a white arrow. Nuclei were stained using DRAQ5. The scale bar represents 20 µm

In **Fig. 7B** PKD and Cortactin showed colocalisations at membrane protrusions in serum-starved control cells (*A-D*), while after 10 minutes of stimulation colocalisation of both makers was dramatically reduced (*E-H*), accompanied by a redistribution of PKD from an extended distribution throughout the cytoplasm to a more aggregated, perinuclear cytoplasmic staining (*E*). A colocalisation of PKD and Cortactin at this time point was more or less restricted to membrane ruffles and the edge of protrusive membrane structures (*G, H*). Panc89 cells stimulated with PDGF for 30 minutes displayed again an increased colocalisation of PKD and Cortactin in membrane protrusions (*I-L*) and cortical, as well as filamentous Actin-rich structures (*O, P*).

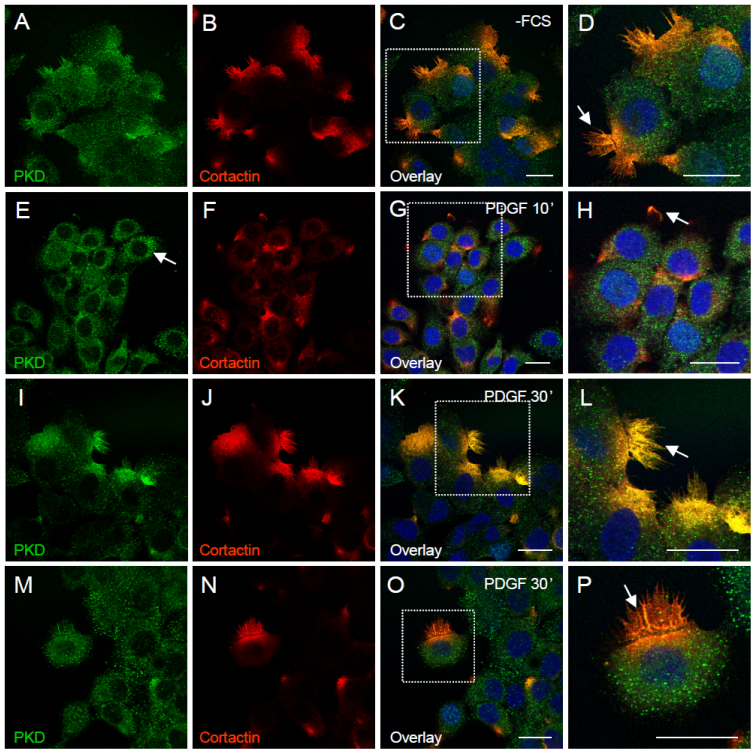

Fig. 7: **(B)** Confocal image sections of Panc89 cells stained for PKD and Cortactin (A-P). 70.000 cells were seeded on Collagen IV coated cover slips, serum starved over night and stimulated with PDGF-BB 30ng/ml for the indicated time points at 37°C. Serum starved cells (-FCS) served as a control. (A-D) Serum starved (-FCS) control. (E-H) Panc89 cells stimulated with PDGF-BB 30ng/ml for 10 min. (I-P) Panc89 cells stimulated with PDGF-BB 30ng/ml for 30 min. Images were taken at 100x magnification. Colocalisation in overlay images is indicated by yellow colour, respective structures are marked by a white arrow. Nuclei were stained using DRAQ5. The scale bar represents 20 µm.

Fig. 7C (*A-J*) shows the localisation of active $pPKD_{S910}$ in relation to Arp3. Colocalisation of both proteins was observed in control cells (*A-C*), as well as after stimulation of 10 (*D-F*), and 30 minutes (*G-J*) respectively. Although in serum-starved controls and after 10 minutes of stimulation the colocalisation was very week and limited to punctuate areas at the edge of membrane protrusions or membrane ruffles (*A-C, D-F*), Panc89 cells stimulated for 30 minutes exhibited a stronger costaining at the edge of membrane protrusions (*G-J*), yet the full extent of the colocalisation was again difficult to asses due to the overall weak staining of the antibodies used. In **Fig. 7C** (*K-V*) $pPKD_{S910}$ and Vinculin colocalisation was analysed. Serum-starved controls showed in some cells a partial colocalisation with Vinculin at the edge of protrusive membrane structures, but not at sites which presumably were focal contact points to the substrate (*L*). As demonstrated for Cortactin after 10 minutes of stimulation, a colocalisation of $pPKD_{S910}$ and Vinculin was drastically reduced and almost completely abolished (*O-R*), while after 30 minutes of PDGF treatment, costaining at the edge of membrane protrusion was enhanced again (*S-V*). $pPKD_{S910}$ staining in Vinculin-positive structures resembling focal contacts to the substratum was neither observed in serum-starved controls, nor after stimulation (*L, P, T*). This is in line with immunohistochemical stainings presented later in this work (*5.16*), which failed to show PKD colocalised with focal adhesions markers Paxillin and Focal adhesion kinase (FAK), whereby Paxillin is a marker for nascently formed focal adhesion contacts (Bryce et *al.*, 2005), while FAK is a more general marker for sites of focal adhesion (Schaller and Parsons, 1994; Calalb *et al.*, 1995; Petit *et al.*, 2000; Lamorte *et al.*, 2003; Valles *et al.*, 2004).

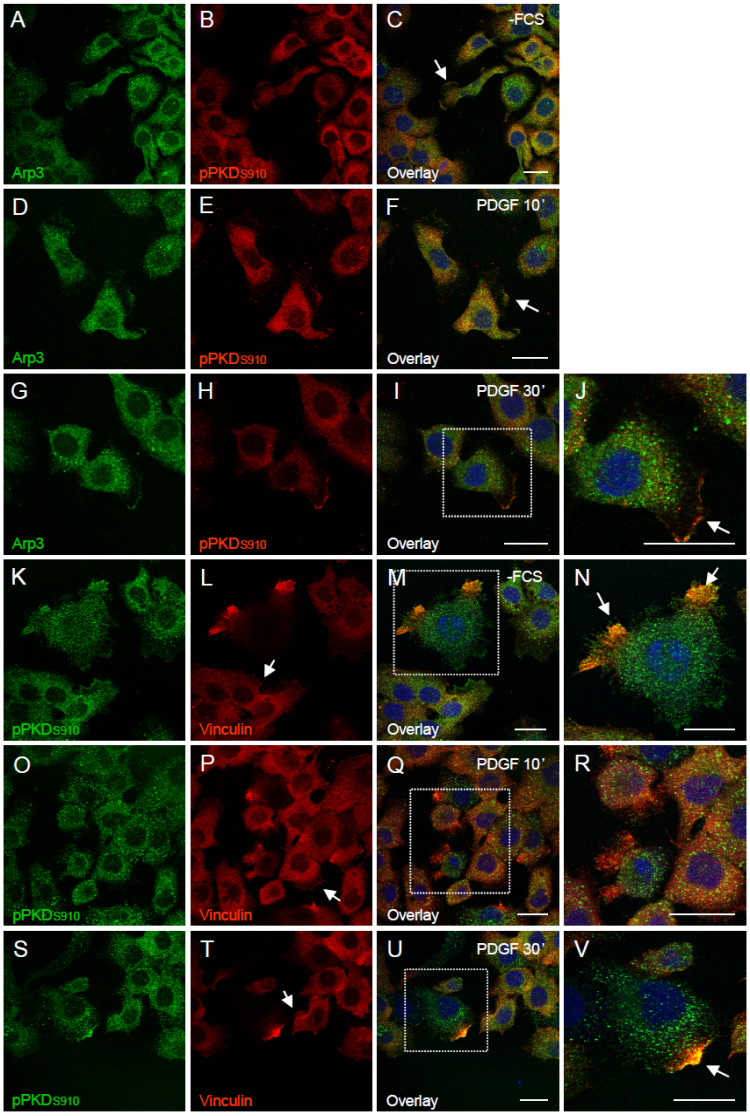

Fig. 7: **(C)** Confocal image sections of Panc89 cells stained for Arp3 and autophosphorylated $pPKD_{S910}$ (A-J) as well as for Vinculin and $pPKD_{S910}$ (K-V). 70.000 cells were seeded on Collagen IV coated cover slips, serum starved over night and stimulated with PDGF-BB 30ng/ml for the indicated time points at 37°C. Serum starved cells (-FCS) served as a control. (A-C; K-N) Serum starved (-FCS) control. (D-F; O-R) Panc89 cells stimulated with PDGF-BB 30ng/ml for 10 min. (G-J; S-V) Panc89 cells stimulated with PDGF-BB 30ng/ml for 30 min. Images were taken by a Leica TCS SP2 confocal microscope at 100x magnification. Colocalisation in overlay images is indicated by yellow colour, respective structures are marked by a white arrow. Nuclei were stained using DRAQ5. The scale bar represents 20 µm.

Fig. 7D again displays the colocalisation of markers Arp3 and Cortactin (A-*L*), as well as Arp3 an F-Actin (*M*-*T*) in Panc89 cells stimulated with PDGF. Serum-starved control cells showed colocalisation of Arp3 and Cortactin in lamellipodia and membrane ruffles (*A*-*D*). After 10 minutes of PDGF stimulation colocalisation of Arp3 and Cortactin was enhanced (*E*-*H*), yet both markers were found to be distributed more concentrated in the cytoplasm around the nucleus, only colocalising at the cell periphery in membrane ruffles at the edge of lamellipodia. After 30 minutes of PDGF treatment both markers were redistributed somewhat more to the cell periphery, staining both structures within the lamellipodia and also membrane ruffles (*I*-*L*). **In Fig. 7D** (*M*-*P*) a colocalisation of Arp3 and F-Actin was observed in some of the serum-starved control cells at membrane protrusions and ruffles, while after 30 minutes of PDGF stimulation the colocalisation was strongly enhanced, with some cells exhibiting almost a complete colocalisation of Arp3 and F-Actin (*Q*-*T*). This strongly intensified colocalisation is in line with the role of PDGF in triggering Actin polymerisation and also remodelling of the Actin cytoskeleton. In addition, structures strongly stained for Cortactin were again found to be Arp3-positive (*A*-*L*), supporting the earlier assumption that

sites which display a colocalisation of PKD with Cortactin **(Fig. 7B)** might also be Arp3 positive.

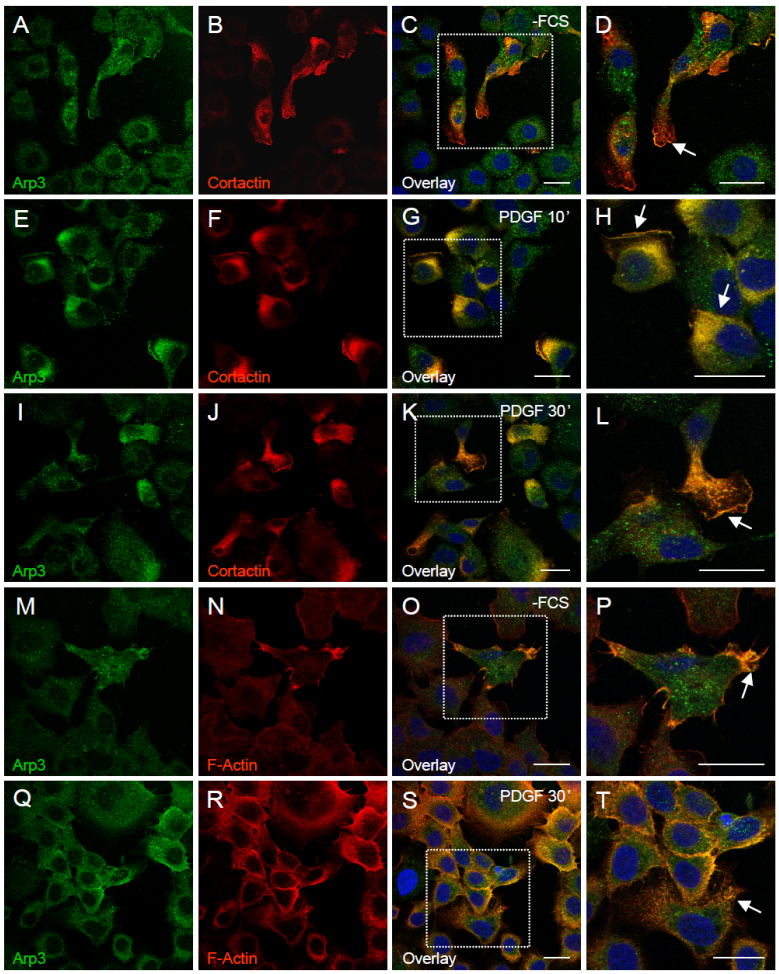

Fig. 7: **(D)** Confocal image sections of Panc89 cells. Mutual colocalisation of respective markers Arp3 and Cortactin (A-L) as well as Arp3 and F-Actin (M-T) in PDGF stimulated and control cells. 70.000 cells were seeded on Collagen IV coated cover slips, serum starved over night and stimulated with PDGF-BB 30ng/ml for the indicated time points at 37°C. Serum starved cells (-FCS) served as a control. (A-D; M-P) Serum starved (-FCS) control cells. (E-H) Panc89 cells stimulated with PDGF-BB 30ng/ml for 10 min. (I-L; Q-T) Panc89 cells stimulated with PDGF-BB 30ng/ml for 30 min. Images were taken at 100x magnification. Colocalisation in overlay images is indicated by yellow colour, respective structures are marked by a white arrow. Nuclei were stained using DRAQ5. The scale bar represents 20 µm.

In **Fig. 7E** (*A-I*) the activation and redistribution of PKD during PDGF stimulation was assessed by costaining active $pPKD_{S910}$ and GM130, a 130 kDa structural element of the Golgi apparatus (Nakamura et *al.*, 1997). GM130 was used as a marker to indicate PKD redistribution to the Golgi compartment. Immunohistochemical stainings were subsequently analysed by confocal microscopy using identical settings of PMT and Offset to compare the obtained results. Images (*A-C*) show the basal state of PKD activation in serum-starved Panc89 cells, with only small amounts of autophosphorylated PKD localised at the Golgi, as indicated by colocalisation with GM130 in some cells (*A-C*). After 10 minutes of PDGF stimulation the overall $pPKD_{S910}$ signal was enhanced and increased amounts of autophosphorylated PKD were seen both at the Golgi, colocalised with GM130, and in the cytoplasm. When compared with serum-starved cells, the cytosolic PKD also seemed to be redistributed, appearing more concentrated in clustered, dot-like structures, no longer extending to the periphery of the cell (*D-E*). After 30 minutes of stimulation $pPKD_{S910}$ still was detected in dot-like structures, but seemed to be somewhat more redistributed throughout the cytoplasm towards the cell periphery (*G-I*). Golgi localised PKD staining, evident from colocalisation with the Golgi marker GM130, remained high, indicating that PKD, once located and activated at the Golgi, stays in place (*G-I*). This is in line with previous data

published by Hausser et *al.* (2002) demonstrating that Golgi-localised PKD, subsequent to activation by upstream kinases at the Golgi compartment, is not exchanged with the cytoplasmic PKD pool.

Summarising data from **Fig. 7E**, autophosphorylation of both, cytoplasmic and Golgi-localised PKD was increased upon PDGF stimulation for 10 minutes, indicating activation of the kinase. Active PKD in the cytoplasm was initially clustered in dot-like structures, while 30 minutes after stimulation $pPKD_{S910}$ was redistributed again more widley throughout the entire cytoplasm, with Golgi localized, active PKD remaining at this compartment.

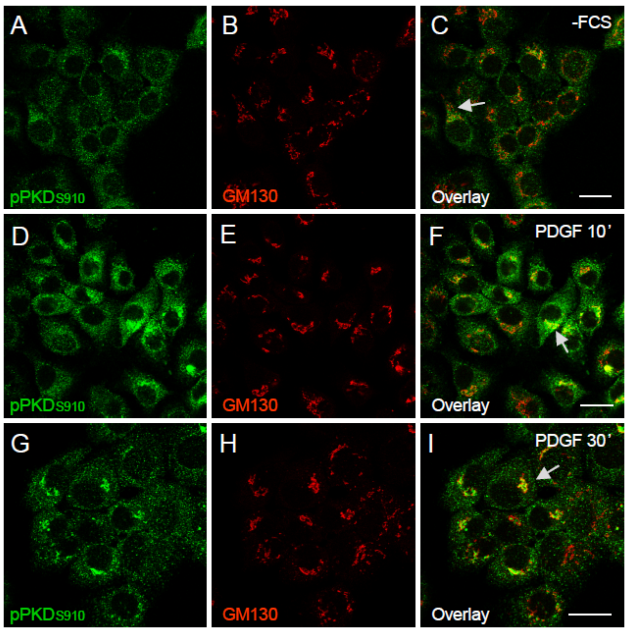

Fig. 7: **(E)** Confocal image sections of Panc89 cells stained for GM130 and autophosphorylated $pPKD_{S910}$ (A-I). 70.000 cells were seeded on Collagen IV coated cover slips, serum starved over night and stimulated with PDGF-BB 30ng/ml for the indicated time points at 37°C. Serum starved cells (-FCS) served as a control. (A-C) Serum starved (-FCS) control. (D-F) Panc89 cells stimulated with PDGF-BB 30ng/ml for 10 min. (G-I) Panc89 cells stimulated with PDGF-BB 30ng/ml for 30 min. Images were taken by a Leica TCS SP2 confocal microscope at 100x magnification using identical PMT and Offset settings to compare $pPKD_{S910}$ auto-phosphorylation in the different samples. Colocalisation in overlay images is indicated by yellow colour, respective structures are marked by a white arrow. The scale bar represents 20 µm.

PDGF stimulation of Panc89 cells also increased the colocalisation of active PKD with F-Actin in cortical and filamentous structures as well as at the edge of membrane protrusions and in ruffles **(Fig. 7A)**. Further, upon PDGF stimulation, time dependent changes in the colocalisation of PKD with Cortactin were noted. Thus, whereas after 30 minute stimulation enhanced colocalisation with Cortactin **(Fig 7B**, *I-L***)** was found in lamellipodia, PDGF stimulation for 10 minutes dramatically reduced the colocalisation of PKD with Cortactin **(Fig 7B**, *E-H***)**. The images point to a redistribution of both proteins at that time point of the stimulation. The same pattern applied for the colocalisation of PKD with Vinculin **(Fig 7C**, *K-V***)**, since after 10 minutes of PDGF treatment colocalisation of PKD and Vinculin was almost completely abolished *(O-R)*. After 30 minutes, PKD and Vinculin colocalised at the edge of membrane protrusions, yet a colocalisation in mature focal contacts was not visible, indicating that the colocalisation with Vinculin does not necessarily point to a putative function of PKD in focal contact structures. The enhanced colocalisation of PKD and Vinculin at the edge of membrane protrusions **(Fig. 7C**, *S-V***)** are therefore rather compatible with data published by DeMali et *al.* (2002), demonstrating a localisation of Vinculin at sites of active Actin remodelling and also implying a transient interaction with the Arp2/3 complex. Due to inherent limitations of the antibodies used, the colocalisation between active $pPKD_{S910}$ and Arp3 in **(Fig. 7C,** *A-J***)** could not be demonstrated to the full extent, yet there seemed to

be an enhanced costaining of both proteins at the edge of membrane protrusions after 30 minutes of PDGF stimulation *(G-J)*. In performing a side-by-side colocalisation of the markers Arp3 and Cortactin, Arp3 staining was found at almost all structures positive for Cortactin **(Fig. 7D,** *A-L***)**, bearing in mind that also PKD was found to colocalise extensively with Cortactin **(Fig. 7B,** *A-P***)**, this points to a much broader overlapping of PKD and Arp3 staining patterns. Taken together, the data obtained so far suggests a putative function for PKD at the F-Actin cytoskeleton, possibly at sites of active Actin remodelling in the cortical Actin network of membrane protrusions, as indicated by the colocalisation with the markers Cortactin, Vinculin, and Arp3.

5.4 Direct binding of PKD to F-Actin *in vitro*

For some PKCs, e.g. PKCδ, PKCε, PKCβII and PKCζ (Lopez-Lluch et *al*, 2001; Prekeris et *al.*, 1998; Blobe et *al.*, 1996; Gomez et *al*., 1995) it has been previously demonstrated that they do not only colocalise with F-Actin, but in fact they directly bind to F-Actin *in vitro*. In contrast, to date, PKD has never been implicated in F-Actin binding or associated with a functional role at the F-Actin cytoskeleton. Screening the PKD sequence for known F-Actin binding motifs, as published by Maciver (1995) or those described for PKCε (LKKQET) by Prekeris et *al.* (1998), revealed no obvious similarities. In order to investigate if the observed colocalisation of PKD with F-Actin is due to an indirect recruitment via interaction within multiprotein complexes at these sites, or by direct binding to the F-Actin cytoskeleton, F-Actin cosedimentation assays were performed *(4.2.7.6)*. In these so called Spin-down assays 5 µM polymerised, purified F-Actin was incubated with either ectopically expressed PKD and control lysates from HEK 293T, respectively, or with purified proteins. Subsequently, samples were subjected to 100.000 g ultracentrifugation separating the polymeric F-Actin fraction with bound interaction partners from the supernatant. Both fractions were normalised, separated via SDS-PAGE and respective proteins were detected by Western blotting. As shown in **Fig. 8A**, both, PKD1 as well as PKD1KD (kinase-dead, K612W), expressed without any tags possibly interfering with the assay, bind to F-Actin *in vitro*. In addition, untagged PKD2 was found to cosediment with F-Actin in Spin-down assays, too (Fig. 8A). The known F-Actin-binding protein Cortactin (Daly, 2004; Weed et *al.*, 2000) was used as positive control, while GFP served as respective negative control for the assays. **Fig. 8B** displays F-Actin cosedimentation assays performed with purified PKD1 and PKD1KD. 1 µg of purified protein was incubated with 5 µM F-Actin. Both purified proteins, PKD1 and PKD1KD, were observed in the pellet fractions, thereby indicating that PKD1 directly binds to F-Actin *in vitro*, independent of its kinase activity. To map the region responsible for mediating PKD binding to F-Actin, several PKD deletion mutants as indicated in **Fig. 8C/D** were subjected to F-Actin cosedimentation assays. A PKD1 mutant with a deletion of amino acids 1-340 (PKD1Δ340-GFP) almost completely failed to cosediment with the pelleted F-Actin fraction, thereby indicating that the deleted amino acids are involved in F-Actin binding. Since the PKD1ΔCRD-GFP mutant still bound to F-Actin, the region responsible was initially mapped to amino acids 1-146. By employing two additional deletion constructs, PKD1Δ1-79 and PKD1Δ1-98, which still dispayed F-Actin binding in this assay, the N-terminal hydrophobic

region and the amino acids up to position 98 could be excluded from being directly involved in F-Actin binding. Accordingly, the putative Actin-binding motif of PKD1 resides within amino acid 99 to 146. In **Fig. 8D**, a sequence alignment for the human isoforms of PKD1, 2, and 3 from amino acids 98-146 is shown. Assuming that binding of PKD to F-Actin is conserved amongst isoforms, as shown for human PKD1 and 2 **(Fig. 8A)**, similar motifs in this sequence region were highlighted in red letters. Using these conserved motifs, peptide competition in spin-down assays can be applied in future studies to narrow PKD down sequences involved. Analysis of the PKD1Δ1-98 deletion mutant in relation to PKD1Δ1-79 indicated a distinct reduction of PKD cosedimented in the pellet fraction of PKD1Δ1-98, pointing to F-Actin binding motifs being located nearby. The binding of PKD to F-Actin in the Δ1-98 mutant however was not completely blocked, as seen for PKD1Δ340-GFP, rather suggesting that the F-Actin binding motif was not missing, but probably compromised. A comparison of PKD1ΔCRD-GFP with PKD1-GFP revealed PKD1ΔCRD-GFP was still efficiently binding to F-Actin, although cosedimentation with the pellet fraction seemed to be somewhat reduced, yet not as strong as for the Δ1-98 mutant. Summarising the data from the cosedimentation assays, the PKD F-Actin binding region was mapped to 46 amino acids from position 99-146, with respective binding motifs likely being located closer to the sequence position 99, than to position 146. Respective PKD mutants can be constructed to precisely identify the Actin binding motif in PKDs. By discovering PKD as a novel F-Actin binding protein and its restricted localisation to cortical F-Actin structures and not to stress fibers, it is very likely that PKD is involved in processes regulating cytoskeletal remodelling. This finding has implications on PKD's potential role in cell motility and directed cell migration.

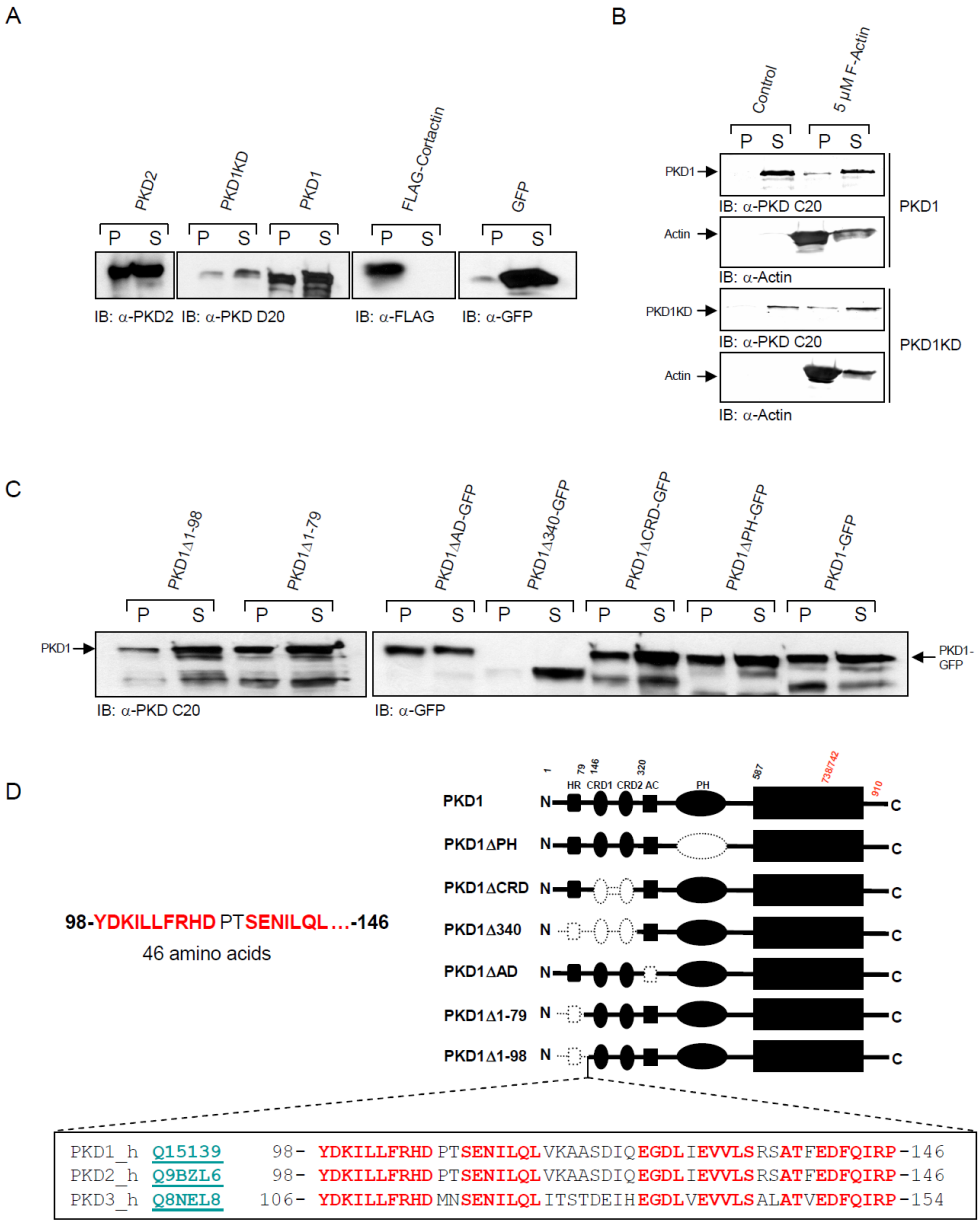

Fig. 8: **(A)** F-Actin cosedimentation assays using PKD1, PKD1KD and PKD2 from HEK 293T total cell lysates (TCL). GFP-Vector and FLAG-Cortactin were included as negative and positive controls respectively. Assays were adapted from Weed et *al.* (2000). F-Actin was removed from TCLs by 100.000 g ultracentrifugation. 50 µg of total protein was incubated with 5 µM F-Actin (AKL99, Cytoskeleton Inc., Denver, USA) for the different F-Actin binding assays. After ultracentrifugation (100.000 g) supernatant and pellet were fractionated and normalised fractions were analysed by SDS-PAGE and Western blotting against the respective proteins. **(B)** F-Actin cosedimentation assays using PKD1 and PKD1KD purified proteins. 1 µg of purified protein was incubated with 5 µM F-Actin for binding assays. After ultracentrifugation supernatant and pellets were again fractionated and analysed by SDS-PAGE and Western blotting against PKD. Assays without F-Actin were included as respective controls **(C)** F-Actin cosedimentation assays to map the F-Actin binding domain of PKD1 using total cell lysates of PKD1-GFP and respective PKD1-GFP deletion mutants, pCDNA3Δ1-79 as well as pCDNA3Δ1-98 constructs indicated in the figure. After removal of the cellular F-Actin cytoskeleton, 50 µg of total protein was incubated with 5 µM F-Actin for the respective F-Actin binding assays. Following ultracentrifugation, fractions were analysed by SDS-PAGE and Western blotting against GFP or PKD respectively. S, Supernatant; P, pellet fraction. **(D)** Schematic representation of PKD1 molecular architecture and domains deleted in the mutant constructs (*dotted white line*) used to map the PKD1 F-Actin-binding domain. *Lower panel*: Sequence alignment of PKD1, 2, 3 human (_h) showing the region responsible for F-Actin binding (PKD1: amino acids 98-146). Conserved motifs in all isoforms are marked in red letters.

5.5 Creation of stable Panc89 cell lines expressing PKD1 and PKD2 wildtype and kinase-dead constructs

To further analyse the *in vivo* function of PKD at the F-Actin cytoskeleton and potential consequences on cell motility, stable Panc89 cell lines expressing PKD1-GFP, PKD1KD-GFP (K612W), PKD2-GFP, and PKD2KD-GFP (K580W) were created. The Panc89 cells were transfected with the indicated constructs and subjected to selection using G418 1mg/ml until cells stopped dying and single clones started to grow. The surviving clones were pooled and subjected to multiple rounds of cell sorting to enhance GFP-expressing cells. Following establishment of stable, growing Panc89 cell lines, the cells were analysed by flow cytometry to determine GFP-expression as shown in **Fig. 9A**. GFP fluorescence in the FL1LOG histograms was plotted relative to the parental Panc89 cells *(A-E)*. All stable cell lines displayed strong GFP-fluorescence, indicating a good expression of tagged transgenes. In addition, cell lines were also analysed by Western blotting. In **Fig. 9B** *blot panel 1* ectopically expressed PKD-GFP fusion proteins were detected using a α-GFP antibody. α-Tubulin was included as a loading control (*blot panel 2, 4, 6*). PKD-GFP autophosphorylation was determined by detecting $pPKD_{S910}$. As expected, wildtype PKD proteins showed strong autophosphorylation, while for kinase-dead PKD1KD and PKD2KD only weak background staining was observed (*blot panel 3*). Activation loop phosphorylation of transgenes was detected using α-$pPKD_{S738/742}$ (*blot panel 5*). PKD1-GFP, as well as PKD1KD-GFP, and PKD2-GFP were transphosphorylated, while PKD2KD-GFP was not stained, possibly indicating a differential activation or localisation of isoforms in the Panc89 cell lines.

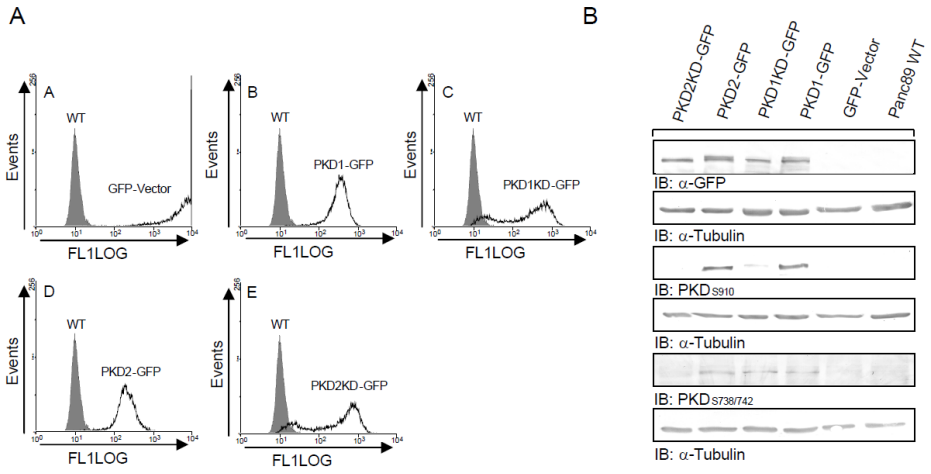

Fig. 9: Characterisation of stable Panc89 cell lines expressing GFP, PKD1-GFP, PKD1KD-GFP, PKD2-GFP and PKD2KD-GFP. **(A)** GFP fluorescence of respective stable Panc89 cell lines: 10.000 cells were analysed by flow cytometry. (A-E) FL1-Log histograms of the GFP expressing cell lines blotted against parental Panc89 control cells. **(B)** Expression and activation state of the respective stable Panc89 cell lines: 50µg total cell lysate per lane. α-Tubulin is included as a loading control (*blot panel 2, 4, 6*). *Blot panel 1*: Transgene expression level detected by α-GFP antibody. The molecular weight of GFP alone was to small to be visualized together with GFP-tagged PKD in the used SDS-PAGE. *Blot panel 3*: PKD autophosphorylation ($pPKD_{S910}$), *blot panel 5*: PKD activation loop phosphorylation state ($pPKD_{S738/742}$).

5.6 Functional Characterisation of stable Panc89 cell lines expressing GFP, PKD1-GFP, PKD1KD-GFP, PKD2-GFP and PKD2KD-GFP

5.6.1 Proliferation of the stable cell lines

In order to further characterise the established stable Panc89 cell lines, proliferation assays **(Fig. 9C)** were performed. The proliferation of the cells was assayed by seeding cell lines in 96 well plates at the appropriate density to be within the linear range of proliferation (5.000 cells/well; *4.2.6.9*). At time points T0, T24, T48 h cells were subjected to crystal violet vitality staining and cell density was measured at OD 550 (*4.2.6.10*). Calculated doubling times for the respective cell lines (*4.2.6.10*) range from close to 16 h for PKD1-GFP to 21 ½ h for GFP-Vector cells **(Fig. 9C)**, with differences for respective wildtype and kinase-dead variants of PKD1 as well as PKD2 of about 2h. All PKD transfectants grew faster then vector control, but there was no apparent correlation with PKD function detectable. In conclusion, when evaluating these results, there were subtle differences in the proliferation of the stable cell lines, which appear, however neglectable for short term cultures, as e.g. for the planned migration assays.

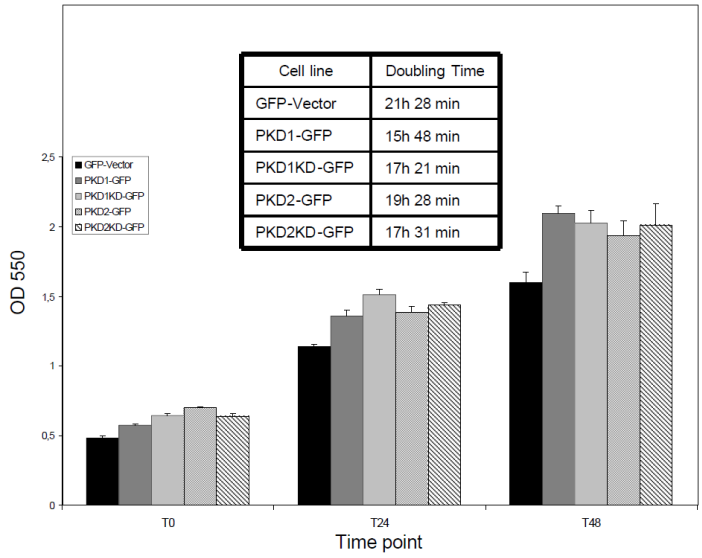

Fig. 9C: Proliferation assays using stable Panc89 cell lines. 5.000 cells were seeded in triplicate wells of three 96 well TC-plates in standard growth media to be within linear range of proliferation. Cells were cultured for 40 h with daily medium exchange then the T0 h plate was subjected to crystal violet staining to determine cell density at OD 550. T24 h and T48 h plates were also stained at the respective time points and cell density was quantified by calculating OD 550 means of triplicate wells as well as respective standard deviations for each cell line and dilution assayed. In order to calculate doubling times, linear equations of growth curves were extrapolated using EXCEL trend line function. Subsequently doubling times for the respective cell lines were calculated using the given linear regression terms.

The established stable Panc89 PKD cell lines were subsequently analysed by confocal immunofluorescence microscopy for PKD localisation in particular focussing on interactions with the F-Actin cytoskeleton

5.6.2 Immunohistochemical analysis of stable Panc89-PKD cells

In order to investigate if the ectopically expressed PKD-GFP variants colocalise with the same cytoskeleton components identified in parental Panc89 cells, cell lines were seeded on Collagen-coated cover slips and subjected to immunohistochemical analysis. As shown in **Fig. 9D**, Panc89 cell lines expressing GFP (*A-D*), PKD1-GFP (*E-H*), PKD1KD-GFP (*I-L*),

PKD2-GFP (*M-P)*, and PKD2KD-GFP (*Q-T*) were stained for F-Actin. Due to the strong ectopic expression of GFP-tagged PKD isoforms, it was, however, very difficult to obtain convincing confocal images. Panc89 cells expressing PKD1-GFP displayed a colocalisation with F-Actin at the edge of membrane protrusions and in ruffles (*E-H*). PKD1KD-GFP colocalised with F-Actin at the edge of membrane protrusions, too (*I-L*). When compared to PKD1-GFP, costaining of PKD2-GFP with F-Actin was not as evident (*M-P*), yet there were areas at the edge of membrane protrusions were both proteins were observed. Investigating Panc89 cells expressing PKD2KD-GFP, only minor areas at the edge of membrane protrusions exhibited a costaining with F-Actin, thus making it very difficult to observe colocalisations at all (*Q-T*). Taken together, PKD1- as well as PKD1KD-GFP were conclusively shown to colocalise with F-Actin, while for the PKD2 constructs the interpretation of data was difficult.

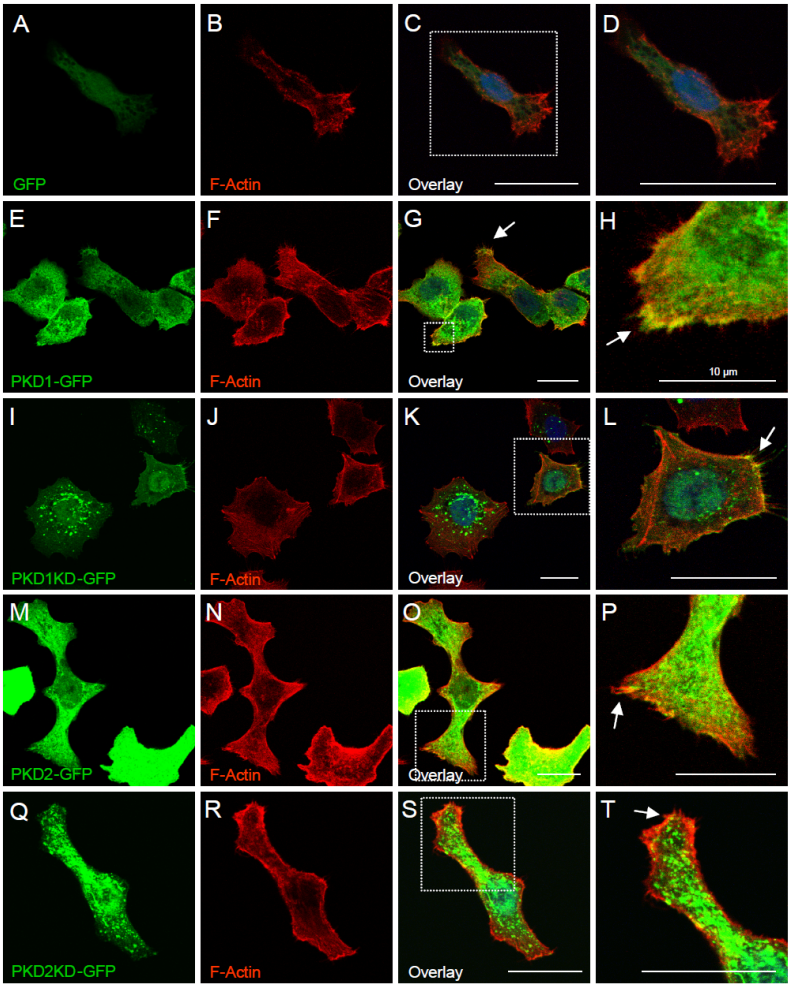

Fig. 9: **(D)** Characterisation of respective stable Panc89 cell lines using confocal immunofluorescence analysis. Image sections of stable Panc89 cells expressing GFP (A-D), PKD1-GFP (E-H), PKD1KD-GFP (I-L), PKD2-GFP (M-P), PKD2KD-GFP (Q-T). Cells were seeded at a density of 100.000 cells on Collagen I coated cover slips. F-Actin was stained using Phalloidine-Rhodamine, nuclei were stained with DRAQ5. Colocalisation in overlay images is indicated by yellow colour and white arrows. Images were taken at 100x magnification. The scale bar represents 20 µm, except for (G, H): 10 µm.

Fig. 9E shows Cortactin staining of stable PKD transfected Panc89 cells. Cells expressing PKD1-GFP (*D-F*) showed a colocalisation with Cortactin at the edge of membrane protrusions and in membrane ruffles. PKD1KD-GFP displayed costaining with Cortactin in membrane protrusion (*G-I*), though they were not as evident as for PKD1-GFP. PKD2-GFP colocalised with Cortactin at the edge of membrane protrusion (*J-L*), while costaining for PKD2KD-GFP with Cortactin (*M-O*) in membrane protrusions again was very weak. These

relatively weak colocalisations in stable cell lines expressing kinase-dead mutants of PKD can be explained due to a prominent localisation of the kinase-deficient fusion proteins in fragmented Golgi structures, whereas only small amounts of kinase-dead PKD were visible in the cytoplasm. In order to visualise this cytoplasmic pool of kinase-dead PKD at all, signals during the acquisition of confocal images had to be strongly intensified, thereby making it very difficult to evaluate the resulting images.

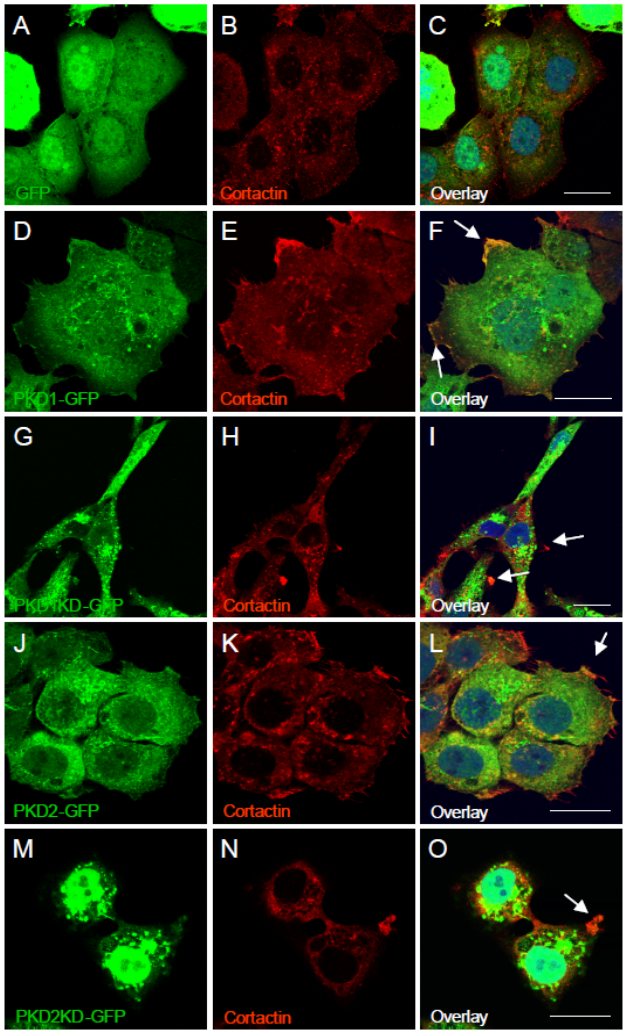

Fig. 9: **(E)** Confocal image sections of respective stable Panc89 cell lines stained for Cortactin: GFP (A-C), PKD1-GFP (D-F), PKD1KD-GFP (G-I), PKD2-GFP (J-L), PKD2KD-GFP (M-O). Cells were seeded at a density of 100.000 cells on Collagen IV coated cover slips. Nuclei were stained with DRAQ5. Colocalisation in overlay images is indicated by yellow colour and a white arrow. Images were taken at 100x magnification. The scale bar represents 20 µm.

To reveal a potential colocalisation of Cortactin-GFP with autophosphorylated-, or transphosphorylated, active PKD, stable Panc89 cell lines expressing Cortactin-GFP were created. Therefore, Cortactin transcript variant 1 (NM_005231) was amplified from Panc89 cDNA and cloned into respective FLAG- as well as GFP-Vectors (*4.2.4*). The expression of the tagged fusion proteins was assessed by transient transfection in HEK 293T cells, followed by Western blotting against Cortactin as well as the respective tags (data not shown). Parental Panc89 cells were transfected with Cortactin-GFP and subjected to selection using G418 1mg/ml. GFP-expressing cells were enhanced by performing multiple rounds of cell sorting, thereby creating a stable Panc89 cell line expressing Cortactin-GFP. Cortactin-GFP cells were seeded on Collagen coated cover slips and processed for

immunohistochemical staining. As expected, Cortactin-GFP in **Fig. 9F** was localised in the cytoplasm and enriched in membrane protrusions as well as in membrane ruffles (*P-X*). Costaining with autophosphorylated $pPKD_{S910}$ also was visible at structures in membrane protrusions as well as in membrane ruffles (*P-R, S-U*). Transphosphorylated $pPKD_{S738/742}$ also colocalised at the edge of membrane protrusions (*V-X*), yet due to limitations of the antibodies used to detect auto- as well as transphosphorylated PKD, both signals were very weak. In conclusion, summarising the data from the immunohistochemical analysis of the stable Panc89 cell lines obtained so far, PKD1- as well as PKD1KD-GFP were shown to colocalise notably with F-Actin and Cortactin, while a clear colocalisation for PKD2-GFP was only observed with the marker Cortactin. Taken together, these data suggest a putative role for PKD1, and maybe also PKD2, at sites positive for F-Actin and Cortactin. In addition Panc89 cells expressing Cortactin-GFP displayed a costaining with both, auto- as well as transphosphorylated PKD, further pointing to an involvement of active PKD at sites of Actin remodelling.

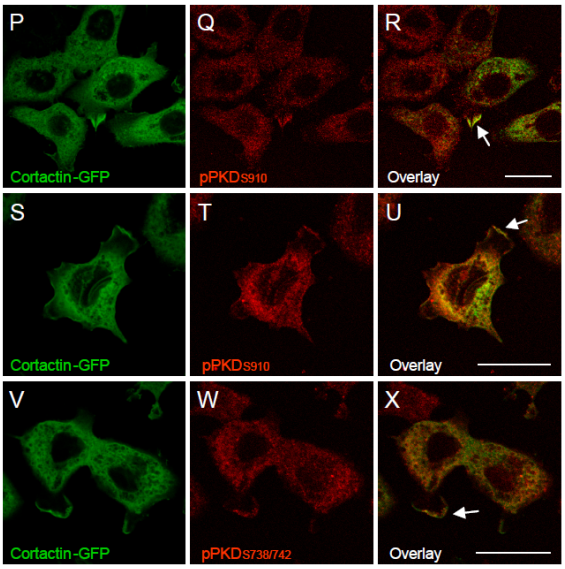

Fig. 9: **(F)** Confocal image sections of stable Panc89 cells expressing Cortactin-GFP (P-X). PKD was stained with α-PKD_{S910} (P-U) and α–$PKD_{S738/742}$ (V-X) antibodies respectively. Colocalisation in overlay images is indicated by a white arrow. Images were taken at 100x magnification. The scale bar represents 20 µm.

To investigate if PKD could also be involved in the organisation of other cytoskeletal components, e.g. Tubulin **(Fig. 10A)**, immunohistochemical stainings using a α-Tubulin antibody were done in the stable Panc89 cells expressing GFP (*A-C*), PKD1-GFP (*D-F*), PKD1KD-GFP (*G-I*), PKD2-GFP (*J-L*) and PKD2KD-GFP (*M-O*). No apparent changes were found in the Tubulin cytoskeletal network of the different cell lines and also no decisive colocalisation with Tubulin was observed in these cells **(Fig. 10A, A-O)**, arguing against a direct function of PKD at the Tubulin cytoskeleton. To further map the intracellular distribution of the ectopically expressed PKD variants, Panc89 transfectants were costained with TGN46, a marker protein for the trans-Golgi Network (TGN) **(Fig. 10B)**. Both, PKD1-GFP as well as PKD2-GFP showed overlapping staining patterns with TGN46, yet due to the massive overexpression of fusion proteins and distribution throughout the cell, often including nuclear staining, no conclusions as to the functional relevance of a costaining with TGN 46 could be done if it would be based on such data only. As shown for (*I-L*) and (*Q-T*), PKD1KD-

and PKD2KD-GFP, respectively, fluorescence signals were strongly clustered in tubular or vesicular structures and showed prominent colocalisation with TGN46, expected from the known role of dominant negative PKDKD in TGN fragmentation. It is inferred from these data that despite overexpression and potential mislocalisation, PKD also homes to its normal, physiological target structures in the cell.

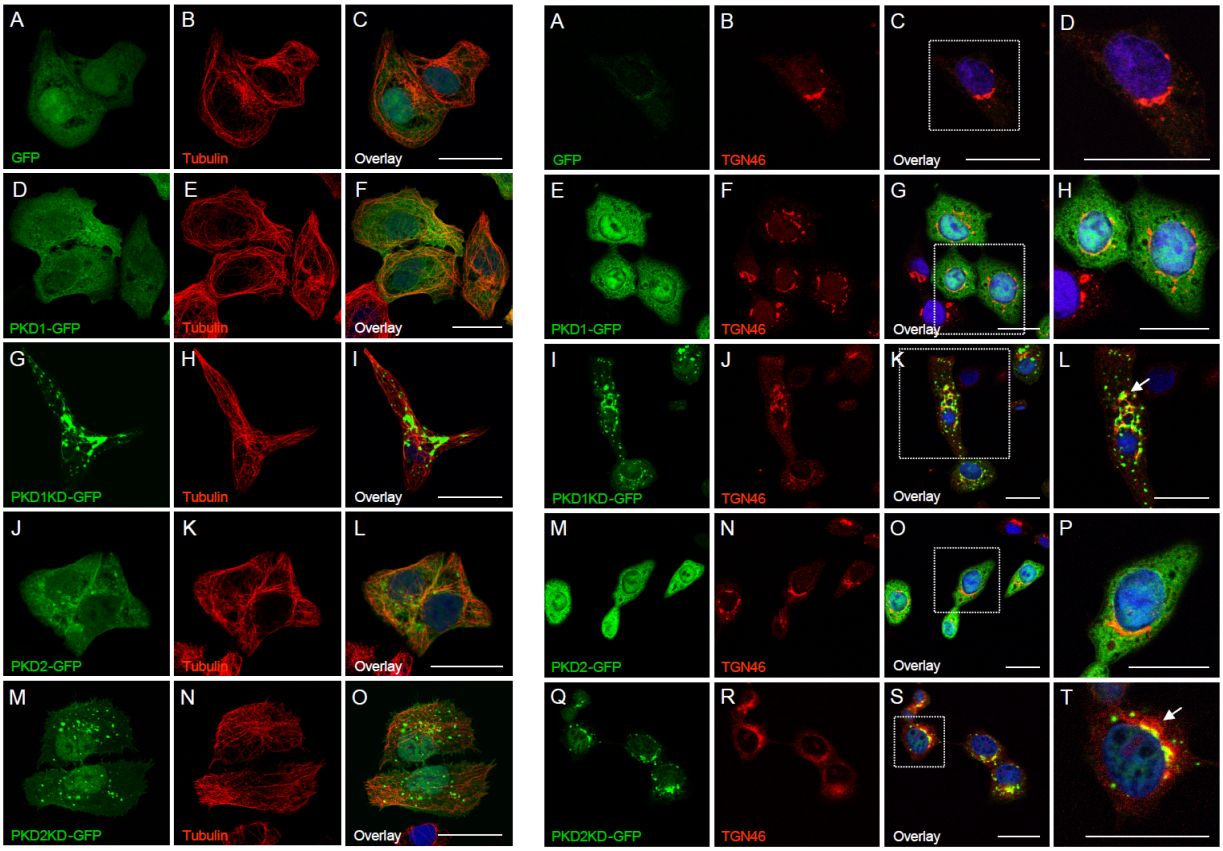

Fig. 10: Further characterisation of respective stable Panc89 cell lines using confocal immunofluorescence analysis. **(A, *left hand panel*)** confocal image sections of stable Panc89 cell lines stained for α-Tubulin: GFP (A-C), PKD1-GFP (D-F), PKD1KD-GFP (G-I), PKD2-GFP (J-L), PKD2KD-GFP (M-O). Cells were seeded at a density of 100.000 cells on Collagen I coated cover slips. Nuclei were stained with DRAQ5. Images were taken at 100x magnification. The scale bar represents 20 µm. **Fig. 10**: **(B, *right hand panel*)** image sections of the stable cell lines stained for TGN46: GFP (A-D), PKD1-GFP (E-H), PKD1KD-GFP (I-L), PKD2-GFP (M-P), PKD2KD-GFP (Q-T). Cells were seeded at a density of 100.000 cells on Collagen I coated cover slips. Following fixation using Methanol/Aceton, cells were processed for immunohistochemistry. Nuclei were stained with DRAQ5. Colocalisation in overlay images is indicated by yellow colour and a white arrow. Images were taken at 100x magnification. The scale bar represents 20 µm.

Analysing the immunohistochemical data from parental as well as stable Panc89 cells, PKD was shown to localise at the cortical F-Actin cytoskeleton and in Actin-rich structures in membrane protrusions, possibly at sites of active Actin remodulation. Colocalisation with respective markers in stable Panc89 cells expressing PKD1- and PKD1KD-GFP was independent of PKD kinase activity. In addition, PKD1 was shown to physically bind to F-Actin *in vitro*, again independent of kinase function, thereby arguing for a putative role of PKD in the regulation of processes involving Actin remodelling. Since both binding to F-Actin, as well as colocalisation with markers at possible sites of PKD action was independent of

kinase activity, PKD-KD variants might be able to act as dominant negative regulators in processes controlled by PKD kinase activity at the F-Actin cytoskeleton.

5.7 Analysis of directed cell migration of stable Panc89 cell lines employing 3D-Transwell migration assays

The modulation of the F-Actin network is a tightly regulated and highly dynamic process. Interference with these functions has serious implications on cell motility, directed migration and also cell adhesion. In order to investigate whether expression of the different PKD isoforms and their respective kinase-dead mutants in Panc89 cells may influence cell migration, 3D migration assays were performed utilising Transwell filter inserts with 8 µm pore diameter (*4.2.6.4*). Parental, as well as stable Panc89 cell lines expressing GFP, PKD1-GFP, PKD1KD-GFP, PKD2-GFP, and PKD2KD-GFP were seeded at equal densities and migration of cells towards an FCS gradient was determined after 40 hours as described in methods (*4.2.6.4*). **Fig. 11A** is representative of at least 3 experiments performed under the same experimental settings. For parental and stable GFP-Vector cells, the median number of migrated cells/visual field was 82.38 and 126.5 respectively. Both, expression of PKD1-(43.25) as well as PKD2-GFP (32.22) drastically reduced migration, while expression of PKD1KD-GFP enhanced migration to 222.9 cells/visual field, whereas PKD2KD-GFP only restored migration to parental/GFP-Vector levels with 88.82 cells/visual field. Respective images of DAPI stained nuclei used for quantification of cell migration are shown below the graph. The impaired migration in PKD1-GFP expressing stable cell lines and the enhanced cell migration upon PKD1KD-GFP expression indicates a possible negative regulatory function of PKD1 in directed cell motility. Overexpression of PKD2-GFP also reduced cell migration to about the same extent as seen in PKD1-GFP expressing stable Panc89 cell lines, yet PKD2KD-GFP only restored migration to vector levels, suggesting that kinase-dead PKD2 was not fully able to act in a dominant negative fashion, possibly due to differences in cellular localisation. To investigate whether the observed migration phenotypes in the stable Panc89 cell lines were caused due to differences in response to the serum stimulus used to induce cell migration on filters, a second set of Transwell migration assays was done without induction by a FCS gradient, seeding Panc89 cells in standard growth media. As demonstrated in **Fig. 11B,** the parental, as well as the stable Panc89 cells exhibited the same migration phenotypes, previously shown following induction by a serum stimulus. Taken together, this result points to a function for PKD in regulating basic Actin dynamics or remodelling of the Actin cytoskeleton, rather then being involved in an upstream signal pathway activated by the extracellular signal. The data shown in **Fig. 11B** is representative of at least 3 experiments performed under the same experimental settings.

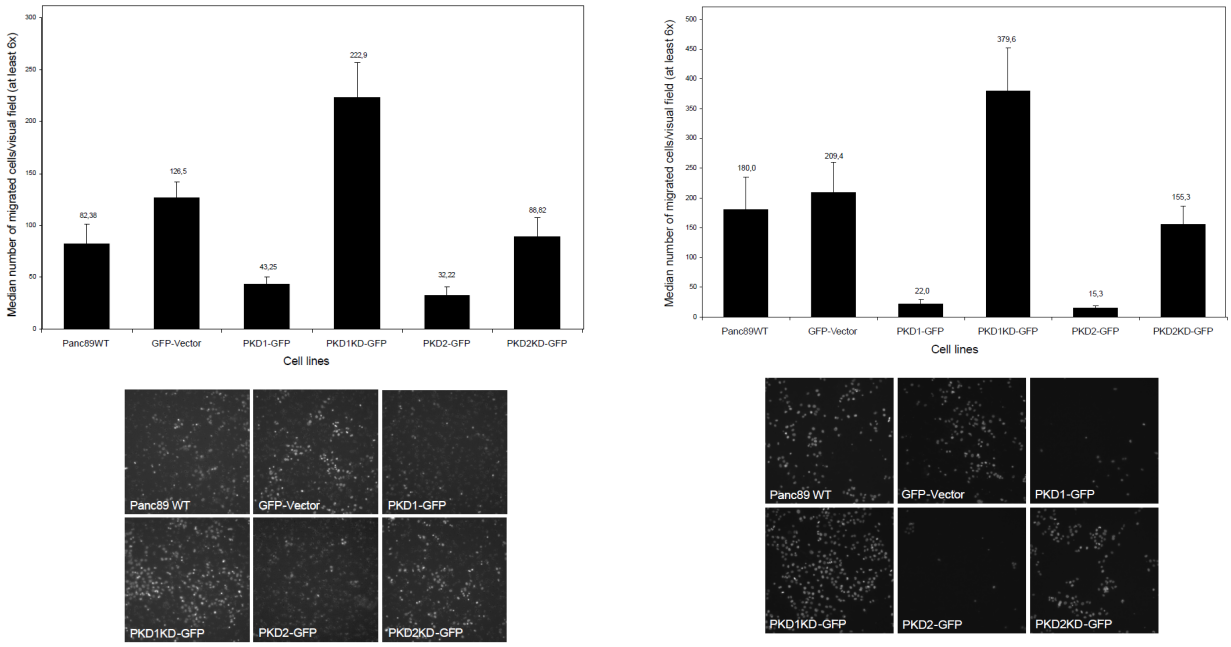

Fig. 11: **(A, *left hand panel*)** Transwell migration assays using Panc89 parental and stable cell lines expressing GFP, PKD1-GFP, PKD1KD-GFP, PKD2-GFP and PKD2KD-GFP. 60.000 cells were seeded on the filters and migration was induced by an FCS gradient of 1% - 10% FCS (top of insert/well) for 40 hours. DAPI stained nuclei of migrated cells were used for quantification and documented by a widefield fluorescence microscope (Leica) equipped with a CCD camera, and a monochromator light source controlled via OpenLab Software (Improvision, UK) at 10x magnification. Results were calculated as median number of migrated cells/visual field (1024 x 1022), with at least 6 images per filter. *Lower panel*: respective images of DAPI stained nuclei used for quantification. The assay is representative of at least 3 experiments performed under the same settings. **Fig. 11**: **(B, r*ight hand panel*):** Transwell migration assays using Panc89 parental and stable cell lines. Cells were incubated on filters in standard growth media containing 10% FCS without a gradient for 40 h. *Lower panel*: respective images of DAPI stained nuclei used for quantification. The assay is representative of at least 3 experiments performed under the same settings.

In **Fig. 11C** results of 9 Transwell migration assays, done with 3 different sorts of the stable Panc89 cell lines are summarised. Differences in relation to stable GFP-Vector cells were marked as statistically significant according to a student paired test by an asterisk (*). When analysing the data of the 9 migration assays performed employing an FCS gradient as stimulus, both, the impaired cell migration in PKD1- as well as PKD2-GFP expressing cell lines as well as the enhanced migration phenotype of stable PKD1KD-GFP cells, were listed as statistically significant relative to GFP-Vector cells. The data together clearly reveal that PKD1- and PKD2-GFP overexpression is negatively associated with cell migration, and corroborating this observation, interference with PKD1 function through dominant negative action of a PKD-KD mutant, promotes cell migration.

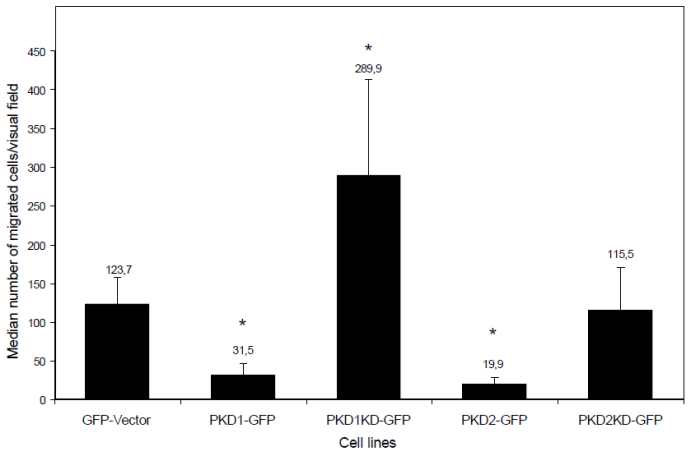

Fig. 11: **(C)** Summarised data of nine independent Transwell migration assays and three different sorts of the stable Panc89 cell lines characterised previously. Means and respective standard deviations for the summarised data of individual assays as described in **Fig. 11 A** were calculated and plotted in the diagram. Differences in relation to GFP-Vector cells were marked as statistically significant according to a student paired test by an asterisk (*).

5.8 Detailed immunohistochemical analysis of PKD1- and PKD1KD- GFP expressing Panc89 cell lines

5.8.1 Triplicate colocalisation of PKD1- or PKD1KD-GFP with F-Actin and Cortactin

To further approach the mechanistic base of the observed PKD mediated regulation of directed cell migration and to elucidate a potential functional link to the documented interaction with F-Actin, the subsequent experiments were performed with PKD1, since only PKD1KD seemed to be able to act in a clearly discernable dominant negative fashion in regulating cell migration.

To narrow down sites and processes were PKD1 kinase activity might be important, immunohistochemical stainings in stable Panc89 cell lines expressing PKD1- **(Fig. 12A,** *F-J, K-O***)** as well as PKD1KD-GFP **(Fig. 12A,** *P-T***)** were done to localise GFP-tagged fusion proteins with F-Actin and the cortical marker Cortactin. Triple colocalisations were marked with white arrows, while costainings of PKD1-GFP with either F-Actin or Cortactin were marked with arrowheads. GFP-Vector cells **(Fig. 12A**, *A-E***)** served as a respective control. In **Fig. 12A** PKD1-GFP was shown to colocalise with F-Actin in membrane protrusions, at structures also positive for Cortactin, indicating the presence of branched F-Actin networks, which are subject to active remodelling processes (*F-J, K-O*). Assessing the images (*K-O*), PKD1-GFP and F-Actin were also present at sites not stained for Cortactin, with some cells showing a colocalisation almost completely enclosing the entire cell periphery (*K-O, white arrowheads*). This either implies a much broader function for PKD1 at the F-Actin cytoskeleton, or most of the colocalisation seen in (*N*) is due to the strong overexpression of PKD1-GFP in the cells. PKD1KD-GFP also was costained with F-Actin in a much broader pattern (*P-T, white arrowheads*), with triplicate colocalisation only at a small area of the cell periphery (*P-T, white arrows*).

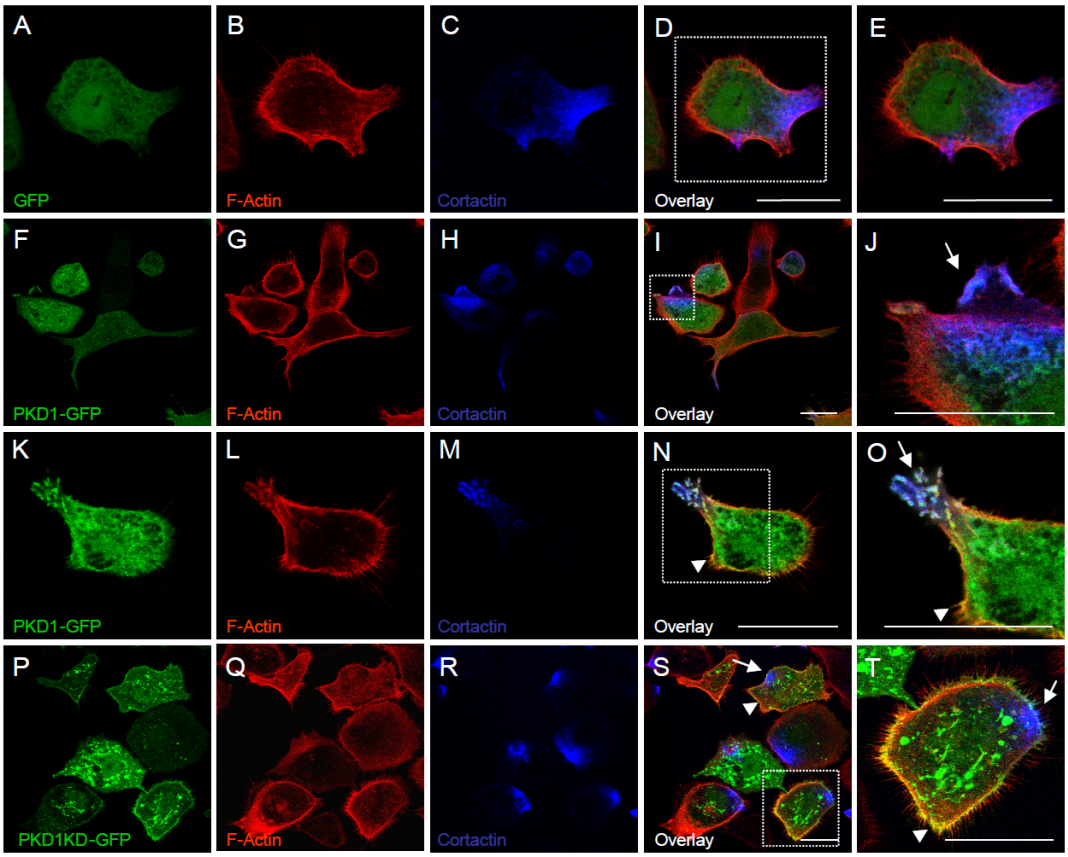

Fig. 12: **(A)** Confocal image sections of stable Panc89 cells expressing GFP (A-E), PKD1-GFP (F-O), PKD1KD-GFP (P-T) stained for F-Actin and Cortactin. Cells were seeded at a density of 100.000 cells on Collagen IV coated cover slips. Colocalisation of PKD1-GFP/PKD1KD-GFP and F-Actin (indicated by white arrowheads), as well as Cortactin (indicated by white arrows). Images were taken at 100x magnification. The scale bar represents 20 µm.

Summarising the data of **Fig. 12A**, colocalisation of all three markers further points to a putative function of PKD1 at the cortical F-Actin network, possibly at Actin branching sites since Cortactin is implicated in facilitating branching itself, or in the stabilisation of branched Actin networks. The broader colocalisation with F-Actin observed at the cell periphery of both PKD1-GFP (K-O) as well as PKD1KD-GFP (P-T) expressing cells, additionally implies a possible function of PKD also at other sites of the F-Actin cytoskeleton.

5.8.2 Stimulation of PKD1- and PKD1KD-GFP cells using PDGF-BB

To further investigate the localisation of PKD1- and PKD1KD-GFP in relation to F-Actin and also Cortactin, the stable cell lines were seeded on Collagen coated cover slips and stimulated with PDGF-BB, as described previously for parental Panc89 cells in *5.3.2*. Following stimulation, cells were processed for immunohistochemical staining (*4.2.8.2*) for selected markers and analysed by confocal microscopy. In **Fig. 12B** (*A-L*) Panc89 cells expressing PKD1-GFP were stained for F-Actin. Serum-starved control cells (*A-D*) as well as cells stimulated with PDGF for 10 (*E-H*), and 30 minutes (*I-L*) respectively displayed a colocalisation of PKD1-GFP with F-Actin in Actin-rich structures of membrane protrusions and in membrane ruffles, which was further enhanced in some cells following PDGF stimulation. Panc89 cells expressing PKD1KD-GFP **(Fig. 12B**, *M-X***)** were also stained for F-

Actin. Serum starved control cells (*M-P*) showed a weak colocalisation of PKD1KD-GFP with F-Actin in ruffles of membrane protrusions, while the colocalisation of PKD1KD-GFP and F-Actin after PDGF engagement for 10 and 30 minutes was enhanced (*Q-T, U-X*).

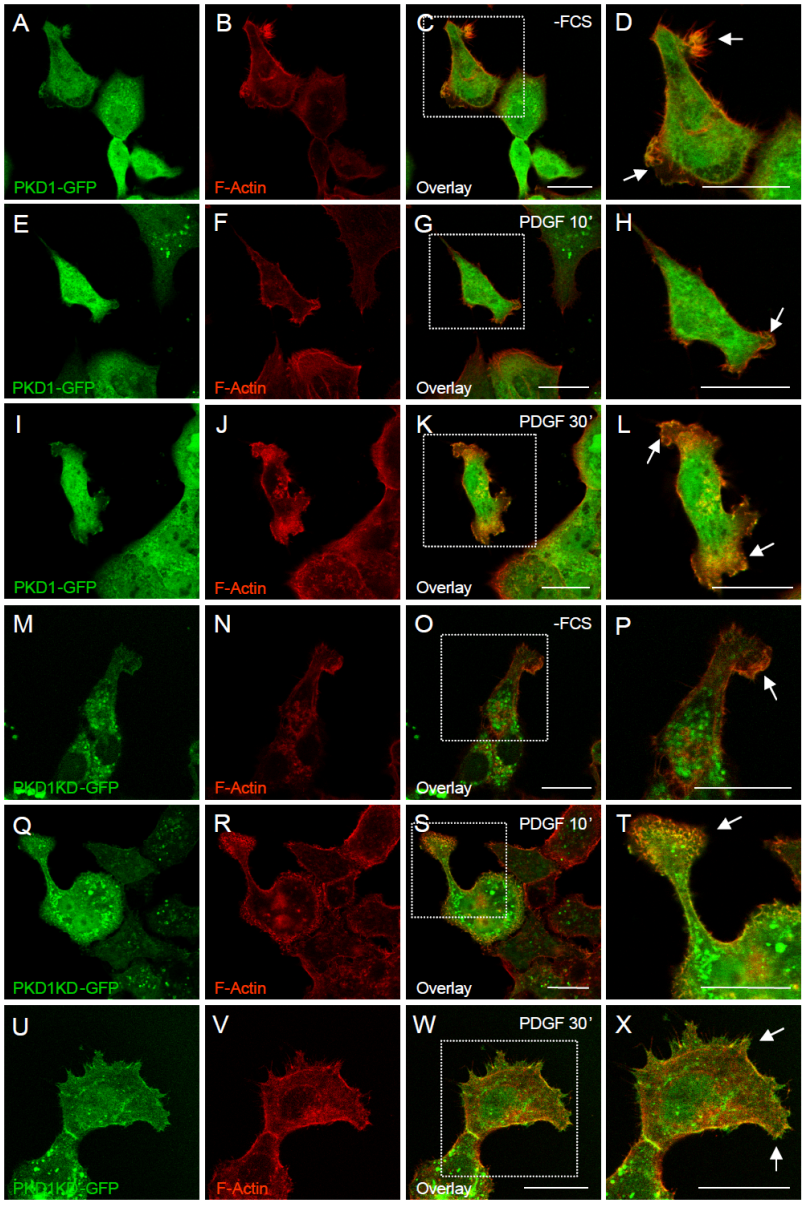

Fig. 12: **(B)** Confocal image sections of Panc89 cells expressing PKD1-GFP (A-L) as well as PKD1KD-GFP (M-X) stained for F-Actin. 70.000 cells were seeded on Collagen IV coated cover slips, serum starved over night and stimulated with PDGF-BB 30ng/ml for the indicated time points at 37°C. Serum starved cells (-FCS) served as a control. (A-D, M-P) Serum starved Panc89 cells. (E-H, Q-T) Panc89 cells stimulated with PDGF-BB 30ng/ml for 10 min. (I-L, U-X) Panc89 cells stimulated with PDGF-BB 30ng/ml for 30 min. Colocalisation in overlay images is indicated by yellow colour and a white arrow. Images were taken at 100x magnification. The scale bar represents 20 µm.

In **Fig. 12C** (*A-L*) Panc89 cells expressing PKD1-GFP were stained for Cortactin. Serum-starved control cells (*A-D*), as well as PDGF-stimulated cells after 10 (*E-H*) and 30 minutes (*I-L*) displayed a colocalisation of PKD1-GFP with Cortactin in lamellipodia and membrane ruffles, further enhanced in some cells following PDGF stimulation. **Fig. 12C** (*M-X*) shows stable Panc89 cells expressing PKD1KD-GFP again stained for Cortactin. Serum-starved controls exhibited only a weak colocalisation at the edge of membrane protrusions, possibly in membrane ruffles, while after 10 (*Q-T*) and 30 minutes (*U-X*) of PDGF stimulation the colocalisation of PKD1KD-GFP with Cortactin at structures within membrane protrusions was enhanced. Taken together, while for PKD1-GFP a distinct colocalisation with F-Actin and Cortactin was shown in serum-starved controls and after PDGF stimulation, the rather weak

colocalisation of PKD1KD-GFP with these markers became clearly discernable following PDGF stimulation. This argues for a recruitment of PKD1KD-GFP from the cytosolic pool to F-Actin-, or Cortactin-positive sites in membrane protrusions, upon PDGF stimulation. The extent of colocalisations with PKD1KD-GFP seemed to be dependent on the expression level and the amount of kinase-dead PKD1 available in the cytoplasm, as seen in **Fig. 12B** (*Q-T*), were a cell strongly expressing PKD1KD-GFP also exhibits a very distinct colocalisation with Actin-rich structures in an area of membrane protrusion and at the cell periphery. PKD1KD-GFP expressed in Panc89 cells therefore might be either present, or is probably recruited to sites of F-Actin remodelling, thereby being able to exert a dominant negative function, as suggested from the Transwell migration assays **(Fig. 11 A-C)**.

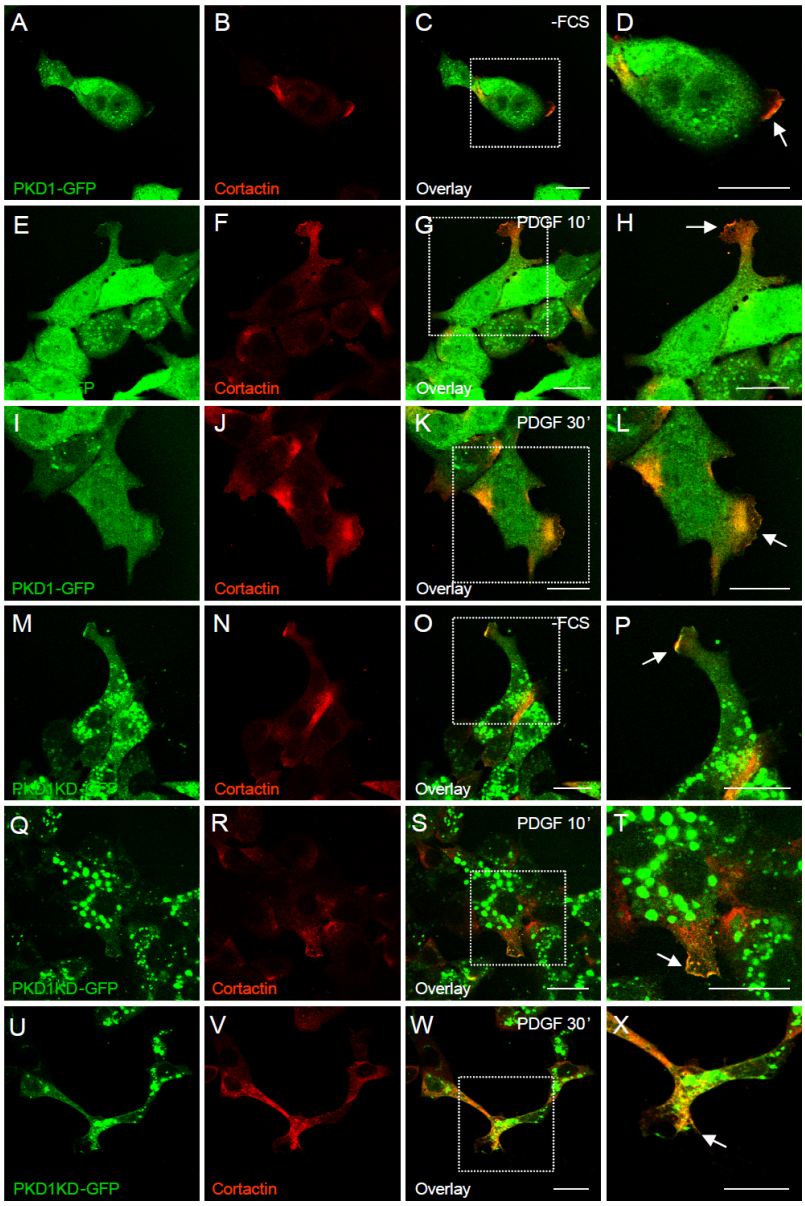

Fig. 12: **(C)** Confocal image sections of Panc89 cells expressing PKD1-GFP (A-L) as well as PKD1KD-GFP (M-X) stained for Cortactin. 70.000 cells were seeded on Collagen IV coated cover slips, serum starved over night and stimulated with PDGF-BB 30ng/ml for the indicated time points at 37°C. Serum starved cells (-FCS) served as a control. (A-D, M-P) Serum starved Panc89 cells. (E-H, Q-T) Panc89 cells stimulated with PDGF-BB 30ng/ml for 10 min. (I-L, U-X) Panc89 cells stimulated with PDGF-BB 30ng/ml for 30 min. Colocalisation in overlay images is indicated by yellow colour and a white arrow. Images were taken at 100x magnification. The scale bar represents 20 µm.

To answer the question, whether endogenous PKD1 in Panc89 cells has a role in cell migration *in vivo*, DNA-based RNA interference was performed.

5.9 Knockdown of PKD1 in Panc89 cells using RNA interference

Parental Panc89 cells were transfected with a PKD1-pSuppressor construct coding for a short interfering RNA (siRNA) specific against the PKD1 isoform and also for a G418 resistance marker. Since transfection efficiency in Panc89 was very low, stable cell clones expressing the PKD1-pSuppressor construct had to be established. Selection of transfected cells was done using G418 1mg/ml, until cells stopped dying. Subsequently cells were subjected to a limited dilution in 96 well plates with an average density of one cell every fourth well. In the case of the Panc89 cells expressing the PKD1-RNAi construct, only 2 clones survived the selection process and the following expansion to individual, stable growing cell lines. The bulk of the clones either stopped growing during the expansion from the limited dilution format, or detached from the surface, dying subsequently. The resulting 2 PKD1 clones were evaluated for a PKD1-knockdown using Western blotting and semi-quantitative RT-PCR analysis (*4.2.2*). As indicated in **Fig. 13B** only clone 9 showed a knockdown in a Western blot against $pPKD_{S910}$ (*blot panel 1*), while clone 6, although the cells were growing on selection, did not display reduced expression of PKD1. α-Tubulin was included as a loading control (*blot panel 2, 4*). Using a PKD3 specific antibody, effects on the expression level of endogenous PKD3 were also excluded (*blot panel 3*). Due to limitations in quality of the α-PKD D20 antibody (Santa Cruz Biotechnology Inc., Santa Cruz, CA, USA), the α-$pPKD_{S910}$ antibody had to be used to characterise the Panc89 PKD1-pSuppressor clones, detecting autophosphorylated PKD. Since the $pPKD_{S910}$ Western blots of Panc89 cells only displayed one band migrating at the approximate molecular mass corresponding to either autophosphorylated PKD1 or PKD2, a semi-quantitative RT-PCR analysis of the 2 clones was added to determine a PKD1-specific RNAi-mediated knockdown. As shown in **Fig. 13B**, the semi-quantitative analysis of PKD isoform expression in the Panc89 PKD1-pSuppressor clones demonstrated a specific knockdown of the PKD1 transcripts, affecting neither PKD2, nor PKD3 expression in PKD1-pSuppressor clone 9 cells. Subjecting the respective cells to Transwell migration assays in the presence of an FCS gradient for 40h **(Fig. 13A)** revealed strongly increased migration of the clone 9 PKD1-knockdown cells, when compared to parental Panc89 cells, or the clone 6 cell line, which did not exhibit a PKD1-knockdown. Since only one clone with a PKD1-specific, yet incomplete, knockdown survived the selection, it is presently difficult to draw firm conclusions on the result obtained with this knockdown clone.

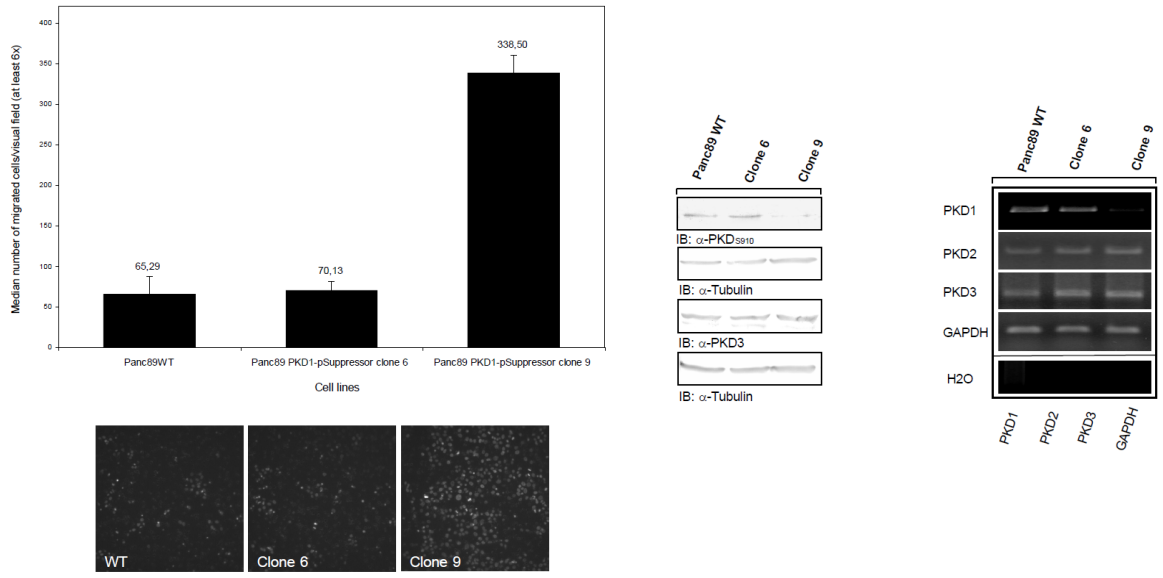

Fig. 13: **(A, *left hand panel*)** Migration assay using stable Panc89 PKD1-pSuppressor clones. Only 2 clones survived the selection process. Migration was induced by an FCS gradient of 1% - 10% FCS (top of insert/well) for 40 hours. DAPI stained nuclei of migrated cells were used for quantification and documented by a widefield fluorescence microscope equipped with a CCD camera, and a monochromator light source controlled via OpenLab Software (Improvision, UK) at 10x magnification. Results were calculated as median number of migrated cells/visual field (1024 x 1022), with at least 6 images per filter. *Lower panel*: respective images of DAPI stained nuclei used for quantification. The assay is representative of at least 3 experiments performed under the same settings. **(B, *right hand panel*)** *Western blots*: Total cell lysates of parental Panc89 cells and PKD1-pSuppressor clones 6 and 9. 80 µg of total protein per lane. PKD expression was detected using α-pPKD$_{S910}$ antibody, while PKD3 was blotted with α-PKD3 antibody. α-Tubulin was included as a loading control. *PCR*: Semi-quantitative RT-PCR of PKD isoforms 1/2/3 and GAPDH from parental Panc89 cells and PKD1-pSuppressor clones 6 and 9. PCR cycles were adjusted to be within the linear range of amplification.

With the cell lines studied, RNAi rescue experiments were not performed, since every genetic manipulation in the Panc89 cells had to be done by establishing stable cell lines, in the case of the Panc89 PKD1-pSuppressor clones this would have taken several months with uncertain outcome, considering the low frequency of established clones. Nevertheless, although only suggestive, these findings are in full accordance with the phenotype of PKD-KD stable transfectants described before. Therefore, the results of PKD1-specific RNA interference in Panc89 cells further support a critical role of PKD1 in directed cell migration *in vivo*.

5.10 Knockdown of PKD1 in Panc1 cells using RNA interference

In parallel to the establishment of PKD1-pSuppressor clones in Panc89 cells, also Panc1 cells were transfected with the respective PKD1-specific RNAi construct to verify the obtained results in a second PDAC cell line. Following selection and limited dilution, multiple cell lines from single clones were established and tested for a PKD1-knockdown using Western blots. In contrast to the Panc89 cells, Panc1 PKD1-pSuppressor clones were not massively lost during the expansion process. In **Fig. 14** respective PKD1-knockdown clones and parental Panc1 cells were characterised in Transwell migration assays. Since the expression of PKD1 in Panc1 cells was very weak, an RNAi-mediated PKD1-knockdown

could not have been simply demonstrated by analysing total cell lysates in Western blots. That's why immunoprecipitations from 2.7 mg of total protein were performed utilising the α-pPKD$_{S910}$ antibody. The immunoprecipitates then were probed again for pPKD$_{S910,}$ yielding to bands in the parental Panc1 cells, with the upper band corresponding to autophosphorylated PKD1, while the lower band was migrating at the appropriate molecular mass of PKD2 ***(Fig. 14B**, blot panel 1)*. Both PKD1-pSuppressor clone 9 as well as clone 17 cells exhibited a PKD1-knockdown (***Fig. 14B***, *blot panel 1*), while the PKD2 protein level was not reduced. Comparing PKD1-pSuppressor clone 9 to 17, there was a weak residual PKD1 band left in clone 9 cells, whereas in clone 17 cells no PKD1 band was visible any more. This is also in line with the stronger PKD2 band seen for the PKD1-pSuppressor clone 17 cells, since more PKD2 would be immunoprecipitated by the α-pPKD$_{S910}$ antibody, following the complete knockdown of PKD1. As shown in **Fig. 14B**, *blot panel 2*, PKD3 expression in the PKD1-knockdown clones was not affected, with Tubulin serving as a loading control (*blot panel 3*). Analysing the cell migration of the Panc1 PKD1-pSuppressor clones **(Fig. 14A)**, only clone 17 cells with complete knockdown of PKD1 showed clearly enhanced migration (median number of cells/visual field: 327.1) when compared to parental Panc1 (median number of cells/visual field: 172.45) and the clone 9 cell line (median number of cells/visual field: 212.22).

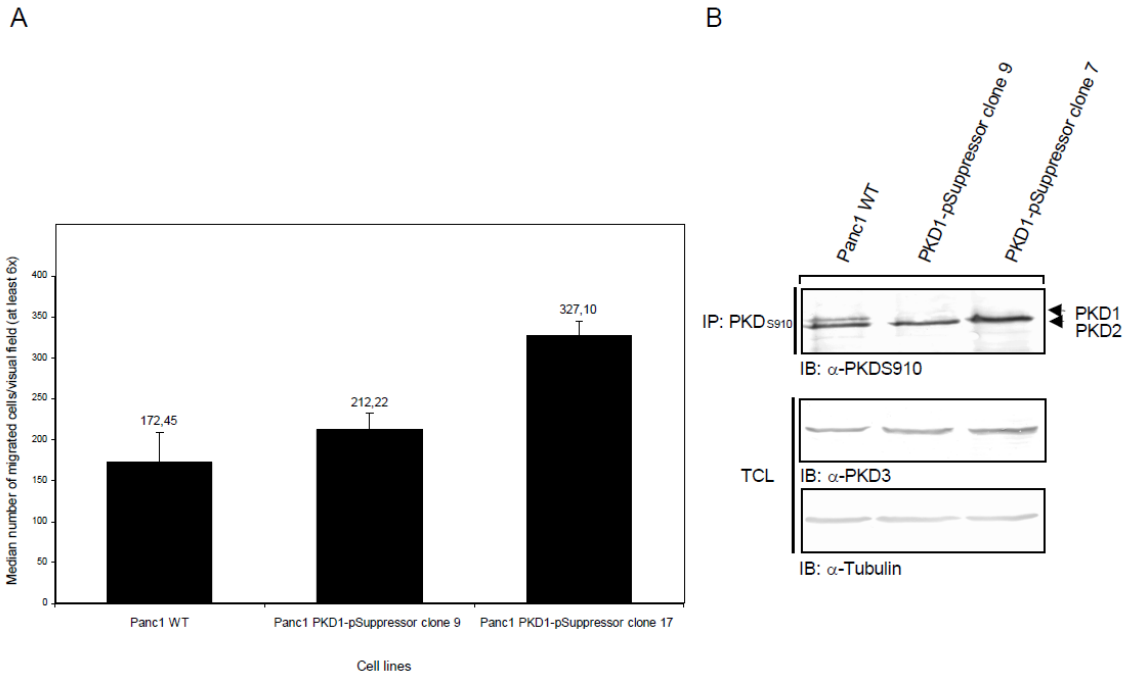

Fig. 14: **(A)** Migration assays using Panc1 PDAC cells. Multiple stable Panc1 PKD1-pSuppressor clones were established and subjected to migration assays. 20.000 cells/insert were seeded in medium containing 1% FCS. Migration was induced by an FCS gradient of 1% - 10% FCS (top of insert/well) for 40 hours. DAPI stained nuclei of migrated cells were used for quantification and documented by a widefield fluorescence microscope equipped with a CCD camera, and a monochromator light source controlled via OpenLab Software (Improvision, UK) at 10x magnification. Results were calculated as median number of migrated cells/visual field (1024 x 1022), with at least 6 images per filter. DAPI stained assays were documented using an epifluorescence microscope with 10x magnification. At least 6 visual fields (1024 x 1022) per filter were photographed. Results were calculated as median number of migrated cells/visual field with at least 6 photos per filter. The assay is representative of at least 3 experiments performed under the same settings. **(B)** *Upper panel*: Immunoprecipitations of PKD1/2 using α-pPKD$_{S910}$ antibody from total cell lysates (2.7mg) of parental Panc1 cells and PKD1-pSuppressor clones to enrich endogenous PKD1/2 proteins. Detection of PKD1/2 was done using α-pPKD$_{S910}$. *Lower panel*: PKD3 expression was detected using α-PKD3 antibody in 100µg of total cell lysates. α-Tubulin was included as a loading control.

Summarising the data of the PKD1 specific RNA interference in Panc1 cells, several clones were established and tested for PKD1-knockdowns (data not shown), but only cells of the complete PKD1-knockdown clone 17 exhibited an increase in cell migration, while other clones, like PKD1-pSuppressor clone 9, displayed an incomplete knockdown and also no enhanced migration when compared to parental Panc1 cells. In addition it has to be noted, that the relative increase in migration observed in PKD1-pSuppressor clone 17 cells was smaller then in the migration assays utilising Panc89 PKD1-knockdown clone 9 cells, possibly pointing to a somewhat different regulation of motility in Panc1 cells **(Fig. 13A).** Concluding from the present data, the regulation of migration in different cell types might be dependent also on different PKD isoforms. PKD1 was shown to act dominant in Panc89 cells, while for Panc1 cells only weakly expressing PKD1 **(Fig. 14B)**, the PKD2 isoform might be more important, as implicated by the relatively small impact of the complete PKD1-Knockdown in the PKD1-pSuppressor clone 17 cells on migration in Transwell assays **(Fig. 14A)**. Taken together, despite the fact that firm conclusions clould not be drawn from the available knockdown-clones, the RNAi experiments in Panc89 and Panc1 cells further support a function of PKD in directed cell migration *in vivo*.

5.11 Coimmunoprecipitations

5.11.1 Coimmunoprecipitations of Cortactin and Paxillin with PKD isoforms in stable Panc89 cells

In order to gain more insight in the regulation of cell migration by PKD, coimmunoprecipitations with markers implicated in the remodelling of the F-Actin cytoskeleton were done *(4.2.7.3)*. Cortactin, which has been shown to extensively colocalise with PKD **(Fig. 7B, 9E)** and Paxillin, a Cortactin binding partner (Bowden et *al.*, 1998), were immunoprecipitated from total cell lysates of the stable Panc89 cell lines expressing GFP, PKD1-GFP, PKD1KD-GFP, PKD2-GFP, as well as PKD2KD-GFP and precipitated complexes were probed for the presence of GFP-tagged PKD fusion proteins **(Fig. 15A)**. Coimmunoprecipitations of Cortactin with PKD are shown in **Fig. 15A**, *upper panel of blots*. Both, PKD 1 and 2 isoforms, as well as the kinase-dead mutants were detected in Cortactin immunoprecipitates of the stable Panc89 cell lines. When analysing the coprecipitations of WT and kinase-dead PKD isoforms, more PKD1KD-GFP than PKD1-GFP and also more

PKD2KD-GFP in relation to PKD2-GFP were found to coprecipitate with Cortactin. Bearing in mind that Cortactin was shown to localise at the TGN, too, where it is implied in the Actin- and Dynamin-dependent transport of cargo (Cao et *al.*, 2005), kinase-dead mutants of PKD disrupting the TGN integrity **(Fig. 10B)** might also trap Cortactin in the same structures, therefore resulting in the enhanced coimmunoprecipitation with kinase-dead PKD 1 and 2.

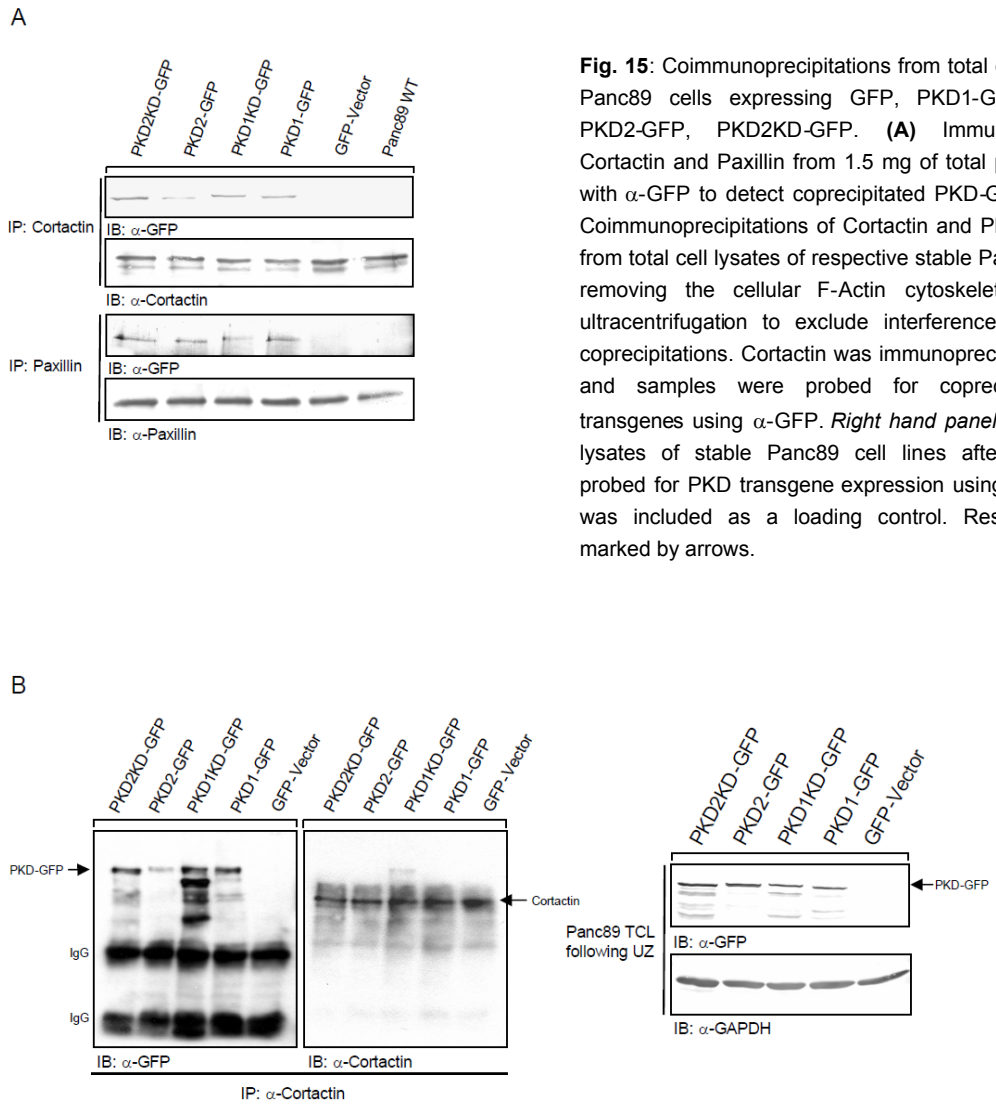

Fig. 15: Coimmunoprecipitations from total cell lysates of stable Panc89 cells expressing GFP, PKD1-GFP, PKD1KD-GFP, PKD2-GFP, PKD2KD-GFP. **(A)** Immunoprecipitations of Cortactin and Paxillin from 1.5 mg of total protein were probed with α-GFP to detect coprecipitated PKD-GFP transgenes. **(B)** Coimmunoprecipitations of Cortactin and PKD-GFP transgenes from total cell lysates of respective stable Panc89 cell lines after removing the cellular F-Actin cytoskeleton by 100.000 g ultracentrifugation to exclude interference of F-Actin in the coprecipitations. Cortactin was immunoprecipitated from lysates and samples were probed for coprecipitated PKD-GFP transgenes using α-GFP. *Right hand panel of blots*: Total cell lysates of stable Panc89 cell lines after ultracentrifugation probed for PKD transgene expression using α-GFP. α-GAPDH was included as a loading control. Respective bands are marked by arrows.

In **Fig. 15A**, *lower panel of blots*, PKD1- and 2-GFP isoforms, as well as the respective kinase-dead mutants were detected in Paxillin immunoprecipitates of the stable cell lines at equal levels. Taken together, these data suggest that PKD not only colocalises by IF to Cortactin positive structures in Panc89 cells, it also physically interacts with Cortactin, indicating a potential molecular and functional link between the regulation of F-Actin remodelling and cell migration. The coprecipitation of PKD with Paxillin, which is a known binding partner of Cortactin, further points to the formation of multi-protein complexes which might be implicated in the regulation of Actin cytoskeleton dynamics. Since both Cortactin and PKD have been shown to be F-Actin binding proteins *in vitro* (**Fig. 8**), the coimmunprecipitations shown in **Fig. 15A** might also be a consequence of an indirect

interaction via F-Actin, known to bind to all the components in question. That's why, in addition to the experimental setup described in **Fig. 15A**, also coprecipitations following the removal of the cellular F-Actin cytoskeleton by 100.000 g ultracentrifugation were performed *(4.2.7.3)*.

5.11.2 Coimmunoprecipitation of Cortactin with PKD isoforms in Panc89 cells following the removal of the F-Actin cytoskeleton

In **Fig. 15B**, *right hand panel of blots*, Panc89 total cell lysates following ultracentrifugation are shown, demonstrating an equal expression of respective WT and kinase-dead PKD isoforms (*blot panel 1*). In this setting GAPDH was used as a loading control (*blot panel 2*). In **Fig. 15B**, *left hand panel of blots*, respective coimmunoprecipitations after the removal of the F-Actin cytoskeleton are displayed. The PKD-GFP transgenes exhibited the same pattern of coprecipitations already observed in **Fig. 15A**, thereby indicating that the coprecipitations were not mediated indirectly via the F-Actin cytoskeleton. Rather the data favour a direct cytosolic interaction. In addition, this might also indicate a possible function for Cortactin as a scaffold protein, recruiting PKD from the cytosol to its putative sites of action at the cortical F-Actin cytoskeleton.

5.11.3 Coimmunoprecipitation of Cortactin and PKD1 in HEK 293T cells following the removal of the F-Actin cytoskeleton

To investigate the interaction of PKD and Cortactin in more detail, total cell lysates of transiently transfected HEK 293T cells coexpressing PKD1-GFP and FLAG-Cortactin, as well as respective vector controls were subjected to 100.000 g ultracentrifugation to remove the F-Actin cytoskeleton. Subsequently, GFP-tagged PKD1 or FLAG-tagged Cortactin, as well as respective controls were immunoprecipitated from the lysates and coprecipitated FLAG-Cortactin or PKD1-GFP was detected in the complexes. As seen in **Fig. 15C**, *left hand panel of blots*, FLAG-Cortactin was specifically coprecipitated with PKD1-GFP, while inversely PKD1-GFP was also coprecipitated with FLAG-Cortactin, yet there was also a weaker background band in the immunoprecipitate from lysates expressing PKD1-GFP and FLAG-Vector (*middle panel of blots*). Western blots of the total cell lysates demonstrating transgene expression are shown at the *right hand side* of **Fig. 15C**. In conclusion, coimmunoprecipitations following removal of the F-Actin cytoskeleton in stable Panc89 cells **(Fig. 15B),** as well as in transiently transfected HEK 293T cells **(Fig. 15C)** demonstrated an interaction of PKD with Cortactin independent of the F-Actin network. Since the interaction of both proteins was observed in 2 different cell lines, this further emphasises the above mentioned putative role for the PKD-Cortactin interaction in the regulation of Actin cytoskeleton remodelling processes.

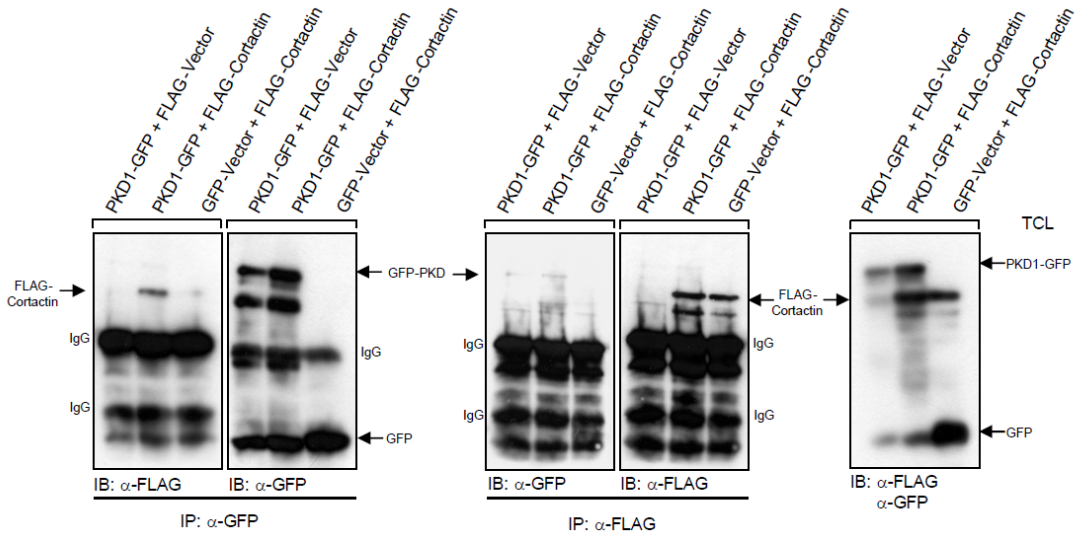

Fig. 15: (C) Coimmunoprecipitations of PKD1-GFP and FLAG-Cortactin from transiently transfected HEK 293T cells. 293T cells expressing PKD1-GFP and FLAG-Cortactin as well as respective FLAG- and GFP-Vector controls were subjected to 100 .000 g ultracentrifugation to remove the cellular F-Actin cytoskeleton. *Left hand panel of blots*: Immunoprecipitations using α-GFP probed for FLAG-Cortactin were stripped and reprobed for GFP expression. *Central panel of blots*: Immunoprecipitations using α-FLAG probed for GFP-PKD were stripped and reprobed for FLAG-expression. *Right hand panel of blots*: Total cell lysates used for immunoprecipitations probed for GFP- and FLAG-transgene expression. Respective bands are marked by arrows.

5.12 Phosphorylation of Cortactin by PKD1 *in vitro*

Since PKD is a protein kinase, an interaction might also involve phosphorylation of consensus motifs in putative substrates. Therefore Cortactin was tested for a possible *in vitro* phosphorylation by PKD1 *(4.2.7.4)*. In **Fig. 16A**, *upper panel*, the autoradiogram of an *in vitro* kinase assay is shown. In the kinase reactions FLAG-Cortactin, expressed in HEK 293T cells, was shown to be phosphorylated by PKD1-GFP, while in the vector control sample and in the PKD1KD-GFP *in vitro* kinase assay, phosphorylation reached only background levels. The *lower panel* in **Fig. 16A** displays the expression of the respective PKD1-GFP/PKD1KD-GFP and FLAG-Cortactin fusion proteins. As illustrated in **Fig. 16B**, both, manual screening, and analysis of the Cortactin amino acid sequence by the software tool *Scansite* (Obenauer et *al.*, 2003) revealed two putative PKD phosphorylation sites at position S113 and S298. A comparison to the optimal consensus sequence L/I/VXRXS/T revealed, that both sides lack an arginine (R) residue in the -2/3 position, yet the also positively charged histidine (H) and lysine (K) residues (-2/3) in the respective motifs might be able to compensate for the arginine. To map the putative phosphorylation sites *in vitro*, S113 and S298 were mutated to alanine, using site-directed mutagenesis and expressed in FLAG- and GFP-Vectors *(4.2.5)*. In addition a double mutant S113A/S298A was constructed. Mutations were verified by sequencing and respective constructs were tested in *in vitro* kinase assays. As shown in **Fig. 16C** using FLAG-purified Cortactin constructs, and WT, as well as kinase-dead purified PKD1, Cortactin was shown to be phosphorylated at position S298, indicated by the reduced phosphorylation of Cortactin using the FLAG-CortactinS298A mutant. However, in other *in vitro* kinase assays performed following immunoprecipitation from transiently transfected

HEK 293T cells (*4.2.7.4*), S113 and, in addition, unspecified sites in the S113A/S298A double mutant were also phosphorylated in some assays (data not shown). A conclusive mapping of all putative PKD *in vitro* phosphorylation sites in Cortactin therefore was not possible. In addition, analysis of phosphoproteomics data on FLAG-Cortactin expressed in HEK 293T cells (produced by Pearson and Hunt), posted on the Nature cell migration gateway website (www.cellmigration.org), did not reveal an *in vivo* phosphorylation at S113, while for S298 no data on *in vivo* phosphorylation was available. To further investigate the phospho-status of S298, FLAG-Cortactin was purified from HEK 293T cells as described in *4.2.7.7*, subsequently separated on a precast NuPaGE 4-12% bis-tris-gradient gel (Invitrogen, Karlsruhe) and subjected to phosphor-mass-spectrometry analysis in cooperation with Dr. Volker Gnau (Proteom-Center, Tübingen). Unfortunately, up to now, no data could be obtained on the phospho-status of S298, yet the analysis is further ongoing. Mapping putative PKD *in vivo* phosphorylation sites in Cortactin utilising the PKD-pMOTIF substrate specific antibody (Doppler et *al.*, 2005) also failed, since the consensus sequences in Cortactin did not match the degenerated motifs, used to generate the antibody, and respective signals in Western blots were weak and not reproducible.

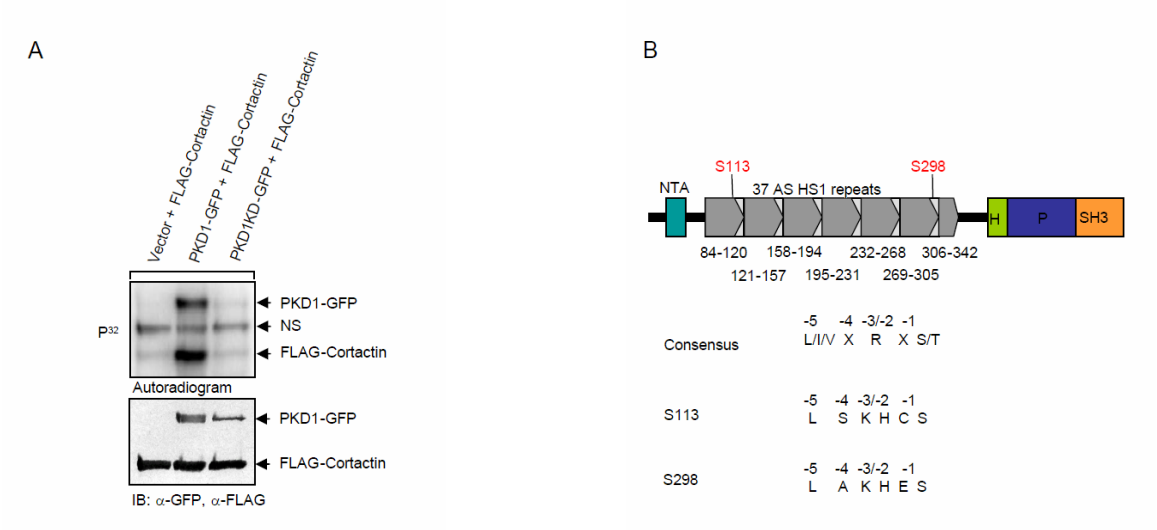

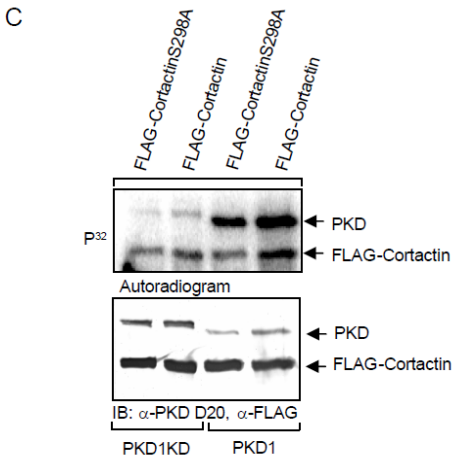

Fig. 16: **(A)** *In vitro* kinase assay using PKD1-GFP, PKD1KD-GFP and vector control as well as FLAG-Cortactin as substrate expressed in HEK 293T cells. *Upper panel*: Autoradiogram of the *in vitro* kinase assay. *Lower panel*: Expression of respective PKD1-GFP/PKD1KD-GFP and FLAG-Cortactin fusion proteins. **(B)** Schematic representation of the domain structure of mammalian Cortactin. NTA, N-terminal acidic domain; H, helical domain; P, proline-rich domain; SH3, SH3 domain. Putative PKD phosphorylation sites are indicated in red colour letters. The optimal PKD phosphorylation consensus site and respective putative sequences in Cortactin are listed below. **(C)** *In vitro* kinase assay using purified PKD1-GFP, PKD1KD-GFP as well as FLAG-Cortactin and FLAG-CortactinS298A fusion proteins as substrates. *Upper panel*: Autoradiogram of the *in vitro* kinase assay. *Lower panel*: Protein levels of PKD1-GFP/PKD1KD-GFP and FLAG-Cortactin/FLAG-CortactinS298A fusion proteins. Respective bands are marked by arrows, NS (non specific).

Regardless of the fact that only an *in vitro*, but no *in vivo* phosphorylation of S298 could be demonstrated, the CortactinS298A mutant was further analysed for functional deficits in Transwell migration assays, to asses if a putative effect on cell migration could be correlated with the PKD1KD migration phenotype.

5.13 Analysis of Cortactin-GFP and CortactinS298A-GFP stable Panc89 cell lines in migration assays

In order to investigate effects of the CortactinS298A mutant on Panc89 cells, a stable cell line was established expressing CortactinS298A-GFP, as described previously for the other stable Panc89 cells lines. In **Fig. 17A**, (*A*-*E*) stable Panc89 cells expressing GFP, PKD1-GFP, PKD1KD-GFP, Cortactin-GFP, (also used in **Fig. 9F**) and CortactinS298A-GFP were analysed by flow cytometry to determine GFP-fluorescence. As seen in the FL1-LOG histograms in **Fig. 17A** *(A-D)*, the stable cell lines exhibited a strong GFP-expression, while the histogram of CortactinS298A-GFP cells (*E*) only showed a weak shift relative to parental Panc89 cells. In **Fig. 17B** the relative expression levels of the respective GFP-tagged transgenes were analysed by Western blot against α-GFP (*blot panel 1*). As expected, CortactinS298A-GFP cells also showed a moderate, but clearly visible expression. **Fig. 17C** displays the results of a Transwell migration assay using the stable Panc89 cell lines characterised in **Fig. 17A/B**. The assay shown is representative of at least 3 experiments performed under the same experimental settings. As expected, PKD1-GFP reduced cell migration (median number of cells/visual field: 41.1) compared to the GFP-Vector cell line (median number of cells/visual field: 122.4), while PKD1KD-GFP enhanced cell migration to a median number of cells/visual field of 375.7. Cortactin-GFP cells reached about GFP-Vector level cell migration (median number of cells/visual field: 127.7), whereas CortactinS298A-GFP again increased cell migration to a median number of cells/visual field of 336. Taken together, a similar phenotype of PKD1KD and the phosphorylation mutant S298 of Cortactin are suggestive of a causal relation and functional link of PKD1 mediated Cortactin phosphorylation in controlling cell migration.

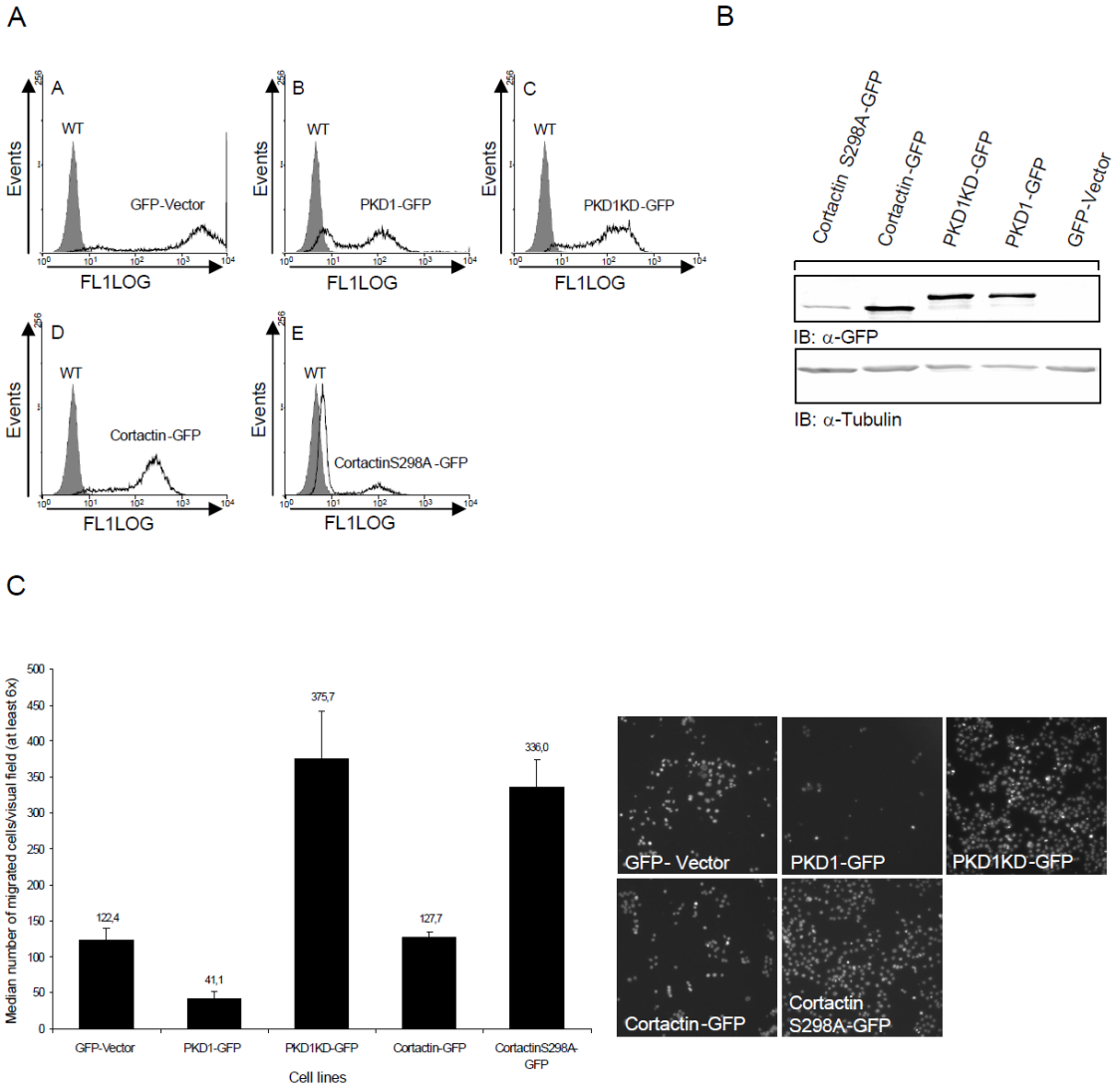

Fig. 17: Characterisation of stable Panc89 cell lines expressing GFP, PKD1-GFP, PKD1KD-GFP, Cortactin-GFP and CortactinS298A-GFP for Transwell migration assays. **(A)** GFP-fluorescence of respective stable Panc89 cell lines: 10.000 cells were analysed by flow cytometry. (A-E) FL1-Log histograms of the GFP expressing cell lines blotted against parental Panc89 control cells. **(B)** GFP-transgene expression in total cell lysates of Panc89 cell lines: 50 µg of protein per lane. **(C)** Transwell migration assays using stable Panc89 cell lines expressing GFP, PKD1-GFP, PKD1KD-GFP, Cortactin-GFP and CortactinS298A-GFP. Migration was induced by an FCS gradient of 1% - 10% FCS (top of insert/well) for 40 hours. DAPI stained nuclei of migrated cells were used for quantification and documented by a widefield fluorescence microscope equipped with a CCD camera, and a monochromator light source controlled via OpenLab Software (Improvision, UK) at 10x magnification. Results were calculated as median number of migrated cells/visual field (1024 x 1022), with at least 6 images per filter. *Right hand panel*: respective images of DAPI stained nuclei used for quantification. The assay is representative of at least 3 experiments performed under the same settings.

5.14 Analysis of Cortactin and CortactinS298A

5.14.1 Immunohistochemistry, F-Actin cosedimentation assays and Actin-coimmunoprecipitations

In the following experiments, Cortactin-GFP and CortactinS298A-GFP were characterised towards their ability to colocalise in cells and bind to F-Actin *in vitro*. As demonstrated in **Fig.**

18A, both, Cortactin-GFP (*A-D*) and CortactinS298A-GFP (*E-H*) colocalised with F-Actin in the Panc89 cells, thereby indicating that the localisation of the CortactinS298A mutant at the F-Actin cytoskeleton was not disturbed. In **Fig. 18B** F-Actin cosedimentation assays were performed using purified FLAG-Cortactin as well as FLAG-CortactinS298A. For the assays 0.5 µg of the purified FLAG-Cortactin was incubated with 10 µg of F-Actin. Following ultracentrifugation, pellet and supernatant fractions were separated, each subjected to SDS-PAGE and blotted with α-FLAG antibody. As shown in **Fig. 18B**, FLAG-Cortactin cosedimented strongly with the F-Actin pellet fraction, while there was only a weak residual band in the supernatant. In contrast, FLAG-Cortactin298A was strongly present in the supernatant and only little was found in the pellet fraction, indicating that the affinity of Cortactin for the F-Actin binding was reduced following the serine to alanine mutation at position 298 within 6th HS1 repeat. Actin-coimmunoprecipitations performed with transiently transfected HEK 293T cells expressing Cortactin-GFP as well as CortactinS298A-GFP are shown in **Fig. 18C**.

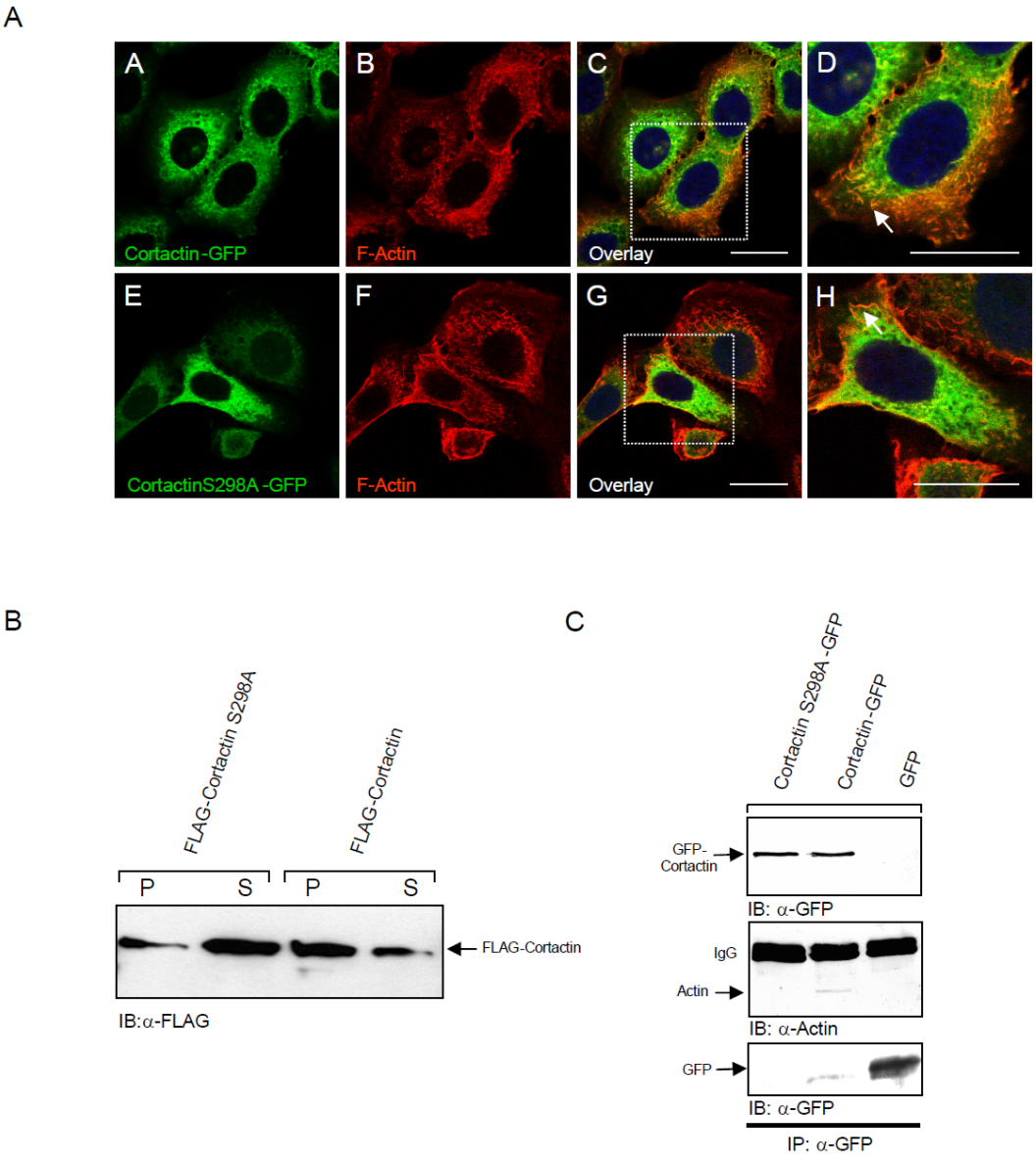

Fig. 18: **(A)** Confocal image sections of stable Panc89 cells expressing Cortactin-GFP (A-D) and CortactinS298A-GFP (E-H) stained for F-Actin. Cells were seeded at a density of 100.000 cells on Collagen IV coated cover slips. Colocalisation in overlay images is indicated by yellow colour and white arrows. Nuclei were stained using DRAQ5. Images were taken at 100x magnification. The scale bar represents 20 µm. **(B)** F-Actin cosedimentation assays using FLAG-Cortactin and FLAG-CortactinS298A purified proteins. 0.5 µg of purified protein was incubated with 10 µg F-Actin for binding assays. After ultracentrifugation (100.000 g) supernatant and pellet were fractionated and normalised fractions were analysed by SDS-PAGE and Western blotting against α-FLAG. **(C)** *Left hand panel of blots*: Coimmunoprecipitation of transiently transfected GFP-Cortactin and GFP-CortactinS298A with Actin in HEK 293T cells. GFP-Cortactin and CortactinS298A were immunoprecipitated and complexes were probed using an α-Actin AC40 antibody. Respective bands are marked by arrows.

The GFP-Vector was used as a control. Following lysis, GFP-tagged Cortactin fusion proteins were immunoprecipitated from total cell lysates and immuncomplexes were probed for the presence of Actin. Since Cortactin is a known F-Actin-binding protein, the coprecipitated Actin, detected following separation on a denaturating SDS-PAGE, very likely originated from the F-Actin pool. As displayed in **Fig.18C**, Actin coprecipitated with Cortactin-GFP immunprecipitates, while in CortactinS298A-GFP and GFP immuncomplexes no, or only a very weak band was visible, further pointing to the fact that under these experimental conditions the binding efficiency of CortactinS298A to F-Actin was also reduced. Since Cortactin was partially shown to localise at the TGN, the effects of the CortactinS298A mutation on TGN structure were also investigated. In **Fig. 18D** confocal image sections of stable Panc89 cell lines expressing GFP, Cortactin-GFP, as well as CortactinS298A-GFP following immunohistochemistry against TGN46 are shown. (*A*-*C*) display GFP-Vector cells stained for TGN46 as reference. Cortactin-GFP (*D*-*F*) and CortactinS298A-GFP (*G*-*I*) cells exhibited a normal Golgi staining, comparable to the GFP-Vector cells (*A*-*C*), indicating that the mutation has no major effect on TGN structure. In addition, transport assays demonstrated that VSV-G protein transport in the CortactinS298A-GFP cells was not notably influenced (Dr. Angelika Hausser, university of Stuttgart, personal communication). Concluding from these data, it seems that the CortactinS298A mutation has no major influence on either TGN structure or on transport from the Golgi to the plasma membrane. As an implication, this also suggests that for these processes Cortactin might not be a PKD substrate.

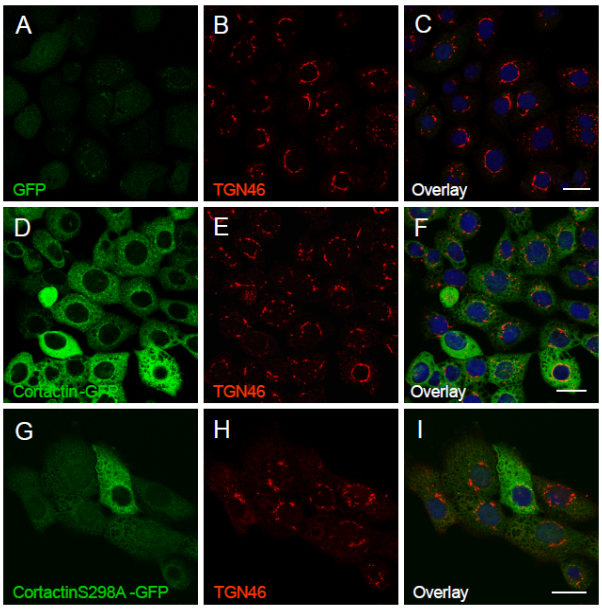

Fig. 18: **(D)** Confocal image sections of stable Panc89 cells expressing GFP (A-C) Cortactin-GFP (D-E) and CortactinS298A-GFP (G-I) stained for TGN46. Cells were seeded at a density of 100.000 cells on Collagen IV coated cover slips. Following Methanol/Aceton fixation cells were processed for indirect immunofluorescence. Nuclei were stained using DRAQ5. Images were taken at 100x magnification. The scale bar represents 20 µm.

5.15 Functions of PKD isoforms and kinase-dead mutants in the invasion of Panc89 cells

Expression of PKD isoforms and kinase-dead variants in Panc89 cells has been shown to influence cell migration in 3D Transwell migration assay. To investigate a role of PKD on the invasive potential of Panc89 cells, combined migration/invasion assays were done using Transwell filters coated with Matrigel™ (BD Bioscience, Heidelberg), which is a basal membrane surrogate only allowing cells to pass the filter membrane, if they are able to degrade the coated matrix *(4.2.6.5)*. In **Fig. 19A** the summarised results of a combined migration and invasion assay for the Panc89 cells expressing GFP, PKD1-GFP, PKD1KD-GFP, PKD2-GFP, as well as PKD2KD-GFP are shown. Bars representing cell migration are coloured black, while invasive cells are displayed in grey. Strongly invasive Colo357 cells (A. Trauzold, university of Kiel, personal communication) were used as a control. Migration of cells was induced by an FCS gradient for 40h. As expected, the effects of the above mentioned constructs on the migration of the stable Panc89 cells were comparable to those seen in **Fig. 11A**, with PKD1KD-GFP enhancing cell migration, while after expression of PKD1- and PKD2-GFP, cell migration relative to the GFP-Vector was impaired. Analysing relative cell invasion through Matrigel™-coated filters, neither construct appeared to have a strong influence. Although plotting invasion relative to the number of migrated cells, PKD1- as well as PKD2-GFP displayed enhanced relative invasion **(Fig. 19B)**. As seen in **Fig. 19B**, [%] invasion was calculated as the number of invading cells/number of migrating cells x 100. Means and respective standard deviations for the summarised data of 4 independent Transwell migration/invasion assays, and three different sorts were displayed in the diagram. Analysing the data, only PKD1-GFP displayed a significantly enhanced invasion relative to GFP-Vector cells, when calculated using the student paired test, whereas relative invasion of the strongly migrating PKD1KD-GFP cells seemed to be reduced, yet the difference was not statistically significant. The same applies for the somewhat enhanced invasion, following the expression of PKD2-GFP. The Colo357 cells used as a positive control also were fairly

invasive, reaching almost PKD1-GFP levels in the assay. Yet, although PKD1-GFP cells exhibited a relative increase in invasion, due to the limited number of cells passing through the Matrigel™-coated filters, the invasive, matrix-degrading potential of the Panc89 cells appeared questionable.

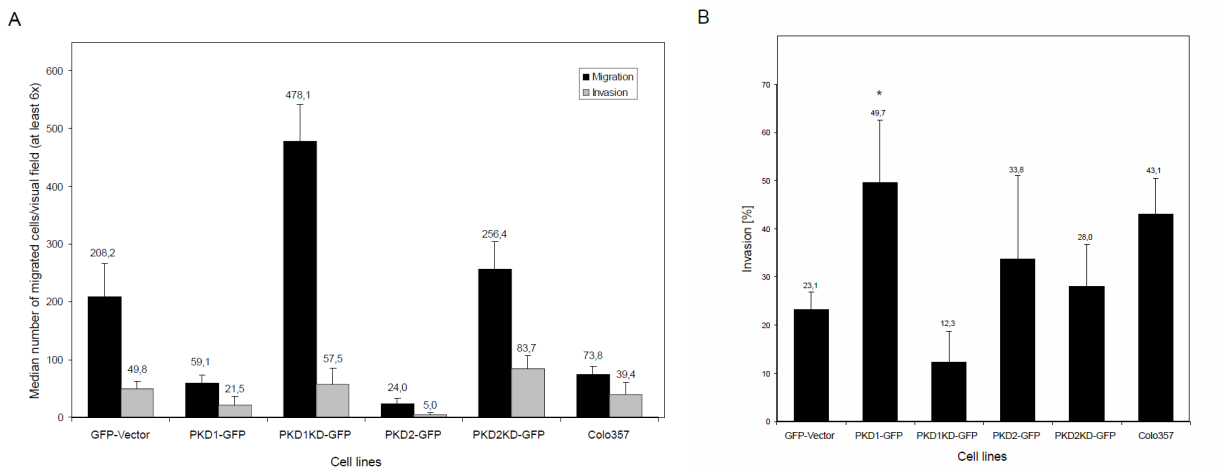

Fig. 19: **(A)** Combined Transwell migration/invasion assay using stable Panc89 cell lines expressing GFP, PKD1-GFP, PKD1KD-GFP, PKD2-GFP, and PKD2KD-GFP. Half of the filters were coated with Matrigel™ (1:5 diluted in RPMI supplemented with 1% FCS and 1mM sodium pyruvate for 30 min at 37°C). 60.000 cells were seeded on the filters and migration was induced by an FCS gradient of 1% - 10% FCS (top of insert/well) for 40 hours. DAPI stained nuclei of migrated cells were used for quantification and documented by a widefield fluorescence microscope equipped with a CCD camera, and a monochromator light source controlled via OpenLab Software (Improvision, UK) at 10 x magnification. Results were calculated as median number of migrated cells/visual field (1024 x 1022), with at least 6 images per filter. The assay is representative of at least 3 experiments performed under the same settings. **(B)** Summarised data of 4 independent Transwell migration/invasion assays and three different sorts of the stable Panc89 cell lines characterised previously. Percent invasion was calculated as number of invading cells/number of migrating cells x 100. Means and respective standard deviations for the summarised data [% Invasion] of individual assays were plotted in the diagram. Differences in relation to GFP-Vector cells were marked as statistically significant according to a student paired test by an asterisk (*).

In order to further investigate the Panc89 cells in respect to their matrix-degrading ability, a second type of *in vitro* invasion assay utilising permeabilised KIF-5 fibroblast layers was done *(4.2.6.6)*. As seen in **Fig. 19C**, confluent KIF-5 layers were overlayed with the respective stable Panc89 cell lines and incubated for 60 h. Then the cells were subjected to a trypan-blue vitality staining to differentiate between living tumour cells and the permeabilised KIF-5 fibroblasts. Documented images of the fibroblast layers (*F*) with the overlayed tumour cells are shown in (*A-E*), and (*G*). As expected the highly invasive Colo357 cells exhibited a strong matrix-degrading activity, documented in (*G*) by the dissolved KIF-5 fibroblast layer. In contrast, the Panc89 cells did not visibly degrade the monolayers. As seen in (*A-C*), and (*E*), GFP-Vector, PKD1-GFP, PKD1KD-GFP, as well as PKD2KD-GFP cells mostly were growing in cell clusters, barely touching the surface of the KIF-5 fibroblasts. Only cells expressing PKD2-GFP (*D*) were extensively attached to the fibroblast monolayer; yet they did not massively destroy the fibroblast layer integrity, as seen in (*G*) by the strongly invasive Colo357 cells.

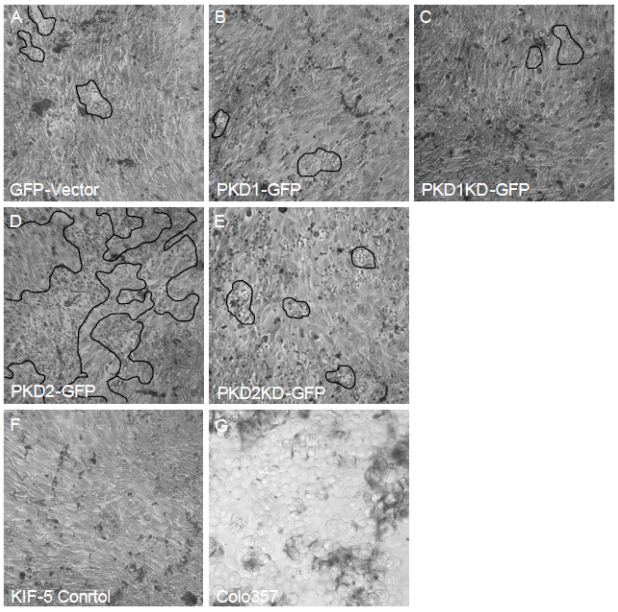

Fig. 19: **(C)** Cell invasion assays in KIF-5 fibroblast layers to show the invasive potential of cancer cells using a modified trypan-blue dye-base model. KIF-5 fibroblasts were grown to a confluent monolayer and permeabilised with DMSO. Then monolayers were overlayed with stable Panc89 cell lines expressing GFP, PKD1-GFP, PKD1KD-GFP, PKD2-GFP, and PKD2KD-GFP at a density of 20.000 cells/well in standard growth media (A-E). A strongly invasive positive control: Colo357 cells (G), and a KIF-fibroblast monolayer (F) as negative control, were also included in the assay. Tumour cells were left to grow for 60 h, daily exchanging the growth media, then cells were stained using trypan blue solution and immediately documented using a widefield fluorescence microscope equipped with a CCD camera, and a white light source controlled via OpenLab Software (Improvision, UK) at 10x magnification using the translucent settings of the software. Live tumour cells were left unstained while permeabilised KIF-5 fibroblasts displayed a blue staining. Disrupted KIF-5 monolayers indicate invasive growth (G).

Concluding from this invasion assay, the matrix-degrading activity of Panc89 cells is rather limited, a fact, which does not allow a comprehensive analysis of the invasive potential of the different stable cell lines. Unfortunately, the establishment of stable Colo357 cells failed. Therefore an investigation of the influence of the different PKD isoforms and kinase-dead mutants has to be done in other cell lines in the future.

Since there were differences in the extent of cell adhesion to the fibroblast layers, as seen in **Fig. 19C** (*D*), cell adhesion assays towards different substrates were performed to investigate this phenotype further.

5.16 Function of PKD isoforms and kinase-dead mutants in cell-substratum adhesion of stable Panc89 cells

In **Fig. 20A** the summarised data of a cell adhesion assay is shown *(4.2.6.7)*. Panc89 cells were seeded in 96 well TC-plates, precoated with the respective substrates as described in the figure legend, and incubated for 1 and ½ h to allow adhesion of cells. Subsequently non-adherent cells were washed away and cell adhesion was assayed by subjecting the plates to crystal violet staining *(4.2.6.10)*. As shown in **Fig. 20A**, cell adhesion in all cell lines was enhanced following coating with Collagen IV, Matrigel™, and Poly-L-Lysine compared to the TC-coat alone. BSA coated wells only incubated with growth media were used as negative controls. Since Matrigel™ has been designed to resemble in composition a basal membrane layer, this is the best coat to comprehensively study cell adhesion phenotypes. Yet, when analysing the adhesion of the stable cell lines towards the above mentioned substrates, no significant differences were witnessed, indicating that the tested PKD isoforms and kinase-dead mutants did not influence cell adhesion of Panc89 cells. This is also in line with the data displayed in **Fig. 20B**, and **C**, were PKD1- and PKD1KD-GFP **(Fig. 20B**, *E-H*, *I-L***)** did not colocalise with the general focal adhesion marker FAK. Also in the case of a second focal adhesion protein, Paxillin **(Fig. 20C)**, no colocalisation was found in either PKD1- and

PKD1KD-GFP, as well as PKD2- and PKD2KD-GFP expressing cell lines (*also discussed in 5.3.2*), further emphasising that PKD isoforms do not influence cell adhesion.

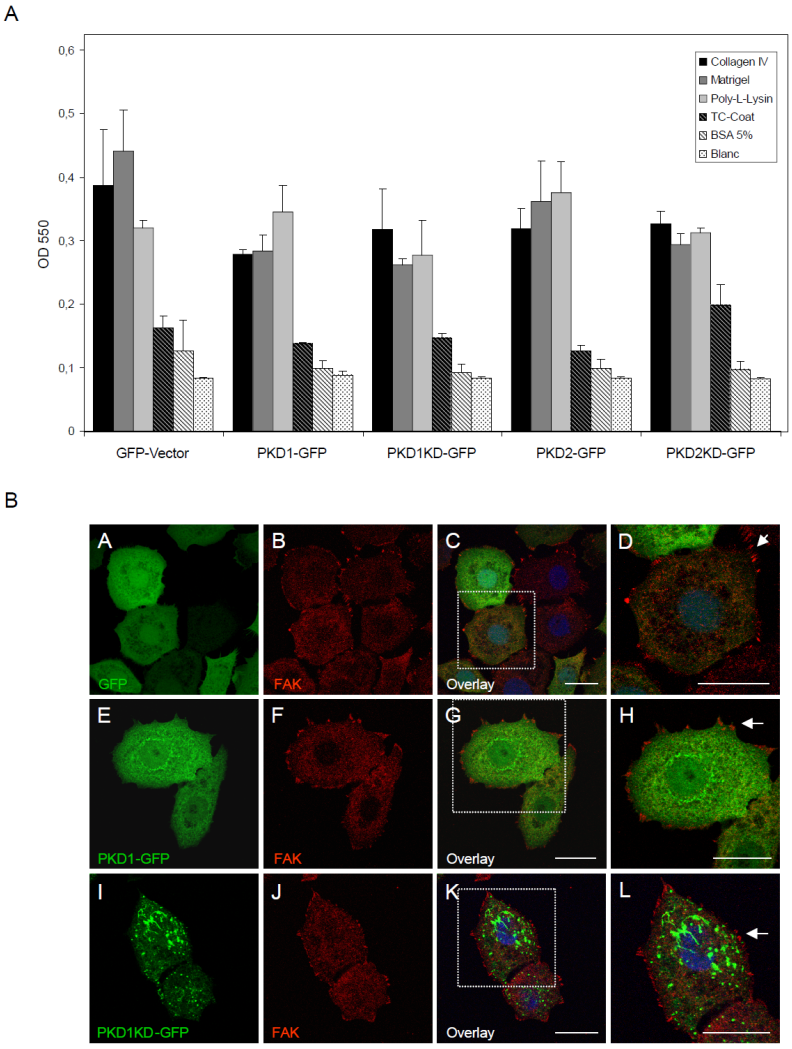

Fig. 20: **(A)** Cellular adhesion assays towards different adhesive substrates were done in 96 well TC-plates coated with *Collagen IV*: 22.5 µg/ml in PBS; *Poly-L-Lysine*: 0.1% (v/v) 1:10 in H_20; *Matrigel*^{TM}: 1:8 dilution in PBS (Phenol-red-free) and as negative control *BSA*: 5% BSA for 1h at 37°C. Stable Panc89 cell lines expressing GFP, PKD1-GFP, PKD1KD-GFP, PKD2-GFP, and PKD2KD-GFP were seeded at a density of 30.000 cells/well in standard growth media. After 1h 30 min cells, which had not adhered were washed away and cell adhesion on different adhesive substrates was quantified using crystal violet staining as described in 4.2.6.10. Relative adhesion was shown by calculating OD 550 means of triplicate wells and respective standard deviations for each cell line and coating condition assayed. **(B)** Confocal image sections of stable Panc89 cell lines stained for Focal adhesion kinase (FAK): GFP (A-D), PKD1-GFP (E-H) and PKD1KD-GFP (I-L). Cells were seeded at a density of 100.000 cells on Collagen IV coated cover slips. Nuclei were stained with DRAQ5. Images were taken at 100x magnification using a Leica TCS SP2 confocal microscope. The scale bar represents 20 µm.

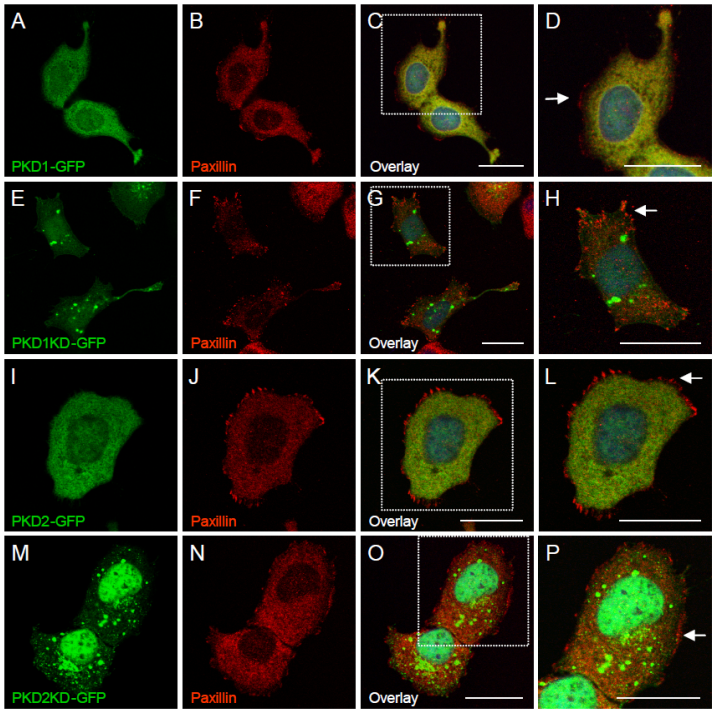

Fig 20: **(C)** Confocal image sections stable Panc89 cell lines stained for Paxillin: PKD1-GFP (A-D), PKD1KD-GFP (E-H), PKD2-GFP (I-L), PKD2KD-GFP (M-P). Cells were seeded at a density of 100.000 cells on Collagen I coated cover slips. Nuclei were stained with DRAQ5. Images were taken at 100x magnification using a Leica TCS SP2 confocal microscope. The scale bar represents 20 µm.

An alternative explanation for the spreaded PKD2-GFP cells on the KIF-5 monolayers **(Fig. 19C)** would be altered cell-to-cell adhesion. To study cell aggregation processes, which are mainly regulated by large, glycosilated, Ca^{2+}-dependent transmembrane proteins called Cadherins, the different stable Panc89 cell lines were cultured in “hanging drops” to induce spheroid formation (*described in 3.3.1*).

5.17 Function of PKD isoforms, kinase-dead mutants and Cortactin in cell-to-cell adhesion of Panc89 cells

5.17.1 Cell aggregation assays using stable Panc89 cell lines

In **Fig. 21A** cell aggregation assays using stable Panc89 cells expressing GFP, PKD1-GFP, PKD1KD-GFP, PKD2-GFP, PKD2KD-GFP, as well as Cortactin-GFP, and CortactinS298A-GFP are shown. The expression of the respective stable transgenes is documented in the Western blots at the *right hand side* of the figure. Cell-to-cell aggregation assays with the stable cells were performed by culturing 6.000 cells for 24 h in “hanging drops”, thereby omitting adhesion of the cells to a growth-supporting surface *(4.2.6.8)*. Since PDAC cells under these conditions tend to form spheroid aggregates, this feature of the cell lines can also be used to assay cell-to-cell adhesion in Panc89 cells. Following incubation for 24 h, the aggregated cells in the droplets were resuspended 10 times and immediately documented using an Axiovert 35 inverted microscope equipped with camera and controller unit (Zeiss) at 10x magnification. In **Fig. 21**, image (*A*) following resuspension, GFP-Vector cells are shown forming small to medium size aggregates, indicating that cell-to-cell adhesion was not very strong. In contrast PKD1-GFP (*B*), PKD1KD-GFP (*C*), as well as PKD2KD-GFP (*E*) expressing cells formed larger, singular aggregates with visibly enhanced cellular aggregation when compared to GFP-Vector cells (*A*). Investigation of cell aggregates formed

by PKD1KD- as well as PKD2KD-GFP expressing stable cell lines also indicated an increased cell aggregation compared to PKD1-GFP cells, since spheroids seemed to be more densely packed. Interestingly, expression of PKD2-GFP in Panc89 cells was not able to markedly increase cellular aggregation relative to GFP-Vectors cells, as seen in (*D*). Expression of Cortactin- (*F*), and CortactinS298A-GFP (*G*) strongly enhanced cell aggregation compared to GFP-Vector cells, with the S298A mutant resulting in the formation of almost completely circumscribed spheroid structures, indicating enhanced aggregation of cells. The assay shown here is representative of at least 3 different experiments performed under the same experimental settings.

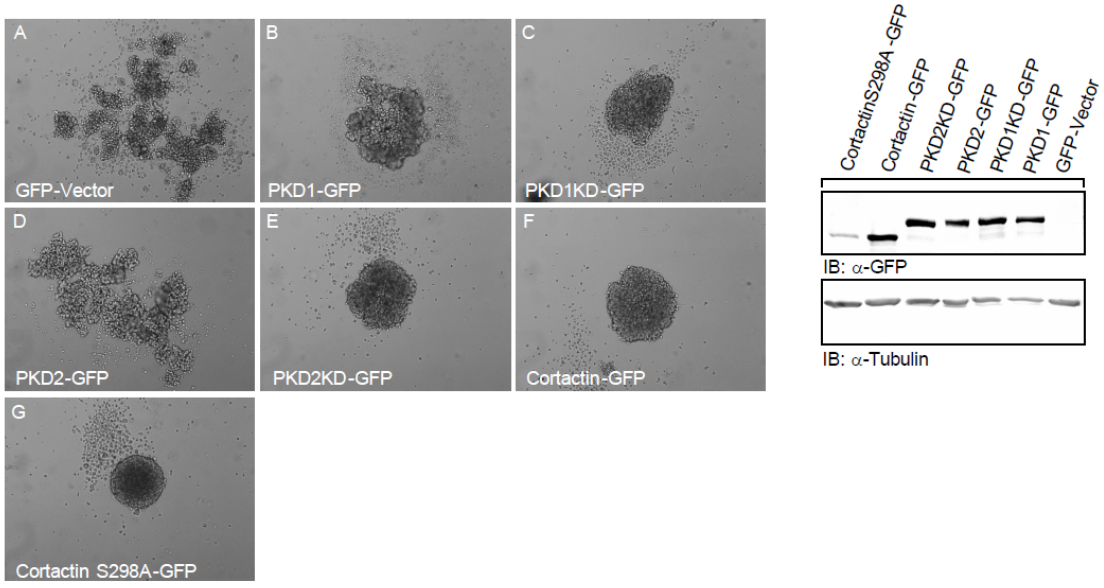

Fig. 21: **(A)** Cell-to-cell adhesion assays using stable Panc89 cells expressing GFP, PKD1-GFP, PKD1KD-GFP, PKD2-GFP, PKD2KD-GFP, Cortactin-GFP, and CortactinS298A-GFP. For aggregation assays 6.000 Panc89 cells of respective cell lines resuspended in 20 µl of standard growth media were dropped on the inner surface of the lid of a 10 cm cell culture dish. The lid was inverted and cells were cultured in "hanging drops" for 24 h. Following aggregation, droplets were resuspended ten times using a 10 µl micropipette. Cell aggregates were documented by an Axiovert 35 inverted microscope equipped with camera and controller unit (Zeiss) at 10x magnification.

Summarising the data, PKD1-, PKD1KD-, as well as PKD2KD-GFP expressing cells showed enhanced cell-to-cell adhesion relative to GFP-Vector cells, with the kinase-dead mutants even exhibiting an increased effect compared to PKD1-GFP. Analysing the packing of the documented spheroid structures, PKD2KD-GFP, amongst the PKD constructs, seemed to mediate the strongest increase in cell aggregation, while PKD2-GFP only was able to slightly enhance cellular aggregation compared to GFP-Vector cells. Cortactin-GFP as well as CortactinS298A-GFP also strongly increased cell aggregation, with the S298A mutant probably having the biggest impact on cell-to-cell adhesion, as seen by the almost perfect circumscribed spheroid structure formed. The increase in adhesion upon overexpression of Cortactin is also in line with published data by Helwani et *al.* (2004) implicating Cortactin in the Cadherin-mediated cellular contact formation, which could also be an explanation for the strongly enhanced cell aggregation seen in the Panc89 cells. Yet, the function of PKD in cell-to-cell aggregation has to be elucidated still further.

5.17.2 Ca^{2+}- and E-Cadherin dependence of cell aggregation in stable Panc89 cell lines

In order to conclusively demonstrate, that the observed cell aggregation was Ca^{2+}-dependent, possibly mediated by Cadherins, like E-Cadherin, the cells were incubated in "hanging drops" with 2mM EGTA included in the standard growth media. As seen in **Fig. 21B** (*A, E, I, M, Q*), Panc89 cells in standard growth media (control) showed the same pattern of aggregate formation seen in **Fig. 21A**, with GFP-Vector cells (*A*) exhibiting the weakest and PKD2KD-GFP expressing cells (*Q*) the strongest cell aggregation. Inclusion of 2mM EGTA in the assay completely abrogated cell adhesion, as seen in (*B, F, J, N, R*) for all stable cell lines. To investigate, if the observed adhesion phenotypes were mediated by E-Cadherin, a likely candidate in the Panc89 cells, 1µg/ml α-HECD-1 antibody was included in the assays. α-HECD-1 (Invitrogen, Karlsruhe) is a monoclonal antibody raised against an epitope in the extracellular domain of *human* E-Cadherin. It can be used, according to the manufacturer's description, for competition experiments as well as for FACS analysis. In addition, binding of α-HECD-1 on parental Panc89 cells was demonstrated via flow cytometry, as seen in **Fig. 22E**. In **Fig. 21B** aggregation assays using a respective isotype control are shown in (*D, H, L, P, T*). In these assays, aggregates of PKD1- and PKD1KD-GFP cells were somewhat fragmented in relation to the untreated controls in (*A, E, I, M, Q*), but nevertheless specific α-HECD-1-mediated phenotypes were clearly visible, as seen in (*C, G, K, O, S*). Following inhibition of cell-to-cell adhesion with α-HECD-1 at a concentration of 1µg/ml, GFP-Vector (*C*) and PKD1-GFP (*G*) cells were almost completely prevented from forming aggregates, whereas PKD1KD-GFP expressing cells showed small, residual aggregates, indicating that cell-to-cell adhesion was not completely blocked by the HECD-1 antibody. In addition PKD2-GFP cells also displayed small, dispersed cell aggregates, while cellular aggregation of PKD2KD-GFP cells was inhibited only to a minor extent by α-HECD-1, as indicated by the large spheroid structure in (*S*), which however showed a clearly reduced packing density when compared to untreated (*Q*), or isotype controls (*T*). Taken together, the data suggest that the cell-to-cell adhesion responsible for the cellular aggregates of GFP-Vector, PKD1-GFP, PKD1KD-GFP, as well as for PKD2-, and PKD2KD-GFP cells is Ca^{2+}-dependent, and at least partially E-Cadherin-mediated. Aggregation of GFP-Vector, PKD1-GFP, PKD1KD-GFP, and also PKD2-GFP cells was strongly dependent on E-Cadherin, whereas aggregates of PKD2KD-GFP expressing cells were largely resistant towards competition with the α-HECD-1 antibody, possibly indicating a shift in Cadherin isotype expression towards other Cadherin subtypes, like P-Cadherin. In addition, small aggregates of PKD1KD-GFP cells following interference with α-HECD-1 indicated a weak residual cell adhesion, which might have been mediated as well by the expression of other Cadherin isoforms.

In **Fig. 21B** right below the images of the aggregation assays, Western blots of total cell lysates from the stable Panc89 cell lines are shown. On the *left hand side* of the figure the expression of the respective GFP-tagged transgenes is displayed, while on the *right hand side* the E-Cadherin expression was analysed using a α-E-Cadherin antibody (BD Bioscience, Heidelberg; *blot panel 1*). E-Cadherin expression in PKD1-GFP cells was equal or slightly increased compared to GFP-Vector cells, whereas in PKD1KD-GFP and to a much

greater extent in PKD2KD-GFP expressing cells, specific E-Cadherin immunoreactive bands were reduced. PKD2-GFP cells, on the other hand, displayed an increase in E-Cadherin expression. In addition there were two fragments visible in the Western blot migrating at approximately 80-100 kDa respectively, which were also stained using the α-E-Cadherin antibody from BD, possibly constituting E-Cadherin fragments, which have been demonstrated in the literature to block cell-to-cell adhesion. Aggregates formed by PKD2KD-GFP cells demonstrated strong cellular adhesion **(Fig. 21B**, *Q***)**, which was largely independent of E-Cadherin expression **(Fig. 21B**, *S***)**. These data are in line with the weak E-Cadherin band in the Western blot **(Fig. 21B**, *left hand side***)**, further pointing to the expression of different Cadherin isoforms, responsible for the observed cellular aggregation phenotypes. PKD1KD-GFP cells display a reduced E-Cadherin expression, too; accordingly, also for this cell line, other cadherins may contribute to cell aggregation.

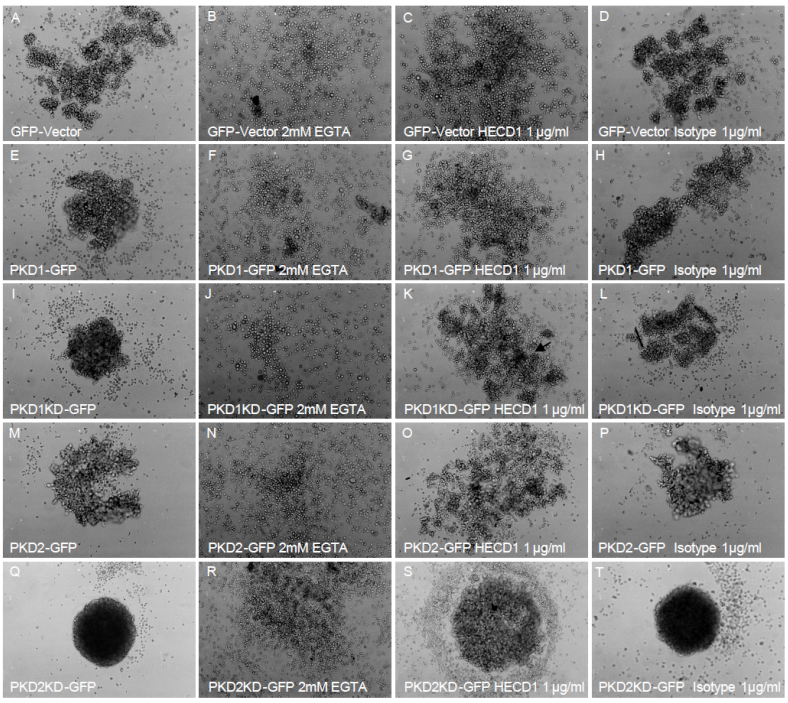

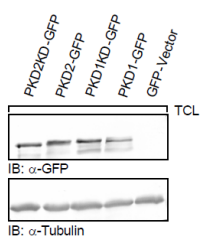

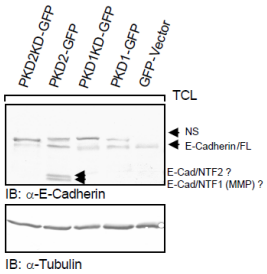

Fig. 21: **(B)** Cell-to-cell adhesion assays using stable Panc89 cells expressing GFP, PKD1-GFP, PKD1KD-GFP, PKD2-GFP, and PKD2KD-GFP. 6.000 Panc89 cells of respective cell lines resuspended in 20 µl of standard growth media were cultured as hanging drops for 24 h. When indicated in the figures, 2mM EGTA, α-HECD-1 (E-Cadherin antibody), as well as the respective isotype control were included in the droplets. Following aggregation, droplets were resuspended ten times using a 10 µl micropipette. Cell aggregates were documented by an Axiovert 35 inverted microscope equipped with camera and controller unit (Zeiss) at 10x magnification. Below the aggregation assays Western blots are shown displaying transgene expression (*right hand side*) and also E-Cadherin expression (*left hand side*). 80 µg of total cell lysate per lane. *Right hand side panel of blots*: PKD-GFP transgene expression (*blot panel 1*). α-Tubulin was included as a loading control (*blot panel 2*). *Left hand side panel of blots*: E-Cadherin expression was detected using α-E-Cadherin antibody (BD Bioscience, Heidelberg; *blot panel 1*). α-Tubulin again was included as a loading control (*blot panel 2*). Respective full length E-Cadherin (FL) and E-Cadherin fragment bands (NTF1/2) are marked by arrows. NS, non specific band.

5.17.3 Processing of E-Cadherin in PKD2-GFP cells

In **Fig. 22A**, a schematic overview of E-Cadherin is shown. As mentioned above, there were two additional bands visible in E-Cadherin Western blots, which were immunoreactive with the BD E-Cadherin antibody and therefore might constitute E-Cadherin fragments. As displayed in **Fig. 22A**, E-Cadherin can be processed by different enzymes, like matrix-metalloproteases (MMPs), serine-proteases, γ-Secretase, or Calpain, yielding different E-Cadherin fragment combinations, which are indicated in the figure. E.g. Noe et *al.* (2000) and Hayashido et *al.* (2005) published the MMP-mediated generation of an 80 kDa, N-terminal E-Cadherin fragment (NTF1), which is shedded into the cell culture supernatant of certain cancer cell lines, being able to abrogate cell-to-cell adhesion by interfering with the homophilic E-Cadherin interaction of neighbouring cells. Possible enzymes involved in this process are Matrilysin, and Stromolysin-1, (Noe et *al.*, 2000), as well as ADAM10, a disintegrin-metalloprotease, which has been implicated in E-Cadherin processing by Maretzky et *al.* (2005). Such an N-terminal fragment would also be an explanation for the reduced cellular aggregation observed in cell adhesion assays, using the stable PKD2-GFP Panc89 cell line. In order to investigate, if the two E-Cadherin fragments identified in **Fig. 21B** were derived of the N-terminal, extracellular part of the E-Cadherin molecule, which is also heavily glycosilated, total cell lysates of the stable Panc89 cells were subjected to deglycosilation by PNGaseF. As shown in the Western blot in **Fig. 22B**, both the full length E-Cadherin in all lysates, as well as the E-Cadherin fragments were deglycosilated, indicating that the fragments contained the N-terminal, extracellular part of E-Cadherin. As mentioned above, the shedding of such an 80 kDa, N-terminal E-Cadherin fragment (NTF1), amongst others, is mediated by MMP cleavage **(Fig. 22A)**. Yet, this cleavage would not explain the second, larger N-terminal fragment observed in the Western blots in **Fig. 21B** and in deglycosilation assays **(Fig. 22B)**. One explanation would be as follows: In addition to this processing by MMPs, both, the full length, as well as residual MMP-processed E-Cadherin (CTF1) can also be cleaved further by γ-Secretase, as indicated in **Fig. 22A**, yielding in the case of full length E-Cadherin, a second N-terminal E-Cadherin fragment (NTF2), which is not shedded in the supernatant and a corresponding CTF2 fragment (Marambaud et *al.*, 2002). Calpain has also been implicated in the processing of E-Cadherin, producing a 100 kDa fragment, which is no longer capable of binding p120, or Catenins, thus resulting in the disruption of E-Cadherin adhesion complexes (Rios-Doria et *al.*, 2002).

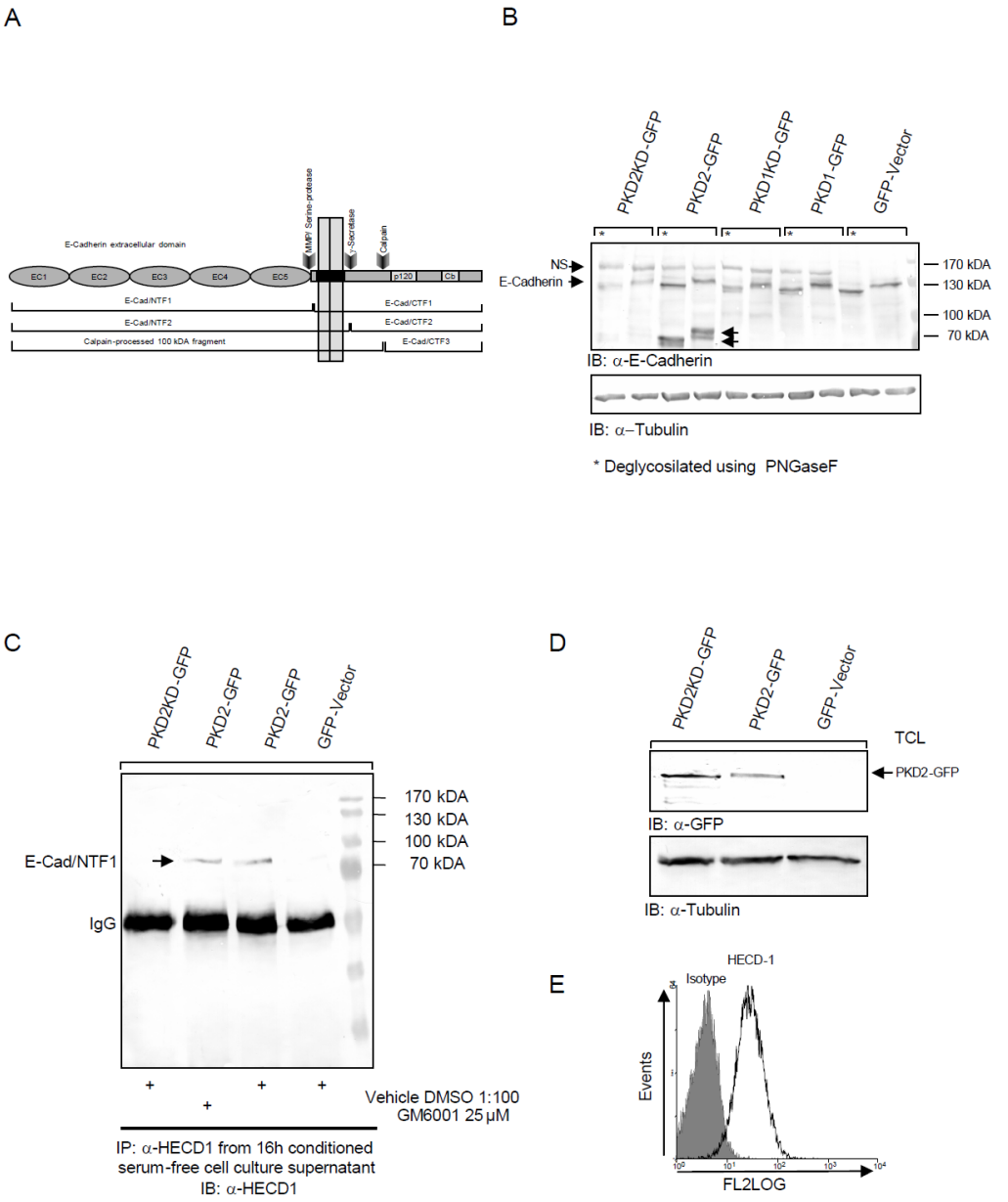

Fig. 22: **(A**) Schematic overview of E-Cadherin structure and processing. Respective fragments generated via cleavage of MMPs, serine-proteases, γ–Secretase or Calpain are marked in the figure. Enzyme cleavage sites are marked with arrows. EC1-5, E-Cadherin extracellular repeat 1-5; p120, p120 binding domain; Cb, Catenin binding domain. **(B)** *Blot panel 1*: 100 µg total cell lysate from each stable Panc89 cell line was either subjected to deglycosilation using PNGaseF (*) or treated respectively omitting PNGaseF. Lysates were blotted against α-E-Cadherin (BD). α-Tubulin was included as a loading control (*blot panel 2*). Down-shift of E-Cadherin bands relative to control indicates deglycosilation. E-Cadherin fragment bands are also affected by deglycosilation, indicating their N-terminal origin. **(C)** Immunoprecipitation of E-Cadherin fragments from conditioned cell culture supernatants of Panc89 GFP-Vector, PKD2-GFP, and PKD2KD-GFP cell lines. Immunoprecipitations were done from 16h conditioned serum-free media using α-HECD-1 antibody. When indicated either the broad spectrum MMP inhibitor GM6001 25 µM, or the respective amount of DMSO vehicle were coincubated. Immuncomplexes were detected also using α-HECD1. **(D)** Total cell lysates of GFP-Vector, PKD2-GFP and PKD2KD-GFP cells used in **(C)** blotted for PKD-GFP transgene expression (*blot panel 1*). α-Tubulin was included as a loading control (*blot panel 2*). **(E)** FL2LOG histogram showing α HECD-1 binding to parental Panc89 cells labelled with α-HECD-1, or a respective isotype control, indicating the antibody used for competition in *Fig. 20 (B)* and immunoprecipitations *Fig. 21 (C)* binds specifically to the extracellular domain of E-Cadherin.

Before the generation of this second, N-terminal fragment was investigated, experiments were done to check, if the 80 kDa fragment seen in the PKD2-GFP lysates in **Fig. 21B** and **22B** was in fact shedded in the cell culture supernatant, thereby being able to interfere with the cellular aggregation of PKD2-GFP expressing cells. In **Fig. 22C** immunoprecipitations of E-Cadherin from 16h conditioned, serum-free cell culture supernatants using the α-HECD-1 antibody are shown. In addition, the broad-band MMP-inhibitor GM6001 as well as the respective vehicle control were included in the assays to analyse if a putative precipitated fragment would be generated by the activity of MMPs or ADAM10, respectively. As demonstrated in the Western blot, an 80 kDa E-Cadherin fragment was specifically shedded by PKD2-GFP expressing cells, and not by the GFP, as well as the PKD2KD-GFP expressing cell lines. Yet, the inhibition of MMPs by the addition of 25 µM GM6001 had no effect on the processing of the fragment, indicating that other proteases are involved in the generation of the 80 kDa, N-terminal E-Cadherin cleavage product. In **Fig. 22D** the transgene expression of the stable cell lines used in **Fig. 22C** is displayed. **Fig. 22E** demonstrates the binding of α-HECD-1 used in immunoprecipitation **(Fig. 22C)** and competition experiments **(Fig. 21B)** to E-Cadherin of parental Panc89 cells.

A

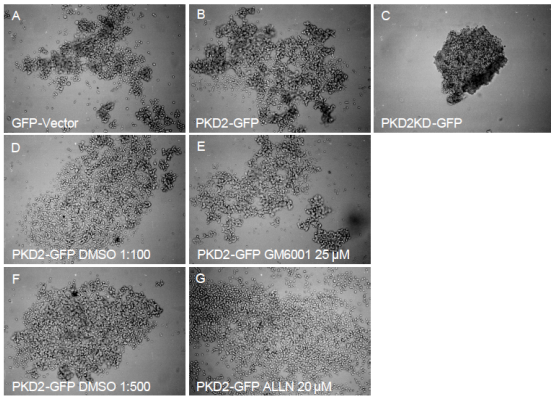

B

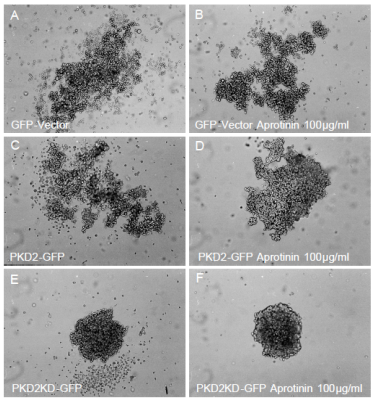

Fig. 23: **(A)** Cell-to-cell adhesion assays using stable Panc89 cells expressing GFP, PKD2-GFP, and PKD2KD-GFP. 6.000 Panc89 cells of respective cell lines resuspended in 20 µl of standard growth media were cultured as hanging drops for 24 h. When indicated in the figures, 20 µM of Calpain inhibitor ALLN, or 25 µM of GM6001 as well as the respective vehicles were included in the droplets of PKD2-GFP expressing cells. Following aggregation, droplets were resuspended ten times using a 10 µl micropipette. Cell aggregates were documented by an Axiovert 35 inverted microscope equipped with camera and controller unit (Zeiss) at 10x magnification. **(B)** Cell-to-cell adhesion assays using stable Panc89 cells expressing GFP, PKD2-GFP, and PKD2KD-GFP. 6.000 Panc89 cells of respective cell lines resuspended in 20 µl of standard growth media were cultured as hanging drops for 24 h. When indicated in the figures, aprotinin (100 µg/ml) as well as the respective vehicle were included in the droplets of the different cell lines. Following aggregation, droplets were resuspended ten times using a 10 µl micropipette and documented as stated above.

In addition to the immunoprecipitation of the 80 kDa E-Cadherin fragment from cell culture supernatants following incubation with GM6001, the MMP inhibitor was also used at a concentration of 25 µM in cell aggregation assays with the PKD2-GFP cell line. As seen in **Fig. 23A**, GFP-Vector, PKD2-, as well as PKD2KD-GFP cells exhibited aggregation

phenotypes expected from previous assays **(Fig. 21 A, B)**. Incubation with GM6001 in "hanging drops" also did not affect aggregation of PKD2-GFP cells relative to the vehicle control **Fig. 23A** (*D, E*), further indicating that the fragments precipitated from the cell culture supernatant were not processed by MMPs, or ADAM10. In order to investigate also a possible Calpain-mediated cleavage of E-Cadherin, which might be involved in the generation of the second, larger E-Cadherin fragment observed in total cell lysates **(Fig. 21B/22B)**, ALLN, a Calpain inhibitor peptide, was included at a concentration of 20 µM in the aggregation assays. Inhibiting Calpain function in PKD2-GFP cells might therefore give a hint, if the 100 kDa fragment observed is indeed processed by Calpain. As displayed in **Fig 23A** (*F, G*), incubation of PKD2-GFP cells with ALLN did not enhance cellular adhesion relative to the vehicle control, which rather points to a γ-Secretase-like cleavage process, being involved in the generation of the larger E-Cadherin fragment.

Since MMPs were not involved in the shedding of the 80 kDa, N-terminal E-Cadherin fragment precipitated from the conditioned cell culture supernatant in **Fig. 22C**, the involvement of other proteases needed to be tested as well. As shown in **Fig. 22A,** in addition to MMPs, also serine-proteases have been published to process Cadherins. Ryniers et *al.* (2002) demonstrated that Plasmin produces an 80 kDa E-Cadherin fragment, which is shedded in the cell culture supernatant, stimulating invasion of cancer cells. In addition Trypsin can catalyse the cleavage of E-Cadherin extracellular fragments *in vitro* (Noe et *al.*, 2000). In the case of PDAC cells, cationic Trypsinogen might be implicated in the processing of E-Cadherin. Ohta et *al.* (1998) showed, that human pancreatic ductal cancer cells express and secrete pancreatic cationic Trypsinogen *in vitro,* which can be spontaneously converted into active Trypsin at acidic pH (pH 4.5-5.5) and might possibly be implicated in the generation of E-Cadherin N-terminal fragments regulating cellular adhesion. To investigate, if serine-proteases are implicated in the regulation of cell-to-cell adhesion of the PKD2-GFP cells by processing the generation of a shedded, N-terminal fragment interfering with the E-Cadherin interaction of neighbouring cells, aprotinin, a serine-protease inhibitor, was included in aggregation assays. As demonstrated in **Fig. 23B**, cell aggregation of PKD2-GFP expressing cells was strongly enhanced (*C, D*) upon incubation with aprotinin at a concentration of 100 µg/ml, while aggregates formed by GFP-Vector (*A, B*) and PKD2KD-GFP (*E, F*) cells were not influenced by aprotinin in relation to the respective vehicle controls. Since aprotinin in aggregation assays was able to reconstitute cell-to-cell adhesion of PKD2-GFP cells, it is very likely that a serine-protease is implicated in the processing of the 80 kDa, extracellular E-Cadherin fragment. However, if this processing is mediated via the Plasminogen/Plasmin-system or by Trypsin, which are both inhibited by aprotinin, has to be investigated further in the future.

In order to substantiate the potential role of PKD in E-Cadherin mediated cell-to-cell adhesion, immunohistochemical stainings were done to analyse the localisation of the respective GFP-tagged PKD isoforms and kinase-dead mutants relative to E-Cadherin in the stable Panc89 cells. As published by Jaggi et *al.* (2005), PKD and E-Cadherin were shown to colocalise at cell junctions. The authors also observed a biochemical interaction of both proteins and reported a phosphorylation of E-Cadherin by PKD1 *in vitro*, the latter of which was associated with enhanced cell adhesion in aggregation assays. To investigate this

further, Panc89 cell lines expressing the various PKD constructs were analysed by confocal microscopy for E-Cadherin expression. In **Fig. 24** image section of GFP-Vector (*A-D*), PKD1- (*E-H*), PKD1KD- (*I-L*), PKD2- (*M-P*), and PKD2KD-GFP (*Q-T*) cells are shown. As seen in (*E-H*), PKD1-GFP colocalised widely with E-Cadherin at membrane structures around the cell periphery, while PKD2-GFP only exhibited limited areas of colocalisation at membrane protrusions (*M-P*). However, neither PKD1KD-GFP (*I-L*) nor PKD2KD-GFP (*Q-T*) displayed colocalisation with E-Cadherin. Concluding from the aggregation assays **(Fig. 21 A/B)** and the immunohistochemical data **(Fig. 24)**, there are indications that PKD1, and maybe also PKD2, are somehow involved in the modulation of E-Cadherin mediated cell-to-cell adhesion, possibly at sites connecting the E-Cadherin transmembrane proteins with the underlying F-Actin cytoskeleton. This is indicated also by the larges areas of colocalisation between E-Cadherin and PKD1-GFP around the periphery of cells (*E-H*), which has been shown also for PKD and F-Actin, in similar structures **(Fig. 12A)**.

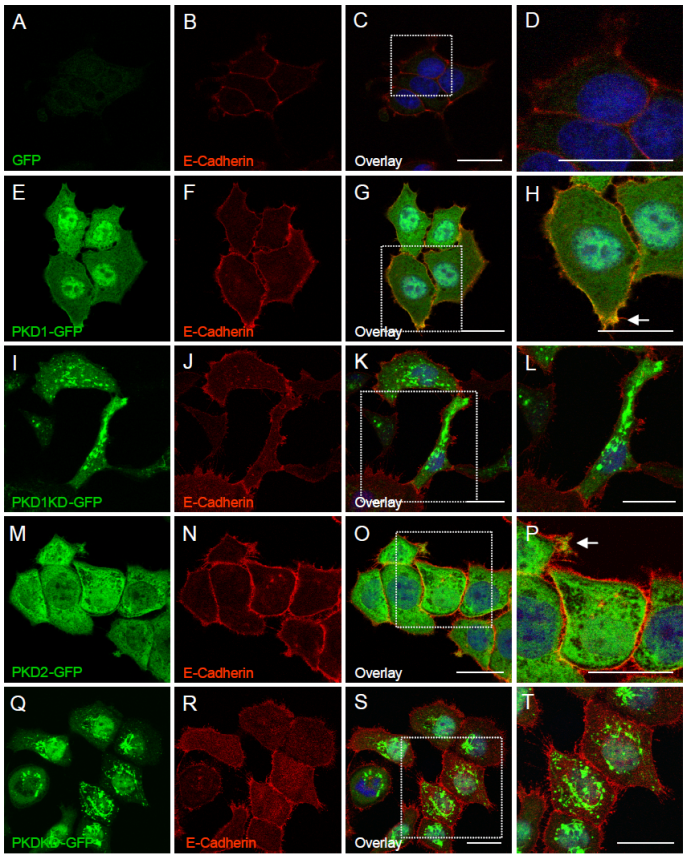

Fig. 24: Confocal image sections of stable Panc89 cell lines stained for E-Cadherin (BD): GFP (A-D), PKD1-GFP (E-H), PKD1KD-GFP (I-L), PKD2-GFP (M-P), PKD2KD-GFP (Q-T) cell lines. Cells were seeded at a density of 100.000 cells on Collagen IV coated cover slips. Nuclei were stained with DRAQ5. Colocalisation in overlay images is indicated by yellow colour and a white arrow. Images were taken at 100x magnification using a Leica TCS SP2 confocal microscope. The scale bar represents 20 µm.

5.18 Expression profiling experiments with stable Panc89 cell lines

In addition to its multiple cellular functions in Panc89 cells, PKD has also been implicated in the control of gene expression (Rykx et *al.*, 2003; VanLint et *al.*, 2002). That's why the different stable PKD1/2-GFP wildtype and kinase-dead expressing cell lines characterised above were also used for expression profiling experiments to investigate the regulation of cancer related genes. The microarray experiments were done in cooperation with Dr. Nicole Hauser (Fraunhofer Gesellschaft, IGB). For the expression profiling, stable cell lines were

cultured without selection for three days, then the cells were harvested and total RNA was prepared using the peQ-Gold-System. Subsequently the RNA preparations were treated with DNAseI (80 Units, 1h 37°C), followed by a phenol-chloroform-purification step. Hybridisation experiments were done in the lab of Dr. N. Hauser using a 1.3 k Cancer array specifically designed as a diagnostic tool for breast cancer studies. 25 µg of total-RNA from parental Panc89 cells, as well as GFP, PKD1-GFP, PKD1KD-GFP, PKD2-GFP, and PKD2KD-GFP expressing cells were subjected to reverse transcription and labelling with Cy3/Cy5-conjugated dNTPs. For each hybridisation experiment, cDNA from GFP-Vector cells was used as control to allow a standardised evaluation of the results relative to the Vector control. The multidimensional raw data acquired from four independent hybridisation experiments of one RNA preparation was then subjected to further data processing steps by our cooperation partner Dr. J. Dippon at the "Institut für Stochastik und Anwendungen" (University of Stuttgart), eliminating genes which exhibited statistically relevant inner- or intra-chip variances. The resulting list of 680 genes, displaying mean log values summarising the gene regulation of the 4 independent experiments relative to the GFP-Vector cohybridisation then was initially analysed by the hierarchical uncentered complete linkage clustering method for genes, using the Gene Cluster Software (Eisen et *al.*, 1998). Cluster subnodes, which exhibited a specific regulation of genes by either, wildtype, or kinase-dead PKD isoforms, plus any given possible respective combination were manually singled out and the resulting list of genes was filtered manually by the following criteria: 1) Genes, which were regulated by a log value < 0.5 relative to Vector control in all hybridisation were eliminated. 2) Genes, which exhibited a regulation between respective wildtype and kinase-dead isoforms < log 0.5 were also filtered out, breaking down the list to 105 genes, as shown in *table 3* (appendix) and the corresponding full linkage hierarchical cluster **Fig. 25 A**. Analysing the regulation of the above mentioned genes in the respective cohybridisations relative to the Vector control, genes which were regulated in PKD1KD-GFP as well as in PKD2KD-GFP cells, with a respective up- or down-regulation of ≥ log 0.5, were listed in *table 4* (appendix). The corresponding cluster analysis is shown in **Fig. 25B**. Genes, which were differentially regulated in PKD1- versus PKD1KD-GFP **(Fig. 25C)**, or in PKD2- versus PKD2KD-GFP **(Fig. 25D)** cells, exhibiting an up- or down-regulation of ≥ log 0.5 are shown in *table 5* and *6* (appendix), respectively. The full linkage hierarchical clusters displaying their regulation are shown in **Fig. 25 C** and **D**.

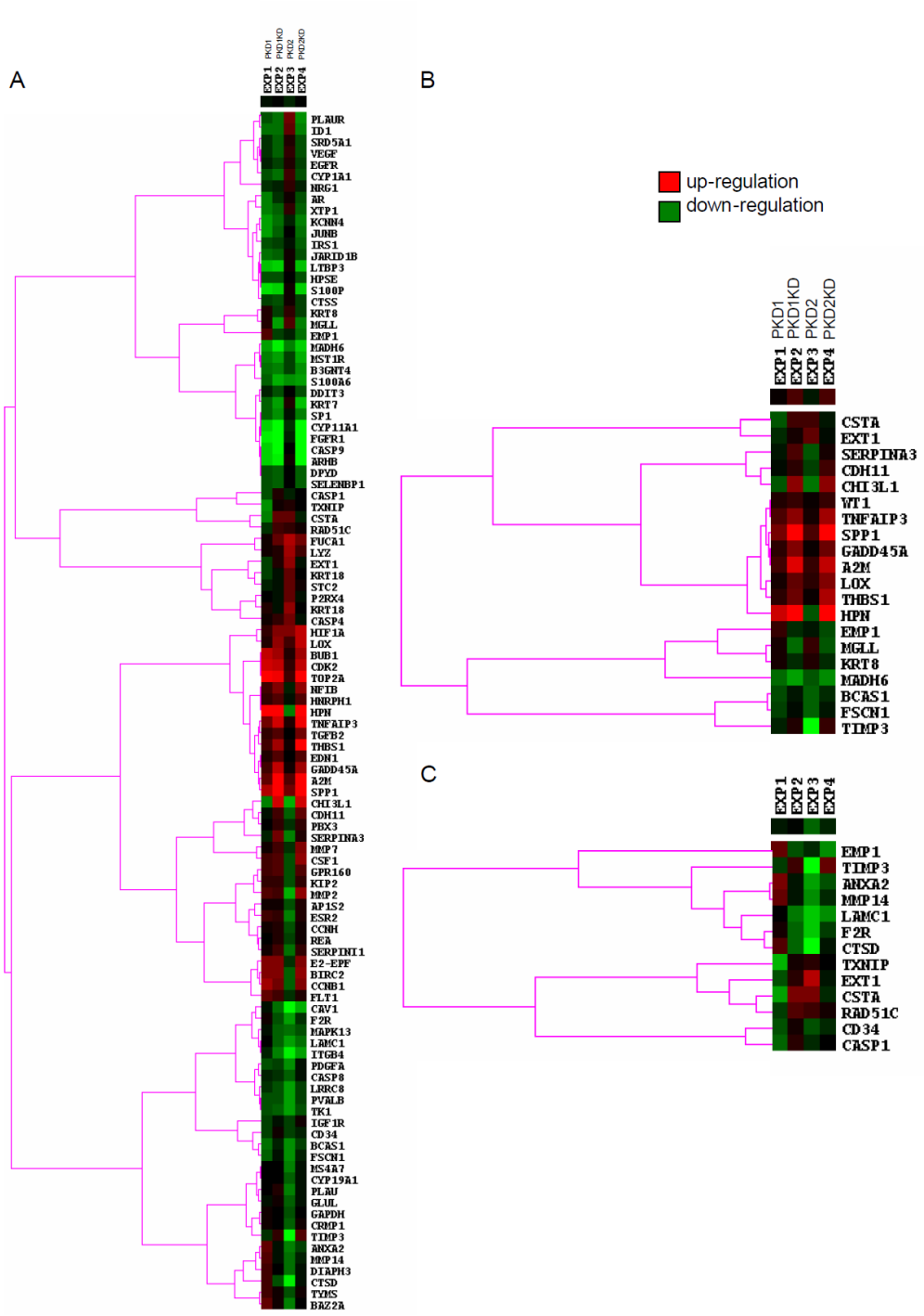

Fig. 25: Cluster analysis of gene profiling experiments with stable Panc89 cell lines. Genes were clustered using the full linkage hierarchical, uncentered cluster method of the Gene Cluster software (Eisen et *al.*, 1998). **(A)** Genes, which exhibited a specific regulation by either wildtype or kinase-dead PKD isoforms and any given possible respective combination were filtered by the following criteria: 1) Genes which were regulated by a log value < 0.5 relative to Vector control in all hybridisation were eliminated. 2) Genes which exhibited a regulation between respective wildtype and kinase-dead isoforms log < 0.5 were also filtered out, resulting in a list of 105 genes (*appendix table 3, Cluster A*). **(B)** Genes, which were regulated in PKD1KD-GFP as well as in PKD2KD-GFP cells with a respective up- or down-regulation relative to their wildtype variants of ≥ log 0.5 were listed in *table 4* (*appendix*) and *Cluster B*. **(C)** Genes, which were differentially regulated in PKD1- versus PKD1KD-GFP cells exhibiting an up- or down-regulation of ≥ log 0.5 are shown in *table 5* (appendix) and *Cluster C*.

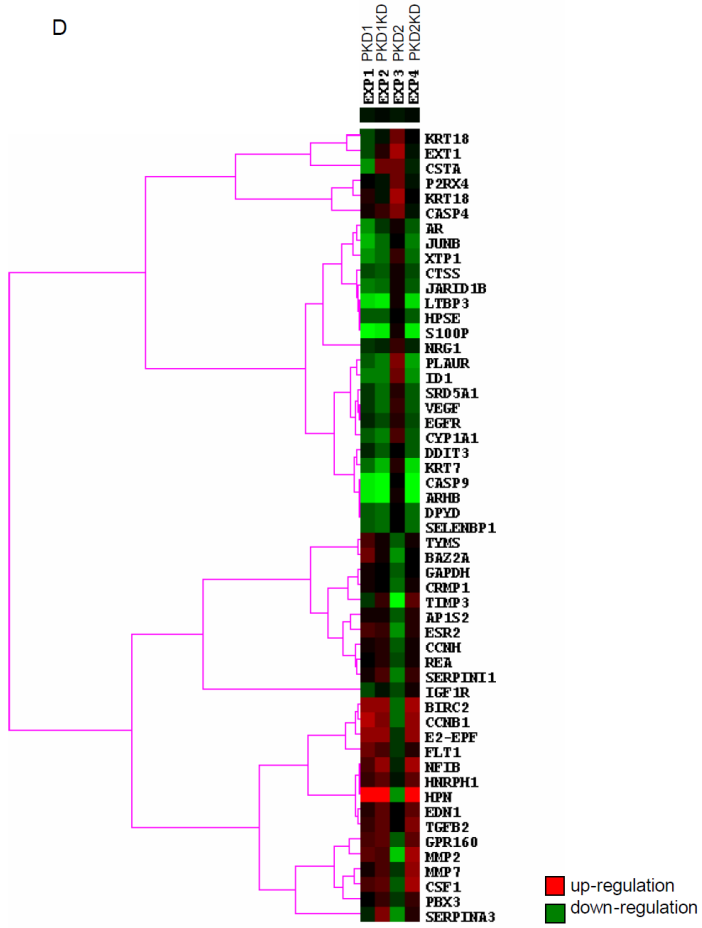

Fig. 25 (D): Cluster analysis of gene profiling experiments with stable Panc89 cell lines. Genes were clustered using the full linkage hierarchical, uncentered cluster method of the Gene Cluster software (Eisen et *al.*, 1998). Genes, which were differentially regulated in PKD2- versus PKD2KD-GFP cells exhibiting an up- or down-regulation of ≥ log 0.5 are shown in *table 6* (*appendix*) and *Cluster D*.

The function and relevance of the individual genes classified above in the respective stable Panc89 cell lines needs to be investigated further. Bearing in mind that PKD has been shown to regulate the nuclear export of histone deacetylases via phosphorylation, and therefore is directly implicated in gene regulation processes, a differential regulation of genes in wildtype versus kinase-dead PKD1/2 expressing cells, as shown in *table 4-6* is very likely to be relevant. The initial analysis performed in this work constitutes a good starting point, yet it is by no means complete, as genes filtered out to reduce complexity might be specifically regulated, as well. The microarray experiments also need to be reproduced with additional RNA samples and genes, which were found to be regulated during the expression profiling, also need independent verification. Genes singled out, and listed above revealed interesting targets. E.g. SPP1 (Secreted phosphoprotein 1), synonym OPN (Osteopontin) is strongly up-regulated in PKD1KD- and PKD2KD-GFP expressing cell lines. SPP1 is a secreted, adhesive glycophosphoprotein containing a RGD consensus motif, which mediates binding to Integrins. Although the functional consequence of SPP1 expression is not completely elucidated, there is good evidence from cell culture experiments with breast cancer cells that it is implicated in enhancing cell migration, pointing to a potential mechanism for increased aggressive behaviour of SPP1-positive breast tumours (Bautista et *al.*, 1994; Senger and Peruzzi, 1996). The function of SPP1 in the migration phenotypes of the stable Panc89 cell lines has still to be analysed, yet it is an interesting target worth while to be investigated

further. Another interesting gene is TIMP3, which is up-regulated in PKD1KD/PKD2KD-GFP cells, whereas in PKD1- and PKD2-GFP expressing cells, it is repressed, indicating a differential regulation via PKD kinase activity **(Fig. 25B)**. TIMP3 (Tissue inhibitor of metalloproteinases-3) is a specific endogenous inhibitor of MMPs and also some disintegrin-metalloproteases, thereby playing a central role in the regulation of the matrix-degrading activity of tumour cells. It is implicated in the regulation of tumour cell invasion and tumour growth. Down-regulation of this gene has been shown to occur in a mouse carcinogenesis model, suggesting that it might play a role in the tumour progression of some cancers (Kang et *al.*, 2000). Plasminogen activators also play an important role in tumour cell invasion. The PLAUR gene **(Fig. 25D)** codes for the urokinase-type Plasmin-activator-receptor (u-PAR). It can specifically catalyze the activation of the urokinase-type Plasmin-activator/Plasmin-system, which is implicated in the degradation of the extracellular matrix and the processing of transmembrane proteins, such as E-Cadherin (Ryniers et *al.*, 2002), enhancing invasion of cancer cells. Since this gene is specifically up-regulated in PKD2-GFP expressing Panc89 cells, it might be implicated in the serine-protease-dependent processing of E-Cadherin, described in *5.17.3*. As mentioned previously, there is still much more work to be done, further cross-referencing the genes with literature data to identify promising candidates, reproducing the gene profiling experiments and also providing independent verification for the regulation of the genes, listed in *table 3-6* **(respective clusters Fig. 25 A-D)**. Yet, even the initial analysis performed so far, showed interesting genes, like SPP1, and PLAUR, which should be investigated more closely in respect to a possible links to the data presented in this work.

5.19 Overview of results

An overview of the most important results, gathered during this study is displayed in **Fig. 26**. As seen in the figure, PKD has been shown to colocalise with, and bind to, F-Actin. PKD1 impaired cell migration, while for PKD1KD expressing cells, migration was enhanced. As described previously, PKD and Cortactin were shown to interact biochemically, as well as to colocalise at the cortical F-Actin cytoskeleton. In addition, PKD phosphorylated Cortactin *in vitro*. Mutation of the potential Cortactin phosphorylation site Ser298 to an alanine residue also increased cell migration in stable Panc89 cells. Since CortactinS298A and PKD1KD phenotypes correlated with respect to their influence on cell migration, Cortactin might be a potential PKD target in the regulation of F-Actin dynamics. The effects on directed migration might therefore be mediated either by Cortactin and/or additional, yet unknown PKD substrates at the respective F-Actin-rich structures **(**for a putative model see *6.1* **Fig. 27)**.
PKD has also been implicated in the literature in the regulation of cell-to-cell adhesion, possibly by the phosphorylation of E-Cadherin itself. As shown in the summary **Fig. 26**, PKD isoforms and kinase-dead mutants influenced Ca^{2+}-dependent cellular adhesion in Panc89 cells in a diverse fashion. PKD2KD, and also PKD1KD to lesser extent, strongly enhanced cell-to-cell adhesion of stable Panc89 cells, yet E-Cadherin expression in the respective cell lines was reduced. At least in the case of PKD2KD cells, aggregation was only partially dependent on E-Cadherin, pointing to the expression of additional Cadherin isoforms. In relation to the vector control, PKD1 also increased cell-to-cell adhesion, yet if this effect is

mediated via a phosphorylation of E-Cadherin, remains to be analysed. PKD2 expressing cells exhibited another interesting feature. Cellular aggregation was very weak, in some assays even resembling the vector control. This could be correlated with shedded, N-terminal E-Cadherin fragments in the supernatant of PKD2 expressing cells, which have been implicated by the literature in the inhibition of cell-to-cell adhesion. Initial results implicated that the fragments found in the cell culture supernatant of PKD2 expressing Panc89 cells were not processed by MMPs, rather by a serine-protease, possibly Plasmin. These findings are also in line with data obtained from expression profiling experiments with the respective stable Panc89 cells, indicating that the PLAUR gene (urokinase-like Plasminogen-activator-receptor) is strongly up-regulated in PKD2 expressing cells, triggering the activation of the uPA-Plasminogen-Plasmin-cascade, which in turn might be implicated in the processing of E-Cadherin.

The cluster analysis of the expression profiling experiments using the stable Panc89 cell lines expressing wildtype and kinase-dead PKD1 and 2 variants also revealed genes generally regulated via PKD kinase activity, independent of the isoform, as well as PKD1/PKD2-specific, differentially regulated genes. An initial cross-referencing with literature data showed interesting candidates, like PLAUR, or SPP1 (Secreted phosphoprotein 1), which is correlated with enhanced cell migration in breast cancer cell lines. Nevertheless, there is much more work to be done, reproducing the microarray data, independently verifying the results, and comprehensively analysing the cluster analysis performed in this work. Taken together, PKD isoforms seem to be involved in the regulation of cancer related genes, which might even be linked to some of the biological effects characterised during the analysis of PKD-function in Panc89 cells.

In addition, as displayed in **Fig. 26**, there were no significant effects visible on to the cell-substratum adhesion of Panc89 cell lines.

The invasive potential of the stable Panc89 cell lines might have been altered by the expression of the different PKD variants, yet due to the limited matrix-degrading ability of the Panc89 cells, a comprehensive analysis was not possible and further experiments need to be done in a more invasive cell line.

Taken together, during this work many interesting aspects concerning a function of PKD in the above mentioned processes have been gathered, yet there is still much more work needed for a comprehensive understanding of PKD action in migration and invasion of cancer cells.

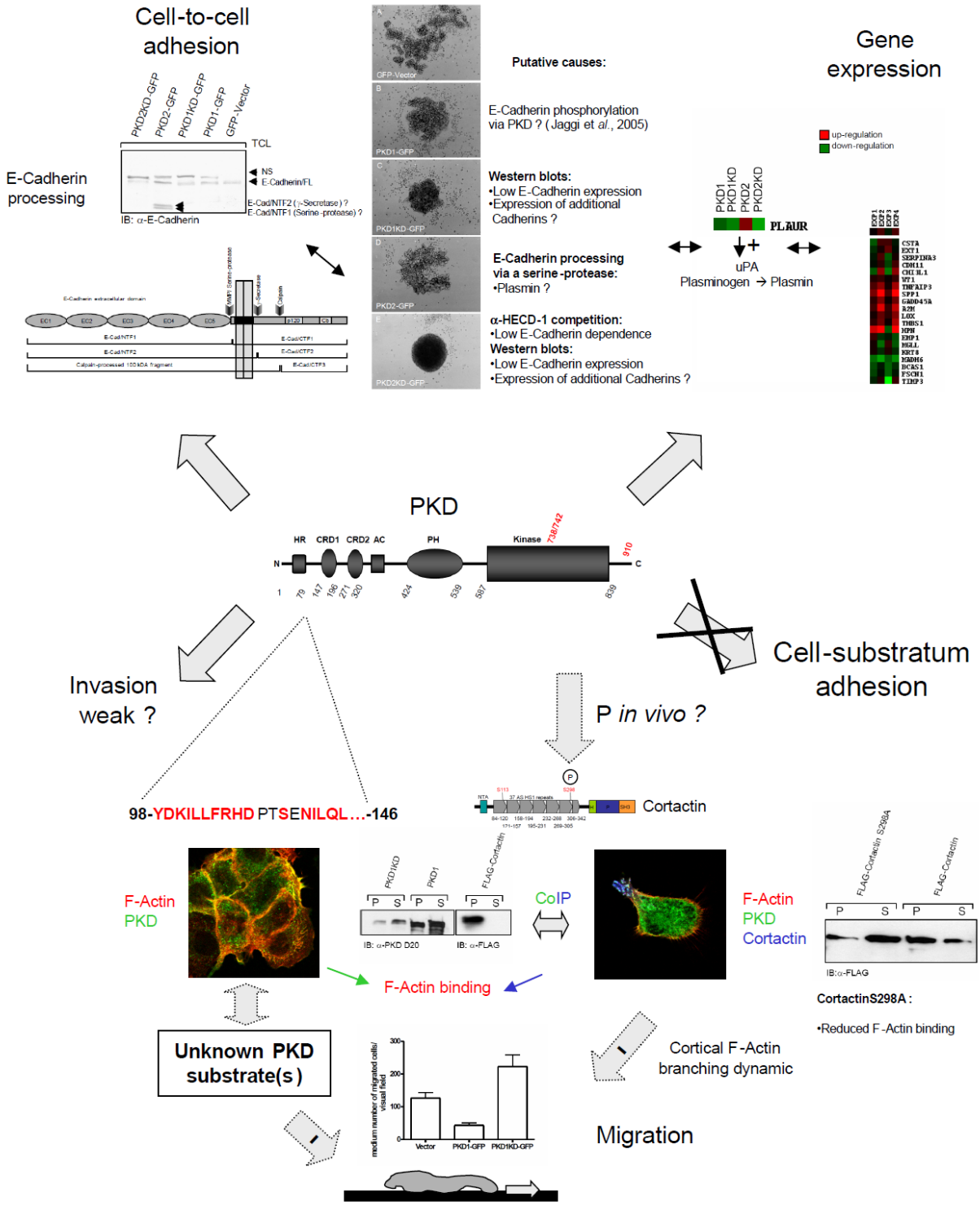

Fig. 26: Schematic overview of the most relevant results obtained during the course of this study. Comments on the figure can be found in 5.19.

6. Discussion

The pancreas ductal adenocarcinoma (PDAC) is one of the most common types of cancer, accounting for a large number of cancer related death. Apart from surgical resection there is no effective therapy. Tumours are mostly resistant against radio-, chemo-, as well as immunotherapy and additional unfortunate characteristics of PDACs include the extraordinary local tumour growth, the fast tumour progression, and its early systemic dissemination. Using PDAC cell lines, this study focused on the potential contribution of PKD which is overexpressed in pancreatic tumors, on their cellular behaviour and functional properties. In particular, the aim was to provide molecular insights in the regulation of processes which are implicated in the progression of pancreatic tumours.
During the course of this work, a role of PKD in cell migration and cellular adhesion of pancreatic cancer cells was revealed. The localisation of PKD at the F-Actin cytoskeleton and its identification as an F-Actin binding protein might even have more general implications on the function of PKD *in vivo*. Since the mapped F-Actin binding region is highly conserved amongst isoforms, as well as between species, this points to a general, as yet undescribed feature of PKD isoforms. They seem to be implicated in functions at the Actin cytoskeletal compartment, possibly in the regulation of F-Actin dynamics and remodelling processes, which influence cell adhesion, motility and cancer progression. Aside from this novel function of PKDs, they are known to play a prominent role in secretory transport and also regulate gene expression. Concerning the latter, another novel aspect of this work is the identification, by gene array analyses, of PKD regulated genes such as Osteopontin and uPAR that have been associated with invasive, metastatic phenotypes of cancer cells.

6.1 Role of PKD at the F-Actin cytoskeleton and in directed cell migration

In this study, PKD has been demonstrated to colocalise with the F-Actin cytoskeleton, as well as with markers Arp3, Cortactin and Vinculin in parental Panc89 cells *(5.3.1)*. Colocalisation with Arp3, a member of the Actin-related Arp2/3 protein complex involved in *de novo* Actin polymerisation and branching of F-Actin networks, indicated sites of active Actin remodelling. Cortactin was initially placed by Bowden et *al.* (1999) into a complex with Paxillin and PKD at invadopodia of breast cancer cells. These authors proposed a role of this protein complex in regulating the extracellular matrix degrading activity of invadopodia. But Cortactin has a much broader spectrum of functions. It is enriched in lamellipodia and localised in membrane ruffles (Wu and Parsons, 1993; Weed et *al.*, 1998). It has been shown to bind to F-Actin and the Arp2/3 complex. In the literature, Cortactin is implicated in the nucleation and/or stabilisation of cortical branched F-Actin networks (Daly, 2004). These data thus suggest a possible function of PKD at the cortical Actin cytoskeleton, too. The here revealed colocalisation of PKD with Vinculin at the edge of membrane protrusions, but not in mature focal contacts, further supports a PKD function at sites of active Actin turnover. Although Vinculin has been shown to bind to Talin and α-Actinin (Jockusch and Isenberg, 1981; Johnson and Craig, 1995a), which are localised with Integrins at focal adhesion contacts to the substratum (Nishizaka et *al.*, 2000; Kiosses et *al.*, 2001), it has also been demonstrated

by DeMali et *al.* (2002) that Vinculin also exhibits a transient interaction with the Arp2/3 complex, which is not present in focal contact sites (Welch et *al*., 1997; DeMali et *al*., 2002). Vinculin might therefore not only be a marker for focal adhesions, it is also localised at sites of active Actin polymerisation or remodelling in protrusive membrane structures, as indicated by its colocalisation and interaction with the Arp2/3 complex. Taken together, these data point to a putative function of PKD at the F-Actin cytoskeleton, possibly exerting its effects at sites of active Actin turnover in the cortical Actin network and in membrane ruffles.

Stimulation of Panc89 cells with PDGF-BB for 30 minutes further enhanced the colocalisation with the above cytoskeletal components *(5.3.2)*. The engagement of PDGF-receptors has been shown to activate both, PKD (Van Lint et *al.*, 1998; Stafford et *al.*, 2003) and Src kinase, the latter is also known to stimulate cell motility by reorganisation of the Actin cytoskeleton (Parsons and Parsons, 1997; Heldin *et al.*, 1998). One of the Src kinase targets involved in this process is Cortactin. The two proteins have been coimmunoprecipitated from a variety of cellular systems (Daly, 2004) and Src has been shown to phosphorylate *murine* Cortactin *in vitro* on three sites: Tyr421, Tyr466 and Tyr482, which are the major sites of phosphorylation in v-Src transformed cells (Huang et *al*., 1998). The ability of Cortactin to promote migration of endothelial cells required the phosphorylation at these sites, and a phosphorylation-deficient mutant of Cortactin was able to act dominant negative on cell migration (Huang et *al.*, 1998). The increased colocalisation of PKD with F-Actin, Cortactin, and Vinculin following stimulation with PDGF-BB for 30 minutes is a further indication for a function of PKD in Actin remodelling processes, possibly via the action at Cortactin, which has been demonstrated to act downstream of a PDGF-Src-signalling cascade regulating Actin turnover and cell migration. It was shown in this work that Cortactin is, at least *in vitro*, a PKD substrate and a PKD-phosphorylation site specific mutant displayed the identical migration phenotype as a PKD1KD mutant *(see also below)*. In addition, another novel finding of this study is the direct molecular interaction of PKD and F-Actin *in vitro*. The F-Actin binding domain of PKD was narrowed down to 46 amino acids in the N-terminal region of PKD starting at sequence position 98 *(5.4)*. A sequence alignment of the relevant amino acids revealed highly conserved motifs both, amongst isoforms, as well as between *human*, *mouse*, and a *Drosophila* PKD orthologue, suggesting that Actin-binding could be a general feature of all PKD kinases. However, PKD does not gernerally localise and bind to the F-Actin cytoskeleton *in vivo*, since it is predominantly found at structures associated with active Actin turnover, as indicated by its colocalisation with the markers Cortactin and Vinculin in membrane protrusions and it was not localised at stress fibers. Therefore one explanation would be a recruitment of PKD by other factors to distinctive sites at the F-Actin network, where it might exert possible functions in the regulation of Actin remodelling. In this context Cortactin would be an ideal candidate to act as a scaffolding protein which could facilitate the recruitment of PKD downstream of a PDGF signal, since PKD and Cortactin were coprecipitated from the supernatant fraction of Panc89 and HEK 293T lysates following the removal of the cellular Actin cytoskeleton, thus indicating a cytosolic interaction of both proteins. If a putative *in vivo* phosphorylation of Cortactin by PKD might involve Actin-binding of one, or both interaction partners, still needs to be addressed, however since PKD is

localised at sites of active Actin turnover it is likely that putative substrates such as Cortactin are phosphorylated at these structures, too.

PKD might also bind directly, independent of other factors to F-Actin *in vivo*, yet how respective sites are sensed and targeted in this case still remains to be elucidated.

Several other kinases are known to bind to the F-Actin cytoskeleton as well, and they were implicated with Actin remodelling processes exhibiting effects on cell motility, cell-substratum-, and cell-to-cell adhesion, or invasion of cancer cells. E.g. the Abl tyrosine kinase has been demonstrated to regulate cytoskeleton remodelling (Hernandez et *al.*, 2004; Woodring et *al.*, 2003) during adhesion, motility, and axon guidance. Consistent with this function, the Abl protein contains Actin-binding sites (McWirther and Wang, 1993; Van Etten et *al.*, 1994; Wang et *al.*, 2001) and localises to dynamic Actin, where it phosphorylates Crk, Crkl (Escalante et *al.*, 2000; Kain and Klemke, 2001), Dok1, and other proteins controlling cytoskeleton dynamics (Van Etten, 1999). Another interesting fact concerning the role of Abl in Actin remodelling processes is its activation by Rin1. Hu et *al.* (2005) described that the Ras-effector Rin1 is an activator of Abl kinase by interacting with its SH3- and SH2-domains, thereby stimulating Abl kinase activity. They were able to show that overexpression of Rin1 in fibroblasts promoted the formation of membrane spikes, as demonstrated for Abl previously, and that knockdown of Rin1 in epithelial cells lines blocked the induction of Crkl phosphorylation, confirming that Rin1 normally functions as an inhibitor of cell motility. Bearing in mind, that Wang et *al.* (2002) identified Rin1 as a PKD substrate, this represents another, potentially relevant connection between PKD and proteins involved in cytoskeletal remodelling processes. Upon PKD mediated phosphorylation at Ser351, Rin1 has been shown to dissociate from Ras, followed by sequestration via 14-3-3 proteins. In turn the release of Ras allows its interaction with Raf, initiating downstream signalling events resulting in the activation of MAPK (Wang et *al.*, 2002), which are regarded as important players in cytoskeleton remodelling processes and cell migration (Huang et *al.*, 2004).

The novel PKC isoenzyme, PKCε, is also an F-Actin binding kinase, involved in oncogenic transformation and Actin nucleation. Tachado et *al.* (2002) showed that cells constitutively expressing PKCε spontaneously acquired a polarised morphology, extending long cellular membrane protrusions. The authors demonstrated that Actin binding sites in the regulatory C1 domain of PKCε were essential for the formation of elongated invadopodia-like structures, increased metalloproteinase activity, and *in vitro* invasion potential. Moreover, PKCε-transformed NIH3T3 fibroblasts showed invasive behaviour and metastases in murine tumour models *in vivo*. Since PKCε is also a direct upstream kinase of PKD (Waldron and Rozengurt, 2003), it might well be implicated in its activation at sites of active Actin turnover at the Actin cytoskeleton. In addition also AKAPs (A-kinase anchoring proteins) have been proposed in the activation process of PKD. Carnegie et *al.* (2004) demonstrated that AKAP-Lbc was involved in the formation of an activation complex for PKD by recruiting the upstream kinase PKCη, as well as synchronising PKA mediated phosphorylation events, releasing activated PKD of the complex. These results have, however, been questioned by others (V. Malhotra, personal communication) and await independent confirmation. Apart from their ability to form multivalent signalling complexes that coordinately regulate the phosphorylation of specific cellular substrates (Colledge and Scott, 1999), AKAPs have also

been implicated as scaffold proteins in the targeting of signal transduction complexes to discrete sites at the cell cytoskeleton, including the centrosome, microtubules, and F-Actin. Recent evidence indicated that Actin-binding proteins such as Gravin (an antigen for the autoimmune disease myasthenia gravis), and WAVE are AKAPs as well (Nauert et *al.*, 1997). Gravin shares significant homology with SSeCKS (clone 72), a cell-cycle-regulated myristylated PKC substrate that has tumour suppressor activity (Frankfort and Gelman, 1995; Lin et *al.*, 1996; Nelson and Gelman, 1997) and has been shown to mediate binding to PKA, PKC and the Actin cytoskeleton (Erlichman et *al.*, 1999), regulating Actin-remodelling events and cell migration during mouse embryogenesis (Gelman et *al.*, 1998). In addition, WASp family members provide a molecular switch converging individual Rho GTPase signals to the Arp2/3 complex (Higgs and Pollard, 1999; Machesky and Gould, 1999). Direct attachment to the Actin cytoskeleton occurs via two conserved Verprolin-binding motifs, and a C-terminal acidic module mediates binding to the Arp2/3 complex (Machesky and Gould, 1999). WAVE1 was also shown to bind both PKA and the Abl tyrosine kinase (Westphal et *al.*, 2000). Since Storz et *al.* (2003) have shown that, upon cellular stress responses towards oxygen radicals, Abl mediates activation of PKD by phosphorylation of a conserved Tyr463 residue in the PH domain, this constitutes another interesting link involving PKD in the modulation of Actin nucleation and remodelling processes, which might affect cell motility and invasion.

During this study PKD has been shown to influence directed migration of Panc89 cells *in vitro*. Following the creation of stable cell lines expressing wildtype and kinase-dead PKD1 and 2 isoforms, PKD1 and 2 were shown to negatively regulate cell migration through Transwell filter inserts, while PKD1KD was able to enhance migration, whereas PKD2KD only restored vector level cell motility, indicating that kinase-dead PKD2 was not fully able to act dominant negative on this function. This can be explained either by differences in localisation, since costaining with the respective markers F-Actin and Cortactin was not as evident, when compared to PKD1KD, or PKD2KD-GFP might also be involved in other processes having negative regulatory effects on migration, thereby in addition reaching only GFP-Vector levels *(5.7)*. E.g. the cell-to-cell aggregation assays revealed the strongest cell adhesion upon overexpression of PKD2KD-GFP, which could be an explanation for the reduced cell motility, when compared to the PKD1KD migration phenotype.

The diverse effects of kinase-dead PKD1 and 2 isoforms on cell migration are also in line with data from the RNAi experiments suggesting that different PKD isoforms might be responsible for regulating cell migration in different cell lines. For example, knockdown of PKD1 caused a strong enhancement of cell migration in Panc89 cells *(5.9)*, whereas in Panc1 cells the complete knockdown PKD1-pSuppressor clone 17 showed only a slightly enhanced migration phenotype *(5.10)*. In addition, in HEK 293T cells stable expression of PKD2KD, but not PKD1KD enhanced cell migration through Transwell filters (Susanne Märtens, university of Stuttgart, personal communication).

Using confocal immunofluorescence, PKD1 as well as PKD1KD were shown to colocalise with F-Actin and Cortactin *(5.6.2; 5.8)*, which was enhanced upon stimulation with PDGF *(5.8.2)*. Both, wildtype and kinase-dead PKD1 were located at, or recruited to, the F-Actin cytoskeleton. Therefore, in principle, it is conceivable that PKD1KD might act dominant

negative on the phosphorylation of putative PKD substrates at these sites, such as Cortactin, thereby promoting cell migration. Cortactin was shown to be phosphorylated *in vitro* at S298, and likely also at unspecified other sites *(5.12)*. Yet, an *in vivo* phosphorylation could not be demonstrated up to now, but a refined analysis of higher sensitivity using mass spectrometry of phosphoproteins is still ongoing and may yield positive results. Irrespective of the outcome of these analyses, the functional role of PKD mediated Cortactin phosphorylation can be deduced from the migration phenotype of stable transfectants of Panc89 cells expressing a phosphorylation mutant of Cortactin, CortactinS298A, which showed enhanced migration just alike the PKD1KD transfectants *(5.13)*. As to the potential mechanism, it could be shown that CortactinS298A displayed weaker F-Actin binding than the wildtype protein in Actin cosedimentation and co-immunoprecipitation assays *(5.14.1)*. Although not formal proof, these data together are in support of Cortactin as a physiological PKD substrate, functioning as a negative regulator of cell migration upon PKD phosphorylation.

Accordingly, integrating the data obtained here and available from literature, a model is proposed to explain the involvement of Cortactin as a PKD substrate in the regulation of migration in Panc89 cells **(Fig. 27)**: PKD and Cortactin were found here to interact biochemically and to colocalise at the F-Actin cytoskeleton. Cortactin was phosphorylated by PKD *in vitro* and mutation of a potential PKD phosphorylation motif in Cortactin (S298) increased cell migration. Cortactin has been implicated to stabilise F-Actin branch points at the cortical F-Actin network (Daly, 2004), whereas mutated CortactinS298A showed reduced F-Actin binding (this study). Since F-Actin branching is a tightly regulated process, interference with the ability of Cortactin to bind to F-Actin, and thereby to stabilise branched Actin networks, might have considerable impact on cell motility. With CortactinS298A acting at least partially dominant negative on endogenous Cortactin in Panc89 cells, the reduced F-Actin binding capacity of CortactinS298A might drive the equilibrium of branch point stabilisation/destabilisation towards a destabilisation of the branched network, in turn allowing increased F-Actin turnover at cortical structures and enhanced cell migration. As demonstrated during the PKD expression analysis in this study, endogenous PKD was strongly expressed in parental Panc89 cells and existed in an active, autophosphorylated, as well as transphosphorylated state. It is proposed that this condition allows Cortactin to be phosphorylated by PKD, thus promoting high efficiency binding to F-Actin. Endogenous Cortactin might be phosphorylated by PKD to such an extent that the equilibrium is shifted towards a stabilisation of F-Actin branches, possibly impairing Actin dynamics and cell motility. Interference by dominant negative kinase-dead PKD1 or CortactinS298A in turn might stimulate the hampered F-Actin turnover, allowing increased Actin dynamics and cell migration, whereas ectopically expressed PKD1 could further enhance F-Actin rigidity and reduce cell motility.

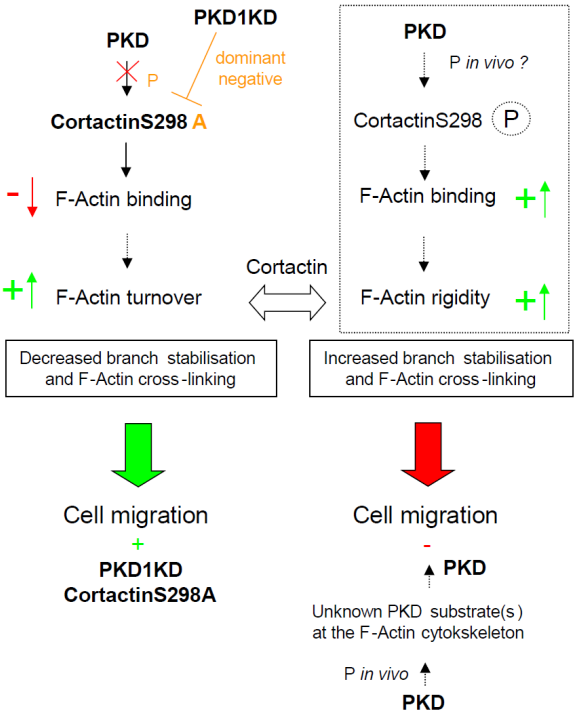

Fig. 27: Putative Model for the regulation of the branching and cross-linking equilibrium of the cortical Actin network by PKD.

An additional role for the Cortactin phosphorylation at S298 within the 6th HS1-repeat is provided by the observation of van Rossum and co-workers. They reported the identification of two alternative splice variants of human Cortactin, present in normal tissues, as well as squamous cell carcinoma cell lines. These variants lack either the 6th or the 5th and 6th repeat, and differ significantly in their ability to bind to F-Actin, to cross-link F-Actin, to activate the Arp2/3-mediated Actin polymerisation, and to induce cell migration *in vitro* (van Rossum et *al.*, 2003). Since the 6th HS1-repeat has been shown to play a vital part in the regulation of the above mentioned processes, phosphorylation of sites in this repeat might alter the Cortactin-F-Actin binding and possibly also cross-linking ability. This is in line with data published by Huang et *al.* (1997), indicating that a phosphorylation by Src at conserved residues modestly inhibited the F-Actin binding activity of Cortactin, but strongly reduced its F-Actin cross-linking activity. A similar effect of Src on the latter parameter was also reported by Bourguignon et *al.* (2001). This suggests another regulatory role for the phosphorylation of Cortactin at S298 by PKD, influencing F-Actin cross-linking and thereby the flexibility and/or turnover of Actin networks. However, the ability of Cortactin to cross-link Actin filaments has also been heavily disputed by others (Weed et *al.*, 2001; Weaver et *al.*, 2001).
PKD has also been implicated in the regulation of cell migration by Prigozhina and Jaggi et *al.* (2004, 2005), however, reaching in part different conlcusions. Prigozhina and co-workers reported that a kinase-dead, dominant-negative mutant of PKD1 specifically blocked budding of secretory vesicles from the TGN to the plasma membrane in NIH3T3 fibroblasts. This had an impact on retrograde membrane flow as wells as submembrane filamentous Actin movement. These cells also showed inhibition of cell motility, which at a first glance contradicts the data reported here. In addition, kinase-dead PKD, defective in binding to the TGN and/or the plasma membrane neither blocked anterograde membrane transport, nor

cell motile functions (Prigozhina et *al.*, 2004). Jaggi et *al.* reported that phosphorylation of E-Cadherin by PKD is associated with altered cellular aggregation and motility of prostate cancer cells. Inhibition of PKD1 activity using the Gö6976 inhibitor in LNCaP cell resulted in decreased cellular aggregation, whereas overexpression of PKD1 in C4-2 prostate cancer cells increased cellular aggregation and decreased cellular motility. Taken together, while in this study and the publication of Jaggi et *al.* (2005), wildtype PKD1 seemed to inhibit cell motility, Prigozhina et *al.* reported PKD1KD to negatively regulate cell migration. This discrepancy might be best explained by several fundamental differences in the studied models. First, the cells studied differ and there is some evidence that regulation of cell migration by PKD might be cell type dependent. Prigozhina and co-workers used NIH 3T3 fibroblasts, while in this work and the publication of Jaggi et *al.* malignant cancer cells were used. Further, own data from the RNAi experiments and the HEK 293T migration assays performed by S. Märtens (Uni Stuttgart) further indicated a cell type and isoform specific regulation of cell motility by PKD. Although cell type and isoform specific differences thus appear to play a role, it is assumed that the differences in the *in vitro* assay system are likely to have a greater influence on the cellular behaviour revealed. Thus, Prigozhina et *al.* measured cell motility by tracking random cell movements on a 2D surface, whereas in this work directed cell migration was assayed using Transwell filter inserts. The same applies for the migration assays in the paper of Jaggi et *al.* As stated by Even-Ram and Yamada (2005), there are discrepancies between the behaviour of cells on 2D surfaces compared to 3D systems, which better represent the microenvironment in living tissues. E.g. cells on 2D substrates exhibit strong exploratory activity of lamellipodia, or filopodia at the leading edge, while strong adhesion to the substrate and actomyosin contractility in the lamellipodia contribute to the forward movement of the cells. Whether structures like lamellipodia exist in 3D environments is still controversially debated. Beningo et *al.* (2004) reported, that under conditions where both ventral and dorsal ECM-support is provided to migrating fibroblasts, instead of the artificial 2D polarity defined only by ventral growth support, the cells acquire a bipolar elongated morphology, resembling fibroblasts *in vivo*. Under these conditions, the cells were also shown by the authors to lack lamellipodia. Yet, however in another study by Heath et *al.* (1989) using fibroblasts embedded in collagen gels, the cells exhibited *in vivo*-like cylindrical cell bodies, major pseudopodial processes, and at the leading edge of advancing pseudopodia, small extensions similar to the lamellipodia seen in cells on glass slides. In addition, small GTPases, like Rac, have been increasingly implicated as regulators of cell directionality during migration. Rac1 has been described as GTPase, which is required for cell spreading and membrane ruffling, whereas RhoA is necessary for intracellular contractility and tension (Ridley et *al.*, 2003). Recently, Pankov et *al.* (2005) placed Rac1 in a central mechanism which determines, whether cell migration is intrinsically random or directionally persistent. The authors demonstrated that decreasing amounts of Rac activity promoted the formation of peripheral lamellae and switched the migration of cells from a random to a directionally persistent pattern. Total Rac1 activity therefore might act as a regulatory switch between patterns of cell migration by a mechanism, which is distinct from chemotaxis. In addition, in three-dimensional rather then two-dimensional cell culture, cells were shown to have lower levels of Rac activity, which was also associated with rapid

directional migration. When comparing motility assays utilising 2D and 3D systems, as it is the case for the 2D cell motility assay used by Prigozhina et *al.* versus 3D systems in this study, this also has to be taken in consideration. Higher Rac1 activity in a 2D system might therefore enhance random migration, while in a 3D environment, like Transwell inserts, the more persistent directed migration through filter pores is assayed. These different features of cell motility, with different underlying regulatory mechanisms can therefore not be compared directly and do not necessarily exclude one another.
Summarising the data, in this and also in the study of Jaggi et *al.*, PKD1 was shown to inhibit directed cell migration using Transwell filter assays. Yet, the conclusions drawn from the respective sets of data differ somewhat. Jaggi and co-workers proposed PKD mediated phosphorylation of E-Cadherin as an essential mechanism, with phosphorylated E-Cadherin promoting enhancement of cell-to-cell adhesion, this in turn causing an inhibition of cell migration. While the work here did not address and cannot rule out a role of E-Cadherin phosphorylation, other PKD targets and actions have been identified that are likely to play an important role in controlling cell migration. However, the proposal of Jaggi et *al.* for a function of PKD in cell-to-cell adhesion processes, appears not unreasonable, considering the data also presented on the effects of the different PKD variants on cell adhesion in this study and might therefore indirectly contribute to the migration phenotypes as well.

6.2 PKD function in cell invasion

PKD1, Cortactin and Paxillin were shown to form a complex in the invadopodia of breast cancer cells, thus suggesting a function for PKD in regulating the matrix degrading potential of these structures. Invadopodia are Actin-rich membrane protrusions, which extend into the extracellular matrix and participate in matrix-degradation events (Chen, 1989; Coopman et *al.*, 1996; Monsky et *al.*, 1994). In addition, Coopman et *al.* (1998) demonstrated a direct correlation between the matrix-degrading ability at sites of invadopodia protrusion and the invasive potential of cancer cells. Membrane-associated metalloproteases, like Separase, or MMP2 are thought to mediate this ECM degradation (Nakahara et *al.*, 1996, 1997; Monsky et *al.*, 1993, 1994) and Actin, as well as Actin-associated proteins such as α-Actinin, Talin, Tensin, Cortactin, and Paxillin are implicated in the extension and formation of the protruding invadopodia (Mueller et *al.*, 1992; Chen, 1989). Since in this work, Cortactin and PKD colocalised in membrane protrusions and the cortical Actin cytoskeleton, interacted in the cytoplasm, and Cortactin was also shown to be a PKD substrate *in vitro*, it is plausible that PKD might be implicated in cancer cell invasion by regulating the formation of invadopodia via an interaction with, or phosphorylation of Cortactin. Yet, the invasion assays performed in this study were not conclusive on a potential function of the different PKD variants in Matrigel™ and KIF-5 fibroblast *in vitro* invasion assays, since the matrix-degrading potential of the Panc89 cells was very low *(5.15)*.
Unfortunately, the establishment of Colo357 cell lines, which would be better suited for invasion assays, expressing the different PKD wildtype and kinase-dead variants, failed. To circumvent this limitation in the future, and to study principal effects on the invasive potential of cancer cells, a further analysis should be done in other, highly invasive cells, e.g. MDA-

MB-231 breast cancer cells, which also have been used in the study of Bowden et *al*. This would allow the investigation of potential effects of the respective PKD isoforms and kinase-dead variants on the formation of invadopodia, as an additional marker for the invasive potential of the cancer cells. The number of invadopodia, indicating the matrix-degrading activity of the respective cell lines, can be measured via microscopic analysis of marker proteins like Cortactin and F-Actin, which colocalise in dot-like structures (Bowden et *al.*, 1999) in cells cultured on an ECM-surrogate, or a Matrigel™-coated supporting surface. PKD might be implicated at different stages of invadopodia formation, either in the assembly of multi-protein complexes which are involved in the generation of invadopodia, or the extension of the structures, since the protrusion of invadopodia involves Actin polymerisation and remodelling.
Therefore PKD could be involved in the modulation of the invasive potential of cancer cells, although a strong impact on invasion could not be shown in this work, using the stable Panc89 cell lines.

6.3 PKD function in cell-substratum adhesion

As shown in the adhesion assays performed during this work, neither coating with Collagen IV, Poly-L-Lysine, nor Matrigel™ did have an significant impact on adhesion towards the respective substrates, when comparing the different stable cell lines. This indicates that PKD seems not to be involved in cell-substratum adhesion processes in Panc89 cells *(5.16)*.
Cell adhesion to the ECM is important for the regulation of many cellular functions, including cell fate decisions and cell motility. In most of the adhesive contacts to the substratum, Integrin receptors mediate the binding to the ECM via their extracellular domains, and interaction via their cytoplasmic part mediates binding to the Actin cytoskeleton (Hynes, 1992; Martin et *al.*, 2002). A large number of proteins is associated with these cytoplasmic domains, which are involved either in strengthening the interaction between the ECM and the cytoskeleton, or in signalling processes at the focal contacts (Critchley, 2000; Geiger et al., 2001; Petit and Thiery, 2000). Yet, recent studies have shown, that the situation is much more complex, and Integrin-mediated adhesions differ in their molecular composition, as well as in their cellular location and function (Zamir and Geiger, 2001). Classical focal adhesions are usually located at the cell periphery, are highly tyrosine phosphorylated, and contain a_5b_3-Integrins, Vinculin and Paxillin. At more central positions of the cell, so-called fibrillar adhesions exist in association with Fibronectin, containing a_5b_1-Integrins, Tensin and little, or no phosphotyrosine (Zamir et *al.*, 1999). They are generated from focal adhesions, following myosin-dependent longitudinal displacement of ECM-associated Fibronectin receptors to the center-region of the cell (Pankov et *al.*, 2000; Zamir et *al.*, 2000). Along the leading edge of motile cells, a third variant of adhesions is found. These small matrix adhesions, termed focal complexes (Nobes and Hall, 1995), are short-lived structures containing mainly b_3-Integrins (Ballestrem et *al.*, 2001), Vinculin (Rottner et *al.*, 1999), Paxillin, α-Actinin (Laukaitis et *al.*, 2001) and possibly also the Arp2/3 complex (DeMali et *al.*, 2002). DeMali et *al.* also showed a direct, but transient interaction of Vinculin and the Arp2/3 complex at the leading edge of cells, where focal complexes are formed, however the Arp2/3 complex was not detected in

mature focal adhesions (Welch et *al.*, 1997; DeMali et *al.*, 2002). This also in line with data presented in this work, whereby Vinculin and endogenous PKD did localise at the leading edge of Panc89 cells, indicating sites of active Actin turnover, yet they were not found to colocalise in structures resembling focal adhesions. In addition PKD1-, PKD1KD-GFP and FAK, as well as PKD1 and 2 wildtype and kinase-dead-GFP and Paxillin, failed to colocalise, further emphasising that PKD isoforms are not implicated at focal contacts, as indicated by the markers FAK and Paxillin. Several groups have also established that the three variants of adhesion described above, represent different stages of interaction with the ECM, thus indicating, that focal complexes are very early forms of focal adhesions, which can be transformed in mature focal contacts to the ECM by the activation of RhoA (Ballestrem et *al.*, 2001; Rottner et *al.*, 1999), or by a external mechanical stimuli (Galbraith et *al.*, 2002; Riveline et *al.*, 2001). In motile cells, focal complexes play a key role in migration processes. At the leading edge, a large number of such matrix adhesions are formed, some of which are induced to develop into stable focal adhesions, which in turn provide anchors to the ECM, allowing the cell to be pushed forward both, at the leading and the trailing edge (Lauffenburger and Horwitz, 1996). However, in this study PKD isoforms did not have significant effects on cell adhesion towards different substrates, and PKD was also not found to localise with focal adhesion markers Paxillin and FAK in mature focal contacts. Yet, the data of DeMali et *al.* (2002) provides evidence, that the colocalisation of PKD and Vinculin at the leading edge of Panc89 cells might implicate PKD in the formation of the transient focal complexes, which are not directly involved in cell adhesion, but may be transformed into stable focal contacts by different stimuli, and are important for cell migration. This is a connection, which needs to be investigated further.

6.4 PKD function in cell-to-cell adhesion

As described above, Jaggi et *al.* also implicated PKD1 in enhancing cell-to-cell adhesion of LNCaP prostate cancer cells, possibly by the phosphorylation of E-Cadherin itself. In this study, the effects of PKD1 and 2 isoforms and kinase-dead variants on cell-to-cell adhesion were investigatated, using spheroid formation. Yet, the effects observed in this cellular aggregation assays were rather diverse *(5.17)*, indicating enhanced cell-to-cell adhesion of the stable Panc89 cell lines PKD1-, PKD1KD-, as well as PKD2KD-GFP, i.e. no apparent correlation could be made with respect to cell aggregation and PKD activity, leaving open the possibility of a kinase independent function of PKD in cell-to-cell interaction. This latter possibility would contradict the conclusions of the Jaggi group. Analysis of the packing density of the documented spheroid structures suggested that PKD2KD-GFP seemed to mediate the strongest increase in cell aggregation, while PKD2-GFP only was able to slightly enhance cellular aggregation compared to GFP-Vector cells *(5.17.1)*.This phenotype could be correlated with E-Cadherin fragments in the cell culture supernatant of PKD2-GFP expressing cells, which are shedded by a serine-protease, possibly Plasmin, or since PDAC cells are analysed here, cationic Trypsin *(5.17.3)*. Plasmin is an interesting candidate because the Plasminogen-activator/Plasmin-system was shown to suppress cell-to-cell adhesion of oral squamous cell carcinoma cells via the proteolysis of E-Cadherin (Hyashido et *al.*, 2005). In addition, initial analysis of the gene profiling experiments using the stable

Panc89 cell lines further emphasised a possible role of the Plasminogen/Plasmin-system in the processing of E-Cadherin, since in PKD2-GFP expressing Panc89 cells, the PLAUR gene has been shown to be specifically up-regulated *(5.18)*. The gene codes for the urokinase-type Plasmin-activator-receptor (u-PAR), which can specifically catalyze the activation of the urokinase-type Plasmin-activator/Plasmin-system, possibly enhancing the E-Cadherin processing in the PKD2 expressing cell line. In summary both, E-Cadherin processing by a serine-protease, like Plasmin, and the generation of the second, lager fragment shown in Western blots by a putative γ-Secretase-like enzyme might account for the reduced cell adhesion in PKD2-GFP cells. This phenotype is also in line with published data from Tan et *al.* (2006), implicating the urokinase-type Plasminogen-activator (uPA) and uPA-receptor (uPAR) controlled Plasmin-cascade in the invasion of pancreatic cancer cells and especially in its early stage cell dissociation.Targeting the Plasmin-cascade may therefore provide novel molecular insights for anti-invasion and anti-metastasis therapies, which might allow modulating the unfavourable early systemic dissemination implicated with the fast progression of pancreatic cancer.

Moreover, the processing of E-Cadherin itself has been shown influence transcription of certain genes. E-Cadherin shedding by ADAM10 was shown to affect β-Catenin translocation and led to an accumulation of β-Catenin in the cytoplasm of affected cells (Maretzky et *al.*, 2005). β-Catenin in turn is known to bind to transcription factors of the Lymphocyte enhancer-binding factor 1/T cell factor pathway (LEF/TCF) pathway (Cowin et *al.*, 2005), thereby regulating the expression of downstream target genes such as c-Myc (He et *al.*, 1998) and Cyclin D1 (Lin et *al.*, 2000; Ryo et al., 2001; Shtutman et *al.*, 1999), which are implicated in cell proliferation and cancer progression. Thus β-Catenin has the potential to be a key regulator of gene transcription involved in the progression of cancer cells, and it has been demonstrated to be an important player in the regulation of the so called, epithelial-mesenchymal transition (EMT). In this process, down-modulation of E-Cadherin mediated cell-to-cell adhesion is involved in regulating tumour progression and metastasis. Originally, EMT occurs as key step during embryonic morphogenesis, involving a developmental switch from a polarised, epithelial phenotype to a highly motile fibroblastoid, or mesenchymal cell. Yet, recent advances in understanding the underlying signalling events involved in governing the EMT in tumours provided evidence, that EMT plays a specific role in the migration of a primary tumour into the circulation. Pathways regulating EMT include TGFβ signals, Ras, autocrine factors, and the canonical Wnt-β-Catenin, Notch-, Hedgehog-, as well as NFκB-signalling cascades. As a key step during EMT progression, the repression of E-Cadherin by transcriptional regulators such as Snail, or Twist has emerged (Huber et *al.*, 2005; Cowin et *al.*, 2005), and this molecular link is currently further investigated, providing evidence for the involvement of new players in the regulation of EMT in tumour cells. Further analysing the Panc89 gene profiling data presented in this work for the differential regulation of pathways involved in governing EMT might provide molecular insights on a putative role of PKD in the regulation of this process. Very recently, novel insights in the structure and molecular composition of adherens junction complexes were published, implicating that the current model describing cell-to-cell adhesion processes is wrong.

In the present model, the Ca^{2+}-dependent cell-to-cell adhesion was thought to be a mediated via a quaternary complex through Cadherin-β-Catenin-α-Catenin towards the F-Actin cytoskeleton. The disruption of the Cadherin-based cell-to-cell adhesion in turn averted normal embryonic development (Larue et *al.*, 1994) and is a common occurrence in metastatic cancers (Thiery, 2002). Cadherin mediated cell adhesion is regulated via distinct interactions of the extracellular and cytoplasmic domains of the protein (Gumbiner, 2000; Foty and Steinberg, 2005). Following homo- or heterophilic interaction of Cadherin molecules on neighbouring cells, the Cadherin cytoplasmic domain was shown to form a high affinity complex with β-Catenin, which was demonstrated to bind with lower affinity to α-Catenin (Aberle et *al*., 1994; Hinck et *al*., 1994; Pokutta and Weis, 2000; Huber and Weis, 2001). In addition several studies showed that α-Catenin interacts with the F-Actin cytoskeleton. Purified α-Catenin was demonstrated to bundle Actin filaments *in vitro* (Pokutta et *al*., 2002), and to interact also with other known Actin-binding proteins, such as Vinculin (Watabe-Uchida et *al.*, 1998; Weiss et *al.*, 1998), α-Actinin (Knudsen et *al.*, 1995), ZO-1 (Itoh et *al.*, 1997), Spectrin (Pradhan et *al*., 2001), Afadin (Pokutta et *al*., 2002), and Formin (Kobielak et *al.*, 2004). Yet, an experimental proof of direct binding of the Cadherin-β-Catenin complex to F-Actin was never provided. That's why recently Yamada et *al.* (2005) tried to answer this unsolved question. Surprisingly, the authors did not find a direct interaction of the Cadherin-β-Catenin complex with the Actin cytoskeleton. They actually were able to show that α-Catenin interaction with β-Catenin, and α-Catenin binding to F-Actin were mutually exclusive, indicating that the present ideas on Cadherin mediated cell-to-cell adhesion were incorrect. In another publication, Drees et *al.* (2005) provided data, that α-Catenin might act as an allosteric protein, with α-Catenin-β-Catenin heterodimers exhibiting a high affinity for Cadherin, whereas α-Catenin homodimers preferentially bound to F-Actin. The authors also showed, using an *in vitro* Pyrene-Actin assay, that the addition of α-Catenin homodimers inhibited Actin polymerisation, which prompted them to present the following revised model: Drees et *al.* found, that α-Catenin bound to E-Cadherin-β-Catenin complexes can dissociate and bind F-Actin in solution. Therefore they proposed that the interaction of E-Cadherin and β-Catenin recruits α-Catenin to adherens junction complexes via a transient binding, which allows subsequent dissociation of α-Catenin, locally increasing its concentration in the vicinity of the apical Actin. Yet, whether this is sufficient to influence the Arp2/3 mediated Actin polymerisation at adherens junctions still needs to be investigated. How the link of Cadherins to the underlying Actin cytoskeleton is accomplished then, is a question which now needs to be addressed again, following the recent advances published by Yamato, and Drees et *al.* Since the interactions in the adherens junctions, following the ligation of Cadherin molecules have shown to be of a transient nature, there is now room for a lot of molecules, which might be implicated in mediating or regulating cell-to-cell adhesion by Cadherins, including Cortactin, and possibly also PKD. In addition to α-Catenin, several other Actin-binding proteins have been shown to localise at adherens junctions, and these proteins might be involved in bridging the gap from the Cadherin-β-Catenin complexes to the Actin cytoskeleton: Ena/VASP (Vasioukhin and Fuchs, 2001), Formin (Kobielak et *al*., 2004), the Arp2/3 complex (Kovacs et *al.*, 2002), and Cortactin (Helwani et *al*., 2004). The Arp2/3

complex and Formin are both implicated in nucleating Actin, whereby Formin polymerises linear filaments, while the Arp2/3 complex is implicated in the nucleation of branched Actin networks. Ena/Vasp on the other hand promotes the continued elongation of existing filaments by binding to the fast growing barbed ends, thereby preventing the binding of capping proteins (Barzik et *al.*, 2005). The localisation of Ena/Vasp and Formin to adherens junctions has also been shown to be dependent on α-Catenin (Kobielak et *al.*, 2004; Vasioukhin et *al.*, 2000). In addition, Formin was demonstrated to interact with α-Catenin (Kobielak et *al*., 2004), although it has also not been shown whether α-Catenin can bind both, Formin and β-Catenin at the same time. Another link, possibly also involving a function of PKD, is the translocation and binding of Cortactin to adherens junctions (Helwani et *al.*, 2004). Cortactin was shown to accumulate with the Arp2/3 complex at cell margins were adhesive contacts were extended. The recruitment of Cortactin also was accompanied by a ligation-dependent biochemical interaction with the Cadherin adhesive complex, and inhibition of Cortactin activity blocked the Arp2/3-dependent Actin assembly at Cadherin-based adhesive sites, significantly reducing the contact zone extension, cell morphology and junctional accumulation of Cadherins in cell-to-cell contact zones. This is also in line with data presented in this study, were ectopic expression of Cortactin-GFP, as well as CortactinS298A-GFP, strongly increased cell aggregation in spheroid formation adhesion assays, with the S298A mutant probably having the biggest impact on cell-to-cell adhesion *(5.16.1)*. Whether a potential phosphorylation of Cortactin by PKD also plays a role in this cellular context, remains to be investigated. However, as for cell migration, enhanced Actin dynamic might enhance cell aggregation, too, since a rapid polymerisation of Actin induced by clustering of Cadherins has been reported (Gates and Pfeiffer, 2005). Taken together, the above mentioned Actin-binding proteins and potential regulatory partners, like PKD, may provide novel molecular means of modifying the state of the Actin cytoskeleton at adherens junctions, thereby regulating or even mediating cell-to-cell adhesion and the link to the underlying cytoskeleton.

6.5 PKD function in transcription of cancer related genes

In addition to its diverse cellular actions at a post-translational level, affecting protein functions through phopsphorylation at internal membranes or the cell periphery, PKD has also been implicated in the control of gene expression (Rykx et *al.* 2003; VanLint et *al.* 2002). This is also in line with data presented by Vega et *al.* (2004) and Dequiedt et *al.* (2005) demonstrating that phosphorylation of HDACs by PKD, and regulation of their nuclear export reveals a novel mechanism linking chromatin modifications and the regulation of gene expression to PKD kinase activity. That's why in this work the different stable PKD1/2-GFP wildtype and kinase-dead expressing cell lines were subjected to gene profiling experiments. Genes, which were generally regulated via PKD kinase activity, independent of the isoform, as well as PKD1/PKD2-specific, differentially regulated genes were identified and displayed in separate clusters *(5.18)*. As can be seen by the size of the clusters, and the respective gene lists, there were much more genes differentially regulated by PKD2 versus PKD2KD expressing cells, then by PKD1 wildtype and kinase-dead variants. This indicates that, at

least in Panc89 cells, mainly PKD2 seems to be implicated in gene regulation. Bearing in mind that processing of E-Cadherin in PKD2-GFP cells also might affect β-Catenin translocation and accumulation in the cytoplasm, thereby regulating the transcription of LEF/TCF controlled genes, this might at least partially be an explanation for the large number of genes, differentially regulated via PKD2 kinase activity. However, the genes, which exhibited the strongest overall regulation were controlled by PKD kinase activity independent of the isoform, such as SPP1 (Secreted phosphoprotein 1, Osteopontin). It is up-regulated in PKD1KD- and PKD2KD-GFP expressing cell lines and codes for a secreted, adhesive glycophosphoprotein implicated in enhancing cell migration in breast cancer cells. According to several publications SPP1 is also implicated with increased invasive potential of breast tumours (Bautista et *al.*, 1994; Senger and Peruzzi, 1996). It is thought to exert its pro-metastatic effects via the interaction with various Integrin and CD44 receptors. Phosphorylation of SPP1 occurs at up to 28 sites distributed throughout the molecule. It contains a protease-hypersensitive region that separates the Integrin- and CD44-binding domains and can be cleaved by the action of Thrombin. However, no direct evidence on the function of Thrombin-processed SPP1 has been reported *in vivo*, up to date. SPP1 has been shown to induce c-Src signalling thereby regulating the dynamic interplay of Integrin- and EGFR-pathways. In addition, the PI3-kinase-Akt pathway might also be a target of SPP1, since SPP1 was documented to protect cells from apoptosis using a murine B-cell line. Osteopontin also has been demonstrated to stimulate the Nuclear factor inducing kinase (NIK), which via the NFκB- and MAPK-pathway mediates uPA secretion and MMP9 activation, enhancing the matrix-degrading potential of cancer cells (Rangaswami et *al.*, 2006). Recently, SPP1 has also been identified as a Hepatocyte nuclear factor 1alpha HNF1alpha (TCF1) target gene in HEK293T cells (Senkel et *al.*, 2005). This transcription factor shows a tissue specific expression patters and its mutation in humans leads to renal cysts, genital malformations, pancreas atrophy, and maturity onset diabetes of the young (MODY5). TCF transcription factors are also implicated in pancreas development, with a supposed function in PDAC tumour progression as well. E.g. TCF2-deficient mice die before gastrulation because of defective visceral endoderm formation, and lack of TCF2 resulted in pancreas agenesis by embryonic day 13.5 (Haumaitre et *al.*, 2005). In addition, SPP1 has also been shown to be a Hoxc8 downstream target gene (Lei et *al.*, 2005). SPP1 expression has been associated with many human carcinomas, although its *in vivo* function is still controversially debated. Crawford et *al.* (1998) demonstrated that SPP null mutant mice exhibited accelerated tumour growth and progression and had a greater number of metastases per animal, when compared to wildtype animals. Taken together, SPP1 seems to be involved in processes controlling tumour cell migration, progression and metastasis, thus being an ideal candidate for further investigation on the function of PKD in the expression of cancer related genes. However, there is still much more work to be done, first of all reproducing the gene profiling experiments and also providing independent verification of the microarray data suggesting a differential gene regulation. Further additional PKD target genes and their respective functions need to be identified.

In conclusion, the study here performed with the pancreas carcinoma cell line Panc89 provided experimental evidence for an important role of PKD in cell migration, cell-to-cell

adhesion and in the regulation of cancer related genes, whereas cell invasion and the cell-substratum adhesion was not influenced by the different PKD isoforms. Concerning underlying molecular mechanisms, the observed interaction of PKD with the F-Actin cytoskeleton and identification of Cortactin as a potential substrate shed first light into the complex interactions involved, suggesting that PKD is an important player in regulating Actin dynamics.

Further work should therefore unravel the molecular details and physiological role of the PKD mediated cytoskeleton regulation that controls such fundamental processes as cell migration and tissue formation.

7. German Summary (Deutsche Zusammenfassung)

Pankreaskarzinome zählen zu häufigsten Tumorarten und sie weisen dabei eine der geringsten 5 Jahre Überlebensraten bei Krebserkrankungen auf. Auf Grund von Resistenzen gegenüber Chemo-, Immuno-, und Radiotherapie besteht die einzige Behandlungsmethode in der Resektion des Primärtumors. Wegen der starken lokalen Tumorprogression und der frühen Metastasierung ist dies aber häufig nicht erfolgreich; die meisten betroffenen Patienten sterben innerhalb eines Jahres. Bis heute ist nicht viel über die molekularen Ereignisse bekannt, die mit der Progression und Metastasierung von Krebszellen einhergehen, jedoch spielen Prozesse wie Apoptose-Resistenz, Veränderung der Zellstruktur, Modulation der Zell-Zell-Adhäsion, verstärkte Zellmigration und verändertes invasives Verhalten der Krebszellen eine wichtige Rolle. In der Fachliteratur wurde auch die Proteinkinase D (PKD) Familie mit diesen Prozessen in Verbindung gebracht, die genauen molekularen Mechanismen sind jedoch noch unklar. Auf Grund von Homologien innerhalb ihrer Kinase Domaine wurden die drei Isoenzyme der PKD Familie: PKD1/PKCμ, PKD2, PKD3/PKCν in eine Subklasse der Calcium/Calmodulin-abhängigen Kinasen (CAMK) eingeordnet. Die *in vivo* Funktion von PKD leitet sich bisher nur von Untersuchungen an Zellmodellen ab, allerdings wird hieraus eine wichtige Rolle bei der Regulation einer ganzen Reihe von fundamentalen zellbiologischen Prozessen postuliert, einschließlich der oben erwähnten Vorgänge, die mit der metastatischen Progression von Krebszellen in Verbindung stehen. Interessanterweise wurde in immunhistologischen Untersuchungen PKD im Pankreaskarzinom überexprimiert gefunden. Ziel dieser Arbeit war es, die Rolle der Proteinkinase D bei der Zellmigration, Invasion, Zell-Substrat-, sowie Zell-Zell-Adhäsion und der Regulation von Krebs-relevanten Genen in Pankreasductaladenokarzinom (PDAK) Zelllinien zu untersuchen. Dazu wurden zunächst mehrere PDAK Linien charakterisiert. In Panc89 Zellen konnte dabei eine starke PKD Expression festgestellt werden. Außerdem war die PKD in dieser Zelllinie auch konstitutiv auto- und transphosphoryliert und damit aktiv, weshalb weitere Untersuchungen sich zunächst auf diese Linie konzentrierten. In diesen Zellen wurde eine molekulare Wechselwirkung von PKD mit dem F-Aktin Zytoskelett festgestellt. Durch konfokale Immunfluoreszenzmikroskopie konnte eine Kolokalisation zwischen PKD und F-Aktin, sowie mit Arp3, einem Teil des Arp2/3 Proteinkomplexes, der für die *de novo* Aktin-Nukleation und die dendritische Verzweigung von Aktin Filamenten verantwortlich ist, festgestellt werden. PKD kolokalisierte auch mit einem subzellulären Pool von Vinculin am Rand von Membranausstülpungen am so genannten „leading edge“ der Zelle. Vinculin markierte in diesem Fall sehr wahrscheinlich transiente Strukturen mit verstärktem Aktinumsatz, die als „fokale Komplexe“ bezeichnet werden. Es konnte aber keine Kolokalisation mit Vinculin-positiven, reifen „fokalen Kontakten“ festgestellt werden. PKD wurde außerdem mit Cortactin, einem Marker, der in Lamellopodien und „membran ruffles“ angereichert ist, kolokalisiert. Laut Literatur, ist Cortactin für die Stabilisierung von F-Aktin-Verzweigungen im kortikalen Aktin Zytoskelett verantwortlich und übt deshalb wichtige Funktionen bei der molekularen Kontrolle der Zellmigration aus. Desweiteren konnte auch eine direkte *in vitro* Bindung von PKD an F-Aktin nachgewiesen werden. Die Aktin-

Bindedomäne wurde dabei auf 46 Aminosäuren im N-terminalen Bereich von PKD, beginnend ab der Aminosäureposition 98 eingegrenzt. Ein Sequenzvergleich der entsprechenden Region zeigte hoch konservierte Motive zwischen den einzelnen PKD Isoformen und auch bei unterschiedlichen Spezies, wie z. B. *Mensch*, *Maus* und *Drosophila* an, was auf eine mögliche konservierte Funktion innerhalb der PKD Familie hindeutet. Außer dieser Bindung von PKD an F-Aktin konnte auch eine direkte Interaktion von PKD und Cortactin nachgewiesen werden. Im *in vitro* Kinasetest wurde Cortactin von PKD am Serin-Rest 298 (Ser298) und an weiteren, noch unbekannten Aminosäuren phosphoryliert. Eine Phosphorylierung an Ser298 konnte in intakten Zellen jedoch bisher nicht nachgewiesen werden. Mit Hilfe von stabil PKD exprimierenden Zelllinien wurde das Migrationsverhalten in 3D Transwell-Migrationsexperimenten untersucht. PKD1 verringerte die gerichtete Zellmigration, während eine Kinase-inaktive Variante (PKD1KD) die Zellmigration verstärkte. Diese Effekte von PKD lassen sich nun entweder durch ein Modell erklären, in dem die Phosphorylierung von Cortactin bei Regulation des Aktinumbaus und der Stabilisierung von Aktin-Verzweigungen eine Rolle spielt, oder aber über die Phosphorylierung bisher noch unbekannter Substrate am Aktin Zytoskelett, welche die Zellmigration negative regulieren. Da jedoch die Mutation von Ser298 in einen Alanin-Rest ebenfalls zu einer Verstärkung der Zellmigration führte, ist es möglich, dass Cortactin ein potentielles physiologisches Substrat von PKD bei der Regulation des Aktinumbaus darstellt.

Aufgrund von Literaturdaten über eine *in vitro* Phosphorylierung von E-Cadherin, wurde PKD mit der Regulation von Zell-Zell-Adhäsionsprozessen in Verbindung gebracht. Daher wurde in dieser Arbeit der Einfluss von unterschiedlichen PKD Isoformen und Kinase-inaktiven (KD) Mutanten auf die Ca^{2+}-abhängige Zell-Adhäsion untersucht. Die Expression einer Kinase-inaktiven PKD2-, und in geringerem Ausmaß auch einer PKD1KD-Mutante, steigerte deutlich die Zell-Zell-Adhäsion der Panc89 Zellen, bei gleichzeitig reduzierter E-Cadherin Expression. Da ein E-Cadherin spezifischer Antikörper nur partiell mit der Ca^{2+}-abhängigen Zell-Aggreagtion interferierte, deutet dies auf die zusätzliche Expression von anderen Cadherin Isoformen in Panc89 Zellen hin, welche die gesteigerte Zell-Zell-Adhäsion bewirkt haben könnten. PKD1 verstärkte in Zellaggregationsversuchen ebenfalls die Zell-Zell-Adhäsion, allerdings ist noch unklar, ob dieser Effekt in Panc89 Zellen über eine mögliche Phosphorylierung von E-Cadherin vermittelt wird. Es bleibt deshalb offen, ob die erhöhte Autoaggreagtionsfähigkeit der PKD überexprimierenden Zellen überhaupt Kinaseaktivität benötigt, wie von anderen postuliert, oder ob eine bloße Proteininteraktion ausreicht. Die Expression von PKD2 in Panc89 Zellen reduzierte dagegen die Aggregation. Dieser Phänotyp konnte mit N-terminalen E-Cadherin Fragmenten im Zellkulturüberstand der stabilen PKD2 exprimierenden Panc89 Linie korreliert werden, was mit Literaturbefunden über andere Krebszellen im Einklang steht. Die Ergebnisse dieser Arbeit deuten darauf hin, dass die E-Cadherin Fragmente im Überstand von PKD2 exprimierenden Panc89 Zellen nicht über die Prozessierung durch Matrix-Metalloproteasen, sondern durch eine Serin-Protease abgespalten werden. Als Kandidaten konnten Plasmin und kationisches Trypsin für die Prozessierung ausgemacht werden. Diese Ergebnisse sind in guter Übereinstimmung mit den „Microarray-Genprofiling“-Experimenten. Hier wurde festgestellt, dass die Expression des PLAUR Gens (urokinase-like Plasminogen-activator-receptor) stark in PKD2

exprimierenden Panc89 Zellen hoch-reguliert ist, was wiederum zu einer verstärkten Aktivierung der uPA-Plasminogen-Plasmin-Kaskade und somit vielleicht auch zur E-Cadherin Prozessierung führt. Die Clusteranalyse der „Microarray“-Experimente ergab zudem weitere Gene, die entweder differentiell durch PKD1/PKD1KD bzw. PKD2/PKD2KD, sowie unabhängig von der PKD Isoform durch entsprechende wildtyp und Kinase-inaktive PKD1 und PKD2 Varianten reguliert wurden. Ein erster Vergleich mit Literaturdaten zeigte interessante Zielgene, wie z.B. das o.g. PLAUR Gen, oder SPP1 (Secreted phosphoprotein 1), das mit der Krebsprogression und dem Migrationsverhalten von Brustkrebszelllinien in Verbindung gebracht wird. Im Rahmen dieser Arbeit konnte jedoch nur eine erste Auswertung der „Genprofiling“-Daten vorgenommen werden, welche aber noch weiterer Reproduktion und unabhängiger Verifizierung bedürfen. Zusammenfassend konnte ein deutlicher Einfluss von PKD auf die Regulation von Krebs-relevanten Genen festgestellt werden, von denen einige möglicherweise mit den zellulären Leistungen in Verbindung stehen, die in dieser Arbeit an den unterschiedlichen stabilen Panc89 Linien identifiziert und molekular charakterisiert wurden.

Im Rahmen dieser Arbeit wurde eine Rolle von PKD bei der Migration und Zell-Adhäsion in Pankreas Krebszellen aufgezeigt und erste Hinweise auf die zugrunde liegenden molekularen Mechanismen erarbeitet. Die Lokalisation von PKD am Aktin Zytoskelett und seine Eigenschaft, als F-Aktin-Bindeprotein zu fungieren, deuten eine mögliche Rolle der PKD Protein-Familie bei der Regulation des Aktinumsatzes und des Aktinumbaus an, was unter anderem auch den Einfluss auf die Zell-Adhäsion und Zellmigration erklären könnte.

Label	Name	ID	Mean of 4 replicats (log)	Mean of 4 replicats (log)	Mean of 4 replicats (log)	Mean of 4 replicats (log)	Mean of 4 replicats (log)
			WT(Cy3)/ Vector(Cy5)	PKD1(Cy3)/ Vector(Cy5)	PKD1KD(Cy3)/ Vector(Cy5)	PKD2(Cy3)/ Vector(Cy5)	PKD2KD(Cy3)/ Vector(Cy5)
				EXP1	EXP2	EXP3	EXP4
A_1_D03	KIP2	NM_006383	-0,3	0,3	0,3	-0,5	0,3
A_1_D11	SPP1	NM_000582	-1,0	1,1	4,2	0,7	4,5
A_1_E05	TK1	NM_003258	-0,3	-0,5	-0,6	-1,0	-0,5
A_1_F03	CTSD	NM_001909	-0,2	0,4	-0,5	-1,5	-0,1
A_1_F09	TIMP3	NM_000362	0,3	-0,3	0,3	-2,7	0,5
A_1_G10	ITGB4	NM_000213	0,9	-0,2	-0,8	-1,5	-1,0
A_1_G15	B3GNT4	NM_030765	0,0	-0,7	-0,8	-0,4	-0,9
A_1_H01	CASP8	NM_032992	-0,5	-0,2	-0,3	-0,6	-0,1
A_1_H02	TOP2A	NM_001067	0,6	1,7	1,5	0,4	1,6
A_1_H17	S100P	NM_005980	0,2	-1,4	-1,3	0,1	-1,3
A_1_H18	A2M	NM_000014	0,5	0,6	2,1	0,5	1,8
A_1_I08	STC2	NM_003714	-0,3	-0,2	-0,1	0,6	0,1
A_1_J05	CRMP1	NM_001313	0,1	0,1	0,0	-0,6	0,1
A_1_L01	CCNB1	NM_031966	0,1	1,0	0,7	-0,6	0,8
A_1_L05	CSF1	NM_000757	0,4	0,4	0,5	-0,5	0,9
A_1_L07	MMP7	NM_002423	0,0	0,1	0,4	-0,3	0,8
A_1_L10	LRRC8	NM_019594	1,3	-0,3	-0,5	-1,0	-0,4
A_1_L13	CYP1A1	NM_000499	-0,7	-0,5	-0,7	0,4	-0,5
A_1_M02	F2R	NM_001992	0,2	0,1	-0,5	-1,0	-0,3
A_1_N07	MMP2	NM_004530	-0,1	0,5	0,4	-1,1	0,9
A_1_N17	HPSE	NM_006665	0,5	-0,5	-0,5	0,0	-0,5
A_1_O06	PBX3	NM_006195	0,0	0,0	0,3	-0,3	0,3
A_1_P06	CYP11A1	NM_000781	-0,5	-1,3	-1,7	-0,3	-1,6
A_1_Q01	CAV1	NM_001753	1,2	-0,1	-0,7	-2,0	-1,1
A_1_Q16	TXNIP	NM_006472	1,4	-0,9	0,1	0,2	0,0
A_1_R04	JUNB	NM_002229	0,1	-1,0	-0,6	0,0	-0,7
A_1_R14	SERPINI1	NM_005025	-0,2	0,1	0,4	-0,7	0,3
A_1_R16	XTP1 (DEPDC1B)	NM_018369	0,0	-0,8	-0,6	0,3	-0,6
A_2_F07	HPN	NM_182983	0,3	1,9	2,9	-0,8	3,2
A_2_F13	MMP14	NM_004995	-0,3	0,5	-0,1	-0,7	-0,2
A_2_G02	KCNN4	NM_002250	0,1	-1,0	-0,7	-0,2	-0,8
A_2_G06	BAZ2A	NM_013449	-0,2	0,6	0,1	-0,8	0,0
A_2_H07	CHI3L1	NM_001276	-0,9	-0,8	1,3	-1,1	1,3
A_2_H18	ANXA2	NM_004039	-0,3	0,6	-0,1	-0,8	-0,4
A_2_I01	KRT7	NM_005556	-0,1	-0,6	-1,0	0,2	-1,2
A_2_J15	ESR2	NM_001437	-0,7	0,4	0,3	-0,8	0,2
A_2_K05	DDIT3	NM_004083	0,5	-0,2	-0,5	0,0	-0,5
A_2_L10	RAD51C	NM_058216	-0,1	-0,3	0,4	0,3	0,1
A_2_M03	GLUL	NM_002065	0,1	-0,1	0,1	-0,6	-0,1
A_2_N05	PDGFA	NM_002607	0,3	-0,5	-0,4	-0,9	-0,1
A_2_N12	IGF1R	NM_000875	-0,4	-0,4	-0,1	-0,4	0,1
A_2_O10	JARID1B	NM_006618	-0,2	-0,7	-0,6	0,1	-0,5
A_2_P09	GADD45A	NM_001924	0,4	0,4	1,2	0,1	1,0
A_2_P13	ARHB	NM_004040	-1,8	-1,3	-1,5	0,1	-1,7
A_2_Q04	HNRPH1	NM_005520	-0,2	0,3	0,5	-0,1	0,5
A_2_Q08	MST1R	NM_002447	0,2	-0,8	-1,0	-0,4	-1,1
A_2_R02	SERPINA3	NM_000624	-0,4	-0,2	0,7	-0,8	0,2
A_2_R11	LTBP3	NM_021070	-0,7	-1,2	-1,3	0,1	-1,2
A_2_R17	ID1	NM_002165	0,2	-0,7	-0,7	0,6	-0,8
A_3_C09	TGFB2	NM_003238	-1,1	0,3	0,5	0,0	0,7
A_3_D02	TYMS	NM_001071	-0,1	0,4	0,1	-0,5	0,1
A_3_E05	REA	NM_007273	-0,1	0,0	0,2	-0,4	0,1
A_3_F03	MGLL	NM_007283	-0,8	0,2	-1,0	0,5	-0,8
A_3_F06	CASP1	NM_032292	1,2	-0,5	0,2	-0,2	0,0
A_3_F07	EGFR	NM_005228	1,0	-0,2	-0,4	0,2	-0,4
A_3_F17	CASP9	NM_001229	-1,2	-1,3	-1,8	0,0	-1,9
A_3_I04	BIRC2	NM_001166	-1,1	0,8	0,8	-0,6	0,9
A_3_J03	THBS1	NM_003246	-0,4	0,4	1,0	0,1	1,6
A_3_J05	PVALB	NM_002854	-0,3	-0,5	-0,5	-1,0	-0,4
A_3_K01	CYP19A1	NM_031226	-0,1	0,0	0,0	-0,6	-0,1
A_3_K11	CCNH	NM_001239	-0,2	0,1	0,2	-0,5	0,1
A_3_M02	LAMC1	NM_002293	-0,1	0,0	-0,6	-1,0	-0,7
A_3_M03	AR	NM_000044	-0,6	-0,8	-0,3	0,1	-0,5
A_3_M08	EXT1	NM_000127	-0,6	-0,4	0,2	0,9	-0,1
A_3_M09	LOX	NM_002317	-2,0	0,2	0,9	0,4	1,2
A_3_M10	IRS1	NM_005544	0,2	-0,5	-0,4	-0,1	-0,6
A_3_N01	S100A6	NM_014624	-0,2	-0,6	-1,1	-0,9	-1,0
A_3_N05	GAPDH	NM_002046	-0,3	0,1	0,0	-0,5	0,0
A_3_O02	FSCN1	NM_003088	1,2	-0,6	-0,1	-0,9	-0,2
A_3_O04	PLAU	NM_002658	-0,2	0,0	0,2	-0,8	-0,1
A_3_O06	BUB1	NM_004336	0,5	1,2	1,0	0,2	1,0
A_3_P05	NRG1	NM_013957	1,0	-0,3	-0,2	0,3	-0,2
A_3_P10	BCAS1	NM_003657	-0,4	-0,7	-0,2	-0,9	-0,4
A_3_Q14	AP1S2	NM_003916	0,0	0,1	0,1	-0,5	0,2
A_3_Q15	GPR160	NM_014373	0,3	0,4	0,5	-0,5	0,5

Table 3: Filtered list of 105 genes displaying mean log values corresponding to the full linkage uncentered hierarchical cluster shown in Fig. 25A

Label	Name	ID	Mean of 4 replicats (log)	Mean of 4 replicats (log)	Mean of 4 replicats (log)	Mean of 4 replicats (log)	Mean of 4 replicats (log)
			WT(Cy3)/ Vector(Cy5)	PKD1(Cy3)/ Vector(Cy5)	PKD1KD(Cy3)/ Vector(Cy5)	PKD2(Cy3)/ Vector(Cy5)	PKD2KD(Cy3)/ Vector(Cy5)
				EXP1	EXP2	EXP3	EXP4
A_3_R07	MADH6	NM_005585	-1,1	-1,0	-1,5	-0,8	-1,3
A_3_R16	CDH11	NM_033664	-0,3	-0,1	0,4	-0,6	0,6
A_4_E07	DIAPH3	NM_030932	-0,3	0,4	0,0	-0,7	-0,1
A_4_E08	TNFAIP3 (A20)	NM_006290	-0,1	0,7	1,3	0,2	1,5
A_4_F06	KRT18	NM_000224	-0,3	-0,4	-0,1	0,6	0,0
A_4_F09	CASP4	NM_001225	-0,4	0,1	0,3	0,7	-0,1
A_4_G10	LYZ	NM_000239	0,5	0,1	0,2	1,0	0,4
A_4_G12	SELENBP1	NM_003944	-0,7	-0,5	-0,6	0,0	-0,6
A_4_G14	FLT1	NM_002019	0,0	0,6	0,4	-0,3	0,2
A_4_H13	DPYD	NM_000110	-0,6	-0,5	-0,6	0,0	-0,6
A_4_I01	PLAUR	NM_002659	0,3	-0,5	-0,7	0,7	-0,9
A_4_J03	SRD5A1	NM_001047	0,2	-0,3	-0,6	0,2	-0,5
A_4_J09	EDN1	NM_001955	-0,4	0,2	0,5	0,0	0,5
A_4_K01	CTSS	NM_004079	-0,5	-0,4	-0,5	0,1	-0,4
A_4_K02	HIF1A	NM_001530	-1,7	0,3	0,8	0,8	1,2
A_4_L01	KRT18	NM_000224	1,1	0,2	-0,1	0,9	0,0
A_4_L05	MS4A7	NM_021201	-0,1	0,0	0,0	-0,8	-0,1
A_4_L13	E2-EPF	NM_014501	0,0	0,8	0,8	-0,3	0,8
A_4_M06	KRT8	NM_002273	0,8	0,2	-0,4	0,3	-0,4
A_4_N11	CDK2	NM_001798	0,5	1,3	1,2	0,3	1,2
A_4_N12	VEGF	NM_003376	0,3	-0,3	-0,6	0,3	-0,5
A_4_N14	FUCA1	NM_000147	0,3	0,1	0,6	1,1	0,7
A_4_O01	SP1	NM_138473	-0,4	-0,6	-0,9	-0,1	-0,8
A_4_O06	P2RX4	NM_032554	-0,2	0,0	-0,1	0,6	-0,1
A_4_P10	FGFR1	NM_023109	-1,3	-1,5	-1,7	-0,2	-1,7
A_4_Q04	MAPK13	NM_002754	-0,1	-0,1	-0,6	-0,7	-0,5
A_4_Q15	CD34	NM_001773	0,2	-0,4	0,1	-0,4	-0,2
A_4_R04	NFIB	NM_005596	-0,9	0,4	0,8	-0,2	0,9
A_4_R07	CSTA	NM_005213	2,2	-0,8	0,6	0,6	-0,2
A_4_R17	EMP1	NM_001423	2,0	0,5	-0,4	-0,2	-0,7

Table 3: Continued list of 105 genes displaying mean log values corresponding to the full linkage uncentered hierarchical cluster shown in Fig. 25A

Label	Name	ID	Mean of 4 replicats (log)	Mean of 4 replicats (log)	Mean of 4 replicats (log)	Mean of 4 replicats (log)	Mean of 4 replicats (log)
			WT(Cy3)/ Vector(Cy5)	PKD1(Cy3)/ Vector(Cy5)	PKD1KD(Cy3)/ Vector(Cy5)	PKD2(Cy3)/ Vector(Cy5)	PKD2KD(Cy3)/ Vector(Cy5)
				EXP1	EXP2	EXP3	EXP4
Genes regulated by PKD1KD and PKD2KD cells ≥ log 0.5							
A_1_D11	SPP1	NM_000582	-1,0	1,1	4,2	0,7	4,5
A_2_F07	HPN	NM_182983	0,3	1,9	2,9	-0,8	3,2
A_1_H18	A2M	NM_000014	0,5	0,6	2,1	0,5	1,8
A_2_P09	GADD45A	NM_001924	0,4	0,4	1,2	0,1	1,0
A_3_J03	THBS1	NM_003246	-0,4	0,4	1,0	0,1	1,6
A_4_E08	TNFAIP3 (A20)	NM_006290	-0,1	0,7	1,3	0,2	1,5
A_3_M09	LOX	NM_002317	-2,0	0,2	0,9	0,4	1,2
A_3_O02	FSCN1	NM_003088	1,2	-0,6	-0,1	-0,9	-0,2
A_3_P10	BCAS1	NM_003657	-0,4	-0,7	-0,2	-0,9	-0,4
A_3_R07	MADH6	NM_005585	-1,1	-1,0	-1,5	-0,8	-1,3
A_4_R17	EMP1	NM_001423	2,0	0,5	-0,4	-0,2	-0,7
A_4_R07	CSTA	NM_005213	2,2	-0,8	0,6	0,6	-0,2
A_3_M08	EXT1	NM_000127	-0,6	-0,4	0,2	0,9	-0,1
Genes regulated by PKD1KD and PKD2KD ≤ log 0.5							
A_1_O01	WT1	NM_024426	0,0	0,3	0,5	0,1	0,5
Genes differentially regulated by PKD1KD and PKD2KD cells versus respective wildtype cell lines ≥ log 0.5							
A_2_H07	CHI3L1	NM_001276	-0,9	-0,8	1,3	-1,1	1,3
A_1_F09	TIMP3	NM_000362	0,3	-0,3	0,3	-2,7	0,5
A_3_R16	CDH11	NM_033664	-0,3	-0,1	0,4	-0,6	0,6
A_3_F03	MGLL	NM_007283	-0,8	0,2	-1,0	0,5	-0,8
A_4_M06	KRT8	NM_002273	0,8	0,2	-0,4	0,3	-0,4
A_2_R02	SERPINA3	NM_000624	-0,4	-0,2	0,7	-0,8	0,2

Table 4: Genes regulated in PKD1KD as well as PKD2KD cells corresponding to the full linkage uncentered hierarchical cluster shown in Fig. 25B

Label	Name	ID	Mean of 4 replicats (log)	Mean of 4 replicats (log)	Mean of 4 replicats (log)	Mean of 4 replicats (log)	Mean of 4 replicats (log)
			WT(Cy3)/ Vector(Cy5)	PKD1(Cy3)/ Vector(Cy5)	PKD1KD(Cy3)/ Vector(Cy5)	PKD2(Cy3)/ Vector(Cy5)	PKD2KD(Cy3)/ Vector(Cy5)
				EXP1	EXP2	EXP3	EXP4
Genes differentially regulated by PKD1/PKD1KD cells ≥ log 0.5							
A_1_F03	CTSD	NM_001909	-0,2	0,4	-0,5	-1,5	-0,1
A_1_F09	TIMP3	NM_000362	0,3	-0,3	0,3	-2,7	0,5
A_1_M02	F2R	NM_001992	0,2	0,1	-0,5	-1,0	-0,3
A_1_Q16	TXNIP	NM_006472	1,4	-0,9	0,1	0,2	0,0
A_2_F13	MMP14	NM_004995	-0,3	0,5	-0,1	-0,7	-0,2
A_2_H18	ANXA2	NM_004039	-0,3	0,6	-0,1	-0,8	-0,4
A_2_L10	RAD51C	NM_058216	-0,1	-0,3	0,4	0,3	0,1
A_3_F06	CASP1	NM_032292	1,2	-0,5	0,2	-0,2	0,0
A_3_M02	LAMC1	NM_002293	-0,1	0,0	-0,6	-1,0	-0,7
A_3_M08	EXT1	NM_000127	-0,6	-0,4	0,2	0,9	-0,1
A_4_Q15	CD34	NM_001773	0,2	-0,4	0,1	-0,4	-0,2
A_4_R07	CSTA	NM_005213	2,2	-0,8	0,6	0,6	-0,2
A_4_R17	EMP1	NM_001423	2,0	0,5	-0,4	-0,2	-0,7

Table 5: Genes differentially regulated by PKD1/PKD1KD cells corresponding to the full linkage uncentered hierarchical cluster shown in Fig. 25C

Label	Name	ID	Mean of 4 replicats (log)	Mean of 4 replicats (log)	Mean of 4 replicats (log)	Mean of 4 replicats (log)	Mean of 4 replicats (log)
			WT(Cy3)/ Vector(Cy5)	PKD1(Cy3)/ Vector(Cy5)	PKD1KD(Cy3)/ Vector(Cy5)	PKD2(Cy3)/ Vector(Cy5)	PKD2KD(Cy3)/ Vector(Cy5)
				EXP1	EXP2	EXP3	EXP4
Genes differentially regulated by PKD2/PKD2KD cells ≥ log 0.5							
A_1_F09	TIMP3	NM_000362	0,3	-0,3	0,3	-2,7	0,5
A_1_H17	S100P	NM_005980	0,2	-1,4	-1,3	0,1	-1,3
A_1_J05	CRMP1	NM_001313	0,1	0,1	0,0	-0,6	0,1
A_1_L01	CCNB1	NM_031966	0,1	1,0	0,7	-0,6	0,8
A_1_L05	CSF1	NM_000757	0,4	0,4	0,5	-0,5	0,9
A_1_L07	MMP7	NM_002423	0,0	0,1	0,4	-0,3	0,8
A_1_L13	CYP1A1	NM_000499	-0,7	-0,5	-0,7	0,4	-0,5
A_1_N07	MMP2	NM_004530	-0,1	0,5	0,4	-1,1	0,9
A_1_N17	HPSE	NM_006665	0,5	-0,5	-0,5	0,0	-0,5
A_1_O06	PBX3	NM_006195	0,0	0,0	0,3	-0,3	0,3
A_1_R04	JUNB	NM_002229	0,1	-1,0	-0,6	0,0	-0,7
A_1_R14	SERPINI1	NM_005025	-0,2	0,1	0,4	-0,7	0,3
A_1_R16	XTP1 (DEPDC1B)	NM_018369	0,0	-0,8	-0,6	0,3	-0,6
A_2_F07	HPN	NM_182983	0,3	1,9	2,9	-0,8	3,2
A_2_G06	BAZ2A	NM_013449	-0,2	0,6	0,1	-0,8	0,0
A_2_I01	KRT7	NM_005556	-0,1	-0,6	-1,0	0,2	-1,2
A_2_J15	ESR2	NM_001437	-0,7	0,4	0,3	-0,8	0,2
A_2_K05	DDIT3	NM_004083	0,5	-0,2	-0,5	0,0	-0,5
A_2_N12	IGF1R	NM_000875	-0,4	-0,4	-0,1	-0,4	0,1
A_2_O10	JARID1B	NM_006618	-0,2	-0,7	-0,6	0,1	-0,5
A_2_P13	ARHB	NM_004040	-1,8	-1,3	-1,5	0,1	-1,7
A_2_Q04	HNRPH1	NM_005520	-0,2	0,3	0,5	-0,1	0,5
A_2_R02	SERPINA3	NM_000624	-0,4	-0,2	0,7	-0,8	0,2
A_2_R11	LTBP3	NM_021070	-0,7	-1,2	-1,3	0,1	-1,2
A_2_R17	ID1	NM_002165	0,2	-0,7	-0,7	0,6	-0,8
A_3_C09	TGFB2	NM_003238	-1,1	0,3	0,5	0,0	0,7
A_3_D02	TYMS	NM_001071	-0,1	0,4	0,1	-0,5	0,1
A_3_E05	REA	NM_007273	-0,1	0,0	0,2	-0,4	0,1
A_3_F07	EGFR	NM_005228	1,0	-0,2	-0,4	0,2	-0,4
A_3_F17	CASP9	NM_001229	-1,2	-1,3	-1,8	0,0	-1,9
A_3_I04	BIRC2	NM_001166	-1,1	0,8	0,8	-0,6	0,9
A_3_K11	CCNH	NM_001239	-0,2	0,1	0,2	-0,5	0,1
A_3_M03	AR	NM_000044	-0,6	-0,8	-0,3	0,1	-0,5
A_3_M08	EXT1	NM_000127	-0,6	-0,4	0,2	0,9	-0,1
A_3_N05	GAPDH	NM_002046	-0,3	0,1	0,0	-0,5	0,0
A_3_P05	NRG1	NM_013957	1,0	-0,3	-0,2	0,3	-0,2
A_3_Q14	AP1S2	NM_003916	0,0	0,1	0,1	-0,5	0,2
A_3_Q15	GPR160	NM_014373	0,3	0,4	0,5	-0,5	0,5
A_4_F06	KRT18	NM_000224	-0,3	-0,4	-0,1	0,6	0,0
A_4_F09	CASP4	NM_001225	-0,4	0,1	0,3	0,7	-0,1
A_4_G12	SELENBP1	NM_003944	-0,7	-0,5	-0,6	0,0	-0,6
A_4_G14	FLT1	NM_002019	0,0	0,6	0,4	-0,3	0,2
A_4_H13	DPYD	NM_000110	-0,6	-0,5	-0,6	0,0	-0,6
A_4_I01	PLAUR	NM_002659	0,3	-0,5	-0,7	0,7	-0,9
A_4_J03	SRD5A1	NM_001047	0,2	-0,3	-0,6	0,2	-0,5
A_4_J09	EDN1	NM_001955	-0,4	0,2	0,5	0,0	0,5
A_4_K01	CTSS	NM_004079	-0,5	-0,4	-0,5	0,1	-0,4
A_4_L01	KRT18	NM_000224	1,1	0,2	-0,1	0,9	0,0
A_4_L13	E2-EPF	NM_014501	0,0	0,8	0,8	-0,3	0,8
A_4_N12	VEGF	NM_003376	0,3	-0,3	-0,6	0,3	-0,5
A_4_O06	P2RX4	NM_032554	-0,2	0,0	-0,1	0,6	-0,1
A_4_R04	NFIB	NM_005596	-0,9	0,4	0,8	-0,2	0,9
A_4_R07	CSTA	NM_005213	2,2	-0,8	0,6	0,6	-0,2

Table 6: Genes differentially regulated by PKD2/PKD2KD cells corresponding to the full linkage uncentered hierarchical cluster shown in Fig. 25D

9 – References

Aberle H., Butz S., Stappert J., Weissig H., Kemler R., Hoschuetzky H. (1994) Assembly of the Cadherin-Catenin complex *in vitro* with recombinant proteins. *J. Cell Sci.* **107**:3655-63

Aspenstrom P., Lindberg U., Hall A. (1996) Two GTPases, Cdc42 and Rac, bind directly to a protein implicated in the immunodeficiency disorder Wiskott-Aldrich syndrome. *Curr. Biol.* **6**:70-5

Ausubel, F. M. (1994) Current protocols in molecular biology. *3. Vols. John Wiley & Sons Inc., USA*

Ayscough K. R. (1998) *In vivo* functions of Actin-binding proteins. *Curr. Opin. Cell Biol.* **10**:102-11

Bagowski C. P., Stein-Gerlach M., Choidas A., und Ullrich A. (1999) Cell-type specific phosphorylation of threonines T654 and T669 by PKD defines the signal capacity of the EGF receptor. *EMBO J*. **20**: 5567-5576

Ballestrem C., Hinz B., Imhof B. A., Wehrle-Haller B. (2001) Marching at the front and dragging behind: differential alpha5beta3-Integrin turnover regulates focal adhesion behavior. *J. Cell Biol.* **155**:1319-32

Bamburg J. R., McGough A., Ono S. (1999) Putting a new twist on Actin: ADF/cofilins modulate actin dynamics. *Trends. Cell Biol.* **9**:364–70

Bankaitis V. A. (2002) Cell biology. Slick recruitment to the Golgi. *Science* **295**:290-1

Baron C. L., Malhotra V. (2002) Role of diacylglycerol in PKD recruitment to the TGN and protein transport to the plasma membrane. *Science* **295**:325-8

Barzik M., Kotova T. I., Higgs H. N., Hazelwood L., Hanein D., Gertler F. B., Schafer D. A. (2005) Ena/VASP proteins enhance Actin polymerisation in the presence of barbed end capping proteins. *J. Biol. Chem.* **280**:28653-62

Bautista D. S., Xuan J. W., Hota C., Chambers A. F., Harris J. F. (1994) Inhibition of Arg-Gly-Asp (RGD)-mediated cell adhesion to Osteopontin by a monoclonal antibody against Osteopontin. *J. Biol. Chem.* **269**:23280-5.

Beningo K. A., Dembo M., Wang Y. L. (2004) Responses of fibroblasts to anchorage of dorsal extracellular matrix receptors. *Proc. Natl. Acad. Sci. USA* **101**:18024-9

Bi E., Zigmond S. H. (1999) Actin polymerisation: Where the WASP stings. *Curr. Biol.* **9**(5):R160-3

Blobe G. C., Stribling D. S., Fabbro D., Stabel S., Hannun Y. A. (1996) Protein kinase C beta II specifically binds to and is activated by F-Actin. *J. Biol. Chem.* **271**:15823-30

Bourguignon L. Y., Zhu H., Shao L., Chen Y. W. (2001) CD44 interaction with c-Src kinase promotes Cortactin-mediated cytoskeleton function and hyaluronic acid-dependent ovarian tumour cell migration. *J. Biol. Chem.* **276**(10):7327-36

Bowden E. T., Barth M., Thomas D., Glazer R. I., and Mueller S. C. (1999) An invasion-related complex of Cortactin, Paxillin and PKCmu associates with invadopodia at sites of extracellular matrix degradation. *Oncogene* **31**:4440-4449

Bradford M. D., Soltoff S. P. (2002) P2X7 receptors activate Protein kinase D and p42/p44 mitogen-activated protein kinase (MAPK) downstream of Protein kinase C. *Biochem. J.* **366**:745-55

Brändlin I., Eiseler T., Salowsky R., and Johannes F. J. (2002) Protein kinase Cμ regulation of the JNK pathway is triggered via phosphoinositide-dependent kinase 1 and Protein kinase Ceta. *J. Biol. Chem.* **277**:45451-7

Brändlin I., Hübner S., Eiseler T., Martinez-Moya M., Horschinek A., Hausser A. Link G., Rupp S., Storz P., and Pfizenmaier K. (2002) Protein kinase C (PKC)eta-mediated PKCμ activation modulates ERK and JNK signal pathways. *J. Biol. Chem.* **277**:6490-6

Bryce N. S., Clark E. S., Leysath J. L., Currie J. D., Webb D. J., Weaver A. M. (2005) Cortactin promotes cell motility by enhancing lamellipodial persistence. *Curr. Biol.* **15**:1276-85

Buday L. (1999) Membrane-targeting of signalling molecules by SH2/SH3 domain-containing adaptor proteins. *Biochem. Biophys. Acta* **1422**:187-204

Calalb M. B., Polte T. R., Hanks S. K. (1995) Tyrosine phosphorylation of Focal adhesion kinase at sites in the catalytic domain regulates kinase activity: a role for Src family kinases. *Mol. Cell Biol.* **15**:954-63

9 – References

Carlier M. F., Jean C., Rieger K. J., Lenfant M., Pantaloni D. (1993) Modulation of the interaction between G-Actin and Thymosinβ4 by the ATP/ADP ratio: possible implication in the regulation of Actin dynamics. *Proc. Natl. Acad. Sci. USA* **90**:5034–38

Carlier M. F., Ressad F., Pantaloni D. (1999) Control of Actin dynamics in cell motility. Role of ADF/Cofilin. *J. Biol. Chem.* **274**:33827-30

Carnegie G. K., Smith F. D., McConnachie G., Langeberg L. K., Scott J. D. (2004) AKAP-Lbc nucleates a Protein kinase D activation scaffold. *Mol. Cell* **15**:889-99

Chan A. Y., Raft S., Bailly M., Wyckoff J. B., Segall J. E., Condeelis J. S. (1998) EGF stimulates an increase in Actin nucleation and filament number at the leading edge of the lamellipod in mammary adenocarcinoma cells. *J. Cell Sci.* **111**:199-211

Chen W. T. (1989) Proteolytic activity of specialised surface protrusions formed at rosette contact sites of transformed cells. *J. Exp. Zool.* **251**:167-85

Chiu T., Rozengurt E. (2001) PKD in intestinal epithelial cells: rapid activation by phorbol esters, LPA, and angiotensin through PKC. *Am. J. Physiol. Cell Physiol.* **280**:C929-42.

Colledge M., Scott J. D. (1999) AKAPs: from structure to function. *Trends Cell Biol.* **9**:216-21

Cooper J. A., Buhle E. L. Jr., Walker S. B., Tsong T. Y., Pollard T. D. (1983) Kinetic evidence for a monomer activation step in Actin polymerisation. *Biochemistry* **22**:2193-202

Coopman P. J., Thomas D. M., Gehlsen K. R., Mueller S. C. (1996) Integrin alpha3beta1 participates in the phagocytosis of extracellular matrix molecules by human breast cancer cells. *Mol. Biol. Cell* **7**:1789-804

Cowin P., Rowlands T. M., Hatsell S. J. (2005) Cadherins and Catenins in breast cancer. *Curr. Opin. Cell Biol.* **17**:499-508

Crawford H. C., Matrisian L. M., Liaw L. (1998) Distinct roles of Osteopontin in host defense activity and tumour survival during squamous cell carcinoma progression *in vivo*. *Cancer Res.* **58**:5206-15

Critchley D. R. (2000) Focal adhesions - the cytoskeletal connection. *Curr. Opin. Cell Biol.* **12:**133-9.

Daly R. J. (2004) Cortactin signalling and dynamic Actin networks. *Biochem. J.* **382**:13-25

Davidson-Moncada J. K., Lopez-Lluch G., Segal A. W., Dekker L. V. (2002) Involvement of Protein kinase D in Fc gamma-receptor activation of the NADPH oxidase in neutrophils. *Biochem. J.* **363**:95-103

Dehio C., Prevost M. C. and Sansonetti P. J. (1995) Invasion of epithelial cells by Shigella flexneri induces tyrosine phosphorylation of Cortactin by a pp60c-Src-mediated signalling pathway. *EMBO J.* **14**:2471-2482

DeMali K. A., Barlow C. A., Burridge K. (2002) Recruitment of the Arp2/3 complex to Vinculin: coupling membrane protrusion to matrix adhesion. *J. Cell Biol.* **159**:881-91

Dequiedt F., van Lint J., Lecomte E., Van Duppen V., Seufferlein T., Vandenheede J. R., Wattiez R., Kettmann R. (2005) Phosphorylation of Histone deacetylase 7 by Protein kinase D mediates T cell receptor-induced Nur77 expression and apoptosis. *J. Exp. Med.* **201**:793-804

Diaz Anel A.M., Malhotra V. (2005) PKCeta is required for beta1gamma2/beta3gamma2- and PKD-mediated transport to the cell surface and the organisation of the Golgi apparatus. *J. Cell Biol.* **169**:83-91

DiMagno E. P. (1999) Pancreatic cancer: clinical presentation, pitfalls and early clues. *Ann. Oncol.10 Suppl.* **4**:140-2

Doppler H., Storz P., Li J., Comb M. J., Toker A. (2005) A phosphorylation state-specific antibody recognises Hsp27, a novel substrate of Protein kinase D. *J. Biol. Chem.* **280**:15013-9

Drees F., Pokutta S., Yamada S., Nelson W. J., Weis W. I. (2005) Alpha-Catenin is a molecular switch that binds E-Cadherin-beta-Catenin and regulates Actin-filament assembly. *Cell* **123**:903-15

Du Y., Weed S. A., Xiong W.-C., Marshall T. D. and Parsons J. T. (1998) Identification of a novel Cortactin SH3 domain-binding protein and its localisation to growth cones of cultured neurons. *Mol. Cell. Biol.* **18**:5838–5851

Eisen M. B., Spellman P. T., Brown P. O., Botstein D. (1998) Cluster analysis and display of genome-wide expression patterns. *Proc. Natl. Acad. Sci. USA* **95**:14863-8

9 – References

Endo K., Oki E., Biedermann V., Kojima H., Yoshida K., Johannes F. J., Kufe D., and Datta R. (2000) Proteolytic cleavage and activation of Protein kinase C [micro] by Caspase-3 in the apoptotic response of cells to 1-beta -D-arabinofuranosylcytosine and other genotoxic agents. *J. Biol. Chem*. **24**:18476-18481

Erlichman J., Gutierrez-Juarez R., Zucker S., Mei X., Orr G. A. (1999) Developmental expression of the Protein kinase C substrate/binding protein (clone 72/SSeCKS) in rat testis identification as a scaffolding protein containing an A-kinase-anchoring domain which is expressed during late-stage spermatogenesis. *Eur. J. Biochem.* **263**:797-805

Escalante M., Courtney J., Chin W. G., Teng K. K., Kim J. I., Fajardo J. E., Mayer B. J., Hempstead B. L., Birge R. B. (2000) Phosphorylation of c-Crk II on the negative regulatory Tyr222 mediates nerve growth factor-induced cell spreading and morphogenesis. *J. Biol. Chem.* **275**:24787-97

Even-Ram S., Yamada K. M. (2005) Cell migration in 3D matrix. *Curr. Opin. Cell Biol.* **17**:524-32

Fawaz F. S., van Ooij C., Homola E., Mutka S. C. and Engel J. N. (1997) Infection with Chlamydia trachomatis alters the tyrosine phosphorylation and/or localisation of several host cell proteins including Cortactin. *Infect. Immun.* **65**:5301–5308

Fedorov A. A., Fedorov E., Gertler F., Almo S. C. (1999) Structure of EVH1, a novel proline-rich ligand-binding module involved in cytoskeletal dynamics and neural function. *Nat. Struct. Biol.* **6**:661-65.

Fogh J., Wright W. C., Loveless J. D. (1977) Absence of HeLa cell contamination in 169 cell lines derived from human tumours. *J. Natl. Cancer Inst.* **58**:209–214

Foty R. A., Steinberg M. S. (2005) The differential adhesion hypothesis: a direct evaluation. *Dev. Biol.* **278**:255-63

Frankfort B. J., Gelman I. H. (1995) Identification of novel cellular genes transcriptionally suppressed by v-Src. *Biochem. Biophys. Res. Commun.* **206**:916-26

Frieden C. (1983) Polymerisation of Actin: mechanism of the Mg2+-induced process at pH 8 and 20 degrees C. *Proc. Natl. Acad. Sci. U S A*. **80**:6513-7

Galbraith C. G., Yamada K. M., Sheetz M. P. (2002) The relationship between force and focal complex development. *J. Cell Biol.* **159**:695-705

Gates J., Peifer M. (2005) Can 1000 reviews be wrong? Actin, alpha-Catenin, and adherens junctions. *Cell* **123**:769-72

Geiger B., Bershadsky A., Pankov R., Yamada K. M. (2001) Transmembrane crosstalk between the extracellular matrix-cytoskeleton crosstalk. *Nat Rev. Mol. Cell Biol.* **2**:793-805.

Gelman I. H., Lee K., Tombler E., Gordon R., Lin X. (1998) Control of cytoskeletal architecture by the Src-suppressed C kinase substrate, SSeCKS. *Cell Motil. Cytoskeleton* **41**:1-17

Glick B.S., Malhotra V. (1998) The curious status of the Golgi apparatus. *Cell* **95**:883-9

Goldschmidt-Clermont P. J., Furman M. I., Wachsstock D., Safer D., NachmiasV. T., Pollard T. D. (1992) The control of Actin nucleotide exchange by Thymosinβ4 and Profilin: a potential regulatory mechanism for Actin polymerisation in cells. *Mol. Biol. Cell* **3**:1015–24

Gomez J., Martinez de Aragon A., Bonay P., Pitton C., Garcia A., Silva A., Fresno M., Alvarez F., Rebollo A. (1995) Physical association and functional relationship between Protein kinase C zeta and the Actin cytoskeleton. *Eur. J. Immunol.* **25**:2673-8

Grutzmann R., Boriss H., Ammerpohl O., Luttges J., Kalthoff H., Schackert H. K., Kloppel G., Saeger H. D., Pilarsky C. (2005) Meta-analysis of microarray data on pancreatic cancer defines a set of commonly dysregulated genes. *Oncogene* **24**:5079-88

Gschwendt M., Dieterich S., Rennecke J., Kittstein W., Mueller H. J., Johannes F. J. (1996) Inhibition of Protein kinase C mu by various inhibitors. Differentiation from Protein kinase C isoenzymes. *FEBS Lett.* **392**:77-80

Gumbiner B. M. (2000) Regulation of Cadherin adhesive activity. *J. Cell Biol.* **148**:399-404

Hall A. (1998) Rho GTPases and the Actin cytoskeleton. *Science* **279**:509-14

Haumaitre C., Barbacci E., Jenny M., Ott M. O., Gradwohl G., Cereghini S. (2005) Lack of TCF2/vHNF1 in mice leads to pancreas agenesis. *Proc. Natl. Acad. Sci. USA* **102**:1490-5

Hausser A., Link G., Bamberg L., Burzlaff A., Lutz S., Pfizenmaier K. and Johannes F. J. (2002) Structural requirements for localisation and activation of Protein kinase C mu (PKC mu) at the Golgi compartment. *J. Cell Biol.* **156**:65-74

Hausser A., Storz P., Hubner S., Brändlin I., Martinez-Moya M., Link G., und Johannes F. J. (2001) Protein kinase C mu selectively activates the mitogen-activated protein kinase (MAPK) p42 pathway. *FEBS Lett.* **492**:39-44

Hausser A., Storz P., Link G., Stoll H., Liu Y. C., Altman A., Pfizenmaier K., and Johannes F. J. (1999) Protein kinase C mu is negatively regulated by 14-3-3 signal transduction proteins. *J. Biol. Chem*. **14**: 9258-9264

Hausser A., Storz P., Martens S., Link G., Toker A. and Pfizenmaier K. (2005) Protein kinase D regulates vesicular transport by phosphorylating and activating Phosphatidylinositol-4 kinase IIIbeta at the Golgi complex. *Nat. Cell Biol.* **7**:880-6

Haussermann S., Kittstein W., Rincke G., Johannes F. J., Marks F., Gschwendt M. (1999) Proteolytic cleavage of Protein kinase Cmu upon induction of apoptosis in U937 cells. *FEBS Lett.* **462**:442-6.

Haworth R. S., Cuello F., Herron T. J., Franzen G., Kentish J. C., Gautel M., Avkiran M. (2004) Protein kinase D is a novel mediator of cardiac Troponin I phosphorylation and regulates myofilament function. *Circ. Res.* **95**:1091-9

Hayashi A., Seki N., Hattori A., Kozuma S. and Saito T. (1999) PKCν, a new member of the Protein kinase C family, composes a fourth subfamily with PKCμ. *Biochim. Biophys. Acta.* **1450**:99-106

Hayashido Y., Hamana T., Yoshioka Y., Kitano H., Koizumi K., Okamoto T. (2005) Plasminogen activator/Plasmin system suppresses cell-to-cell adhesion of oral squamous cell carcinoma cells via proteolysis of E-Cadherin. *Int. J. Oncol.* **27**:693-8

He T. C., Sparks A. B., Rago C., Hermeking H., Zawel L., da Costa L. T., Morin P. J., Vogelstein B., Kinzler K. W. (1998) Identification of c-Myc as a target of the APC pathway. *Science* **281**:1509-12

Heath J. P., Peachey L. D. (1989) Morphology of fibroblasts in Collagen gels: a study using 400 keV electronmicroscopy and computer graphics. *Cell Motil. Cytoskeleton* **14**:382-392

Heldin C. H., Ostman A., Ronnstrand L. (1998) Signal transduction via Platelet-derived growth factor receptors. *Biochem. Biophys. Acta.* **1378**:F79-113

Helwani F. M., Kovacs E. M., Paterson A. D., Verma S., Ali R. G., Fanning A. S., Weed S. A. and Yap A. S. (2004) Cortactin is necessary for E-Cadherin-mediated contact formation and Actin reorganisation. *J. Cell Biol.* **164**:899–910

Hernandez S. E., Krishnaswami M., Miller A. L., Koleske A. J. (2004) How do Abl family kinases regulate cell shape and movement? *Trends Cell Biol.* **14**:36-44

Higgs H. N., Pollard T. D. (1999) Regulation of Actin polymerisation by Arp2/3 complex and WASp/Scar proteins. *J. Biol. Chem.* **274**:32531-4

Higgs H. N., Pollard T. D. (2000) Activation by Cdc42 and PIP_2 of Wiskott-Aldrich syndrome protein (WASp) stimulates Actin nucleation by Arp2/3 complex. *J. Cell Biol.* **150**:1311-20

Hinck L., Nathke I. S., Papkoff J., Nelson W. J. (1994) Dynamics of Cadherin/Catenin complex formation: novel protein interactions and pathways of complex assembly. *J. Cell Biol.* **125**:1327-40

Hu H., Bliss J. M., Wang Y., Colicelli J. (2005) Rin1 is an Abl tyrosine kinase activator and a regulator of epithelial-cell adhesion and migration. *Curr. Biol.* **15**:815-23

Huang C., Jacobson K., Schaller M. D. (2004) MAP kinases and cell migration. *J. Cell Sci.* **117**:4619-28

Huang C., Liu J., Haudenschild C. C., Zhan X. (1998) The role of tyrosine phosphorylation of Cortactin in the locomotion of endothelial cells. *J. Biol. Chem.* **273**:25770-6

Huang C., Ni Y., Wang T., Gao Y., Haudenschild C. C., Zhan X. (1997) Down-regulation of the filamentous Actin crosslinking activity of Cortactin by Src-mediated tyrosine phosphorylation. *J. Biol. Chem.* **272**:13911-5

Huber A. H., Weis W. I. (2001) The structure of the beta-Catenin/E-Cadherin complex and the molecular basis of diverse ligand recognition by beta-Catenin. *Cell* **105**:391-402

Huber M. A., Kraut N., Beug H. (2005) Molecular requirements for epithelial-mesenchymal transition during tumour progression. *Curr. Opin. Cell Biol.* **17**:548-58

9 – References

Hurd C., and Rozengurt E. (2001) Protein kinase D is sufficient to suppress EGF-induced c-Jun Ser 63 phosphorylation. *Biochem. Biophys. Res. Commun.* **2**:404-408

Hurd C., Waldron R. T., and Rozengurt E. (2002) Protein kinase D complexes with C-Jun N-terminal kinase via activation loop phosphorylation and phosphorylates the C-Jun N-terminus. *Oncogene* **14**:2154-2160

Hynes R. O. (1992) Integrins: versatility, modulation, and signalling in cell adhesion. *Cell* **69**:11-25

Iglesias T. and Rozengurt E. (1999) Protein kinase D activation by deletion of its cysteine-rich motifs. *FEBS Lett.* **454**:53-6

Iglesias T., Cabrera-Poch N., Mitchell M. P., Naven T. J., Rozengurt E., Schiavo G. (2000) Identification and cloning of Kidins220, a novel neuronal substrate of Protein kinase D. *J. Biol. Chem.* **275**:40048-56

Iglesias T., Matthews S., and Rozengurt E. (1998b) Dissimilar phorbol ester binding properties of the individual cysteine-rich motifs of Protein kinase D. *FEBS Lett.* **437**:19-23

Iglesias T., und Rozengurt E. (1998a) Protein kinase D activation by mutations within its pleckstrin homology domain. *J. Biol. Chem.* **273**:410-416

Itoh M., Nagafuchi A., Moroi S., Tsukita S. (1997) Involvement of ZO-1 in Cadherin-based cell adhesion through its direct binding to alpha-Catenin and Actin filaments. *J. Cell Biol.* **138**:181-92

Jaggi M., Rao P. S., Smith D. J., Wheelock M. J., Johnson K. R., Hemstreet G. P., Balaji K. C. (2005) E-Cadherin phosphorylation by Protein kinase D1/Protein kinase C{mu} is associated with altered cellular aggregation and motility in prostate cancer. *Cancer Res.* **65**:483-92

Jamora C., Takizawa P. A., Zaarour R. F., Denesvre C., Faulkner D. J., Malhotra V. (1997) Regulation of Golgi structure through heterotrimeric G proteins. *Cell* **91**:617-26

Jamora C., Yamanouye N., van Lint J., Laudenslager J., Vandenheede J. R., Faulkner D. J., and Malhotra V. (1999) G-mediated regulation of Golgi organisation is through the direct activation of Protein kinase D. *Cell* **98**:59-68

Janmey P. A. (1994) Phosphoinositides and calcium as regulators of cellular Actin assembly and disassembly. *Annu. Rev. Physiol.* **56**:169–91

Jemal A., Murray T., Samuels A., Ghafoor A., Ward E., Thun M. J. (2003) Cancer statistics, 2003. *CA Cancer J Clin.* **53**:5-26

Jockusch B. M., Isenberg G. (1981) Interaction of alpha-Actinin and Vinculin with Actin: opposite effects on filament network formation. *Proc. Natl. Acad. Sci. USA* **78**(5):3005-9

Johannes F. J., Horn J., Link G., Haas E., Sieminski K., Wajant H., und Pfizenmaier K. (1998) Protein kinase Cμ downregulation of TNF induced apopotosis via enhancement of NFκB dependent protective genes. *Eur. J. Biochem*. **257**:47-54

Johannes F. J., Prestle J., Eis S., Oberhagemann P., Pfizenmaier K. (1994) PKCmu is a novel, atypical member of the Protein kinase C family. *J. Biol. Chem.* **269**:6140-8

Johnson R. P., Craig S. W. (1995) F-Actin binding site masked by the intramolecular association of Vinculin head and tail domains. *Nature* **373**:261-4

Kain K. H., Klemke R. L. (2001) Inhibition of cell migration by Abl family tyrosine kinases through uncoupling of Crk-Cas complexes. *J. Biol. Chem.* **276**:16185-92

Kang S. H., Choi H. H., Kim S. G., Jong H. S., Kim N. K., Kim S. J., Bang Y. J. (2000) Transcriptional inactivation of the Tissue inhibitor of metalloproteinase-3 gene by DNA hypermethylation of the 5'-CpG island in human gastric cancer cell lines. *Int. J. Cancer* **86**:632-5

Kapus A., Szaszi K., Sun J., Rizoli S., Rotstein O. D. (1999) Cell shrinkage regulates Src kinases and induces tyrosine phosphorylation of Cortactin, independent of the osmotic regulation of Na+/H+ exchangers. *J. Biol. Chem.* **274**:8093-102

Katsube T., Takahisa M., Ueda R., Hashimoto N., Kobayashi M., and Togashi S. (1998) Cortactin associates with the cell–cell junction protein ZO-1 in both *Drosophila* and *mouse*. J. *Biol. Chem.* **273**: 29672-29677

9 – References

Keleg S., Buchler P., Ludwig R., Buchler M. W., Friess H. (2003) Invasion and metastasis in pancreatic cancer. *Mol. Cancer* **2**:14

Kelleher J. F., Atkinson S. J., Pollard T. D. (1995) Sequences, structural models, and cellular localisation of the Actin-related proteins Arp2 and Arp3 from Acanthamoeba. *J. Cell Biol.* **131**:385-97

Kessels M. M., Engqvist-Goldstein A. E., Drubin D. G. (2000) Association of mouse Actin-binding protein 1 (mAbp1/SH3P7), an Src kinase target, with dynamic regions of the cortical actin cytoskeleton in response to Rac1 activation. *Mol. Biol. Cell* **11**:393-412

Kim A. S., Kakalis L. T., Abdul-Manan N., Liu G. A., Rosen M. K. (2000) Autoinhibition and activation mechanisms of the Wiskott-Aldrich syndrome protein. *Nature* **404**:151-8

Kim J., Yu W., Kovalski K., Ossowski L. (1998) Requirement for specific proteases in cancer cell intravasation as revealed by a novel semi-quantitative PCR-based assay. *Cell* **94**:353-62

Kinley A. W., Weed S. A., Weaver A. M., Karginov A. V., Bissonette E., Cooper J. A. and Parsons J. T (2003). Cortactin interacts with WIP in regulating Arp2/3 activation and membrane protrusion. *Curr. Biol.* **13**:384–393

Kinnunen T., Kaksonen M., Saarinen J., Kalkkinen N., Peng H. B. and Rauvala H. (1998) Cortactin-Src kinase signalling pathway is involved in N-syndecan-dependent neurite outgrowth. *J. Biol. Chem.* **273**:10702–10708

Kiosses W. B., Hahn K. M., Giannelli G., Quaranta V. (2001) Characterisation of morphological and cytoskeletal changes in MCF10A breast epithelial cells plated on Laminin-5: comparison with breast cancer cell line MCF7. *Cell Commun. Adhes.* **8**:29-44

Kiosses W. B., Shattil S. J., Pampori N., Schwartz M. A. (2001) Rac recruits high-affinity Integrin alpha5beta3 to lamellipodia in endothelial cell migration. *Nat. Cell Biol.* **3**:316-20

Klinkenbijl J. H., Jeekel J., Sahmoud T., van Pel R., Couvreur M. L., Veenhof C. H., Arnaud J. P., Gonzalez D. G., de Wit L. T., Hennipman A., Wils J. (1999) Adjuvant radiotherapy and 5-fluorouracil after curative resection of cancer of the pancreas and periampullary region: phase III trial of the EORTC gastrointestinal tract cancer cooperative group. *Ann Surg.* **230**:776-82; discussion 782-4

Knudsen K. A., Soler A. P., Johnson K. R., Wheelock M. J. (1995) Interaction of alpha-Actinin with the Cadherin/Catenin cell-to-cell adhesion complex via alpha-Catenin. *J. Cell Biol.* **130**:67-77

Kobayashi K., Kuroda S., Fukata M., Nakamura T., Nagase T., Nomura N., Matsuura Y., Yoshida-Kubomura N., Iwamatsu A., Kaibuchi K. (1998) p140Sra-1 (specifically Rac1-associated protein) is a novel specific target for Rac1 small GTPase. *J. Biol. Chem.* **273**:291-5

Kobielak A. , Pasolli H. A., Fuchs E. (2004) Mammalian Formin-1 participates in adherens junctions and polymerisation of linear Actin cables *Nat. Cell Biol.* **6**:21-30

Kovacs E. M., Goodwin M., Ali R. G., Paterson A. D., Yap A. S. (2002) Cadherin-directed Actin assembly: E-Cadherin physically associates with the Arp2/3 complex to direct Actin assembly in nascent adhesive contacts. *Curr. Biol.* **12**:379-82

Kozma R., Ahmed S., Best A., Lim L. (1995) The Ras-related protein Cdc42Hs and Bradykinin promote formation of peripheral Actin microspikes and filopodia in Swiss 3T3 fibroblasts. *Mol. Cell Biol.* **15**:1942-52

Krueger E. W., Orth J. D., Cao H., McNiven M. A. (2003) A dynamin-cortactin-Arp2/3 complex mediates Actin reorganisation in growth factor-stimulated cells. *Mol. Biol. Cell* **14**:1085-96

Kyriazis A. P., Kyriazis A. A., Scarpelli D. G., Fogh J., Rao M. S., Lepera R. (1982) Human pancreatic adenocarcinoma line Capan1 in tissue culture and the nude mouse: morphologic, biologic, and biochemical characteristics. *Am. J. Pathol.* **106**:250–260

Lamorte L., Rodrigues S., Sangwan V., Turner C. E., Park M. (2003) Crk associates with a multimolecular Paxillin/GIT2/beta-PIX complex and promotes Rac-dependent relocalisation of Paxillin to focal contacts. *Mol. Biol. Cell* **14**:2818-31

Larue L., Ohsugi M., Hirchenhain J., Kemler R. (1994) E-Cadherin null mutant embryos fail to form a trophectoderm epithelium. *Proc. Natl. Acad. Sci. USA* **91**:8263-7

Lauffenburger D. A., Horwitz A. F. (1996) Cell migration: a physically integrated molecular process. *Cell* **84**:359-69

Laukaitis C. M., Webb D. J., Donais K., Horwitz A. F. (2001) Differential dynamics of alpha5 Integrin, Paxillin, and alpha-Actinin during formation and disassembly of adhesions in migrating cells. *J. Cell Biol.* **153**:1427-40

Lei H., Wang H., Juan A. H., Ruddle F. H. (2005) The identification of Hoxc8 target genes. *Proc. Natl. Acad. Sci. USA* **102**:2420-4

Lemonnier J., Ghayor C., Guicheux J., Caverzasio J. (2004) Protein kinase C-independent activation of Protein kinase D is involved in BMP-2-induced activation of stress mitogen-activated protein kinases JNK and p38 and osteoblastic cell differentiation. *J. Biol. Chem.* **279**:259-64

Lieber M., Mazzetta J., Nelson-Rees W., Kaplan M., Todaro G. (1975) Establishment of a continuous tumour-cell line (Panc1) from a human carcinoma of the exocrine pancreas. *Int. J. Cancer* **15**:741–747

Liljedahl M., Maeda Y., Colanzi A., Ayala I., Van Lint J., and Malhotra V. (2001) Protein kinase D regulates the fission of cell surface destined transport carriers from the trans-Golgi network. *Cell* **3**:409-420

Lin S. Y., Xia W., Wang J. C., Kwong K. Y., Spohn B., Wen Y., Pestell R. G., Hung M. C. (2000) Beta-Catenin, a novel prognostic marker for breast cancer: its roles in cyclin D1 expression and cancer progression. *Proc. Natl. Acad. Sci. USA* **97**:4262-6

Lin X., Tombler E., Nelson P. J., Ross M., Gelman I. H. (1996) A novel Src- and Ras-suppressed Protein kinase C substrate associated with cytoskeletal architecture. *J. Biol. Chem.* **271**:28430-8

Lopez-Lluch G., Bird M. M., Canas B., Godovac-Zimmerman J., Ridley A., Segal A. W., Dekker L. V. (2001) Protein kinase C-delta C2-like domain is a binding site for Actin and enables Actin redistribution in neutrophils. *Biochem. J.* **357**:39-47

Maa M. C., Wilson L. K., Moyers J. S., Vines R. R., Parsons J. T., Parsons S. J. (1992) Identification and characterisation of a cytoskeleton-associated, epidermal growth factor sensitive pp60c-Src substrate. *Oncogene* **7**:2429-38

Machesky L. M., Gould K. L. (1999) The Arp2/3 complex: a multifunctional Actin organiser. *Curr. Opin. Cell Biol.* **11**:117-21

Machesky L. M., Hall A. (1997) Role of Actin polymerisation and adhesion to extracellular matrix in Rac- and Rho-induced cytoskeletal reorganisation. *J. Cell Biol.* **138**:913-26

Machesky L. M., Insall R. H. (1998) Scar1 and the related Wiskott-Aldrich syndrome protein, WASp, regulate the Actin cytoskeleton through the Arp2/3 complex. *Curr. Biol.* **8**:1347-56

Maciver S. K. (1995) Microfilament organisation and Actin-binding proteins in *The Cytoskeleton* (*Pryme, H., ed.), JAI press inc., Greewich CT, London, UK*

Maeda Y., Beznoussenko G. V., van Lint J., Mironov A. A., and Malhotra V. (2001) Recruitment of Protein kinase D to the trans-Golgi network via the first cysteine-rich domain. *EMBO J.* **21**: 5982-5990

Manning G., Whyte D. B., Martinez R., Hunter T. und Sudarsanam S. (2002) The protein kinase complement of the human genome. *Science* **298**:1912-1934

Marambaud P., Shioi J., Serban G., Georgakopoulos A., Sarner S., Nagy V., Baki L., Wen P., Efthimiopoulos S., Shao Z., Wisniewski T., Robakis N. K. (2002) A Presenilin-1/gamma-Secretase cleavage releases the E-Cadherin intracellular domain and regulates disassembly of adherens junctions. *EMBO J.* **21**:1948-56

Maretzky T., Reiss K., Ludwig A., Buchholz J., Scholz F., Proksch E., de Strooper B., Hartmann D., Saftig P. (2005) ADAM10 mediates E-Cadherin shedding and regulates epithelial cell-to-cell adhesion, migration, and beta-Catenin translocation. *Proc. Natl. Acad. Sci. USA*. **102**:9182-7

Marklund U., Lightfoot K., Cantrell D. (2003) Intracellular location and cell context-dependent function of Protein kinase D. *Immunity* **19**:491-501

Martin K. H., Slack J. K., Boerner S. A., Martin C. C., Parsons J. T. (2002) Integrin connections map: to infinity and beyond. *Science* **296**:1652-3

Matthews S. A., Dayalu R., Thompson L. J., Scharenberg A. M. (2003) Regulation of Protein kinase Cnu by the B-cell antigen receptor. *J. Biol. Chem.* **278**:9086-91

Matthews S. A., Rozengurt E., Cantrell D. (2000) Protein kinase D. A selective target for antigen receptors and a downstream target for Protein kinase C in lymphocytes. *J. Exp. Med.* **191**:2075-82

9 – References

Matthews S., Rozengurt E., and Cantrell D. (1999) Characterisation of serine 916 as an *in vivo* autophosphorylation site for Protein kinase D/Protein kinase Cμ. *J. Biol. Chem.* **272**:26543-26549

Matthwes S., Pettit G. R., and Rozengurt E. (1997) Bryostatin 1 induces biphasic activation of Protein kinase D in intact cells. *J. Biol. Chem.* **272**:20245-20250

McWhirter J. R., Wang J. Y. (1993) An Actin-binding function contributes to transformation by the Bcr-Abl oncoprotein of Philadelphia chromosome-positive human leukemias. *EMBO J.* **12**:1533-46

Meitner P. A., Kajiji S. M., LaPosta-Frazier N., Bogaars H. A., Jolly G. A., Dexter D. L., Calabresi P., Turner M. D. (1983) "COLO357," a human pancreatic adenosquamous carcinoma: growth in artificial capillary culture and in nude mice. *Cancer Res.* **43**:5978–5985

Miki H., Sasaki T., Takai Y., Takenawa T. (1998a) Induction of filopodium formation by a WASp-related Actin-depolymerising protein N-WASp. *Nature* **391**:93-6.

Miki H., Suetsugu S., Takenawa T. (1998b) WAVE, a novel WASp-family protein involved in Actin reorganisation induced by Rac. *EMBO J.* **17**:6932-41

Mishima M., Nishida E. (1999) Coronin localises to leading edges and is involved in cell spreading and lamellipodium extension in vertebrate cells. *J. Cell Sci.* **112**:2833-42

Mitchison T. J., Cramer L. P. (1996) Actin-based cell motility and cell locomotion. *Cell* **84**:371–79

Monsky W. L., Kelly T., Lin C. Y., Yeh Y., Stetler-Stevenson W. G., Mueller S. C., Chen W. T. (1993) Binding and localisation of M(r) 72,000 matrix metalloproteinase at cell surface invadopodia. *Cancer Res.* **53**:3159-64

Monsky W. L., Lin C. Y., Aoyama A., Kelly T., Akiyama S. K., Mueller S. C., Chen W. T. (1994) A potential marker protease of invasiveness, Seprase, is localised on invadopodia of human malignant melanoma cells. *Cancer Res.* **54**:5702-10

Moore P. S., Sipos B., Orlandini S., Sorio C., Real F. X., Lemoine N. R., Gress T., Bassi C., Kloeppel G., Kalthoff H., Ungefroren H., Loehr M., Scarpa A. (2001) Genetic profile of 22 pancreatic carcinoma cell lines. Analysis of K-ras, p53, p16 and DPC4/Smad4. *Virchows Arch.* **439**:798–802

Morgan R. T., Woods L. K., Moore G. E., Quinn L. A., McGavran L., Gordon S. G. (1980) Human cell line (COLO 357) of metastatic pancreatic adenocarcinoma. *Int. J. Cancer* **25**:591–598

Mueller S. C., Yeh Y., Chen W. T. (1992) Tyrosine phosphorylation of membrane proteins mediates cellular invasion by transformed cells. *J. Cell Biol.* **119**:1309-25

Mullins R. D., Heuser J. A., Pollard T. D. (1998) The interaction of Arp2/3 complex with Actin: nucleation, high-affinity pointed end capping, and formation of branching networks of filaments. *Proc. Natl. Acad. Sci. USA* **95**:6181–86

Naisbitt S., Kim E., Tu J. C., Xiao B., Sala C., Valtschanoff J., Weinberg R. J., Worley P. F., Sheng M. (1999) Shank, a novel family of postsynaptic density proteins that binds to the NMDA receptor/PSD-95/GKAP complex and Cortactin. *Neuron* **23**:569-82

Nakahara H., Howard L., Thompson E. W., Sato H., Seiki M., Yeh Y., Chen W. T. (1997) Transmembrane/cytoplasmic domain-mediated membrane type 1-matrix metalloprotease docking to invadopodia is required for cell invasion. *Proc. Natl. Acad. Sci. USA* **94**:7959-64

Nakahara H., Nomizu M., Akiyama S. K., Yamada Y., Yeh Y., Chen W. T. (1996) A mechanism for regulation of melanoma invasion. Ligation of alpha6beta1 Integrin by Laminin G peptides. *J. Biol. Chem.* **271**:27221-4.

Nakamura N., Lowe M., Levine T. P., Rabouille C., Warren G. (1997) The vesicle docking protein p115 binds GM130, a cis-Golgi matrix protein, in a mitotically regulated manner. *Cell* 89:445-55

Nauert J. B., Klauck T. M., Langeberg L. K., Scott J. D. (1997) Gravin, an autoantigen recognised by serum from myasthenia gravis patients, is a kinase scaffold protein. *Curr. Biol.* **7**:52-62

Nelson P. J., Gelman I. H. (1997) Cell-cycle regulated expression and serine phosphorylation of the myristylated Protein kinase C substrate, SSeCKS: correlation with culture confluency, cell cycle phase and serum response. *Mol. Cell Biochem.* **175**:233-41

Newton, A. C. (2002) Analysing Protein kinase C activation. *Methods Enzymol* **345**:499-506

Nishikawa K., Toker A., Johannes F. J., Songyang Z., Cantley L. C. (1997) Determination of the specific substrate sequence motifs of Protein kinase C isozymes. *J. Biol. Chem.* **272**:952-60

Nishikawa K., Toker A., Wong K., Marignani P. A., Johannes F. J., and Cantley L. C. (1998) Association of Protein kinase Cμ with type II Phosphatidylinositol 4-kinase and type I Phosphatidylinositol-4-phosphate 5-kinase. *J. Biol. Chem.* **273**:23126-23133

Nishizaka T., Shi Q., Sheetz M. P. (2000) Position-dependent linkages of Fibronectin-Integrin-cytoskeleton. *Proc. Natl. Acad. Sci. USA* **97**:692-7

Nobes C. D., Hall A. (1995) Rho, Rac, and Cdc42 GTPases regulate the assembly of multimolecular focal complexes associated with Actin stress fibers, lamellipodia, and filopodia. *Cell* **81**:53-62

Noe V., Fingleton B., Jacobs K., Crawford H. C., Vermeulen S., Steelant W., Bruyneel E., Matrisian L. M., Mareel M. (2001) Release of an invasion promoter E-Cadherin fragment by Matrilysin and Stromelysin-1. *J Cell Sci.* **114**:111-118

Oancea E., Bezzerides V. J., Greka A., Clapham D. E. (2003) Mechanism of persistent Protein kinase D1 translocation and activation. *Dev. Cell* **4**:561-74

Obenauer J. C., Cantley L. C,, Yaffe M. B.(2003) Scansite 2.0: Proteome-wide prediction of cell signalling interactions using short sequence motifs. *Nucleic Acids Res.* **31***:3635-41*

Ochs H. D. (1998) The Wiskott-Aldrich syndrome. *Semin. Hematol.* **35**:332-45

Ohoka Y., and Takai Y. (1998) Isolation and characterisation of Cortactin isoforms and novel Cortactin-binding protein, CBP90. *Genes to Cells* **3**: 603–612

Ohta T., Tajima H., Fushida S., Kitagawa H., Kayahara M., Nagakawa T., Miwa K., Yamamoto M., Numata M., Nakanuma Y., Kitamura Y., Terada T. (1998) Cationic Trypsinogen produced by human pancreatic ductal cancer has the characteristics of spontaneous activation and gelatinolytic activity in the presence of proton. *Int. J. Mol. Med.* **1**:689-92

Okabe T., Yamaguchi N., Ohsawa N. (1983) Establishment and characterisation of a carcinoembryonic antigen (CEA)-producing cell line from a human carcinoma of the exocrine pancreas. *Cancer* **51**:662-668

Panchal S. C., Kaiser D. A., Torres E., Pollard T. D., Rosen M. K. (2003) A conserved amphipathic helix in WASp/Scar proteins is essential for activation of Arp2/3 complex. *Nat. Struct. Biol.* **10**:591-8

Pankov R., Cukierman E., Katz B. Z., Matsumoto K., Lin D. C., Lin S., Hahn C., Yamada K. M. (2000) Integrin dynamics and matrix assembly: Tensin-dependent translocation of alpha5beta1 Integrins promotes early Fibronectin fibrillogenesis. *J. Cell Biol.* **148**:1075-90

Pankov R., Endo Y., Even-Ram S., Araki M., Clark K., Cukierman E., Matsumoto K., Yamada K. M. (2005) A Rac switch regulates random versus directionally persistent cell migration. *J. Cell Biol.* **170**:793-802

Pantaloni D., Carlier M. F. (1993) How Profilin promotes Actin filament assembly in the presence of Thymosinβ4. *Cell* **75**:1007–14

Paolucci L., Sinnett-Smith J., Rozengurt E. (2000) Lysophosphatidic acid rapidly induces Protein kinase D activation through a pertussis toxin-sensitive pathway. *Am. J. Physiol. Cell Physiol.* **278**:C33-9

Parsons J. T., Parsons S. J. (1997) Src family protein tyrosine kinases: cooperating with growth factor and adhesion signalling pathways. *Curr. Opin. Cell Biol.* **9**:187-92

Paunola E., Mattila P. K., Lappalainen P. (2002) WH2 domain: a small, versatile adapter for Actin monomers. *FEBS Lett.* **513**:92-7

Permert J., Hafstrom L., Nygren P., Glimelius B. (2001) SBU-group; *Swedish Council of Technology Assessment in Health Care*. A systematic overview of chemotherapy effects in pancreatic cancer. *Acta. Oncol.* **40**:361-70

Petit V., Boyer B., Lentz D., Turner C. E., Thiery J. P., Valles A. M. (2000) Phosphorylation of tyrosine residues 31 and 118 on Paxillin regulates cell migration through an association with Crk in NBT-II cells. *J. Cell Biol.* **148**:957-70

Petit V., Thiery J. P. (2000) Focal adhesions: structure and dynamics. *Biol. Cell.* **92**:477-94

Pokutta S., Drees F., Takai Y., Nelson W. J., Weis W. I. (2002) Biochemical and structural definition of the l-Afadin- and Actin-binding sites of alpha-Catenin. *J. Biol. Chem.* **277**:18868-74

Pokutta S., Weis W. I. (2000) Structure of the dimerisation and beta-Catenin-binding region of alpha-Catenin. *Mol. Cell* **5**:533-43

Pollard T. D., Blanchoin L., Mullins R. D. (2000) Molecular mechanisms controlling Actin filament dynamics in nonmuscle cells. *Annu. Rev. Biophys. Biomol. Struct.* **29**:545-76

Pollard T. D., Cooper J. A. Q (1984) Quantitative analysis of the effect of *Acanthamoeba* profilin on Actin filament nucleation and elongation. *Biochemistry* **23**:6631–41

Pradhan D., Lombardo C. R., Roe S., Rimm D. L., Morrow J. S. (2001) alpha-Catenin binds directly to Spectrin and facilitates Spectrin-membrane assembly *in vivo*. *J Biol. Chem.* **276**:4175-81

Prehoda K. E., Lee D. J., Lim W. A. (1999) Structure of the enabled/VASP homology 1 domain-peptide complex: a key component in the spatial control of Actin assembly. *Cell* **97**:471–80

Prehoda K. E., Scott J. A., Mullins R. D., Lim W. A. (2000) Integration of multiple signals through cooperative regulation of the N-WASp-Arp2/3 complex. *Science* **290**:801-6

Prekeris R., Hernandez R. M., Mayhew M. W., White M. K., Terrian D. M. (1998) Molecular analysis of the interactions between Protein kinase Cepsilon and filamentous Actin. *J. Biol. Chem.* **273**:26790-8

Prestle J., Pfizenmaier K., Brenner J. and Johannes F. J. (1996) Protein kinase Cμ is located at the Golgi compartment. *J. Cell Biol.* **134**:1401-10

Prigozhina N. L. and Waterman-Storer C. M. (2004) Protein kinase D-mediated anterograde membrane trafficking is required for fibroblast motility. *Curr. Biol.* **14**:88-98

Rangaswami H., Bulbule A., Kundu G. C. (2006) Osteopontin: role in cell signalling and cancer progression. *Trends Cell Biol.* **16**:79-87

Rennecke J., Rehberger P. A., Furstenberger G., Johannes F. J., Stohr M., Marks F., and Richter K. H. (1999) Protein kinase Cmu expression correlates with enhanced keratinocyte proliferation in normal and neoplastic mouse epidermis and in cell culture. *Int. J. Cancer* **1**:98-103

Rey O., Reeve J. R., Zhukova E., Sinnett-Smith J., Rozengurt E. (2004) G protein-coupled receptor-mediated phosphorylation of the activation loop of Protein kinase D: dependence on plasma membrane translocation and Protein kinase Cepsilon. *J. Biol. Chem.* **279**:34361-72

Rey O., Sinnett-Smith J., Zhukova E., und Rozengurt E. (2001a) Regulated nucleocytoplasmic transport of Protein kinase D in response to G protein-coupled receptor activation. *J. Biol. Chem.* **52**: 49228-49235

Rey O., Young S. H., Cantrell D. and Rozengurt E. (2001b) Rapid Protein kinase D translocation in response to G protein-coupled receptor activation. *J. Biol. Chem.* **276**:32616-26

Ridley A. J., Schwartz M. A., Burridge K., Firtel R. A., Ginsberg M. H., Borisy G., Parsons J. T., Horwitz A. R. (2003) Cell migration: integrating signals from front to back. *Science* **302**:1704-9

Ridley A. J. (2001) Rho GTPases and cell migration. *J. Cell Sci.* **114**: 2713–2722

Ridley A. J., Paterson H. F., Johnston C. L., Diekmann D., Hall A. (1992) The small GTP-binding protein Rac regulates growth factor-induced membrane ruffling. *Cell* **70**:401-10

Rinnerthaler G., Geiger B., Small J. V. (1988) Contact formation during fibroblast locomotion: involvement of membrane ruffles and microtubules. *Cell Biol.* **106**:747-60

Riol-Blanco L., Iglesias T., Sanchez-Sanchez N., de la Rosa G., Sanchez-Ruiloba L., Cabrera-Poch N., Torres A., Longo I., Garcia-Bordas J., Longo N., Tejedor A., Sanchez-Mateos P., Rodriguez-Fernandez J. L. (2004) The neuronal protein Kidins220 localises in a raft compartment at the leading edge of motile immature dendritic cells. *Eur. J. Immunol.* **34**:108-18

Rios-Doria J., Day K. C., Kuefer R., Rashid M. G., Chinnaiyan A. M., Rubin M. A., Day M. L. (2003) The role of Calpain in the proteolytic cleavage of E-Cadherin in prostate and mammary epithelial cells. *J. Biol. Chem.* **278**:1372-9

9 – References

Riveline D., Zamir E., Balaban N. Q., Schwarz U. S., Ishizaki T., Narumiya S., Kam Z., Geiger B., Bershadsky A. D. (2001) Focal contacts as mechanosensors: externally applied local mechanical force induces growth of focal contacts by an mDia1-dependent and ROCK-independent mechanism. *J. Cell Biol.* **153**:1175-86

Rohatgi R., Ho H. Y., Kirschner M. W. (2000) Mechanism of N-WASp activation by Cdc42 and phosphatidylinositol 4, 5-bisphosphate. *J. Cell Biol.* **150**:1299-310

Rohatgi R., Nollau P., Ho H. Y., Kirschner M. W., Mayer B. J. (2001) Nck and phosphatidylinositol 4,5-bisphosphate synergistically activate Actin polymerisation through the N-WASp-Arp2/3 pathway. *J. Biol. Chem.* **276**:26448-52

Rosenblatt J., Peluso P., Mitchison T. J. (1995) The bulk of unpolymerised Actin in *Xenopus* egg extracts is ATP-bound. *Mol. Biol. Cell* **6**:227–36

Rottner K., Hall A., Small J. V. (1999) Interplay between Rac and Rho in the control of substrate contact dynamics. *Curr. Biol.* 9:640-8

Rozengurt E., Sinnett-Smith J., Van Lint J., Valverde A. M. (1995) Protein kinase D (PKD): a novel target for diacylglycerol and phorbol esters. *Mutat. Res.* **333**:153-60

Rykx A., De Kimpe L., Mikhalap S., Vantus T., Seufferlein T., Vandenheede J. R., Van Lint J. (2003) Protein kinase D: a family affair. *FEBS Lett.* **546**:81-6.

Ryniers F., Stove C., Goethals M., Brackenier L., Noe V., Bracke M. Vandekerckhove J., Mareel M., Bruyneel E. (2002) Plasmin produces an E-Cadherin fragment that stimulates cancer cell invasion. *J. Biol Chem.* **383**:159-65

Ryo A., Nakamura M., Wulf G., Liou Y. C., Lu K. P. (2001) Pin1 regulates turnover and subcellular localisation of beta-Catenin by inhibiting its interaction with APC. *Nat. Cell Biol.* **3**:793-801

Safer D., Nachmias V. T. (1994) Beta-Thymosins as Actin binding peptides. *Bioessays* **16**:473–79

Sambrook J., Fritsch E. F., Maniatis T. (1998) Molecular cloning. A laboratory manual. 2nd ed. *Cold Spring Habor Press, Cold Spring Habor, NY*

Schafer D. A., Jennings P. B., Cooper J. A. (1996) Dynamics of capping protein and Actin *assembly in vitro*: uncapping barbed ends by polyphosphoinositides. *J. Cell Biol.* **135**:169–79

Schafer D. A., Welch M. D., Machesky L. M., Bridgman P. C., Meyer S. M., Cooper J. A. (1998) Visualisation and molecular analysis of Actin assembly in living cells. *J. Cell Biol.* **143**:1919-30

Schaller M. D., Parsons J. T. (1994) Focal adhesion kinase and associated proteins. *Curr. Opin. Cell Biol.* **6**:705-10

Schoenwaelder S. M., Burridge K. (1999) Bidirectional signalling between the cytoskeleton and Integrins. *Curr. Opin. Cell Biol.* **11**:274-86

Schwob E., Martin R. P (1992). New yeast Actin-like gene required late in the cell cycle. *Nature* **355**:179–82

Senger D. R., Ledbetter S. R., Claffey K. P., Papadopoulos-Sergiou A., Peruzzi C. A., Detmar M. (1996) Stimulation of endothelial cell migration by vascular permeability factor/vascular endothelial growth factor through cooperative mechanisms involving the alpha5beta3 Integrin, Osteopontin, and Thrombin. *Am. J. Pathol.* **149**:293-305

Senkel S., Lucas B., Klein-Hitpass L., Ryffel G. U. (2005) Identification of target genes of the transcription factor HNF1beta and HNF1alpha in a human embryonic kidney cell line. *Biochem. Biophys. Acta.* **1731**:179-90

Shtutman M., Zhurinsky J., Simcha I., Albanese C., D'Amico M., Pestell R., Ben-Ze'ev A. (1999) The cyclin D1 gene is a target of the beta-Catenin/LEF-1 pathway. *Proc. Natl. Acad. Sci. USA* **96**:5522-7

Sidorenko S. P., Law C.-L., Klaus S. J., Chandren K. A., Takata M., Kurosaki T., und Clark E. A. (1996) Protein kinase Cμ (PKCμ) associates with the B cell antigen receptor complex and regulates lymphocyte signalling. *Immunity* **5**:353-363

Sinnett-Smith J., Zhukova E., Hsieh N., Jiang X., Rozengurt E. (2004) Protein kinase D potentiates DNA synthesis induced by Gq-coupled receptors by increasing the duration of ERK signalling in swiss 3T3 cells. *J. Biol. Chem.* **279**:16883-93

Sipos B., Moser S., Kalthoff H., Torok V., Lohr M., Kloppel G. (2003) A comprehensive characterisation of pancreatic ductal carcinoma cell lines: towards the establishment of an in vitro research platform. *Virchows Arch.* **442**:444-52

Stafford M. J., Watson S. P., Pears C. J. (2003) PKD: a new Protein kinase C-dependent pathway in platelets. *Blood* **101**:1392-9

Staib L., Link K. H., Beger H. G. (1999) Immunotherapy in pancreatic cancer - current status and future. *Langenbecks Arch. Surg.* **384**:396-404

Storz P., Döppler H., and Toker A. (2004) Protein kinase Cδ selectively regulates Protein Kinase D-dependent activation of NFκB in oxidative stress signalling. *Mol. Cel.l Biol.* **24**:2614-26

Storz P., Doppler H., Johannes F. J. and Toker A. (2003) Tyrosine phosphorylation of Protein kinase D in the pleckstrin homology domain leads to activation. *J. Biol. Chem.* **278**:17969-76

Storz P., Hausser A., Link G., Dedio J., Ghebrehiwet B., Pfizenmaier K., und Johannes F. J. (2000) Protein kinase C [micro] is regulated by the multifunctional chaperon protein p32. *J. Biol. Chem*. **32**: 24601-24607

Sturany S., van Lint J., Gilchrist A., Vandenheede J. R., Adler G., Seufferlein T. (2002) Mechanism of activation of Protein kinase D2 (PKD2) by the CCK(B)/Gastrin receptor. *J. Biol. Chem.* **277**:29431-6

Sturany S., Van Lint J., Muller F., Wilda M., Hameister H., Hocker M., Brey A., Gern U., Vandenheede J., Gress T., Adler G., and Seufferlein T. (2001) Molecular cloning and characterisation of the human Protein kinase D2. A novel member of the Protein kinase D family of serine/threonine kinases. *J. Biol. Chem.* **276**:3310-3318

Suetsugu S., Miki H., Takenawa T. (1999) Identification of two human WAVE/SCAR homologues as general Actin regulatory molecules which associate with the Arp2/3 complex. *Biochem. Biophys. Res. Commun.* **260**:296-302

Svitkina T. M., Borisy G. G. (1999) Arp2/3 complex and Actin depolymerising factor/Cofilin in dendritic organisation and treadmilling of Actin filament array in lamellipodia. *J. Cell Biol.* **145**:1009–26

Tachado S. D., Mayhew M. W., Wescott G. G., Foreman T. L., Goodwin C. D., McJilton M. A., Terrian D. M. (2002) Regulation of tumour invasion and metastasis in Protein kinase Cepsilon-transformed NIH 3T3 fibroblasts. *J. Cell Biochem.* **85**:785-97

Tan M., Xu X., Ohba M., Ogawa W., Cui M. Z. (2003) Thrombin rapidly induces Protein kinase D phosphorylation, and Protein kinase Cdelta mediates the activation. *J. Biol. Chem.* **278**:2824-8

Tan X., Egami H., Nozawa F., Abe M., Baba H. (2006) Analysis of the invasion-metastasis mechanism in pancreatic cancer: Involvement of Plasmin(ogen) cascade proteins in the invasion of pancreatic cancer cells. *Int. J. Oncol.* **28**:369-74

Thiery J. P. (2002) Epithelial-mesenchymal transitions in tumour progression. *Nat. Rev. Cancer.* **2**:442-54

Tilney L. G., Bonder E. M., Coluccio L. M., Mooseker M. S. (1983) Actin from Thyone sperm assembles on only one end of an Actin filament: a behavior regulated by Profilin. *J. Cell Biol.* **97**:112-24

Tilney L. G., Bonder E. M., DeRosier D. J. (1981) Actin filaments elongate from their membrane-associated ends. *J. Cell Biol.* **90**:485–94

Tobacman L. S., Korn E. D. (1983) The kinetics of Actin nucleation and polymerisation. *J. Biol. Chem.* **258**:3207-14

Trauzold A., Schmiedel S., Sipos B., Wermann H., Westphal S., Röder C., Klapper W., Arlt A., Lehnert L., Ungefroren H., Johannes F. J. and Kalthoff H. (2003) PKCμ prevents CD95-mediated apoptosis and enhances proliferation in pancreatic tumour cells. *Oncogene* **22**:8939-47

Uhle S., Medalia O., Waldron R., Dumdey R., Henklein P., Bech-Otschir D., Huang X., Berse M., Sperling J., Schade R., Dubiel W. (2003) Protein kinase CK2 and Protein kinase D are associated with the COP9 signalosome. *EMBO J.* **22**:1302-12

Uruno T., Liu J., Li Y., Smith N. and Zhan X. (2003) Sequential interaction of Actin-related proteins 2 and 3 (Arp2/3) complex with Neural Wiscott–Aldrich syndrome Protein (N-WASp) and Cortactin during branched Actin filament network formation. *J. Biol. Chem.* **278**:26086–26093

Uruno T., Liu J., Zhang P., Fan Y.-X., Egile C., Li R., Mueller S. C. and Zhan X. (2001) Activation of Arp2/3 complex-mediated Actin polymerisation by Cortactin. *Nat. Cell Biol.* **3**:259–266

Vaduva G., Martin N. C., Hopper A. K. (1997) Actin-binding Verprolin is a polarity development protein required for the morphogenesis and function of the yeast Actin cytoskeleton. *J. Cell Biol.* **139**:1821-33

Valles A. M., Beuvin M., Boyer B. (2004) Activation of Rac1 by Paxillin-Crk-Dock180 signalling complex is antagonised by Rap1 in migrating NBT-II cells. *J. Biol. Chem.* **279**:44490-6

Valverde A. M., Sinnett-Smith J., Van Lint J., Rozengurt E. (1994) Molecular cloning and characterisation of Protein kinase D: a target for diacylglycerol and phorbol esters with a distinctive catalytic domain. *Proc. Natl. Acad. Sci. USA* **91**:8572-6

Van Etten R. A. (1999) Cycling, stressed-out and nervous: cellular functions of c-Abl. *Trends Cell Biol.* **9**:179-86

Van Etten R. A., Jackson P. K., Baltimore D., Sanders M. C., Matsudaira P. T., Janmey P. A. (1994) The COOH terminus of the c-Abl tyrosine kinase contains distinct F- and G-Actin binding domains with bundling activity. *J. Cell Biol.* **124**:325-40

Van Lint J., Ni Y., Valius M., Merlevede W., and Vandenheede J. R. (2002) Platelet-derived growth factor stimulates Protein kinase D through the activation of phospholipase Cγ and Protein kinase C. *J. Biol. Chem.* **273**:7038-7043

Van Lint J., Rykx A., Maeda Y., Vantus T., Sturany S., Malhotra V., Vandenheede J. R., Seufferlein T. (2002) Protein kinase D: an intracellular traffic regulator on the move. *Trends Cell Biol.* **12**(4):193-200

Van Rossum A. G., de Graaf J. H., Schuuring-Scholtes E., Kluin P. M., Fan Y. X., Zhan X., Moolenaar W. H., Schuuring E. (2003) Alternative splicing of the Actin-binding domain of human Cortactin affects cell migration. *J. Biol. Chem.* **278**:45672-9

Vasioukhin V., Bauer C., Yin M., Fuchs E. (2000) Directed Actin polymerisation is the driving force for epithelial cell-to-cell adhesion. *Cell* **100**:209-19

Vasioukhin V., Fuchs E. (2001) Actin dynamics and cell-to-cell adhesion in epithelia. *Curr. Opin. Cell Biol.* **13**:76-84.

Vega R. B., Harrison B. C., Meadows E., Roberts C. R., Papst P. J., Olson E. N., McKinsey T. A. (2004) Protein kinases C and D mediate agonist-dependent cardiac hypertrophy through nuclear export of Histone deacetylase 5. *Mol. Cell Biol.* **24**:8374-85

Vertommen D., Rider M., Ni Y., Waelkens E., Merlevede W., Vandenheede J. R., und van Lint J. (2000) Regulation of protein kinase D by multisite phosphorylation. Identification of phosphorylation sites by mass spectrometry and characterisation by site-directed mutagenesis. *J. Biol. Chem.* **26**: 19567-19576

Vinson V. K., De La Cruz E. M., Higgs H. N., Pollard T. D. (1998) Interactions of Acanthamoeba Profilin with Actin and nucleotides bound to Actin. *Biochemistry* **37**:10871–80

Vuori K. and Ruoslahti E. (1995) Tyrosine phosphorylation of p130Cas and Cortactin accompanies Integrin-mediated cell adhesion to extracellular matrix. *J. Biol. Chem.* **270**:22259–22262

Waldron R. T. and Rozengurt E. (2003) Protein kinase C phosphorylates Protein kinase D activation loop Ser744 and Ser748 and releases autoinhibition by the pleckstrin homology domain. *J. Biol. Chem.* **278**:154-63

Waldron R. T., Rey O., Iglesias T., Tugal T., Cantrell D., und Rozengurt E. (2001) Activation loop Ser744 and Ser748 in Protein kinase D are transphosphorylated *in vivo*. *J. Biol. Chem.* **35**:32606-32615

Waldron R.T., Rey O., Zhukova E., Rozengurt E. (2004) Oxidative stress induces Protein kinase C-mediated activation loop phosphorylation and nuclear redistribution of Protein kinase D. *J. Biol. Chem.* **279**:27482-93

Wanebo H. J. (2000) The challenge of early gastric cancer: the need to optimise microstaging and therapy. *Gastric Cancer* **3**:121-122

Wang Y., Miller A. L., Mooseker M. S., Koleske A. J. (2001) The Abl-related gene (Arg) nonreceptor tyrosine kinase uses two F-Actin-binding domains to bundle F-Actin. *Proc. Natl. Acad Sci. USA* **98**:14865-70

Wang Y., Waldron R. T., Dhaka A., Patel A., Riley M. M., Rozengurt E., Colicelli J. (2002) The Ras effector Rin1 directly competes with Raf and is regulated by 14-3-3 proteins. *Mol. Cell. Biol.* **22**:916-26

Watabe-Uchida M., Uchida N., Imamura Y., Nagafuchi A., Fujimoto K., Uemura T., Vermeulen S., van Roy F., Adamson E. D. Takeichi M. (1998) alpha-Catenin-Vinculin interaction functions to organise the apical junctional complex in epithelial cells. *J. Cell Biol.* **142**:847-57

Weaver A. M., Heuser J. E., Karginov A. V., Lee W.-L., Parsons J. T. and Cooper J. A. (2002) Interaction of Cortactin and N-WASp with Arp2/3 complex. *Curr. Biol.* **12**:1270–1278

Weaver A. M., Karginov A. V., Kinley A. W., Weed S. A., Li Y., Parsons J. T., Cooper J. A. (2001) Cortactin promotes and stabilises Arp2/3-induced Actin filament network formation. *Curr. Biol.* **11**:370-4
Weed S. A., Du Y. and Parsons J. T. (1998) Translocation of Cortactin to the cell periphery is mediated by the small GTPase Rac1. *J. Cell Sci.* **111**:2433–2443

Weed S. A., Karginov A., Schafer D. A., Weaver A. M., Kinley A. W., Cooper J. A. and Parsons J. T. (2000) Cortactin localisation to sites of Actin assembly in lamellipodia requires interactions with F-Actin and the Arp2/3 complex. *J. Cell Biol.* **151**:29–40

Weed S. A., Parsons J. T. (2001) Cortactin: coupling membrane dynamics to cortical Actin assembly. *Oncogene* **20**:6418-34

Weiss E. E., Kroemker M., Rudiger A. H., Jockusch B. M., Rudiger M. (1998) Vinculin is part of the Cadherin-Catenin junctional complex: complex formation between alpha-Catenin and Vinculin. *J. Cell Biol.* **141**:755-64

Welch M. D., DePace A. H., Verma S., Iwamatsu A., Mitchison T. J. (1997) The human Arp2/3 complex is composed of evolutionarily conserved subunits and is localised to cellular regions of dynamic Actin filament assembly. *J. Cell Biol.* **138**:375–84

Welch M. D., Mallavarapu A., Rosenblatt J., Mitchison T. J. (1997) Actin dynamics *in vivo*. *Curr. Opin. Cell Biol.* **9**:54-61

Westphal R. S., Soderling S. H., Alto N. M., Langeberg L. K., Scott J. D. (2000) Scar/WAVE-1, a Wiskott-Aldrich syndrome protein, assembles an Actin-associated multi-kinase scaffold. *EMBO J.* **19**:4589-600

Westphal S., Kalthoff H. (2003) Apoptosis: targets in pancreatic cancer. *Mol. Cancer* **2**:6

Woodring P. J., Hunter T., Wang J. Y. (2003) Regulation of F-Actin-dependent processes by the Abl family of tyrosine kinases. *J. Cell Sci.* **116**:2613-26

Wu H. and Montone K. T. (1998) Cortactin localisation in Actin-containing adult and fetal tissues. *J. Histochem. Cytochem.* **46**:1189–1191

Wu H., and Parsons J. (1993) Cortactin, an 80/85-kilodalton pp60/Src substrate, is a filamentous Actin-binding protein enriched in the cell cortex. *J. Cell Biol.* **120**:1417–1426

Wu H., Reynolds A. B., Kanner S. B., Vines R. R. and Parsons J. T. (1991) Identification and characterisation of a novel cytoskeleton-associated pp60/Src substrate. *Mol. Cell. Biol.* **11**:5113–5124

Yamada S., Pokutta S., Drees F., Weis W. I., Nelson W. J. (2005) Deconstructing the Cadherin-Catenin-Actin complex. *Cell* **123**:889-901

Yeaman C., Ayala M. I., Wright J. R., Bard F., Bossard C., Ang A., Maeda Y., Seufferlein T., Mellman I., Nelson W. J., Malhotra V. (2004a) Protein kinase D regulates basolateral membrane protein exit from trans-Golgi network. *Nat. Cell Biol.* **6**:106-12

Yeaman C., Grindstaff K. K., Nelson W. J. (2004b) Mechanism of recruiting Sec6/8 (exocyst) complex to the apical junctional complex during polarisation of epithelial cells. *J. Cell Sci.* **117**:559-70

Yeo C. J., Cameron J. L. (1999) Improving results of pancreaticoduodenectomy for pancreatic cancer. *World J. Surg.* **23**:907-12

Zamir E., Geiger B. (2001) Molecular complexity and dynamics of cell-matrix adhesions. *J. Cell Sci.* **114**:3583-90

Zamir E., Katz B. Z., Aota S., Yamada K. M., Geiger B., Kam Z. (1999) Molecular diversity of cell-matrix adhesions. *J. Cell Sci.* **112**:1655-69

Zamir E., Katz M., Posen Y., Erez N., Yamada K. M., Katz B. Z., Lin S., Lin D. C., Bershadsky A., Kam Z., Geiger B. (2000) Dynamics and segregation of cell-matrix adhesions in cultured fibroblasts. *Nat. Cell Biol.* **2**:191-6

Zettl M. and Way M. (2001) New tricks for an old dog? *Nat. Cell. Biol.* **3**:E74–E75

Zhan X., Hu X., Hampton B., Burgess W. H., Friesel R. and Maciag T. (1993) Murine Cortactin is phosphorylated in response to Fibroblast growth factor-1 on tyrosine residues late in the G1 phase of the BALB/c 3T3 cell cycle. *J. Biol. Chem.* **268**:24427–24431

Zhukova E., Sinnett-Smith J., Rozengurt E. (2001) Protein kinase D potentiates DNA synthesis and cell proliferation induced by Bombesin, Vasopressin, or phorbol esters in Swiss 3T3 cells. *J. Biol. Chem.* **276**:40298-305

Zigmond S. H. (1993) Recent quantitative studies of Actin filament turnover during cell locomotion. *Cell. Motil. Cytoskeleton*. **25**:309-16

Zigmond S. H. (1996) Signal transduction and Actin filament organisation. *Curr. Opin. Cell Biol.* **8**:66-73

Zugaza J. L., Sinnett-Smith J., van Lint J., and Rozengurt E. (1996) Protein kinase D (PKD) activation in intact cells through a Protein kinase C-dependent signal transduction pathway. *EMBO J.* **15**:6220-6230

Zugaza J. L., Waldron R. T., Sinnett-Smith J., and Rozengurt E. (1997) Bombesin, Vasopressin, Endothelin, Bradykinin and Platelet-derived growth factor rapidly activate Protein kinase D through a Protein kinase C-dependent signal transduction pathway. *J. Biol. Chem.* **272**:23952-23960

Publications

Brändlin I., Hübner S., Eiseler T., Hausser A., Rupp S., Pfizenmaier K., Johannes F.-J. (2001) PKCη-PKCμ interaction and mutual regulation: Modulation of ERK and JNK signal pathways *in vivo*. S*ignal Transduction* **1**: 93

Brändlin I., Hübner S., Eiseler T., Martinez-Moya M., Horschinek A., Hausser A., Link G., Rupp S., Storz P., Pfizenmaier K., Johannes F.-J. (2002) Protein kinase C (PKC)eta-mediated PKCmu activation modulates ERK and JNK signal pathways. *J. Biol. Chem.* **277**:6490-6

Brändlin I., Eiseler T., Salowsky R., Johannes F.-J. (2002) Protein kinase C(mu) regulation of the JNK pathway is triggered via Phosphoinositide-dependent kinase 1 and Protein kinase C(epsilon). J*. Biol. Chem.* **277**:45451-7

Danksagung

Ich möchte mich hiermit bei allen bedanken, die zur Verwirklichung und zum erfolgreichen Abschluss der Arbeit beigetragen haben:

Herrn Prof. Dr. Klaus Pfizenmaier möchte ich für die Möglichkeit zur Durchführung meiner Promotion, für seine fachliche Unterstützung, die wissenschaftlichen Diskussionen und sein stetes Interesse an meiner Arbeit danken.

Mein Dank gilt auch Herrn Prof. Dr. Peter Scheurich für die Beurteilung meiner Arbeit als Mitberichterstatter und für seine wissenschaftliche Unterstützung im Laufe meiner Promotion.

Besonders möchte ich mich auch noch bei Dr. Angelika Hausser für die intensive Betreuung und fortwährende Unterstützung, sowie Motivation bedanken, die wesentlich zum Gelingen dieser Arbeit beigetragen hat.

Des Weiteren gilt mein Dank auch unseren Kooperationspartnern: Prof. Dr. H. Kalthoff (Christian-Albrechts-Universität, Kiel) für die Bereitstellung der PDAC Zellen, sowie Dr. Nicole Hauser (Fraunhofer Institut, IGB) und Dr. J. Dippon (Uni Stuttgart) für die Hilfe bei den „Geneprofiling“-Experimenten bzw. der Datenauswertung.

Danken möchte ich auch Eva Behrle und Olaf Selchow für die fachliche Unterstützung bei der Mikroskopie und speziell Eva für die netten Gespräche während der vielen Stunden am Mikroskop.

Ich möchte auch allen Mitarbeitern der PKD-Arbeitsgruppe: Suse, Gisela, Sylke, Kornelia, Chiara, Miriam… sowie allen anderen IZI-Mitarbeitern für die gute Arbeitsatmosphäre, Zusammenarbeit und Hilfsbereitschaft während meiner Promotion Danke sagen.

Bedanken möchte ich mich auch noch bei meinem Vater für seine Unterstützung während der Durchführung meiner Arbeit.

Vielen Dank an alle !